



HAL
open science

Multiscale organization of the human cortex: from anatomo-functional cognitive networks to gene expression

Claudia Cioli

► **To cite this version:**

Claudia Cioli. Multiscale organization of the human cortex: from anatomo-functional cognitive networks to gene expression. Imaging. Université Pierre et Marie Curie - Paris VI, 2015. English. NNT : 2015PA066412 . tel-01599241

HAL Id: tel-01599241

<https://theses.hal.science/tel-01599241>

Submitted on 2 Oct 2017

HAL is a multi-disciplinary open access archive for the deposit and dissemination of scientific research documents, whether they are published or not. The documents may come from teaching and research institutions in France or abroad, or from public or private research centers.

L'archive ouverte pluridisciplinaire **HAL**, est destinée au dépôt et à la diffusion de documents scientifiques de niveau recherche, publiés ou non, émanant des établissements d'enseignement et de recherche français ou étrangers, des laboratoires publics ou privés.



Université Pierre et Marie Curie

École doctorale informatique, télécommunications et électronique

Laboratoire d'Imagerie Biomédicale (LIB)

Équipe Systèmes dynamiques anatomo-fonctionnels chez l'homme, altération et récupération fonctionnelle (ADSH)

Organisation multi-échelle du cortex humain: des réseaux anatomo-fonctionnels à l'expression des gènes

Par Claudia CIOLI

Thèse de doctorat de Sciences et technologies de l'information et de la communication

Dirigée par Yves Burnod et Habib Benali

Présentée et soutenue publiquement le Septembre 30, 2015

Devant le jury composé de:

POTIER, Marie-Claude, <i>DR CNRS</i>	Rapporteur
TORO, Roberto, <i>Prof. Universidad de Valparaíso, Chili</i>	Rapporteur
COLLIOT, Olivier, <i>DR CNRS</i>	Examineur
FROUIN, Vincent, <i>Chercheur-Ingénieur CEA</i>	Examineur
ABDI, Hervé, <i>Prof. University of Texas, USA</i>	Examineur
BOURGINE, Paul, <i>Prof. Open University, UK</i>	Examineur
BENALI, Habib, <i>DR INSERM</i>	Directeur de Thèse
BURNOD, Yves, <i>DR INSERM</i>	Directeur de Thèse



Université Pierre et Marie Curie

École doctorale informatique, télécommunications et électronique

Laboratoire d'Imagerie Biomédicale (LIB)

Équipe Systèmes dynamiques anatomo-fonctionnels chez l'homme, altération et récupération fonctionnelle (ADSH)

Multiscale organization of the human cortex: from anatomo-functional cognitive networks to gene expression

Par Claudia CIOLI

Thèse de doctorat de Sciences et technologies de l'information et de la communication

Dirigée par Yves Burnod et Habib Benali

Présentée et soutenue publiquement le Septembre 30, 2015

Devant le jury composé de:

POTIER, Marie-Claude, *DR CNRS*

TORO, Roberto, *Prof. Universidad de Valparaíso, Chili*

COLLIOT, Olivier, *DR CNRS*

FROUIN, Vincent, *Chercheur-Ingénieur CEA*

ABDI, Hervé, *Prof. University of Texas, USA*

BOURGINE, Paul, *Prof. Open University, UK*

BENALI, Habib, *DR INSERM*

BURNOD, Yves, *DR INSERM*

Rapporteur

Rapporteur

Examineur

Examineur

Examineur

Examineur

Directeur de Thèse

Directeur de Thèse

Abstract

This work is conceived in the present panorama of fast development of large databases gathering experimental results about the organization of the human brain at different scales. This abundance of information calls for an intra and inter-disciplinary effort aimed to synthesize this information in a coherent way.

The aim of this thesis was to contribute to this effort for knowledge synthesis to better understand the multiscale organization of the cerebral cortex. The work followed two paths: an intra-disciplinary effort to bring together results produced by the brain imaging community with particular focus on Resting State and Task Based MRI experiments; an inter-disciplinary attempt to draw a link between the anatomo-functional organization of the cortex as emerging from brain imaging studies and the cortical patterns of gene expression as revealed by recently published atlases of the adult human brain transcriptome.

The thesis is organized into three parts: Part I is devoted to the study of the anatomo-functional organization of the human cortex starting from brain imaging studies.

In the first chapter of Part I we showed using multiscale clustering, that anatomo-functional networks (including Resting State and Task Based networks (referred to also as cognitive networks) as obtained in brain imaging experiments) are topologically organized across the cortex as two rings and that these two rings correspond to two different ways of information processing. A first ring called VSA–Visual Somatosensory Auditory– carries out real time, high fidelity processing of sensory-motor and multimodal information. A second ring called PTF–Parieto, Temporo, Frontal– and while it encompasses the cognitive networks implementing language, memory and emotions, it is responsible for multi-temporal information processing and characterized by a stronger autonomous component.

In the second chapter of Part I we deepened the analysis of the organization of these networks at a finer level. To do so we built a graph of topographical similitude among several hundreds of cognitive networks covering all the domains, sensory-motor, language, memory, emotional and vital needs. This analysis allowed not only to find again the ring organization but also to establish relations and continuity across different cognitive domains. We finally propose a global scheme to describe the organization of cognitive networks across the anatomo-functional regions of the cortex. This scheme is determined by: 1) poles of

connections of cerebral areas with the rest of nervous structures; 2) functional gradients connecting these poles within parietal, frontal and temporal regions.

In Part II we studied the link between cortical gene expression and the anatomo-functional organization of the cortex both in term of their topography and in term of their function, focusing in particular on information processing and memory formation.

In the first chapter of Part II we showed using multidimensional statistical techniques –such as CA and DiCA – that the ensemble of genes the most differentially expressed across the cortex are organized according to the ring architecture. The advantage of this method is to reveal the members of the gene families the most spatially differentiated. We focused on family of genes with specific synaptic properties in neuronal information processing namely ionic channels and proteins implied in neurotransmitter release. We showed that the expression of different protein isoforms is coherent with the information processing performed by each of the two rings. We found proteins supporting precise and high fidelity information processing (such as ionic channel SCN1A, KCNA1 and release proteins SYT2 and CPLX1), more expressed across VSA networks, while proteins favoring spontaneous activity production (such as ionic channel SCN3A, KCNG1 and release proteins SYT5 and CPLX3), more expressed in the PTF ensemble.

In the second chapter of Part II we studied on a finer scale this dual organization analyzing the topographical relation between specialized networks–visual, motor, language, memory etc.–and the proteins controlling information processing (ionic channels and neurotransmitter release), short term memory (calcium-dependent kinases), long term memory (actin, tubulin) and development (guidance and growth factors). Short-term and long term memory involves a cascade of transformation: glutamate NMDA receptor activation signaling co-occurrence of inputs, calcium inflow prolonged by CaMK auto-phosphorylation producing a short term memory, and actin polymerization increasing the spine surface for long-term memory encoding. The expression of genes coding for these 3 families of proteins is highest in the cerebral cortex, with a differential distribution of subunits in the cortical regions. The glutamate receptor NR2B responsible of sustained activities of working memory and strong plasticity is higher in cognitive regions PTF; NR2A which produces shorter activation and limits plasticity is higher in sensorymotor VSA regions; GRIN3A, which delay maturation is more expressed in PTF. The CaMK isoforms CaMK2D higher in cognitive regions PTF and CaMK2G higher in sensorymotor regions VSA produce two modes of actin polymerization, with CaMK2D favoring strong consolidation. There is also a contrast between temporal and frontal regions. CaMK1G in frontal regions produces longer duration of short term memory than CaMK4 in temporal regions. Genes coding for proteins regulating the actin network, are either more expressed in the frontal regions (ACTN2 gene coding for alpha-actinin2), or in the temporal regions (actin-related protein ACTR3) suggesting different mode of long-term memory encoding. Furthermore, genes coding for alpha and beta tubulin, which regulate the microtubule dynamics, and thus axon and den-

drites growth, are also more expressed in the frontal regions where very slow maturation allows for learning-dependent network remodeling.

In Part III we present the platform that we developed to favor knowledge integration between databases of cognitive networks and databases of gene expression and to foster research. The platform is based in part on the studies presented in Part I and Part II.

In perspective we show how the type of analyses we perform could help to better understand, in Alzheimer disease, the relation between the gradient associated to gene expression and the pattern of propagation of the disease across cortical regions. Similarly the preferential expression of genes implicated in ASD could help to better understand the cognitive networks and cognitive functions which are impaired. Finally a more precise knowledge of the genes the most expressed in different cortical areas can help adapting the parameters necessary to model the dynamic processes (activation, plasticity) in the different areas of the cortex.

Résumé

Ce travail est conçu dans le panorama actuel de développement rapide de grandes bases de données qui rassemblent des ensembles de résultats expérimentaux sur l'organisation anatomo-fonctionnelle du cerveau humain à différentes échelles; l'abondance d'informations demande un effort intra et interdisciplinaire pour les synthétiser de façon cohérente. Le but de cette thèse est de contribuer à cet effort de synthèse. Le travail suit deux chemins: l'effort intra)disciplinaire pour relier et synthétiser les résultats produits par la communauté de l'imagerie cérébrale, avec une focalisation particulière sur les Réseaux de Repos et les Réseaux Cognitifs; l'effort inter-disciplinaire pour relier l'organisation anatomo-fonctionnelle du cortex cérébral telle qu'elle émerge des ensembles de résultats en imagerie cérébrale, et les expressions des gènes révélées par les bases de données publiées très récemment sur le transcriptome humain.

Cette thèse est organisée en trois parties: la Partie I est consacrée à l'étude de l'organisation anatomo-fonctionnelle du cortex à partir des études d'imagerie cérébrale.

Dans le premier chapitre de la partie I, nous montrons en utilisant des méthodes de clustering multi-échelle que les réseaux anatomo-fonctionnels (incluant les réseaux de repos et les réseaux activés par des tâches cognitives) sont topologiquement organisés sur la surface corticale comme deux anneaux entrelacés, et que ces deux anneaux implémentent deux modes de traitement de l'information. Le premier anneau appelé VSA (Visuel-Somatoteur-Auditif) effectue des traitements sensorimoteurs (et multimodaux) en temps réel, avec une haute fidélité par rapport aux entrées et sorties reliées au monde extérieur. Un second anneau, appelé PTF (Parieto-Temporo-Frontal) qui implémente le langage, la mémoire sémanique et épisodique, les émotions, les fonctions et rythmes vitaux) effectue des traitements multi-temporels, plus autonomes par rapport aux sources extérieures.

Dans le second chapitre de la Partie I, nous approfondissons l'analyse de ces réseaux à un niveau de résolution plus fin. Pour cela, nous construisons un graphe des similitudes topographiques entre des centaines de réseaux cognitifs dans tous les domaines, sensori-moteurs, pour le langage, la mémoire, les émotions, les besoins vitaux, etc. Cette analyse nous permet de retrouver l'organisation d'ensemble en deux grands anneaux, mais aussi d'établir des relations de continuité ' corticotopique' entre les différents domaines cognitifs. Nous décrivons finalement un schéma d'ensemble pour décrire l'organisation des

réseaux cognitifs à partir de régions anatomo-fonctionnelles de référence. Ce schéma est déterminé par: 1) des pôles de connection des aires cérébrales avec les autres structures nerveuses; (2) des gradients fonctionnels reliant ces pôles par les réseaux entre régions pariétales, frontales, et temporales.

Dans la Partie II, nous étudions les liens entre l'expression corticale des gènes et l'organisation anatomo-fonctionnelle du cortex, à la fois en terme de similitude topographique et de congruence de fonction, en se focalisant en particulier sur le traitement de l'information et la mémorisation.

Dans le premier chapitre de la Partie II nous montrons, en utilisant des techniques statistiques multidimensionnelles - tels que l'Analyse des Correspondances, et l'Analyse Discriminante des Correspondances - que l'ensemble des gènes les plus différenciellement exprimés sur le cortex sont organisés suivant l'architecture en deux anneaux. L'avantage de cette méthode statistique est de révéler les gènes les plus différenciés dans chaque famille de gènes. Nous nous focalisons sur les familles de gènes spécialisés dans le traitement de l'information, comme les canaux membranaires et les protéines contrôlant la libération des vésicules de neurotransmetteurs. Nous montrons que l'expression des différents isoformes, compte tenu de leurs propriétés fonctionnelles, est cohérent avec les modes spécifiques de traitement de l'information dans chacun des deux anneaux. Nous trouvons des protéines plus spécialisées pour le traitement de l'information précis dans le temps et fidèle par rapport aux entrées (canaux SCN1A, KCNA1, contrôlant la libération SYT2, CPLX1), plutôt dans l'anneau VSA qui effectue les traitements en temps réel avec le monde extérieur, et des protéines plus spécialisées dans l'activité plus soutenue et plus spontanée (canaux SCN3A, contrôlant la libération CPLX3) dans l'anneau PTF qui effectue les traitements multi-temporels, plus autonomes par rapport au monde extérieur.

Dans le second chapitre de la Partie II, nous étudions à une échelle spatiale plus fine cette organisation en deux anneaux, en différenciant les régions anatomo-fonctionnelles spécialisées (pour le langage, la mémoire, les émotions, les besoins vitaux, etc.). En plus des qui contrôlent le traitement de l'information (canaux ioniques et libération du neurotransmetteur), nous nous focalisons aussi sur celles qui contrôlent la mémoire à court terme (récepteur glutamate NMDA et CaMK calcium-dependent kinases), la mémoire à long terme (cytosquelette actine et tubuline), et le développement (facteurs de croissance et facteurs de guidage des axones). La mémorisation à court et long terme se fait par une cascade de transformations: le récepteur NMDA au glutamate signale la co-occurrence des entrées et génère un flux entrant de calcium, qui produit l'autophosphorylation des CaMK (mémoire à court terme) et la polymérisation de l'actine qui augmente la surface des épines dendritiques et donc le poids synaptique (support de la mémoire à long terme). L'expression des gènes qui codent ces trois familles de protéines est plus fort dans le cortex cérébral, avec une distribution différentielle des sous-unités et des isoformes dans les régions corticales. Ainsi le récepteur au glutamate NR2B, responsable des activités soutenues de la mémoire de travail, et d'une plasticité très forte, s'exprime plus dans PTF, alors que le récepteur NR2B,

qui produit des activations plus courtes et moins de plasticité, s'exprime plus dans les régions VSA. Le gène GRIN3A, qui retarde la maturation, s'exprime plus dans PTF. Pour les isoformes de la CaMK, CaMK2D s'exprime plus dans les régions cognitives PTF, et CaMK2G s'exprime plus dans les régions sensori-motrices VSA. Ces deux isoformes de la CaMK produisent deux formes différentes de polymérisation de l'actine, avec la CaMK2D qui favorise des consolidations fortes, avec des mémoires persistantes. Il existe aussi un contraste entre les régions pariétales et frontales. La CaMK1G dans les régions frontales produit des mémorisations à court terme plus longues, de l'ordre de l'heure, alors que la CaMK4, dans les régions temporales, produit des mémorisations à court terme plutôt de l'ordre de la minute. Les gènes qui codent les protéines qui régulent les réseaux d'actine, sont soit plus exprimées dans les régions frontales (ACTN2 codant l'alpha-actinine 2), soit dans les régions temporales (actin-related protein ACTR3), suggérant des modes différents de mémorisation de l'information. De plus, les gènes qui codent pour les différents isoformes des tubulines alpha et beta, qui régulent finement la dynamique des microtubules, et donc la croissance des axones et des dendrites, sont aussi plus exprimés dans les régions frontales où la maturation lente des neurones pendant deux décennies permet de modeler fortement les réseaux en fonction de l'apprentissage.

Dans la Partie III, nous présentons la plate-forme que nous avons développée, pour intégrer dans une même représentation les données d'imagerie cérébrale et les données d'expression génétique, et pour faciliter la recherche présentée dans les Parties I et II.

En perspective, nous montrons comment les analyses que nous faisons peuvent aider à mieux comprendre la relation, dans la maladie d'Alzheimer, entre les gradients d'expression des gènes et la propagation de la pathologie dans les réseaux corticaux. De même dans le spectre autistique, l'expression préférentielle des gènes à risque peut aider à mieux comprendre les réseaux cognitifs et les fonctions cognitives qui sont déficitaires. Finalement une meilleure connaissance des gènes les plus exprimés dans les différentes régions corticales peut aider à adapter les paramètres des modèles des processus dynamique (activation, plasticité) aux caractéristiques spécifiques des réseaux corticaux.

Contents

1	Introduction	1
1.1	Motivation	1
1.2	Context	5
1.2.1	Brain imaging databases	5
1.2.2	Gene expression: the Allen Institute’s human brain transcriptome database	7
1.3	This Dissertation: contents	8
1.3.1	Anatomo-functional organization of the cortex: the dual intertwined rings architecture	9
1.3.2	Anatomo-functional organization of cortical gene expression	9
1.3.3	Heuristic: focusing on expression of families of genes known to be involved in information processing and memory formation	10
1.4	This Dissertation: plan	12
1.5	This Dissertation: personal contributions	17
1.6	Publications from this Dissertation	18
1.6.1	Journal articles	18
1.6.2	Peer-Reviewed Abstracts	18
1.6.3	Others	19
I	Cortical organization of anatomo-functional networks: rings and gradients	21
2	The dual intertwined rings architecture	23
2.1	Graphical abstract	23
2.2	Abstract	23
2.3	Introduction	24
2.4	Results	27
2.4.1	Extraction of the most representative RSNs in the group: robustness	27
2.4.2	RSNs Specialization: overlap between RSNs and TBNs	28
2.4.3	RSNs topography: overlap between RSNs and the Brodmann Areas.	30
2.4.4	Corticotopy of the RSNs clusters: the dual intertwined rings architecture	31
2.4.5	Anatomical connections within and between the dual rings.	35

2.5	Discussion	36
2.5.1	Method of RSNs extraction and RSNs coverage	37
2.5.2	Comparison of the dual intertwined architecture with other RSNs results	38
2.5.3	Real-time integration in the VSA ring and multi-temporal integration in the PTF ring	40
2.5.4	Topological advantages of the intertwining	42
2.5.5	Development of the dual intertwined rings architecture	42
2.5.6	Evolution of the dual intertwined ring architecture	43
2.5.7	Conclusion	43
2.6	Materials and Methods	43
2.6.1	Resting-state database	43
2.6.2	Pre-processing	44
2.6.3	Functional network identification by spatial Independent Component Analysis (NEDICA)	44
2.6.4	Clustering methods	44
2.6.5	RSNs specialization: overlap with TBNs	45
2.6.6	RSNs distribution: overlap with BAs regions	45
2.6.7	Anatomical Fiber tracting	46
2.6.8	Representation of the results	47
3	Gradients of cognitive networks	51
3.1	Graphical abstract	52
3.2	Abstract	53
3.3	Introduction	54
3.3.1	fMRI: single study vs meta-analysis	55
3.3.2	Data-driven meta-analysis: the Neurosynth framework	55
3.4	Results	57
3.4.1	Lexical Map: 1000 cognitive terms	57
3.4.2	Topographic Map: 1000 cognitive categories	60
3.4.3	Anatomo-functional gradients of cognitive tasks across the cortex	62
3.5	Methods	73
3.5.1	Neurosynth: inverse inference maps	74
3.5.2	CorText: lexical extraction	75
3.5.3	Cognitive terms: lexical and topographical similarity	76
3.6	Conclusions	77

II	Cortical organization of gene expression in relation with anatomo-functional networks	79
4	Cortical gene expression match the temporal properties of large-scale functional networks	81
4.1	Graphical abstract	82
4.2	Abstract	83
4.3	Introduction	83
4.4	Materials and Methods	87
4.4.1	Data Base	87
4.4.2	Labeling of cortical regions by VSA or PTF rings	87
4.4.3	Statistical Analysis I: Correspondence Analysis (CA)	87
4.4.4	Statistical Analysis II: Discriminant Correspondence Analysis (DiCA)	88
4.5	Results	89
4.5.1	Gene expression spontaneously separates the rings	89
4.5.2	Cortical gene expression predicts the assignment of cortical regions to the rings	90
4.5.3	Correlation between gene expressions	92
4.5.4	The proteins coded by genes most differentiated between cortical regions belong to families of proteins involved in neuronal information processing such as ionic channels and neurotransmitter release	92
4.5.5	Determination of genes the most expressed in VSA and PTF for the ionic channels and transmitter release functional classes	94
4.6	Discussion	98
4.6.1	Sodium and potassium channels	100
4.6.2	Calcium channels	101
4.6.3	Synaptotagmins	101
4.6.4	Complexins	102
4.6.5	Synaptobrevins	102
4.7	Conclusions	103
4.8	Remark: Regions are organized according to gradients based on their gene expression profile	103
5	Gradients of synaptic genes properties across cognitive networks	107
5.1	Graphical abstract	108
5.2	Abstract	109
5.3	Introduction	110
5.4	Materials and Methods	112
5.4.1	Data Base	112
5.4.2	Anatomo-functional regions	112
5.4.3	Statistical Analysis: Discriminant Correspondence Analysis (DiCA)	113
5.5	Results	113

5.5.1	Single gene expression profiles	115
5.5.2	Organization of brain regions by gene expression	116
5.5.3	Organization of cortical regions by gene expression	118
5.5.4	Differential expression of genes in families involved in information processing and memory formation	120
5.5.5	Gradients of gene expression in the cerebral cortex	137
5.6	Discussion	139
5.6.1	Main axes of gene expression in cerebral regions and cortical regions	139
5.6.2	Neoteny of language regions	141
5.6.3	Gradients of gene expression	142
5.6.4	Multiscale anatomo-functional congruence	143
5.6.5	Transcription factor FOXP2 and growth factor MET: language and autism	156
5.7	Conclusions	156
5.8	Remark I: The anatomo-functional synapse: multiscale scenarios in different cortical regions	157
5.8.1	Perform a visuomotor task: cortical motor, visual and parietal visuomotor regions	158
5.8.2	Memorize-recognize faces and events: temporal fusiform and parahippocampal regions	159
5.8.3	Produce goal-directed sequences of actions: superior frontal regions	160
5.8.4	Produce sentences: network relating audition-phonation, temporal and frontal regions	163
5.9	Remark II: Synaptic proteins evolution and the tethering hypothesis	165

III Tools development 169

6 LinkRbrain: a web-based platform to analyze spatial correlation of gene expression and cognitive networks 171

6.1	Graphical abstract	171
6.2	Abstract	171
6.3	Introduction	172
6.4	Data sources	174
6.5	Methods	174
6.5.1	Text mining	175
6.5.2	From probes to expression of genes	175
6.5.3	Topographical distances	175
6.5.4	Visualization	176
6.6	LinkRbrain as a multi-scale, integrative explorer	178
6.6.1	From cognitive functions to functional-anatomical architecture	179
6.6.2	From genetic expression to cognitive functions	181

6.7	LinkRbrain as comparator of brain networks of cognitive functions	182
6.8	LinkRbrain as a comparator of user results with the literature	182
6.9	Conclusion	183
7	Conclusions and future work	187
7.1	Conclusions	187
7.2	Future work	192
7.2.1	Alzheimer disease	192
7.2.2	Autism Spectrum Disorder	194
7.2.3	Models	196
	Bibliography	201
A	Supplementary Material	227

Introduction

This work is conceived in the present panorama of fast development of large databases gathering experimental results about the organization of the human brain at different scales. This abundance of information calls for an intra and inter-disciplinary effort aimed to synthesize this information in a coherent way.

In this dissertation we explore the relations between brain imaging and transcriptomics databases, to better understand the multiscale organization of the cerebral cortex. We study the relation between gene expression and cognitive networks, both in term of their cortical topography and in term of their function, focusing in particular on information processing and memory formation.

1.1 Motivation

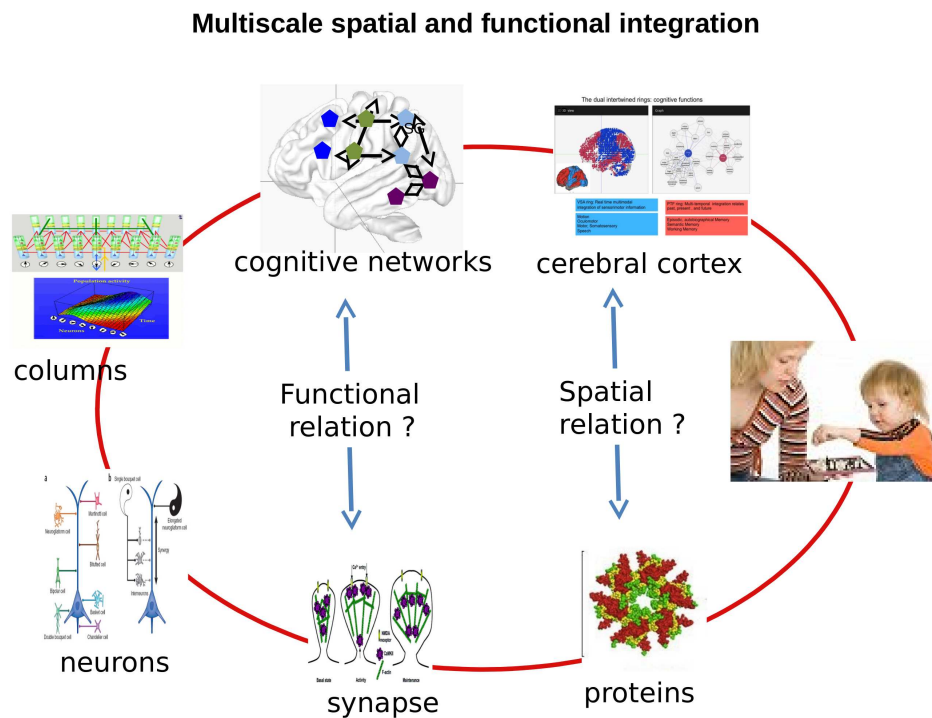


Fig. 1.1.: Spatiotemporal multiscale organization of the cortex

Figure 1.1 summarizes the multiscale functional architecture of the human brain, starting from the behavioral and cognitive level, and zooming toward the cerebral and cortical networks, and then toward the local networks of cortical columns, neurons, synapses, un-

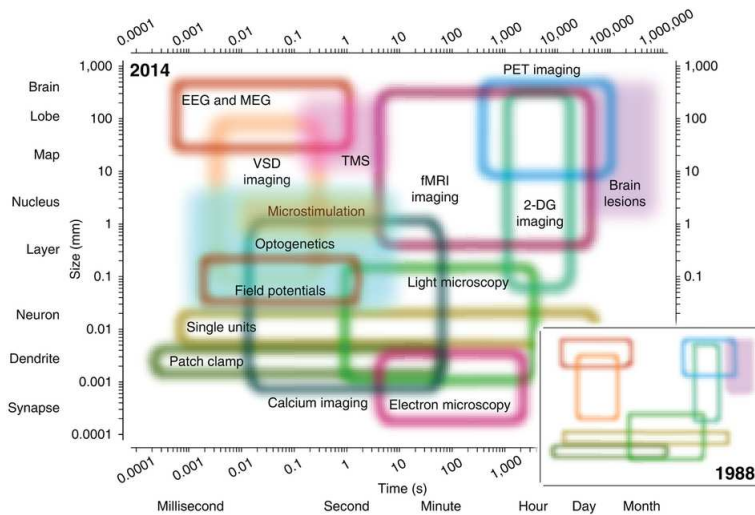


Fig. 1.2.: The spatiotemporal domain of neuroscience and the evolution of the main techniques of investigation. Source: [236]

til molecules within synapses. All these levels have been studied in term of information processing and memory formation. For example, at the behavioral and cognitive levels, psychology and artificial intelligence describe interaction between visual and motor information to manipulate objects, between phonation and audition to communicate, and at the same time, information storage to memorize new words and rules through verbal communication.

At the brain level, brain imaging techniques, for example fMRI techniques, have revealed a very large set of sensorymotor and cognitive networks specialized for information processing and storage, as for example visuomotor processing in parietal areas, speech and sentence processing in dorsal temporal areas and ventral frontal regions, episodic memory in ventral temporal regions, working memory and rules processing in dorsal frontal areas, etc.

At the finer level of local neuronal networks, neurophysiology have shown that all forms of processing and memory are based on prototypical networks of neurons, the cortical columns. Cortical columns are processing units which combine locally different types of information (sensory, motor or cognitive) provided by different layers of the column, and store the congruences among these different types of information, as for example the congruency between visual, proprioceptive, tactile and motor information.

At the level of a single neuron, electrophysiological techniques have revealed how information is processed by the axodendritic system thanks to a set of ionic channels, and how memory processes are determined by pre and post synaptic plasticity and remodeling as a consequence of the coactivation of several synapses belonging to the same neuron.

Molecular biology and genetics have deciphered the function of proteins involved in information processing and memory formation at the synaptic level. Among these proteins are ionic channels, receptors, cytoskeleton proteins and transcription factors. These families of proteins are composed by several isoforms or subunits differentiated among them by the

fine tuning of their molecular structure. This variety of molecular structures confers to these families of proteins a large repertoire of temporal and dynamical properties. Figure 1.1 illustrates two important questions: 1) what is the spatial relation between gene expression and the anatomo-functional organization of the cerebral cortex; 2) what is the functional relation between the synaptic proteins coded by these genes and the specialized functions of cognitive networks which are spatially matched with the gene expression patterns.

To understand how the cortex works and how it gives rise to the variety of human behaviors, it is necessary to understand how these different scales interact together. To this purpose, researchers have combined a variety of techniques at different scale in space and time (see for a set of techniques Figure 1.2 from [236]) to find out which are the relations between distribution and dynamics of proteins at the synaptic and neuronal level, how proteins interactions shape the way neurons process and store information, how different neurons and networks of neurons are reciprocally organized in maps and cognitive networks, which are the anatomical and genetic pathways leading to the genesis of neuronal and cognitive networks.

1.1.0.1 Multiscale research strategies

Since many diseases are due to molecular deficits and have effects at all levels, synaptic, neuronal, networks and cognitive, researchers have developed integrated multiscale strategies to understand and cure these diseases.

For example, in Alzheimer disease, researchers have found specific molecules which are dysfunctional, like beta-amyloid peptide and tau proteins. They produce lesions at the neuronal level (reviewed in [73]): Tau accumulate in the cell body of the neuron as neurofibrillary tangle, in the dendrites as neuropil threads, and in the axons forming the senile plaque. At the neuronal circuit level, these lesions produce losses of synapses and neurons. At the level of cortical networks, there is a progression of the tau pathology which involves specific networks from the entorhinal cortex, through the hippocampus, to the isocortex. At the psychological and clinical level, there are progressive deficits starting from memory losses to language alterations and then to sensorymotor dysfunctions.

As another example, in Autism, researchers (see for example [262, 221]) have found a variety of genes which are dysfunctional, like cell-cell adhesion proteins, receptors of transcription factors, axon guidance proteins, etc. They have synthesized their combined synaptic and cellular effects by showing that the main category of genes associated with ASD is related to the development and function of neuronal circuits, and in synaptogenesis, such as, cell adhesion molecules which are major organizers of excitatory glutamatergic and inhibitory GABAergic synapses, and contribute to the activity-dependent formation of neuronal circuits. This set of genes is responsible after birth for synaptic homeostasis that allows neurons to maintain an optimal level of activity which plays an important role in the

activity-dependent refinement of brain connections during development and the first years of life. Furthermore, at the network level, they found that there is a dysmaturation of cortical thickness in the temporal lobes and within these the fusiform and middle temporal gyri. These brain regions are crucial to social cognition which is a specific cognitive deficits in ASD.

Beyond multiscale strategies, researchers have formed large consortia to share their data in genetics and brain imaging.

For example ADNI (Alzheimer Disease NeuroImaging) is a global research consortium to share genetic and brain imaging data on Alzheimer Disease. This multisite, longitudinal study assesses clinical, brain imaging, genetic and biospecimen biomarkers through the process of normal aging to early mild cognitive impairment (EMCI), to late mild cognitive impairment (LMCI), to dementia or AD. The IMAGEN consortium is a European research project investigating mental health and risk taking behaviour in teenagers. Research methods include psychological measures (self-report questionnaires, behavioural assessment, interviews), neuroimaging of the brain, as well as blood sampling for genetic analyses. The ENIGMA Consortium [258] produce large-scale collaborative analyses of neuroimaging and genetic data to relate measures of brain volume, integrity, receptor distribution, or chemical composition, with functions of candidate genes—such as growth factors, transcription factors, guidance molecules, or neurotransmitters and their transporters. Many of these had already been implicated in the risk for psychiatric illness, and imaging offered the opportunity to study differences in brain connectivity or function, in carriers of genetic variants associated with disease risk. These consortia have shown a set of specific relation between genes and networks, including anatomical, functional, and cognitive networks.

Concerning Anatomical networks, researchers working with ADNI data have shown that cortical thickness in different regions allows to automatically discriminate between patients with Alzheimer's disease (AD) or mild cognitive impairment (MCI) and elderly controls (CN). By cumulating data from ADNI, IMAGEN, and 3 other consortia (30000 individuals from 50 cohorts with MRI scans) researchers have conducted genome-wide association studies of the volumes of seven subcortical regions [120]. They found that genetic variants influencing the volumes of the putamen and caudate nucleus clustered near developmental genes that regulate apoptosis, axon guidance and vesicle transport. The ENIGMA consortium (ENIGMA) has performed a genome-wide association study GWAS identifying common variants in the genome associated with hippocampal volume, subcortical volumes and white matter microstructure to understand how schizophrenia, bipolar illness, major depression and attention deficit/hyperactivity disorder (ADHD) affect the brain.

Concerning Functional networks, researchers working on IMAGEN fMRI data and the Allen Gene expression atlas [222] have shown that functional Resting State Networks are correlated with a set of 136 genes significantly enriched for ion channels and axonal con-

nectivity. Polymorphisms in this set of genes significantly affect Resting State functional connectivity in a large sample of healthy adolescents, showing that RSN correlate with the orchestrated activity of dozens of genes linked to ion channel activity and synaptic function. Concerning cognitive networks, analysis of the IMAGEN data showed that a significant proportion of the brain response to facial expressions is predicted by common genetic variance (captured by $\sim 500,000$ single nucleotide polymorphisms) in a subset of 25 regions constituting the face network [66].

The recent development of open databases about brain imaging and transcriptomics gives a unique opportunity to connect the anatomo-functional organization of the cortex with the topographic organization of gene expression. Previous studies showed that different cerebral structures (e.g., hippocampus, cerebellum) present characteristic gene expression, and that this is true, even if with weaker differences for distinct areas of the cerebral cortex [117, 101]. However what is poorly understood is the relation between the functional role of proteins and gene expression at the synaptic and cellular level and the functional specialization of different cognitive and sensorymotor cerebral networks.

The aim of this thesis was to contribute to this effort for knowledge synthesis following two paths: an intra-disciplinary effort to bring together results produced by the brain imaging community with particular focus on Resting State and Task Based MRI experiments; an inter-disciplinary attempt to draw a link between the anatomo-functional organization of the cortex as emerging from brain imaging studies and the cortical patterns of gene expression as revealed by recently published atlases of the adult human brain transcriptome.

This thesis is organized into three parts: Part I of the thesis will be devoted to the study of the anatomo-functional organization of the human cortex starting from brain imaging studies; Part II will study the link between cortical gene expression and the anatomo-functional organization of the cortex; Part III will introduce a platform developed to favor knowledge integration and to foster research based in part on the studies presented in Part I and Part II. In the next section we will give some context for Part I and Part II.

1.2 Context

1.2.1 Brain imaging databases

1.2.1.1 Anatomical and Resting State networks (RSNs): human connectome databases

There is a consensus on the anatomical organization of cortical areas. Historically, based on pure anatomical observations the human cerebral cortex have been divided in four main lateral **cortical lobes**: frontal lobe, parietal lobe, occipital lobe and temporal lobe; a mesial

lobe, the limbic lobe and an internal portion the insular cortex. This represent the first level of the topographic organization of the human cortex. At a smaller scale each lobe is characterized by crests (**gyri**) and valleys (**sulci**) result of the grey matter folding. The main gyri and sulci are stable across individuals. Gyri are not only different for their position across the different cortical lobes but also because they differ for their cytoarchitectural organization. **Brodmann Areas** (BAs) describe the heterogeneity of cortical areas cytoarchitectonic and their boundaries follow mainly those of the main sulci. These areas are connected among them by local cortico-cortical connection and long range connections linking non contiguous regions. **Diffusion Tensor Imaging** (DTI) technique has brought a large number of results on the precise anatomy of these long-range connections, and these data are shared by the scientific community. Another method to analyze the functional relations between areas are the **Resting State Networks** (RSNs). Cerebral activity of participants is measured with an MRI scan while people are not performing any particular task. The **Human Connectome project** (HCP) has provided open databases of experimental results on anatomical connections and Resting State Networks. Another fundamental initiative in the field of data sharing with particular focus on Resting State Networks is the **International Neuroimaging Data-sharing Initiative** (INDI).

1.2.1.2 Task based cognitive networks (TBNs): the Neurosynth database

Functional Magnetic Resonance Imaging (fMRI) maps cognitive tasks (human behavior) to cortical anatomy. Participants to fMRI experiments are asked to perform task according to a predefined paradigm while scanning their brain activity. The result of the experiment consists in so called **Task Based Networks** (TBNs) relating cortical areas to the task performed. TBNs studies are important not only to get spatial information about cognitive networks organization but also to have some hints about the time-scale associated with different tasks and consequently with the cortical regions implementing them. Trying to solve the problem of poor statistical power of experiments—given the small cohorts of participants ($N \sim 10$)—the differences in experimental paradigms and MRI machine models it was started a movement of meta-analysis studies. Statistical methods were developed to exploit the peaks of activations extracted manually from a set of trustworthy studies about a task of interest to obtain more statistical sound results. The **BrainMap** project [157], was the first to try to scale up this process accumulating several hundreds of articles manually tagged according to top-down ontologies with the cognitive task performed in the experiment and the MNI/Talairach coordinates for the peaks of activations found as the result of the experiment. In 2011 Tal Yarkoni implemented an automated and open source framework to perform meta-analysis of large chunks of fMRI literature collecting a database of about 4000 articles in its first release (now around 10000): the **Neurosynth** platform. The framework include a set of scripts able to automatically extract peaks of activations from tables found in fMRI articles, do a basic ranking of terms used all along the text of the paper based on their frequency of occurrence and create a database relating each paper with

its *doi* (digital object identifier) to a set of coordinates and a set of terms. Together with his collaborator he also implemented a set of statistical scripts to analyze this database and return meta-analytic probability maps for each term, based on thousands of papers.

1.2.2 Gene expression: the Allen Institute's human brain transcriptome database

Neurons are very specialized cells and as such they undergo a massive process of RNA transcription. Since in general they do not duplicate their chromatin is constantly unfolded and ready for transcription operations [243]. This transcription activity is fundamental for the production of proteins regulating all neuronal processes from the more general as metabolism (90% of neuronal metabolism is devoted to maintain a functional resting state potential) to the more specific such as information processing and memory formation. It is well known in mice at least for genes implied in cortical morphogenesis that they are expressed according to gradients [219, 218]: it means that their expression is differential across the cortex with poles of maximal expression and dieing out moving away from these regions of preferential expression. Moreover there is evidence—from comparative studies of PSD composition in vertebrates—that synaptic composition in mammals (mouse) not only varies according to the neuronal phenotype like (for example if they belong to glutamatergic or GABAergic neurons [218]), but also in relation to their position across the cortical sheet [297].

In humans only recently for the strong postmortem constraint has been possible to study the whole genome transcriptome. In particular the **Allen Institute** was the first to produce and make available to the scientific community a detailed atlas of human cerebral transcriptome (ABA) in healthy adults (2 complete brains and 4 left halves). Previously only large anatomical areas had been analyzed as for example in [142, 50]. For each specimen the ABA contains measures conducted for about 60000 probes corresponding to about 21000 genes in at least 180 samples for cortical hemisphere. While these data represent a unique source to study gradient of gene expression across the cortex and it is not difficult to produce systematic analyses for the entire bulk of data, a very challenging task is to make sense of these results. Three are the main difficulties underlying the interpretation path: the first is that a large proportion of genes is still part of the so called Ignorome [205] so that their function is currently unknown; the second is that the cellular function of genes is not homogeneously studied across different tissues and developmental stages; for example CAMKs proteins playing a central role in neurons for short memory formation had been studied till not long ago preeminently in cardiac tissues. Third databases such as **GeneCards** or **Gene Ontology**, while they represent a precious source to have ideas about family of genes, general properties and related pathways, are still too weak in capturing and offering to the user precise and systematically exploitable information about differences in

functionality of genes according to differences in molecular structure, tissue of expression and developmental stage.

1.2.2.1 Neurosynth and the Allen Brain Institute database of gene expression

Recently Tal Yarkoni extended the Neurosynth platform to include transcriptomics data from the Allen Brain Institute. In [84] they quantify the spatial similarity between over 20,000 genes studied by the ABI and 48 psychological topics derived from lexical analysis of neuroimaging articles. The result is a comprehensive set of gene/cognition mappings called the Neurosynth-gene atlas. In [84] it is shown how the platform is able to independently replicate known gene/cognition associations (e.g., between dopamine and reward). Furthermore the framework allows to discover new associations between genes and cognitive networks representing thus a method to generate hypotheses about the genetic dimension of functional networks.

1.3 This Dissertation: contents

This project started in 2012 one year after the publication of Neurosynth [295] and the year of the first paper by the Allen Institute [117]. This conjuncture was a unique opportunity to start studying in a systematic way the eventual relations between the organization of cognitive networks and the spatiotemporal properties of proteins.

The conjunction of these two projects brought us together data coming from two far away worlds –brain imaging and molecular biology– by providing us a common reference frame where to integrate data in a spatiotemporal fashion: the spatial part represented by the MNI coordinates system and the temporal part represented by the time constants proper to proteins and dynamics of protein networks. The data coming from the Allen Institute were indeed unique in their nature since it was the first study to provide the mRNA expression of the entire human genome on a comprehensive grid of samples across all cerebral structures. This type of information is complementary respect to one obtained to GWAS-like analysis. The two main questions we wanted to answer using these data were: which is the anatomo-functional organization of the human cortex and which is the relation between gene expression and this anatomo-functional organization in term of processing and storage of information. In order to answer this question we adopted a strategy consisting in starting with the correlation of the databases at a large scale and successively zooming in towards finer level of spatial resolution.

1.3.1 [Anatomo-functional organization of the cortex: the dual intertwined rings architecture](#)

We first studied the organization of cortical anatomo-functional networks using two sets of databases and statistical techniques. A first study aimed to interpret a group of reproducible Resting State Networks. The comparison of these networks with Task Based Networks (as from [157]) and fibers tracts allowed us to reveal two large ensemble of regions, called the two rings VSA and PTF, opposed by their topography and by the type of functions implemented: real-time, stimulus driven for VSA, multi-temporal, more spontaneous and internally driven for PTF. We called this anatomo-functional organization the **two intertwined rings architecture**.

A second study parallel to the first one started from the database of Neurosynth and used text mining and meta-analytic methods allowed us to extract about **1000 cognitive networks**. The analysis of the cortical overlap of these networks performed using community detection algorithms revealed again a main superstructure made of the same two large clusters and at the same time revealed the finer structure of cognitive networks organized within each of the two large clusters.

Finally based on a spatial reference frame represented by a set of anatomo-functional regions we proposed a global scheme to describe the **organization of cognitive networks across the cortex**. This scheme is determined by: 1) poles of connections of cortical areas with the rest of the cerebral regions: the visual pole, the motor pole, the auditory pole, the pole of vital functions linked to the Hypothalamus, the pole of episodic memory linked to the Hippocampus, the pole of emotional recruitment linked to the Amygdala; 2) functional gradients connecting these poles in correspondence of parietal, frontal and temporal regions.

1.3.2 [Anatomo-functional organization of cortical gene expression](#)

When the first result of the Allen Institute on the systematic analysis of gene expression across the human cerebral cortex [117] was published, we were struck by the similitude between the topography of gene expression (obtained for a set of about 1000 genes) and the anatomo-functional architecture forming two intertwined rings that we had just defined.

We then studied the relation between the cortical gene expression patterns and the two intertwined rings architecture by means of multivariate statistical techniques such as Correspondence Analysis (CA) and Discriminant Correspondence Analysis (DiCA). Results confirmed that the main organization of gene expression is given by the dichotomy between the anatomo-functional regions belonging to the two rings. In particular DiCA analysis allowed in conjunction with the bootstrap resampling technique, to identify which genes were the most associated (preferentially expressed in) with one of the two rings.

We then investigated gene expression gradients at a finer spatial scale in relation with cog-

nitive networks made of doublets or triplets of cortical regions forming a tessellation of the cortex. Results revealed **four main gradients** of gene expression: two gradients related to the two rings, a gradient maximal in VSA and a gradient maximal in PTF ring, and two gradients related to a ventro-dorsal organization of the cerebral cortex, a gradient maximal in ventral regions (occipito temporal) and a gradient maximal in dorsal regions (frontal, motor and parietal). These four groups identify four groups of genes. This analysis gave us a list of genes maximally expressed in each of the four poles.

We then wanted to understand the meaning for this particular configuration looking at the function of these genes: is there a functional correspondence between the role of a protein at the neuronal level and the cognitive functions a region is involved in? This relation if it exist was not trivial. Databases reporting proteins properties are usually not precise enough and they do not take into account how different proteins can be expressed in different tissues or at different developmental stages still playing a role.

1.3.3 Heuristic: focusing on expression of families of genes known to be involved in information processing and memory formation

Given the difficulties encountered in interpreting the results about genes' distribution, we had to elaborate a more precise strategy. Since the main result was that genes are organized in two ensembles of cortical regions related to two distinct way of processing and storing information (the two intertwined ring architecture), we should find gene families differentially expressed participating to synaptic dynamics for information processing and memory.

We thus focused on families of proteins (and the genes they are coded by) with known synaptic function in information processing and memory. Experimental results indeed show that memory and information processing at the synaptic and cellular level (e.g., LTP) can be seen as a cascade of molecular transformations with temporal effects lasting longer through the successive steps of the cascade. We exemplified this cascade by a stair in Figure 1.3: at each step a new molecular process with a longer duration can be triggered by the previous one, from millisecond, the operation time of typical ionic channels, up to years in well consolidated memories stored in spines and dendritic morphologies. For each step of the stairs we identified protein families with a well established role in information processing and storage. This is clearly far from being exhaustive but it allowed us to verify if indeed there was a correlation between the function of key proteins for information processing and storage, and their poles of expression in correspondence to particular anatomo-functional regions. It is then possible to simply add new families to be more and more precise.

Starting from the first step of Figure 1.3 we find the families of ionic channels subunits: SCNs (sodium channels), KCNs (potassium channels) and CACNs (calcium channels). These proteins are the basic bricks of neuronal information processing since controlling the propagation of action potentials in axons and the interactions of post-synaptic potentials in dendrites. The KCN family counts alone about 100 members with different temporal characteristics important for the regulation and duration of stimuli effects. The precision reached by some family members can be of the order of milliseconds allowing ultra precise synchronization between different sensory-motor functions.

Another process important in shaping information processing is presynaptic neurotransmitter release. There are several families regulating the complex dynamic of this process and their role is to control on one hand the precision of release with respect to an afferent action potential, on the other hand the degree of spontaneity that is the capacity of the synaptic button to release neurotransmitter independently from the arrival of an action potential. Among these families two are particularly interesting, synaptotagmins (SYTs) and complexins (CPLXs) which molecular and functional properties have been understood recently.

The third step relating information processing to memorization is controlled by NMDA glutamate receptor able to modify the influx of calcium when there is a simultaneous presence of pre-synaptic activity (glutamate release) and post-synaptic (voltage depolarization). This hebbian association at the molecular level make of NMDA glutamate receptor the principal doorway toward memorization.

We studied the results for different families of glutamate and GABA receptors. NMDA receptors in the synapse are strongly influenced by the activation of receptors for neuromodulators such as serotonin, dopamine, acetylcholine and norepinephrine. There exists a tight association at the molecular level between NMDA glutamate receptors and neuromodulator receptors, with specific effect depending upon the different receptor isoforms. We analyzed the distribution of families of receptor for these four neuromodulators (not represented on the figure).

Short term memory is the capacity of a neuron to activate and stay active also when the stimulus is not there anymore. This capacity has its molecular support in the process of autophosphorylation of CaMKs proteins: thanks to the calcium influx produced by NMDA receptors, CaMKs modulate its phosphorylation in a prolonged way as a threshold function of calcium level. Here again, we analyzed the different CaMK isoforms which can support different forms of short term memory.

Long-term memory has been linked to the molecular process of actin polymerization which changes the shape of synaptic spines. This change in spine configuration leads to a modified synaptic weight and so to a different importance for that input to the neuron. Researchers

have found a strong link between different state of polymerization of actin in relation with different types of CaMKs and different types of actin networks (like actinin ACTNs, actin-related proteins ARPs and ACTRs). Short term and long term memories in human interfere with the maturation of neuronal networks (growth of dendrites and axons), as in frontal cortex, lasting decades. A next step relating long term memory and network construction is controlled by microtubules networks . These microtubules have dynamical properties of elongation strongly dependent on their composition on tubulin subunits (TUBs.) They can play an important role in learning-dependent reorganization of the axodendritic neural network. Indeed, studies in adults (Allen, more studies) show that protein which play a role in the construction of neuronal networks during development keep playing a major role during adulthood in the homeostatic processes necessary to neuronal functioning and synaptic plasticity. We focused on protein families known to be particularly important for the development of the cortical neural network, with two families of growth factors, epidermal growth factors (EGFs) and fibroblast growth factors (FGFs), and three families of protein involved in cellular recognition and axon guidance: semaphorins (SEMs), ephrins (EPHs) and C-lectins (CLECs). The choices do not pretend to be exhaustive but allow to evaluate the distribution of the protein isoforms of playing an important role in information processing and memory at different time scales.

With this scheme in mind, the essential problem to solve becomes the comprehension of the relation between the properties of genes differentially distributed in the cortex and the properties of corresponding cognitive networks, in term of memorization and information processing as exemplified in Figure 1.4. The statistical analyses reveal which members of the family are more expressed in a given anatomo-functional region of the cortex (map of the differential expression for isoforms/subunits of a family of genes). Comparison of functional properties of different isoforms differentially expressed (*Pubmed*) allowed to propose a multiscale scenario between the different protein cellular properties and different information and memory processing underlying cognitive functions.

1.4 This Dissertation: plan

The presentation of the result is organized in direct relation with the scientific production developed in the course of my PhD; in particular each sets of results is presented in the form of an article. Each chapter is introduced by a brief introduction and a graphical abstract. We added at the end of the papers supplementary remarks that can be eventually skipped. Chapters are organized as in the following (see also Figure 1.5).

Part I: Cortical organization of anatomo-functional networks: rings and gradients

Chapter 1: Introduction

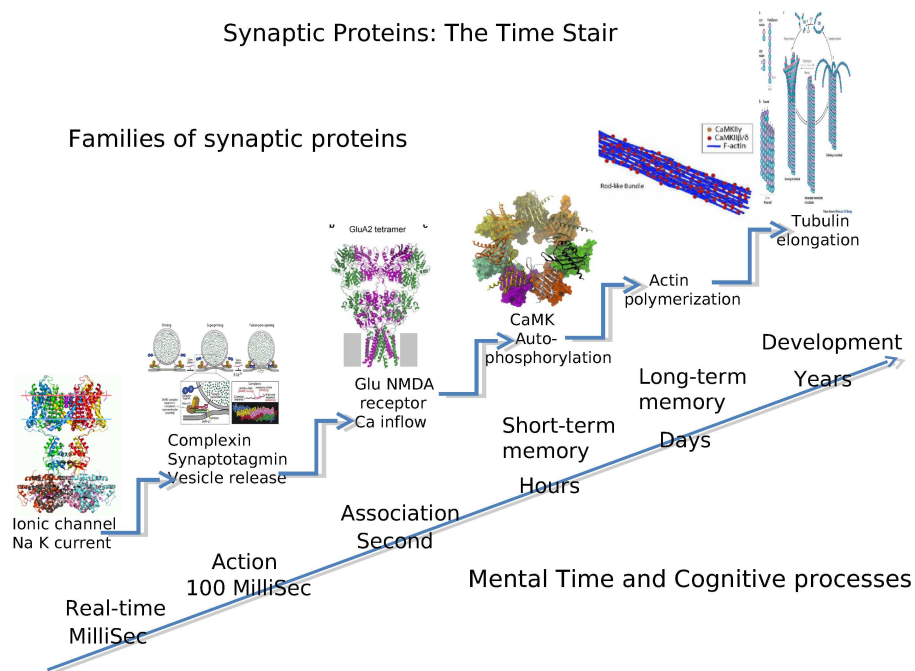


Fig. 1.3.: Stairway to memory formation: from information processing to synaptic remodeling. Experimental results show that memory and information processing at the synaptic and cellular level (e.g., LTP) can be seen as a cascade of molecular transformations with temporal effects lasting longer through the successive steps of the cascade.

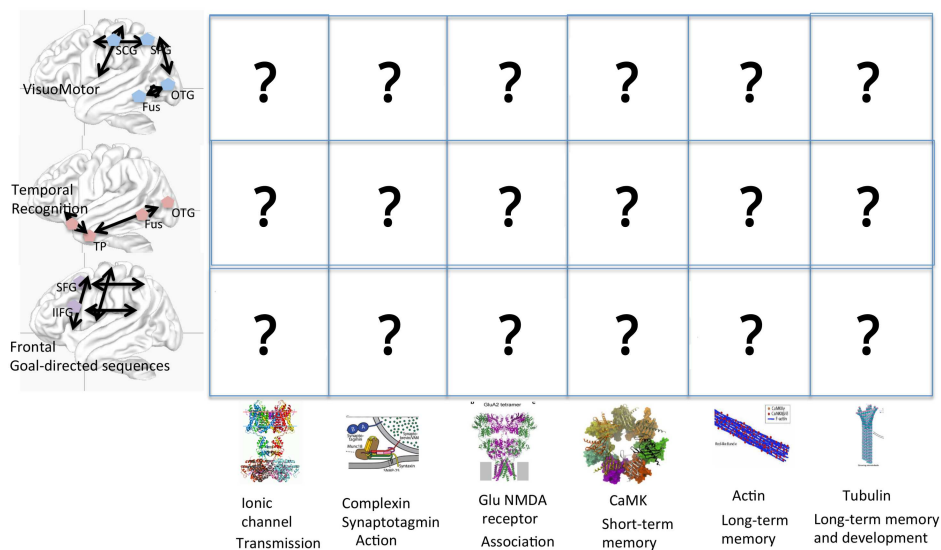


Fig. 1.4.: The central question of this dissertation: which is the relation between the cellular properties of genes differentially expressed across the cortex and the functional properties of cognitive networks, in term of memorization and information processing?

Chapter 2: The dual intertwined rings architecture of anatomo-functional and cognitive cortical networks. In this chapter we used a multi-scale clustering approach to interpret Resting State Networks (RSNs) from an anatomo-functional point of view and shed light on the question how does the brain integrate multiple sources of information

to support normal sensori-motor and cognitive functions? To do so we extracted using ICA (Independent Component Analysis) 32 highly intersubject reproducible RSNs—using independent databases provided by the 1000 Functional Connectomes Project—and we compared them with: (i) Brodmann Areas (BAs) in order to better capture their topographical/cytoarchitectonic relation across the cortex, (ii) with fiber bundles of white matter (as from Human Connectome Project) to complete the anatomical view on a 3-dimensional base; (iii) with Task Based Networks (TBNs – as from BrainMap) to better understand their cognitive-neuronal function and have ideas on the characteristics time constants. The results tell us that anatomo-functional networks are topologically organized across the cortex as two rings (from comparison to BAs and fiber bundles) and that these two rings correspond to two different ways of information processing (from comparison with TBNs). A first ring called VSA—Visual Somatosensory Auditory— carries out real time, high fidelity processing of sensory-motor and multimodal information. A second ring called PTF—Parieto, Temporo, Frontal—is responsible for multi-temporal information processing and while it encompasses the cognitive networks implementing language, memory and emotion it is characterized by a stronger autonomous component. The results of this work were published in *Mesmoudi et al. PlosOne, 2013*.

Chapter 3: Organization of the gradients of cognitive networks on the cortical surface.

In this chapter we investigate how cognitive networks are organized across cortical regions. Using the Neurosynth database, we first built a lexical map (graph) of 1000 cognitive categories (concerning sensory, motor, language, emotion, semantic and episodic memory, etc..), and build a topographical map (graph) of all the overlaps between the corresponding cognitive networks. At a global level we found that the main organization of these cognitive networks (in term of overlaps) reproduces the two intertwined rings architecture, obtained with a totally different method. Furthermore, this graph shows many overlaps between different cognitive networks revealing the continuity of underlying neural processes. At a finer level to better understand the organization of cognitive networks across the cortical surface we chose a set of 21 anatomo-functional regions, (1) forming like BAs a tessellation of the cortex covering the entire cortical surface without overlaps, (2) organized as Brodmann areas along the main cortical gradients, (3) directly comparable with the tessellation and the sampling proposed in the Allen atlas of genetic expression, (4) forming a more precise description of the dual ring architecture. (5) differentiated by a global sensory-motor or cognitive specialization. Cognitive networks are organized on the gradients formed within and between the 21 anatomo-functional cortical regions. Each anatomo-functional region represents a pole for specific groups of cognitive tasks. We propose a scheme to describe the organization of cognitive networks across the cortex. This scheme is determined by 1) poles of connections of cerebral regions with the other brain regions: 2) the functional gradients connecting these poles along parietal, frontal and temporal gradients. These results were partially published in *Cioli et al. OHBM 2013 – Seattle - USA, 2013*.

Part II: Cortical organization of gene expression in relation with anatomo-functional networks

Chapter 4: Cortical gene expression match the temporal properties of large-scale functional networks. In this chapter we studied the cortical organization of gene expression for about 1000 genes found as the most differentially expressed by the Allen Institute. To do so we used mRNA postmortem measures of local expression as provided by the Allen Institute. Samples are reported across about 400 cortical regions of two complete human brains of healthy adult donors. Using multidimensional statistical techniques –such as CA and DiCA – that the 1000 genes the most differentially expressed across the cortex are organized according to the two intertwined rings architecture. Among these 1000 genes we found genes playing fundamental roles in neuronal information processing (such as Ionic Channels) and neurotransmitter release (such as Synaptotagmins, Synaptobrevins and Complexins). We found that members of a same family of genes have their pole of expression in different rings. We adopted then a new heuristic consisting in analyzing entire families of genes with a known neuronal function to find eventual differences between the molecular properties of member preferentially expressed in different rings. In this chapter we analyzed family of genes with specific synaptic properties of neuronal information processing namely ionic channels and proteins implied in neurotransmitter release. The advantage of this method is to reveal the members of the families the most spatially differentiated. We showed that the expression of different isoforms is coherent with the information processing performed by each of the two rings. We found proteins supporting precise and high fidelity information processing, more expressed across VSA networks while proteins favoring spontaneous activity production more expressed in the PTF ensemble. The results presented in this chapter were published in *Cioli et al. PlosOne, 2014*.

Chapter 5: Gradients of synaptic genes properties across cognitive networks. In this chapter we studied the relation between cortical gradients of gene expression and anatomo-functional cortical networks a finer scale. The interest was to go closer to the spatial scale of cognitive networks to study if it exists a relation between cognitive functions and groups of genes. Since cognitive functions often overlap among them we chose to define a set of disjoint anatomo-functional regions based on the Allen Institute anatomical labels. We used this time the entire set of genes measured by the Allen Institute. We studied these data in relation to the anatomo-functional cortical regions by means of multivariate statistical technique called Discriminant Correspondence Analysis (DiCA). For completeness to better understand the overall picture we also studied gene expression in relation to the entire set of cerebral structures. To draw a link between genes' pole of expression and anatomo-functional regions this time at the functional level we focused the analysis of the results on three class of genes: genes involved in information processing, genes participating to memory formation (short term and long term) and genes taking part to networks genesis. The results obtained confirm that: 1) the patterns of expression of the human genome

across cerebral areas are mainly dictated by anatomical and cytoarchitectural constraints; 2) the differential gene expression across the cerebral cortex also follows anatomy and cytoarchitectonic more than functional specialization; 3) the cortical regions with the most distinctive patterns of gene expression are also the more phylogenetically ancient namely visual and motor areas on the VSA side and parahippocampal and temporal pole regions on the PTF side. Furthermore we found that regions implicated in the implementation of language result the most average regions in term of gene expression. Finally the systematic study of families of genes coding for proteins covering central roles in synaptic activity (information processing, neurotransmission, short and long term memory, networks genesis and homeostasis) showed strong congruence between the preferential expression of genes, the cellular properties of the proteins they code, and the cognitive function implemented in anatomo-functional regions. These results point out to the existence of differential synapses whose composition in terms of proteins varies based on the anatomo-functional specialization of the region they belong to. The results presented in this chapter are in course of submission (*Cioli et al.*).

Part III: Tools development

Chapter 6: LinkRbrain: web-based platform to analyze spatial correlation of gene expression and cognitive networks. In this chapter we propose a web-based platform meant to integrate the scientific knowledge about brain organization called LinkRbrain. In particular in this first version of the platform we gathered fMRI task-based results (as obtained in Chapter 2), standard anatomical labels (Talairach Atlas) and gene expression data (Allen Institute Transcriptome Atlas). These different sources of data are linked together thanks to a common spatial framework given by the MNI system of coordinates. The platform can provide information about similarities among groups of cognitive networks, groups of genes or a group of networks and a group of genes. This information is delivered to the user in four different ways: 3D and 2D visualization directly on the brain, as a graph or as a list stating distribution similarities. Finally the platform allows to compare new data provided by the user against the core data of the platform itself. The description of the platform has been published *Mesmoudi et al. Journal of Neuroscience Methods, 2015.*

Chapter 7: Conclusions and future work. In perspective we show how the type of analyses we perform could help to better understand, in Alzheimer disease, the relation between the gradient associated to gene expression and the pattern of propagation of the disease across cortical regions. Similarly the preferential expression of genes implicated in ASD could help to better understand the cognitive networks and cognitive functions which are impaired. Finally a more precise knowledge of the genes the most expressed in different cortical areas can help adapting the parameters necessary to model the dynamic processes (activation, plasticity) in the different areas of the cortex.

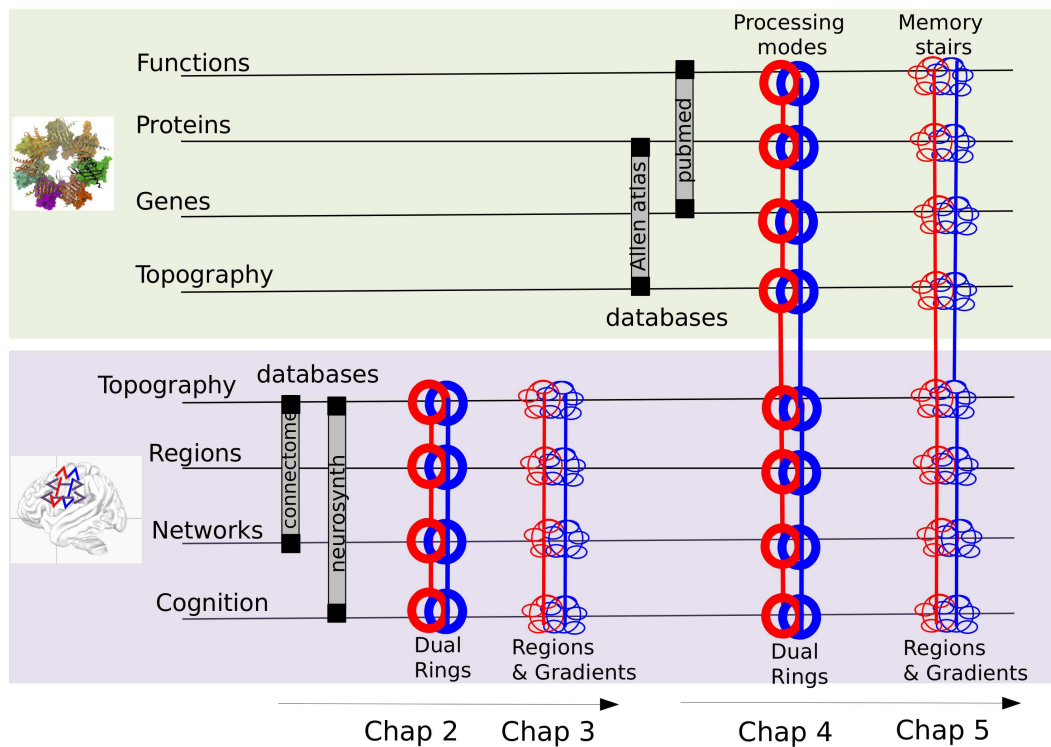


Fig. 1.5.: Plan of the dissertation: this scheme shows the progression of the work in the different chapters. First we analyzed the brain imaging databases at two level of resolution (two large scale regions and then 21 anatomo-functional regions) and then we analyzed the correlation between gene expression and anatomo-functional regions at these two levels of resolution.

1.5 This Dissertation: personal contributions

Chapter 2: My contribution was to systematically study the cortical organization of cognitive networks using the Neurosynth database as described in Chapter 3. This work allowed to compare cognitive networks obtained from two independent databases: the BrainMap database (obtained with top-down methods) and the Neurosynth database obtained in a bottom-up fashion.

Chapter 3: I was the principal contributor of the work presented in this chapter. The results presented were partially published in *Cioli et al., OHBM 2013* and they will be further structured for future publication.

Chapter 4: I was the main contributor of the work described in this chapter; the results are published in *Cioli et al., PlosOne 2014*.

Chapter 5: I was the main contributor of the work described in this chapter; the results are in course of submission as *Cioli et al.*

Chapter 6: My contribution for this chapter is represented by: 1) the cognitive networks (as derived in Chapter 3) used in the platform; 2) the discussion/proposition of methods to compare and display data.

1.6 Publications from this Dissertation

The results of this dissertation appeared in the following publications:

1.6.1 Journal articles

- Mesmoudi S., Rodic M., **Cioli C.**, Cointet J. P., Yarkoni T., Burnod Y., *LinkRbrain: Multi-scale data integrator of the brain*, Journal of Neuroscience Methods, Volume 241, 15 February 2015, Pages 44-52.
DOI: <http://dx.doi.org/10.1016/j.jneumeth.2014.12.008>.
- **Cioli C.**, Abdi H., Beaton D., Burnod Y., Mesmoudi S., *Differences in Human Cortical Gene Expression Match the Temporal Properties of Large-Scale Functional Networks*. PLoS ONE 9(12): e115913. 2014.)
DOI: <http://dx.doi.org/10.1371/journal.pone.0115913>.
- Mesmoudi S., Perlberg V., Rudrauf D., Messe A., Pinsard B., Hasboun D., **Cioli C.** et al., *Resting State Networks' Corticotopy: The Dual Intertwined Rings Architecture*. PLoS ONE 8(7): e67444. 2013.
DOI: <http://dx.doi.org/10.1371/journal.pone.0067444>

1.6.2 Peer-Reviewed Abstracts

- **Cioli C.**, Abdi H., Beaton D., Burnod Y., Mesmoudi S., *Integration of functional cerebral networks and genetic expression: the dual intertwined rings architecture of the cerebral cortex for real-time vs multi-temporal information processing*, Proceedings in the 21th Annual Meeting of the Organization for Human Brain Mapping, Honolulu, USA, 2015.
- **Cioli C.**, Cointet J. P., Mogoutov A., Reuillon R., Messé A., Benali H., Rudrauf D., Yarkoni T., Burnod Y., Mesmoudi S., *Systematic analysis of task-based fMRI database: comparison between lexical and topographic maps*, Proceedings in the 19th Annual Meeting of the Organization for Human Brain Mapping, Seattle, USA, 2013.

- Mesmoudi S., **Cioli C.**, Rodic M., Messé A., Mogoutov A., Cointet J. P., Benali H., Rudrauf D., Yarkoni T., Burnod Y., *Synthesizing the task-based fMRI literature with the CARMA Matrix*, Proceedings in the 19th Annual Meeting of the Organization for Human Brain Mapping, Seattle, USA, 2013.
- Mesmoudi S., Perlberg V., Rudrauf D., Messé A., Pinsard B., Hasboun D., **Cioli C.** et al., *The dual organization of functional integration in cortical networks*, Proceedings in the 19th Annual Meeting of the Organization for Human Brain Mapping, Seattle, USA, 2013.

1.6.3 Others

- **Cioli C.**, Abdi H., Beaton D., Burnod Y., Mesmoudi S., *Differences in human cortical gene expression match the temporal properties of large-scale functional networks*, Journées de Recherche en Imagerie et Technologies de la Santé (RITS), Dourdan, France, 2015.

Part I

Cortical organization of anatomo-functional
networks: rings and gradients

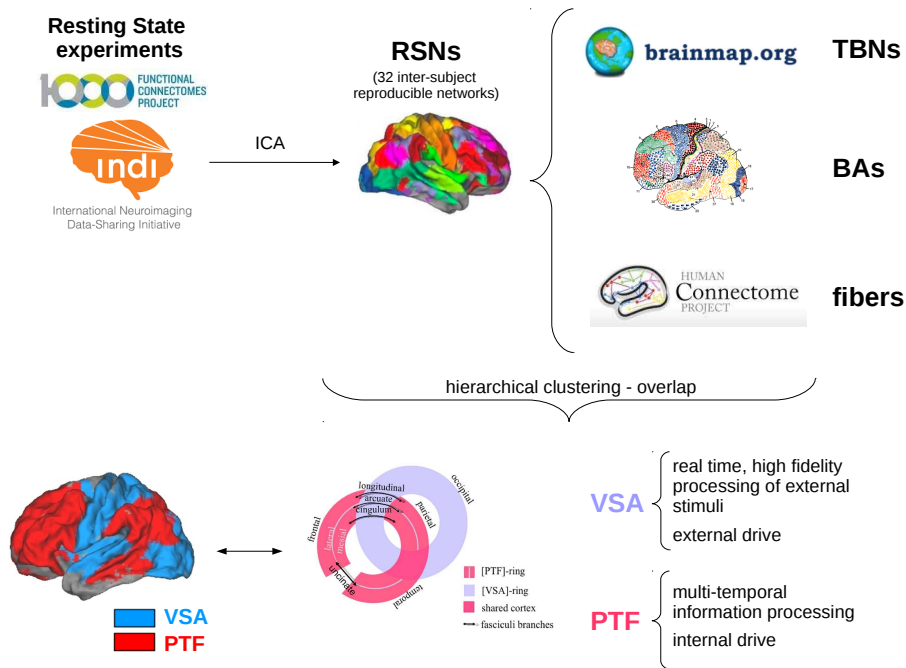
The dual intertwined rings architecture of anatomo-functional and cognitive cortical networks

In this chapter we propose an anatomo-functional model of the human cortex—called the two intertwined rings architecture—based on the integration of anatomical and functional data. The goal of the study was 1) to interpret resting state data (from 1000 Connectome project) using task based networks (BrainMap meta-analysis derived networks) in order to give them a functional and temporal (dynamical) dimension; 2) to study their topological properties by means of Brodmann Areas and fiber connections (data from the Human Connectome Project). The model proposed aims to shed light on how the brain integrates multiple sources of information to support normal sensori-motor and cognitive functions. Figures from 2.4 to 2.7 show the main results of this work published in *Mesmoudi et al., PLoSOne 2013*.

2.1 Graphical abstract

2.2 Abstract

How does the brain integrate multiple sources of information to support normal sensori-motor and cognitive functions? To investigate this question we present an overall brain architecture (called *the dual intertwined rings architecture*) that relates the functional specialization of cortical networks to their spatial distribution over the cerebral cortex (or *cor-ticotopy*). Recent results suggest that the resting state networks (RSNs) are organized into two large families: 1) a sensorimotor family that includes visual, somatic, and auditory areas and 2) a large association family that comprises parietal, temporal, and frontal regions and also includes the default mode network. We used two large databases of resting state fMRI data, from which we extracted 32 robust RSNs. We estimated: (1) the RSN functional roles by using a projection of the results on task based networks (TBNs) as referenced in large databases of fMRI activation studies; and (2) relationship of the RSNs with the Brodmann Areas. In both classifications, the 32 RSNs are organized into a remarkable architecture of two intertwined rings per hemisphere and so four rings linked by homotopic



connections. The first ring forms a continuous ensemble and includes visual, somatic, and auditory cortices, with interspersed bimodal cortices (auditory-visual, visual-somatic and auditory-somatic, abbreviated as VSA ring). The second ring integrates distant parietal, temporal and frontal regions (PTF ring) through a network of association fiber tracts which closes the ring anatomically and ensures a functional continuity within the ring. The PTF ring relates association cortices specialized in attention, language and working memory, to the networks involved in motivation and biological regulation and rhythms. This *dual intertwined architecture* suggests a dual integrative process: the VSA ring performs fast real-time multimodal integration of sensorimotor information whereas the PTF ring performs multi-temporal integration (i.e., relates past, present, and future representations at different temporal scales).

2.3 Introduction

To perform sensorimotor and cognitive functions, the brain needs to coordinate and integrate the activity of different regions that process multiple sources of information [269, 271, 260, 30, 86]. This integration is based on correlated activities that can be seen, for example, in the coherent brain networks revealed by resting-state magnetic functional imaging [21, 22].

Recent results suggest that these resting state networks (RSNs) are organized according to some general anatomo-functional principles [296, 239, 31, 19, 72, 247, 156]. First, RSNs appear to be similar to the Task-Based Networks (TBNs) that emerge from the analysis of

large ensembles of activation studies collected with different cognitive tasks found in very large functional imaging databases [247, 156]. These TBNs can be used as a reference set to infer the sensorimotor and cognitive functions of cortical networks revealed by RSNs. Second, several studies have shown that RSNs can be grouped into two major families, a *sensorimotor family* and an *association family*, that rely on two different modes of integration [296, 239, 31, 19, 72, 162]. In the *sensorimotor family*, the RSNs encompass a set of topographically adjacent Brodmann Areas (BAs), that includes the processing hierarchies of primary and secondary unimodal areas, and bimodal sensorimotor areas. In the *association family*, the RSNs encompass a topographically discontinuous set of BAs distributed over temporal, parietal, and frontal areas characterized by strong functional coupling between distant regions. These association networks correspond to the RSNs, previously described as the (1) default mode, (2) dorsal attentional, (3) ventral attentional, and (4) frontoparietal control networks (see, e.g., [16, 59, 63, 85, 110, 109, 272]). Similar results have been obtained using different RSNs extraction and clustering methods, either topographical (local vs. large scale functional connectivity [296]), hierarchical [72], or based on stepwise connectivity [239].

Here, we further investigate the relationship between the functional and anatomical organizations of the RSNs. Several previous studies have already described various RSNs clusters obtained from direct temporal correlations between RSNs, a pattern suggesting global organizational principles, but the topographies of the RSNs on the cortical surface depend on the methods and parameters used (e.g., the preselected number of components in an ICA analysis [296, 72]).

For this reason, we chose to characterize anatomo-functional clusters of RSNs from their overlap with two reference sets (i.e., Brodmann Areas (BAs) and TBNs) to confirm the two principles suggested by the RSN literature: (1) RSNs connect adjacent BAs in sensorimotor regions or connect distant areas in associative regions specialized in higher cognitive functions (e.g., language, attention, working memory) and (2) RSNs resemble TBNs and their specialization can be inferred from the closest TBNs. Furthermore, we expected to find correlations between RSNs groups overlapping TBNs functional groups and RSNs groups overlapping groups of BAs, which are either adjacent (local connectivity) or extend over different brain regions.

In an initial step, we used two different groups of subjects, and for each group we automatically determined the number of RSNs, on the basis of their representativeness. This method was robust because it produced two similar sets of 32 RSNs, with greater representativeness in two independent groups of subjects. Then, we inferred the RSNs functional roles from the overlap of the RSNs with 18 reference TBNs extracted from large databases of fMRI activations obtained during sensorimotor and cognitive tasks [156]. Similarly, we characterized the RSNs topography and topological features from their overlap with the Brodmann Areas, in order to determine the RSNs spanning adjacent cortical regions (e.g.,

BA17 and BA18), as well as those extending to distant regions (e.g., between the BA39 parietal area and the BA46 frontal area). We then extracted functional groups of RSNs from the $\text{RSN} \times \text{TBN}$ matrix and independently extracted anatomical groups from the $\text{RSN} \times \text{BA}$ matrix, using general classification methods (such as expectation maximization, see Method section). As an advantage of this method, these two well-defined reference sets (i.e., BAs and TBNs) are characterized independently of the RSNs extraction.

Remarkably, RSNs clusters having the same topography as sensorimotor and bimodal TBNs are found on adjacent BAs clusters. In turn, the RSNs, that have the same topography as the TBNs specialized in higher cognitive functions, emotions and biological regulations, are organized on networks linking distant parietal, frontal, temporal, and cingulate regions (PTF family). Our results showed that these two sets of cortical networks have a remarkable architecture that comprises two intertwined rings per hemisphere and so four rings linked by homotopic connections, an architecture that we called *the dual intertwined rings architecture*.

The first of these intertwined rings in each hemisphere is continuous over the cortex, organized in a concentric manner around the inferior parietal cortex, and relates visual, auditory, somatosensory and motor cortices with interspersed bimodal regions. This circular organization optimally integrates these sensorimotor modalities. We call this ring: the visual-sensorimotor-auditory (VSA) ring. The second ring in each hemisphere relates parietal, temporal, and frontal regions dedicated to higher cognitive functions (e.g., language, episodic memory, social interactions, self) with systems dedicated to emotions, basic biological regulations (e.g., hunger, thirst) and biological rhythms. We call this ring the Parieto Temporo Frontal (PTF) ring.

We called these two rings *intertwined* because the parietal region of the PTF ring (BAs 39 and 40) is at the center of the VSA ring and the PTF ring does not form a continuum over the cerebral cortex, but is closed through long-range association fiber tracts [234]. Taking into account the variety of sensorimotor and cognitive functions within each ring, the dual architecture of the rings suggests that each set of functions shares common basic neural principles. We hypothesize that the networks forming the two rings implement two different temporal integration processes: real-time integration of sensory and motor interactions with the world in the VSA ring and what we refer to as *multi-temporal integration* in the PTF ring, (i.e., the construction of interacting past, present and future representations, at different temporal scales).

2.4 Results

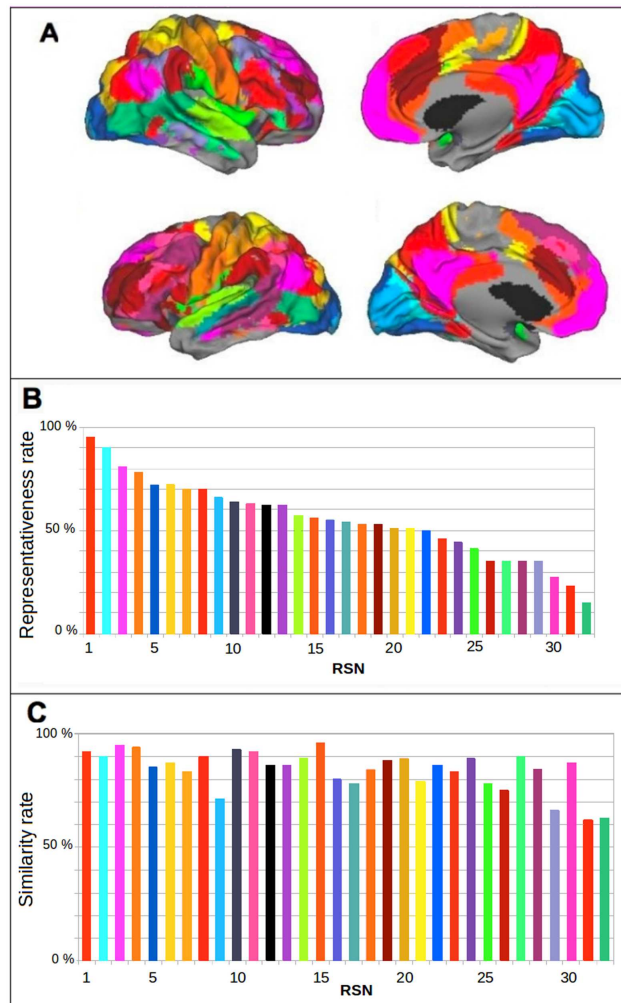


Fig. 2.1.: Mapping and representativeness of RSNs and similarities in two different populations. (A) Mapping of the 32 Resting State Networks (RSNs), on the right hemisphere (above) and the left hemisphere (below), on the lateral face (left) and the medial face (right). (B) Representativeness of the 32 RSNs. The color of each bar corresponds to the color of the RSNs network in Figure 1A and the RSNs are labeled with their representativeness rank. (C) Spatial similarity rate between equivalent RSNs in the Cambridge and Beijing populations.

2.4.1 Extraction of the most representative RSNs in the group: robustness

We used two independent databases of resting state activity: the first was from a population of subjects from Cambridge ($N = 197$) and the second was from a population of subjects from Beijing ($N = 180$). We started with the Cambridge database. We first applied spatially independent components analysis (sICA) to the voxel time series across each subject's brain. This provided one voxel factor scores matrix per subject. The matrices of all subjects were then concatenated into a group factor score matrix that was used in a hierar-

chical cluster analysis. From this analysis, we obtained 264 classes of voxels from which we selected 32 representative classes as the 32 most representative RSNs. These RSNs were observed in at least 10% of the subjects (see Figure 2.1A and Figure 2.1B). The first 20 classes were observed in at least 50% of the subjects (Figure 2.1B). We labeled each RSN with its representativeness rank in the population (Figure 2.1B). We then used the same general method with the independent database of subjects from Beijing. This analysis also yielded 32 RSNs. The RSNs found in the Cambridge database were very similar to those found in the Beijing database (Figure 2.1C). The similarity rate was as high as 60%, showing that the 32 identified RSNs were highly representative and robust within and between independent populations.

2.4.2 RSNs Specialization: overlap between RSNs and TBNs

Previous results have shown that RSNs are similar to TBNs extracted from a large database of activation studies across a variety of behavioral tasks [247, 156]. A systematic statistical analysis of thousands of datasets of brain activation scans obtained during behavioral tasks (sensory, motor, cognitive, and emotional) has previously revealed the existence of clusters of activation corresponding to TBNs (available online at www.brainmap.org). We computed the overlaps between our 32 RSNs and the 18 reference TBNs (Figure 2.2B).

The RSNs are represented along the vertical axis of the matrix and sorted according to their maximum overlap with the TBNs. The $\text{RSN} \times \text{TBN}$ matrix revealed a dual organization. The upper part of this matrix is nearly diagonal and reveals RSNs related to TBNs specialized in sensorimotor and cognitive functions (see Table in Figure 2.2C). The lower part of the matrix reveals RSNs that correspond mainly to the Default Mode Network (*DMN*, TBN# 13, involved in social interactions) but also to several TBNs such as TBN number 15 (working memory and attention), 18 (language), 4 (emotion and interoception), and 2 (olfaction, taste, and reward). Since the TBNs database did not describe the specialization of subcortical structures, we focused on the cerebral cortex: RSN#10 and 12 corresponding to sub-cortical networks were eliminated from subsequent analyses. In order to further categorize the major RSNs families according to their overlap with TBNs, we used a clustering method based on mixture distributions (see Methods section). Figure 2.2B shows the $\text{RSN} \times \text{TBN}$ matrix, in which RSNs along the vertical axis are sorted on the basis of the afore mentioned clustering method. The 18 TBNs on the horizontal axis of the $\text{TBN} \times \text{RSN}$ matrix were based on a meta-analysis of cognitive brain-imaging articles [156] (the TBNs were labeled *ICN* in this reference). For further details concerning the correspondence between RSNs and TBNs, see Table in Figure 2.2C.

Six RSNs clusters based on TBNs overlap were identified (see Figure 2.2B). Cluster $C_{\text{TBN}\#1}$ matches visual areas; cluster $C_{\text{TBN}\#2}$ and $C_{\text{TBN}\#3}$ somatomotor regions; clusters $C_{\text{TBN}\#4}$ and $C_{\text{TBN}\#5}$ the auditory regions, and cluster $C_{\text{TBN}\#6}$ mainly large association networks

(TBN# 18, 15, 13, 4, 1, 2 and 7). corresponds to four major functional entities: (1) for language (TBN# 18) in the left hemisphere; (2) for attention and working memory in the right hemisphere (TBN# 15); (3) for social interaction, self, memory recall and anticipation (TBN# 13) in a bilateral network corresponding to DMN; (4) for basic biological regulation, olfaction, taste and emotion (TBN# 2, 4).

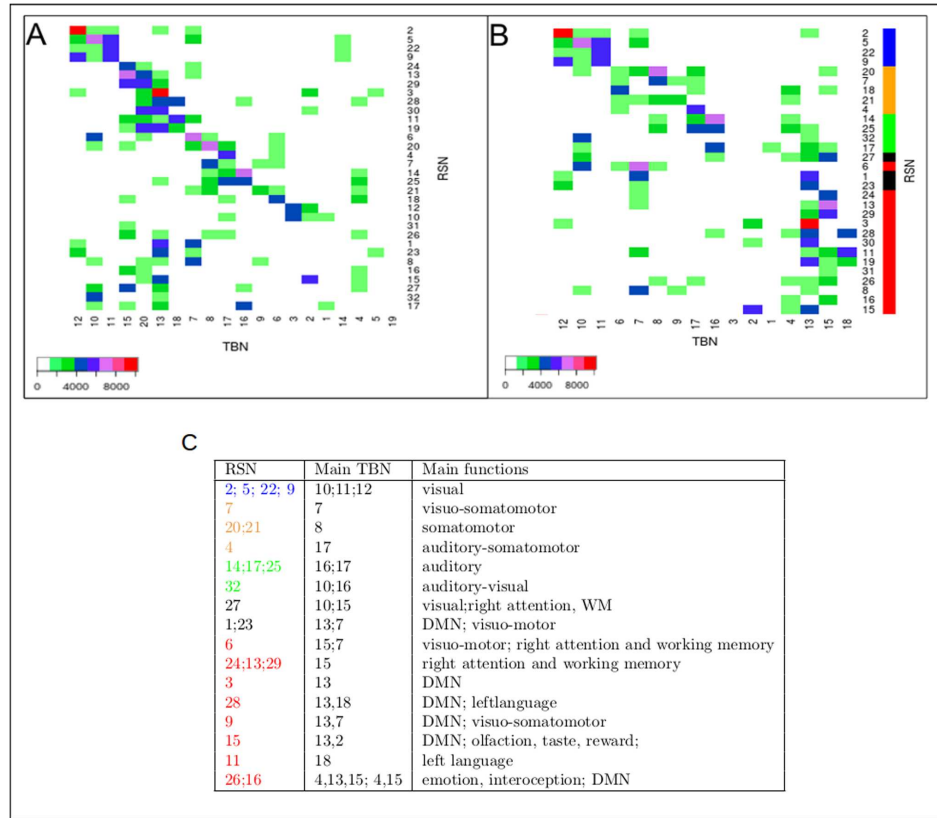


Fig. 2.2.: RSN \times TBN overlap matrix. (A) RSN \times TBN matrix showing overlaps (topographical similarity) between the 32 Resting State Networks (RSN, vertical axis) and the 18 reference Task Based Networks (TBNs, horizontal axis). The RSN are labeled as in Figure 2.1 and the TBNs are labeled as in [156]. The RSNs and TBNs are ranked according to the maximum of their overlaps. (B) RSN \times TBN matrix reorganized by applying an Expectation Maximization (EM) algorithm to display the RSN clusters having similar overlaps with the TBNs (see text for details). The RSN \times TBN clusters are: $C_{TBN\#1}(RSN\#2, 5, 22, 9)$, $C_{TBN\#2}(20, 7, 18, 21)$, $C_{TBN\#3}(4)$, $C_{TBN\#4}(14, 25)$, $C_{TBN\#5}(32, 17, 27)$ and $C_{TBN\#6}(6, 1, 23, 24, 13, 29, 3, 28, 30, 11, 19, 31, 26, 8, 16, 15)$. The color bars (at the right of Figure 2.2) indicate: visual (blue), somatomotor (orange), auditory (green), left, right and bilateral RSN (red), and RSNs of intermediate region (black). Scale bars represents the number of shared voxels. (C) This table shows the correspondence between RSNs and TBNs obtained by the maximal overlap between them, with the main sensory-motor and cognitive functions of the TBNs. The masks, labels and functions of TBNs are taken from [156]. The labels of RSNs correspond to their representativeness in the group of subjects, as in Figure 2.1. The colors used for RSNs labels, are the same as color bars in Figure 2.2B.

These clustering results were confirmed by another method [196] (see Method section), with a similar significance level (i.e., $p = .00002$).

2.4.3 RSNs topography: overlap between RSNs and the Brodmann Areas.

We computed the overlap matrix between the 30 RSNs and the Brodmann Areas (BAs) and, in order to limit the size of the matrix, we then regrouped small adjacent BAs, thereby obtaining 28 extended BAs (see Figure 2.3A).

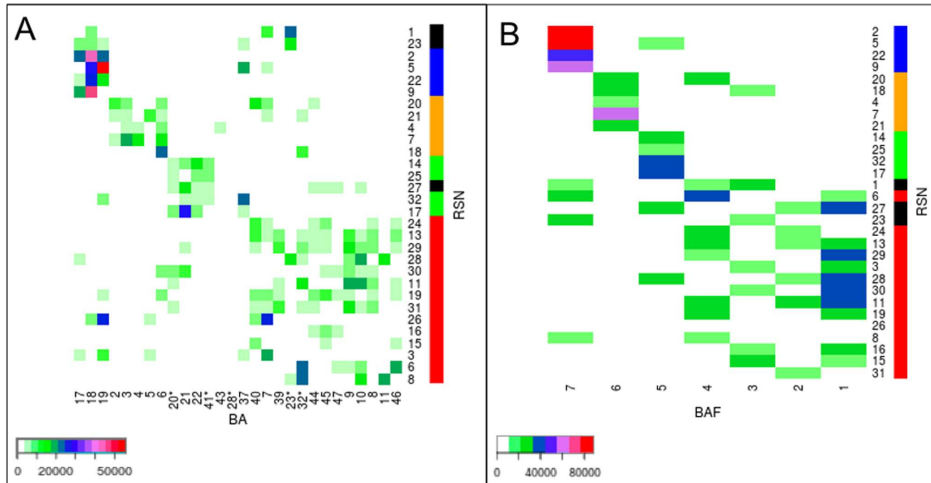


Fig. 2.3.: RSN \times BA overlap matrix. (A) Matrix of $30RSN \times 28BA$ (Brodmann Area). 20^* : $BA20 + BA38$, 41^* : $BA41 + 42$, 28^* : $BA28 + BA34 + BA35 + BA36$, 32^* : $BA32 + BA24 + BA25$, 23^* : $BA23 + BA29 + BA30 + BA31$, (B) Matrix of $30RSN \times 7BAF$ (Brodmann Area Family), see the details concerning the BAFs and RSNs in the text. Both matrices are reorganized by applying the same Expectation Maximization (EM) algorithm as in Figure 2.2C, to reveal the RSNs clusters with a similar topography on the cortical surface. The RSNs are ranked on the vertical axis according to this clustering. BA \times RSN matrix clusters: $C_{BA\#1}(RSN\#1, 23, 2, 5, 22, 9)$, $C_{BA\#2}(20, 21)$, $C_{BA\#3}(4, 7, 18)$, $C_{BA\#4}(14, 25, 27, 32, 17)$, $C_{BA\#5}(24, 13, 29, 28, 30, 11, 19, 31, 26, 16)$, $C_{BA\#6}(3, 15)$ and $C_{BA\#7}(6, 8)$. BAF \times RSN matrix clusters: $C_{BAF\#1}(RSN\#2, 22, 9, 5)$, $C_{BAF\#2}(4, 7, 21)$, $C_{BAF\#3}(18)$, $C_{BAF\#4}(20)$, $C_{BAF\#5}(25, 14, 17, 32)$, $C_{BAF\#6}(27, 28, 11, 29, 13, 19, 6, 26, 18, 20, 8$ and $24)$, $C_{BAF\#7}(3, 15, 30, 16)$, $C_{BAF\#8}(31)$, $C_{BAF\#9}(23)$ and $C_{BAF\#10}(1)$. Color bars (to the right of Figure 2.3A and Figure 2.3B) indicate: visual (red), somatomotor (orange), auditory (green), left, right and bilateral RSNs (red) and as in Table in Figure 2.2C, RSNs of intermediate region are in (black). Scale bars represent the number of shared voxels.

We applied the same clustering algorithm as described above, to the RSN \times BA matrix. Figure 2.3A displays the RSN \times BA matrix, where RSNs along the vertical axis and BAs along the horizontal axis are sorted according to the results from the cluster analysis. Eight clusters were obtained (see the legend of Figure 2.3A). There were three RSNs clusters that remained localized and appeared on the upper part of the matrix diagonal. These three clusters corresponded to visual (BA# 17, 18, 19), somatomotor (BA# 2, 3, 4, 5, 6) and auditory

(BA# 42, 43, 22, 21) areas. The lower part of the matrix including $C_{BA\#5}$, $C_{BA\#6}$ and $C_{BA\#7}$ corresponded to associative-parietal (40,39), temporal areas (20,21) and all frontal and cingulate areas.

The results obtained for the RSNs and BAs were very close to those obtained for the RSNs and TBNs (see Table in Figure 2.4A). The $C_{BA\#2}$ and $C_{BA\#3}$ correspond to the $C_{TBN\#2}$ and $C_{TBN\#3}$ somatic clusters and the $C_{TBN\#4}$ corresponds to the $C_{TBN\#4}$ and $C_{TBN\#5}$ auditory clusters. Finally, the $C_{TBN\#5}$, $C_{TBN\#6}$ and $C_{TBN\#7}$ correspond to $C_{TBN\#6}$ (large association networks). For a cluster $C_{TBN\#1}$, in addition to RSN# 2, 22, 5 and 9 included in the visual $C_{TBN\#1}$ cluster, two other RSN# 23 and 1, were associated with this cluster. RSN# 23 and 1 were balanced between the two clusters: $C_{TBN\#1}$ and $C_{TBN\#6}$.

In order to confirm the topographical organization of RSNs given by the RSN6BA matrix, we regrouped the BAs into large continuous regions. We call these regions the Brodmann Area Families (BAFs), based on their anatomo-functional interpretation: occipital visual regions BAF7 (BA# 17, 18, 19), central somatomotor BAF6 (BA# 2 until 6), temporal auditory BAF5 (BA# 41, 42, 21, 22, 37), cingular BAF4 (BA# 23 posterior and 32 anterior), inferior frontal BAF3 (BA# 44, 45, 47), superior frontal BAF2 (respectively BA# 8, 9 and 46), and anterior frontal BAF1 (BA# 10 and 11). These results are shown in the BAF6RSN overlap matrix in Figure 2.3B. Ten clusters were obtained by applying the Mixture Distribution Algorithm (see Figure 2.3B). The results obtained for the RSNs and BAFs were very close to those obtained for the clustering based on the BAs overlap and the TBNs overlap. $C_{TBN\#1}$ corresponds to visual clusters ($C_{TBN\#1}$), $C_{TBN\#2}$, $C_{TBN\#3}$ and $C_{TBN\#4}$ correspond to somatic clusters $C_{TBN\#2}$ and $C_{TBN\#3}$ and $C_{TBN\#5}$ corresponds to the auditory clusters $C_{TBN\#4}$ and $C_{TBN\#5}$. Finally, all the RSNs of clusters $C_{TBN\#6}$, $C_{TBN\#7}$, $C_{TBN\#8}$, $C_{TBN\#9}$ and $C_{TBN\#10}$ correspond to $C_{TBN\#6}$, with the exception of RSN# 27, which was balanced between the two clusters, $C_{TBN\#5}$ and $C_{TBN\#6}$.

The results obtained using a second clustering method [196] show the same distribution as the first clustering method. The similarity significance for the results obtained from RSN6BA is $p = 2.35 \times 10^{-10}$ and from RSN \times BAF is $p = 1.06 \times 10^{-8}$.

2.4.4 Corticotopy of the RSNs clusters: the dual intertwined rings architecture

The various approaches used to analyze the relationships between the RSNs, TBNs and BAs (see Table in Figure 2.4A) thus all converge to a pattern which suggests that the RSNs can be grouped into two families characterized by their topography and their functions.

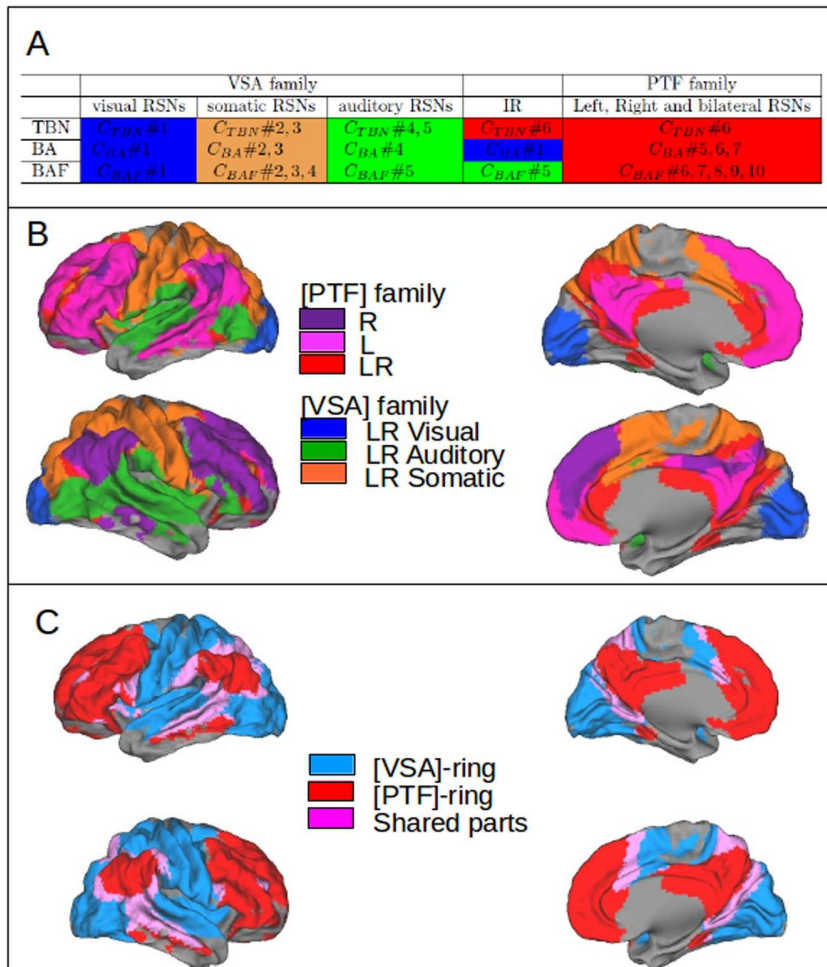


Fig. 2.4.: Mapping of VSA and PTF families. (A) Comparison of clustering results on the 3 matrices $TBN \times RSN$, $BA \times RSN$ and $BAF \times RSN$. All clustering results are obtained from the same method: Mixture Distribution Algorithm. $C_{i\#j}$ is a cluster of RSNs obtained from matrix $(RSN \times i)$, $i \in \{TBN, BA, BAF\}$, $j = 1 \dots p$ where p is the number of clusters. IR: Intermediate Regions are represented by RSN# 1, 23, 27 (B) Mapping of the 2 families which group the RSNs, according to the clustering based on functional specialization (as shown in Figure 2.2) and the clustering based on cortical topography (shown in Figure 2.3), giving both the same results: VSA family formed by 3 clusters, LR (Left and Right = bilateral) Visual RSNs, in blue; LR Auditory RSNs in green and LR somatomotor RSNs in orange, with similar colors as in Table in Figure 2.2C. PTF family: R (right lateralized) RSNs in dark purple, L (left lateralized) RSNs in light purple and LR (bilateral) RSNs in red, distributed over the parietal, frontal, temporal and cingular regions. (C) The two intertwined rings per hemisphere: the visual, somatomotor and auditory RSNs clusters shown in Figure 2.4 and grouped in the VSA family form the VSA ring, in blue, and the RSNs of the PTF family, distributed over the parietal, temporal, frontal and cingular regions form the PTF ring, in red. The overlap between the two families is shown in purple. The two rings are intertwined as shown in Figure 2.7.

Twenty-seven of the 30 RSNs were specialized within one of the two families. Three RSNs (27, 1, and 23) had more balanced overlaps with the two families.

The first family comprises three contiguous clusters which share similar anatomo-functional principles (see Tables in Figure 2.2C and Figure 2.4A): The visual cluster overlaps with TBNs specialized for vision: not only with low-level vision in primary areas, but also to higher level vision in secondary areas. The somatomotor not only cluster overlaps with TBNs specialized for tactile and motor functions, but also with bimodal functions, visuo-motor and auditory-motor. The auditory cluster overlaps not only with primary and secondary regions, but also with regions involved in speech processing and bimodal auditory-visual integration. We call this set of clusters the visual-somatomotor-auditory (VSA) family of RSNs. We then mapped this VSA family, first with 3 colors corresponding to the 3 clusters (Figure 2.4B) and then with a unique color to show the topography of the whole VSA family (Figure 2.5A).

The second family comprises RSNs that are distributed over several, not fully contiguous, association cortices in the parietal, temporal, and frontal regions. Because this family encompasses a large set of cognitive functions distributed over the parietal, frontal, and temporal regions (see Table Figure 2.2C), we call it the PTF family. Table in Figure 2.2C shows that RSNs in this family overlap (1) with bilateral TBNs specialized for self-referential and social interactions (DMN); (2) with bilateral TBNs specialized for biological regulations, olfaction, taste, interoception and reward;(3) with left-lateralized TBNs specialized for language and (4) with right-lateralized TBNs specialized for working memory and attention. We then mapped the PTF family first by showing the 3 clusters, bilateral and lateralized, in 3 different colors (see Figure 2.4B) and then with a unique color to show the topography of the whole PTF family, as shown in Figure 2.5A2.

When the VSA and PTF families are mapped together onto the cortical surface (Figure 2.4B and Figure 2.4C) or displayed independently (in Figure 2.5A), the mapping results reveal a remarkable 3-D structure forming two intertwined rings per hemisphere and so four rings linked by homotopic connections. The ring formed by the VSA family in each hemisphere is continuous, as shown in Figure 2.5A1. Conversely, the ring formed by the PTF family in each hemisphere is discontinuous over the cortical mantle (see Figure 2.5A2), but is closed by the major cortical fiber tracts, as shown in Figure 2.6A. The topological model of the two rings within each hemisphere is shown in Figure 2.7. We call these two rings the VSA and the PTF rings. The 3D rings extend both on the lateral and on the medial face of each hemisphere. The two families in both hemispheres are thus forming pairs of VSA rings and pairs of PTF rings. The homologous rings within each pair are symmetrical as shown in Figure 2.5B. All the RSNs of the VSA family are bilateral and extend in homologous regions of the left and right VSA rings, with a very accurate symmetrical organization between the two hemispheres. The RSNs of PTF family are either bilateral and extend on the left and right PTF rings or lateralized and restricted to one ring, corresponding

to the right-lateralized TBNs for attention and working memory and the left-lateralized TBNs for language.

The VSA ring (Figure 2.5A1) forms a continuous cortical ring, with several sectors organized around sensory and motor maps (visual, auditory, and somatomotor), with unimodal hierarchical cortices around these primary maps and interspersed bimodal associative regions (visuomotor, auditory-visual, and auditory-motor): VS for bimodal visual and somatomotor processing, SA for bimodal auditory and somatomotor processing, related to tongue control and important for speech and VA for bimodal visuo-auditory integration. These different regions are radially distributed and bimodal sectors are interspersed between unimodal sectors. Thus, the VSA ring forms a continuous ring with six alternating sectors, monomodal and bimodal sectors. The VSA ring circles a central inferior parietal zone, which does not belong to the VSA ring but to the PTF ring (see below) and corresponds to BA# 39 and 40. This central position suggests that this sector of the PTF ring might receive, transform, and integrate all combinations of monomodal and bimodal information computed by the VSA ring. The VSA ring extends on the medial side, with two medial sectors in direct continuity with the lateral sectors. The shape of the ring is related to the topographical organization of four major cortical sulci: the calcarine sulcus (visual), the intraparietal sulcus (visuomotor), the central sulcus (somatomotor), and the superior temporal sulcus (auditory and auditory-visual).

The PTF ring (Figure 2.5A2) comprises the parietal, temporal, and frontal regions, including cingular regions, that, together, form a second ring. This ring is not entirely continuous over the cortical mantle, but features ring closure, as soon as one considers the fiber tract systems that massively and directly connects cortical components of the family which are not contiguous over the cortical mantle (see next paragraph). Figure 2.5A2 shows three sectors of this ring on the lateral aspect of each hemisphere and three sectors on the medial aspect. (1) The lateral parietal sector (IP) consists of supramodal parietal areas BA# 39 and 40; (2) the lateral temporal sector (IT) consists of supramodal temporal areas BA# 20 and 21; (3) the lateral frontal sector (IF) consists of supramodal frontal regions, in the IFG (BA# 44, 45, 47) and the SFG (BA# 8, 9, 46), as well as in frontopolar regions (BA#10); (4) The medial frontal sector, (mF), consists of the anterior cingulate cortex, the anterior medial prefrontal cortex and the orbitofrontal cortex (BA# 11); (5) the medial parietal sector (mP) consists of the precuneus and posterior cingulate cortex; and (6) the ring can be extrapolated to the medial temporal sector (mT) containing the medio-temporal and parahippocampal regions. The lateral and medial aspects of the PTF ring can be superimposed.

We describe the VSA and PTF rings within each hemisphere as being *intertwined* (see Figure 2.5B), because associative parietal regions of the PTF ring are at the center of the VSA ring and are connected with other regions of the PTF ring via long-range association tracts passing under the VSA ring, as shown in Figure 2.6. In the following, using diffusion

weighted imaging (DWI) results, we verified that the topography of the well-known long-range fiber tracts connect discontinuous regions of the PTF ring and close this ring.

2.4.5 Anatomical connections within and between the dual rings.

We compared the topography of the two RSNs families with the underlying cortical fiber tract systems (see Method section). To do so, we computed the 3D masks corresponding to each RSN family, as shown in Figure 2.6, and identified the long distance fiber tracts specifically associated with each family (see Figure 2.6A, for the PTF ring and Figure 2.6B, for the VSA ring). The PTF ring presents discontinuities at the level of the cortical mantle (Figure 2.6A).

Actually the PTF ring is topographically cut by the VSA ring, isolates, like an island, the inferoparietal sector of the PTF ring from the rest of the ring in the middle of the VSA ring. However, the tractography results revealed that long distance association tracts constitute the structural backbone of the topological continuity of the PTF ring (Figure 2.6A). The lateral parietal and frontal sectors are connected by parieto-frontal connections, formed by the inferior and superior longitudinal fasciculi. The lateral temporal, lateral parietal and lateral frontal sectors are connected by the arcuate fasciculus. The medial frontal and parietal sectors (including the anterior and posterior cingulate regions) are connected by the cingulum. Finally, the anterior lateral frontal and temporal regions are connected via the uncinatus fasciculus. It can therefore be considered that the PTF ring is *intertwined* with the VSA ring and is complete, thanks to the long distance cortical connections passing below the VSA ring. The backbone of the connections underlying the VSA ring is quite different in its organization from that of the long distance cortical connections underlying the PTF ring. Long distance VSA ring connections are mainly cortico-subcortical, rather than corticocortical and connect the cortex to the sub-cortical structure via major projection fiber tract systems, in accordance with the sensorimotor specialization of the VSA ring. No obvious major structural differences appear between the short-range connections intrinsic to the two rings. The 3D mapping of the relationships between the two RSNs families and the infrastructure of long range connectivity reveals the manner in which these two rings are intertwined, thanks to these connections (Figure 2.6; schematic representation in Figure 2.7).

2.5 Discussion

We investigated the large-scale topographical organization of cortical RSNs networks, and we analyzed their correlations with TBNs, BAs, and fiber tracts between areas. We extracted the 32 most representative RSNs in a large group of subjects and verified that these RSNs were the same in another independent group. Then we investigated the RSNs topographical organization by measuring their overlap with BAs and inferred their functional specialization by measuring their overlap with TBNs. We used this approach because the TBNs extracted from large databases and the BAs are well-defined, independently of the RSNs. The overlap between RSNs and TBNs (provided by the $RSN \times TBN$ matrix) revealed clusters that correspond to the major specializations of visual, auditory, somatomotor, and also bimodal functions. It also showed a large cluster that encompasses all higher cognitive functions, as well as emotions and basic needs. The overlap between the RSNs and BAs ($RSN \times BA$ matrix) revealed RSN clusters, which link (1) adjacent cortical regions (e.g. BA#17 with BA#18) and (2) other clusters that link distant regions (e.g., parietal BA#39 with frontal BA#46). Furthermore, the results showed that both properties are closely related. RSNs clusters having the same topography as the sensorimotor and bimodal regions (VSA family: visual-somatomotor-auditory), link adjacent areas. RSNs clusters having

the same topography as the TBNs corresponding to higher cognitive functions, emotions and basic needs, also link distant cortical regions: parietal, frontal, temporal, and cingulate (PTF family: parieto-temporo-frontal). These highly significant results are also robust because similar results are obtained with different clustering methods (see [196, 161]).

The topography of these two families of RSNs over the cortical mantle is quite remarkable and can be described by two intertwined rings per hemisphere and so four rings linked by homotopic connections. The VSA family forms a continuous ring, in which the three bimodal functions are interspersed between the three monomodal regions. The PTF family encompasses parietal, temporal, frontal, and cingulate regions and it forms a second ring, which is discontinuous over the cortical mantle but closed through systems of long-range fiber tracts, both laterally and on the mesial wall. We described the architecture of the PTF and VSA rings as *intertwined* because a subset of associative parietal regions of the PTF ring is at the center of the VSA ring and these regions are connected with other regions of the PTF ring via long-range association tracts passing under the VSA ring. Using tractography from DWI, we verified that the topography of the corresponding well-known long-range fiber tracts connected these discontinuous regions of the PTF ring.

2.5.1 Method of RSNs extraction and RSNs coverage

We used the sICA method [207] on a large group of subjects (198 healthy subjects) to extract RSNs. Because it computes the individual sICA decomposition, prior to clustering of similar effects across subjects, NEDICA (see Methods section) can account for possible high inter-subject variability. Moreover, with the criteria we proposed, in order to automatically define the classes from the similarity tree, we could control the relevance of these classes with respect to individual sICA decompositions. When considering highly representative classes as was done in the present study the number and spatial distributions of the resulting functional networks are similar to those extracted with other group ICA techniques. We selected a large number of components ($K = 100$) in order to identify even small networks having a high functional specificity. We found that 32 RSNs were representative and robust across subjects. We compared the RSNs from two different groups (Cambridge and Beijing) and confirmed that the RSNs with the highest representativeness had similar cortical topographies in both groups. Several parts of the cortex are not covered by the 32 RSNs: the temporal pole, some infero-temporal regions, and a part of the mesial paracentral lobule. The RSNs overlapping with these regions had a low representativeness and greater variability in the groups and did not appear among the first 32 RSNs that were retained for further analysis. Nevertheless the dual intertwined rings architecture can be easily extrapolated to these missing regions. The paracentral region encompasses the somatomotor TBNs in the VSA ring. The infero-temporal regions encompass the TBNs, in the PTF ring, associated with higher cognitive functions, language and, memory. This

conjecture will have to be validated by future studies, using methods that can extend the coverage of extracted RSNs.

Likewise, it would be of interest to consider the relationships between the dual ring architecture and subcortical systems. Since subcortical-cortical pathways have a topographical organization (e.g., thalamic projections), we can predict that the VSA and PTF rings should project towards separate regions of the thalamus, basal ganglia, and cerebellum. We have limited our analysis to the cerebral cortex for two reasons. First, subcortical TBNs were not available in the TBNs database. Second, the RSNs extracted from subcortical structures were not robustly linked to regions of the cerebral cortex and were not included in the analysis. These two limitations might be overcome by using new tools for the extraction of cortico-subcortical RSNs and by extending the TBNs database to subcortical structures.

2.5.2 Comparison of the dual intertwined architecture with other RSNs results

Although the remarkable organization of intertwined rings, has not been previously discussed as such, most published results dealing with the organization of RSNs present patterns that are compatible with this architecture. RSNs reflect intrinsic functional correlations between the activities of different regions of the brain and a variety of methods have been used for RSNs identification [21, 239, 247, 59, 63, 85, 110, 15, 71, 17, 273]. Different methods produced similar RSNs, with differences that partly depend on the pre-defined number of RSNs covering the cortical mantle, since the RSNs can be extracted at different scales.

Similarly to the findings of several other studies, the RSNs of the VSA family accurately matched the sensorimotor cortices, with different RSNs corresponding either to the central visual areas or to the peripheral areas and with the RSNs in the motor areas associated with either the hand or the mouth [296].

Other RSNs of the VSA family covered intermediate, adjacent bimodal regions forming bridges between primary unimodal areas [156]: between visual and motor areas (e.g., for visually-guided actions: grasping, reaching), between somatomotor and auditory areas (e.g., for phonation and speech) and between visual and auditory areas (e.g., for naming pictures).

The VSA ring can be described with three sensorimotor regions corresponding to primary and higher order unimodal areas and three interspersed bimodal regions. The circular structure of the VSA ring can be compared to the results of the method called *stepwise functional connectivity* [238]: when starting from primary sensory areas, RSNs correlations first arise in adjacent bimodal areas and extend to the VSA ring, and only after to the PTF

ring. The global recruitment of the PTF ring is consistent with studies that have revealed a high degree of intrinsic functional connectivity between high order associative regions of the parietal, frontal, temporal, and cingular cortices [30].

RSNs in the PTF family correspond to RSNs classically reported by other studies, such as the highly reproducible DMN network, together with similar RSNs that correspond to lateral fronto-parietal connections in the PTF ring, the fronto-parietal control network, the dorsal attentional network and the ventral attentional network [86, 31, 16, 59, 63, 85, 110, 109, 272, 71]. Our classification into two families, based on overlaps with BAs and TBNs, confirmed previous works searching for hierarchy of RSN cluster obtained when extracting clusters using only the resting state data [296, 72, 162, 238, 166].

Several methods (e.g., hierarchical cluster analysis [72], Gaussian Bayesian network [166] and fuzzy-c-means clustering algorithms [162]) gave results consistent with a two cluster organization: the first cluster comprising visual areas and primary somatosensory and auditory areas, and the second one comprising the default mode, fronto-parietal, dorsal attentional, and ventral attentional networks. In our study we show that two similar families can be obtained also by a different method measuring overlaps between RSNs, TBNs, and BAs. However, here we structure the topography of these two families of RSNs into intertwined rings and characterize their functional specialization in relation with two sets of TBNs.

Long distance cortico-cortical connections are essential to support a dual intertwined ring architecture. When the ring topography is visually compared with the main cortico-cortical fiber tract systems [37], the geometrical similarities between the dual ring architecture and the long-range fiber tracts is striking. Furthermore, using tractography from DWI data in three subjects, we controlled that the pattern of long-range connectivity of the PTF ring well matched its geometry and completed its closure. The dual intertwined architecture is thus consistent with studies that have demonstrated significant correlations between structural and functional connectivity, even if RSNs can also correspond to polysynaptic pathways [272, 124, 245, 146].

In previous reports, RSNs corresponding to the PTF ring have often been broken down into two subsets of networks called taskpositive and task-negative systems [86]. The task-negative network (i.e., the default mode network), shows a decrease in activity during task performance [31, 244, 112, 185, 10, 217] while the task-positive network is activated during goal-directed and cognitively demanding tasks. In these experiments, the task concerns executive functions, while regions of DMN activation are more active in internal tasks related to self, memory recall and internal thoughts. In the intertwined ring architecture, this dichotomy can be related to the topography of the PTF ring. On the mesial wall, the ring relates the DMN network to regions of the anterior part of the ring that are important for internal functions of biological regulation and biological rhythms. On the lateral part of

the PTF ring, the intertwining relates the parieto-frontal network of the PTF ring (executive functions) to the VSA ring essential for integration of interactions with the external world.

As defined in this paper, the topography of the rings and their components are stable even though the RSNs, composing the rings, can vary because their identifications vary with the methods, the parameters [296], or even they are dynamic and may change over time [44, 149]. The rings are stable because they are defined as sets of well-defined BAs and robust statistically defined TBNs [156, 246]. The dual intertwined architecture can be viewed as an organizational scheme describing the changing topography of the flexible RSNs within the fixed architecture of the two rings. Similarly, task related activations in individual experiments are highly flexible, reflecting the variety of tasks and experimental conditions. Recent studies have directly compared the resting state networks (intrinsic networks) and the networks activated during a set of tasks (extrinsic networks) at the participant level [188]. These results demonstrated that there is a weak correspondence between individual TBN and RSN, for RSNs that we have classified in the VSA ring and a strong correspondence for RSNs that we have classified in the PTF ring. In the framework of the dual ring architecture, these results suggest that individual TBN tend to activate specific parts of the VSA ring, spreading over local functional links, while activations spread in a more extended over parts of the PTF ring, through long-range connections.

2.5.3 Real-time integration in the VSA ring and multi-temporal integration in the PTF ring

The dual intertwined architecture seems to underline also a dual integrative process: the VSA ring performs fast real-time multimodal integration of sensorimotor information, to control interactions with the environment while the PTF ring performs multi-temporal integrations (i.e., relating past, present, and future representations at different temporal scales), as described below. Sensorimotor processing in the VSA ring implies strong *real time* constraints, designed to link various sources of auditory, visual and somatomotor information together and to control actual behavior. These real-time interactions are important, not only within each modality as sensory or motor, but also for all of their bimodal interactions: between visual and motor (e.g., grasping, reaching, imitation) between auditory and somatomotor information (e.g., recognizing and producing phonemes) and between auditory and visual information (important for communication).

Our results show that the PTF ring implements at least four main groups of functions (TBNs, Table in Figure 2.2C): (1) biological regulation, olfaction, taste, and emotion, (2) working memory and attention, (3) self-referential functions and social cognition and (4) language. The common neural processes supporting these functions (in contrast to sensorimotor real-time processes,) integrate different sources of information in a “multi-temporal”

fashion, at different time-scales, including recall from the past and projections into the future.

Biological regulations and rhythms (in the medial and anterior part of the PTF ring: TBN#2,4 in [156]), operate at different time scales, and are strongly influenced by (1) the hypothalamus and hormonal regulations ranging from minutes to days and months and by (2) the dopaminergic system involved in drive, reward and reinforcement, ranging from minutes to hours. Similarly, emotions are prolonged reactions, which last much longer than the induced emotional sensory stimuli: olfaction and taste produce neural effects which last much longer than those produced by real-time vision, hearing, or touch.

Planning and working memory (in the lateral frontal network of the PTF ring) are based on the integration of information across time by sustained neuronal activations and are able to integrate in the same sequence, several sensory and motor events separated by long and variable delays (review in [93, 176, 191, 61, 190, 151]).

Self-referential functions (in the medial fronto-parietal part of the PTF ring) require information to be integrated at different temporal scales from the past (memory), the present and the future [30, 112, 217, 275, 199, 232, 292]. These regions are active both when subjects consider their present mental states and when they make inferences about the mental states of others (theory of mind and social cognition) [64, 95, 231, 200]. Such processes can last for minutes to hours

Language processing (left temporo-parieto-frontal part of the PTF ring) requires the formation of meaningful conceptual representations integrating events and their consequences over long time lines. It is striking to observe that the regions in the PTF ring match regions that are more strongly activated for words having a meaning than for pseudo-words, which, by contrast, are processed only in the VSA ring [19]. The PTF ring has a topography quite similar to brain activations related to semantic processing [31, 19, 28]. In contrast, speech processing requires realtime processing of visual form perception, motor articulation and auditory perception and, accordingly, the corresponding TBNs are in the VSA ring.

The dual process that we postulate across the two rings (i.e., real-time and multi-temporal integration), are close to the dual process proposed by Fuster [92, 94] with both perception-action cycles and working memory (WM) processes. A perception-action cycle requires temporal contiguity between different signals. By contrast, WM based on sustained neuronal activation is critical to the integration of information across time in goal-directed behavior, reasoning and language bridging time in the perception/action cycle. WM has a retrospective function of retention and a prospective function of anticipation and preparation for forthcoming actions. It allows the temporal structures of strategies, melodies, sentences, scripts, etc. to be stored in memory [92, 94]. Furthermore, the WM processes depend on interactions between large-scale networks of the cerebral cortex, involving the

coactivation of several non-contiguous cortical areas (e.g., a lateral prefrontal region and, concomitantly, a region of the posterior cortex).

2.5.4 Topological advantages of the intertwining

As an important topological advantage, the dual intertwined rings architecture creates multiple interfaces between the two rings within each hemisphere for a large variety of cognitive and sensorimotor functions. First, the intertwined architecture forms three large interfaces between the two rings, which correspond to three large sulci: the precentral sulcus, the STS sulcus, and the intraparietal sulcus. The precentral sulcus forms a VSA-PTF interface for tasks associating multi-temporal goals, and subgoals (frontal areas) with real-time command of each action (somatomotor areas). The STS sulcus forms a second VSA-PTF interface for tasks associating real-time speech (superior temporal areas) with the multi-temporal signification of words (inferior temporal areas). The intra-parietal sulcus forms a third VSA-PTF interface for tasks involving the real-time visuomotor processing of scenes and events and multi-temporal processing of these scenes in terms of social interactions. Second, the intertwining architecture places the associative parietal areas BA#39 and 40 (which are part of the PTF ring) in the central hole of the VSA ring at the confluence of visual, spatial, somatosensory and auditory processing streams (see [153]). This same BA39 region is also related to the medial part of the PTF ring that is implied in the representations of intentions and social interactions. The BA39 can thus transform the real time observation of actions, scenes, and events processed in the VSA ring, in longer term predictions and interpretations related to intentions and social interactions processed in the PTF ring (see [83, 102]). Third, the intertwined architecture places the VSA somatomotor regions in a central position between the PTF parietal and frontal areas, which are themselves connected by the parieto-frontal network. Somato-motor regions can command actions depending both on goals and subgoals (links with frontal regions) and the interpretation of scenes (links with parietal regions).

2.5.5 Development of the dual intertwined rings architecture

A significant finding that emerged when measuring RSNs in children is that developing RSNs are quite similar to the adults' RSNs [79, 81, 87, 254, 145] and it is even possible to detect these RSNs in preterm infants [70, 248]. Interactions progressively change from being predominately anatomically local in young children, to interactions spanning longer cortical distances in young adults, with the segregation of local regions and the integration of distant regions [248, 213, 80, 274] (but this result should be confirmed to exclude possible motion artefact [212, 266]). The distributed cerebral networks of the association cortex have a late development in terms of myelination and cortical surface area [121], thereby facilitating increased long-range correlations. In the dual ring framework, this suggests that the VSA and the PTF rings are present at birth. The RSNs of the VSA ring mature

first and can facilitate the fast development of sensorimotor functions during the first years. The RSNs of the PTF ring mature more slowly and can facilitate the further development of higher cognition. Stronger functional inter-regional connectivity mediates higher level control functions, leading to a more mature cognition.

2.5.6 Evolution of the dual intertwined ring architecture

Previous results comparing monkey and human brains strongly suggest an expansion in humans of the associative parietal, temporal, and frontal areas, with greater functional specialization [121, 215, 267]. In humans, the inferior parietal lobule includes two Brodmann cytoarchitectonic areas that are absent in the monkey (areas 39 and 40). Long-distance networks exist in monkeys, with a functional equivalent of the human DMN [146, 180, 178, 179], but monkeys lack the lateralized fronto-parietal RSNs implicated in language functions [146, 179, 129]. In the dual ring framework, these results strongly suggest the development of the PTF ring during evolution, but also the parallel development of the intertwined architecture, with an expansion of parietal areas of the PTF ring in the center of the VSA ring, connected both to lateral fronto-temporal and medial parietoprefrontal regions. This architectural evolution could be important for human language, because it could relate the processing of words and sentences in the temporo-frontal network with the interpretation of scenes and social interactions in the medial parieto-prefrontal regions.

2.5.7 Conclusion

To conclude, because the dual intertwined rings architecture integrates large set of anatomical, functional, and cognitive results, it can broaden our understanding of the functional properties of the cerebral cortex and the corticotopy of sensorimotor and cognitive functions. In turn, the functional interpretation of the dual ring architecture (real time vs. multi-temporal integration) could inspire new models of the neural basis of these sensorimotor and cognitive functions.

2.6 Materials and Methods

2.6.1 Resting-state database

Resting-state fMRI data were acquired from 198 healthy volunteers (age: 18-30) (from FCP Classic-Cambridge,). Another similar database comprising 170 healthy volunteers (age: 18-26) (from INDI Beijing enhanced) was used to confirm the results obtained from the first onset of volunteers. Both databases are freely available from the NITRC (http://fcon_1000.projects.nitrc.org) [187, 174, 198]. Acquisition param-

eters for the Cambridge databases were: $TR = 3000ms$, 47 contiguous slices, 119 volumes, matrix size = 72×72 , voxel size = $3 \times 3 \times 3mm^3$; and for the Beijing databases were: $TR = 2000ms$, 33 contiguous slices, 225 volumes, matrix size = 72×72 , voxel size = $3 \times 3 \times 3mm^3$; For each individual in both populations, a T1-weighted sagittal MP-RAGE structural image was obtained from the same databases.

2.6.2 Pre-processing

Individual time-series were corrected for slice-timing, within run motion and smoothed (FWHM = $5mm$) using the FSL software (<http://www.fmrib.ox.ac.uk/fsl/>). A nonlinear transformation, used to register the fMRI volumes into the MNI standard space, was calculated as the combination of a linear transformation (using FLIRT), between the averaged fMRI volume and the T1 volume in the subject space and a nonlinear transformation (using FNIRT) was used between the T1 volume in the individual space and the T1 template in the MNI standard space. Then, the FA and ADC images were registered on a $1 \times 1 \times 1mm^3$; standard space image (MNI152 space), using a nonlinear registration procedure.

2.6.3 Functional network identification by spatial Independent Component Analysis (NEDICA)

Group functional networks were identified using a two-step procedure, the NEDICA method [207]. The first step consisted in applying a spatial independent component analysis (sICA) to each individual fMRI-series, with a fixed number of components ($K = 100$). The second step consisted in identifying reproducible spatial components across subjects, by means of hierarchical clustering. RSNs were then identified according to their representativeness in the studied population $R(RSN_i)$: the number of subjects in which RSN_i is present was divided by the total number of subjects (among group-representative clusters identified for at least 10% of the subjects). Finally, the corresponding T-maps were thresholded at $p < .05$, with a false discovery rate procedure used as a control for multiple comparisons.

2.6.4 Clustering methods

The aim of this work is to build methods for sample classification and selection of RSNs networks in order to identify the various functional and anatomical RSNs groups. Our method is based on a Bayesian approach to density estimation and clustering using mixture distributions [161]. For our data sets comprising multinomial variables (values overlap between RSNs and TBNs, BAs or BAFs), we used the approach involving mixture distributions having Gaussian components fitted by maximum likelihood, for which the EM algorithm has a closed-form. This algorithm allows the automatic determination of the number of

distributions in the mixture. One of the most common motivations for using Gaussian distributions is to obtain robust estimates for the RSNs groups. To evaluate the accuracy of Bayesian classification, we compared this technique with the community structure detection algorithm [196] to evaluate if the results of the two methods agreed sufficiently closely. Indeed, if we consider that each data set is a network overlap, the community structure method assumes that the network of interest divides naturally into subgroups. The number and size of the groups are thus determined by the network itself. The true community structure or group can be quantified by using the modularity measure [197]) which is defined as the number of edges falling within groups minus the expected number in an equivalent network with edges placed at random. The accuracy of a Bayesian classification is assessed by comparing the classification with community structure detection algorithm. The results of the accuracy assessment are summarized in a confusion matrix which displays the number of correct and incorrect predictions made by the Bayesian model compared with the community structure detection algorithm. The estimate of accuracy is then simply the ratio of correct predictions to the total number of predictions.

2.6.5 RSNs specialization: overlap with TBNs

We characterized the functional properties of the 32 RSNs by computing their overlaps with the TBNs extracted from large databases of fMRI activation, during sensorimotor and cognitive tasks. This analysis was carried out using the following measurement of topological similarity:

$$D(RSN_i, TBN_j) = \frac{RSN_i \cap TBN_j}{RSN_i \cup TBN_j}$$

where RSN_i are the binary thresholded T-map of the RSN_i and the masks of TBN_j [156].

We then constructed a similarity matrix between each RSN and each TBN. Each RSN was then characterized by its overlap with the TBNs specialized in cognitive functions (see [247, 156]). In order to find RSNs clusters with similar functional specializations, the similarity matrix was reorganized by applying an Expectation Maximization (EM) algorithm as described in [161]. The reorganization of this similarity matrix provided several clusters functionally characterized by TBNs (see Figure 2.2C).

2.6.6 RSNs distribution: overlap with BAs regions

We characterized the anatomical organization of the 32 RSNs by computing their overlaps with Brodmann areas. The Brodmann areas (BAs) numbered from 1 to 47 were grouped

into 28 regions (the small adjacent regions were regrouped) to limit the size of the matrix ($BA_q, q = 1 \dots 28$):

$$D(RSN_i, BA_q) = RSN_i \cap BA_q$$

where RSN_i are the binary thresholded T-map of the RSN_i and $q = 1 \dots 28$. The resulting similarity matrix was reorganized by applying the same Mixture Distribution Algorithm as that described above. The RSNs clusters were then defined and characterized anatomically by the Brodmann atlas. To confirm this result and show that it does not depend on the number of BAs regions, we grouped the 28 BAs regions into 7 families ($BAF_p, p = 1 \dots 7$), related to the occipital lobe (BA# 17, 18, 19), the central sulcus (BA# 2, 3, 4, 5, 6), the temporal lobe (BA# 41, 42, 21, 22, 37), the cingular cortex (BA# 23, 32), the inferior frontal cortex (BA# 44, 45, 47), the superior frontal cortex (BA# 8, 9, 46) and the anterior frontal cortex (BA# 10, 11). The RSNs were then anatomically localized using the spatial overlap ratio between the RSNs and the BAFs:

$$D(RSN_i, BAF_p) = RSN_i \cap BAF_p \text{ where } p = 1 \dots 7$$

Next, we constructed a similarity matrix between each of the (RSN_i, BAF_p) pairs, which were then reorganized by applying the same clustering method.

2.6.7 Anatomical Fiber tracting

We compared the topography of RSNs, made of non-adjacent cortical regions, with underlying cortical fiber tracts. The data used in the preparation of this work were obtained from the Human Connectome Project (HCP) database¹. The HCP project is supported by the National Institute of Dental and Craniofacial Research (NIDCR), the National Institute of Mental Health (NIMH) and the National Institute of Neurological Disorders and Stroke (NINDS). HCP is the result of contributions from co-investigators from the University of California, Los Angeles, the Martinos Center for Biomedical Imaging at Massachusetts General Hospital (MGH), the Washington University and the University of Minnesota.

A diffusion spectrum MRI scan was acquired in a normal human subject, imaged in vivo at 3 Tesla with an isotropic spatial resolution of $2mm$ and 515 diffusion samples ($b = 0$ every 15 volumes) with a peak gradient intensity $G_{max} = 90mT/m$. Diffusion orientation density functions (ODFs) were reconstructed using the 3D discrete Fourier transform of the modulus of the measured signal. From the directions of the ODF maxima,

¹<https://ida.loni.ucla.edu/login.jsp>

paths were computed with a streamline tractography algorithm (parameters: Euler integration; angular threshold 35 degrees; step length 0.2 mm; 8 random seeds within voxels) and smoothed using a B-Spline filter. Next, fiber tracts were registered into the standard MNI space by means of a linear transform computed using FSL (FMRIB, Oxford, UK: www.fmrib.ox.ac.uk/fsl/). Finally, the ring masks were used to filter tracks and keep fibers which end within rings. All diffusion data processing and visualization was carried out using the TrackVis software (MGH, Massachusetts, USA: www.trackvis.org/).

2.6.8 Representation of the results

The functional structures were mapped onto a standard human brain surface using the Caret software (<http://brainvis.wustl.edu/>).

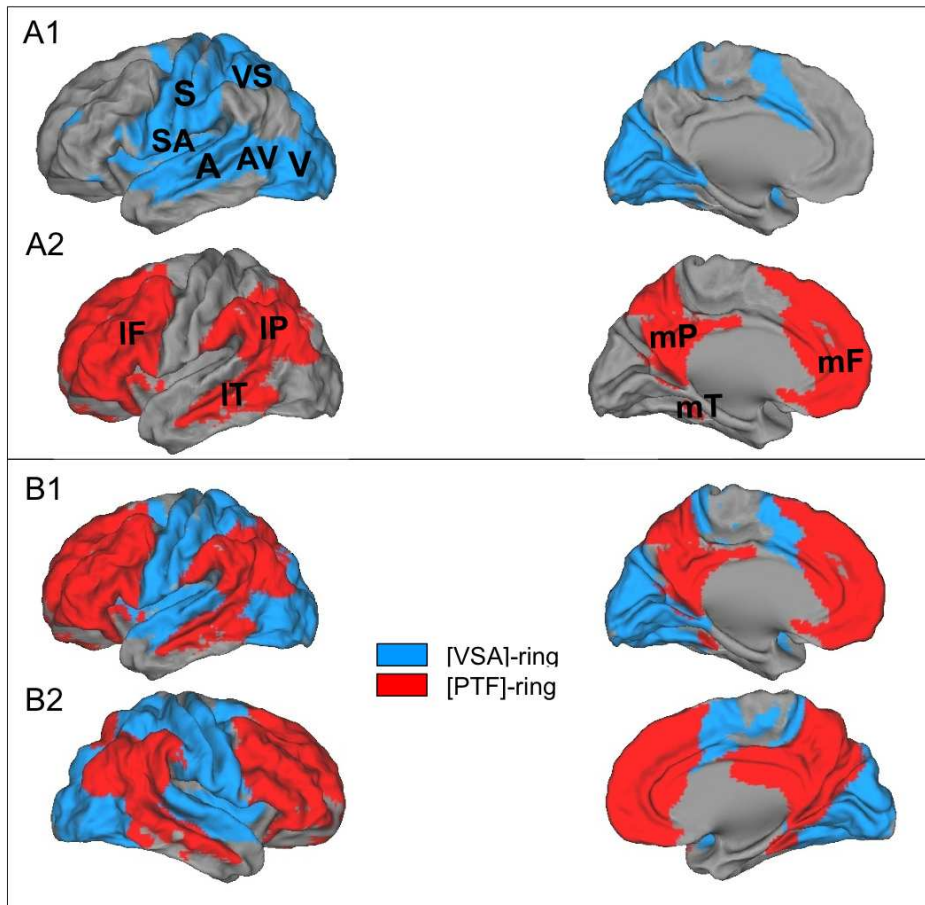


Fig. 2.5.: The dual intertwined rings architecture. (A1) The VSA ring, in blue, forms a continuous cortical ring organized around primary cortices: visual (V), auditory (A) and somatomotor (S) with interspersed bimodal regions: visuo-somatomotor (VS), auditory-somatomotor (SA) and visuo-auditory (VA). (A2) The PTF ring, in red, forms a ring discontinuous over the cortical mantle but closed by major cortical fiber tracts (see Figure 2.6), with 3 regions, parietal, temporal and frontal on the lateral (l) aspect of each hemisphere (IP,IT,IF) and 3 regions parietal, temporal and frontal, on the medial (m) aspect (mP,mT,mF). (B) The two rings are intertwined: the PTF ring, in red, is placed in foreground, to show that it is not continuous over the cortical mantle but interrupted by the VSA ring and is closed by major cortical fiber tracts passing below the VSA ring, as shown in Figure 2.6.

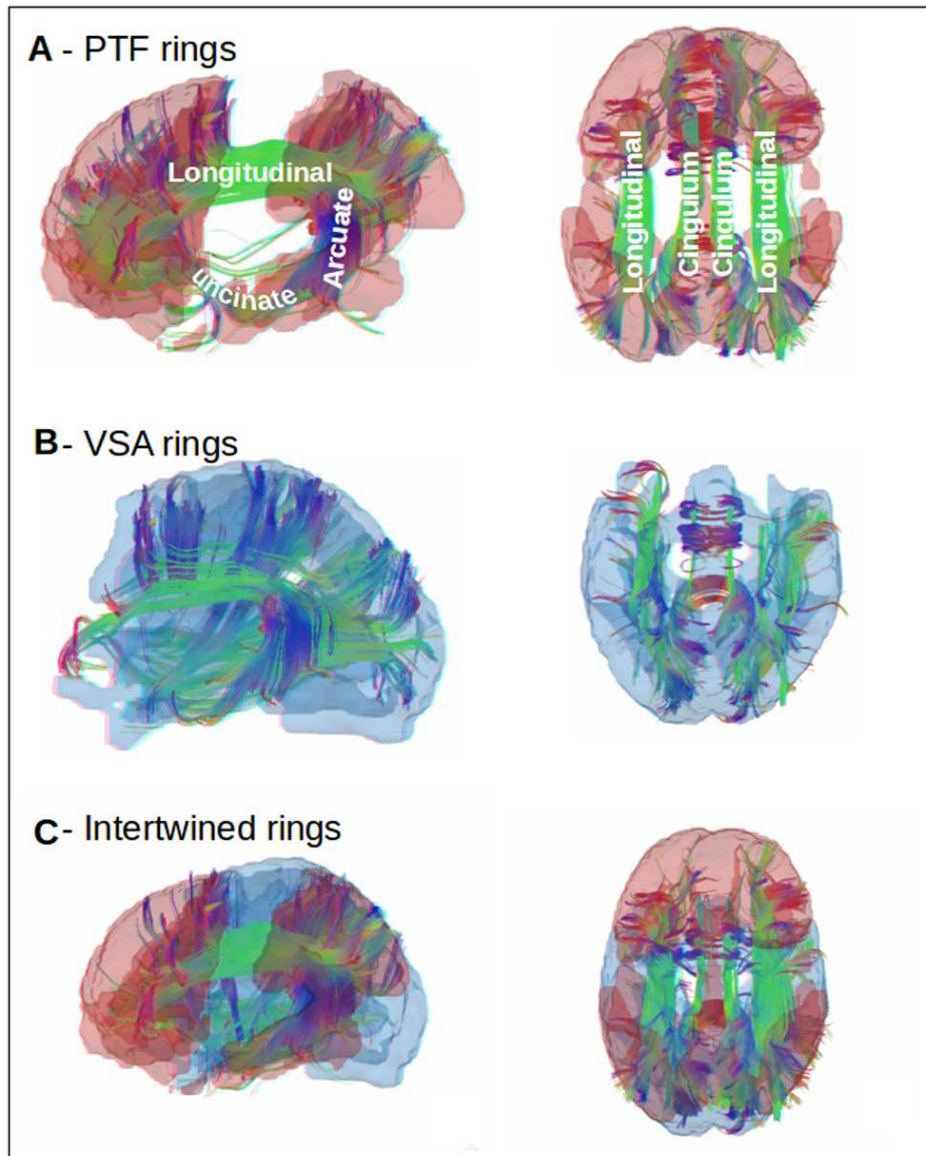


Fig. 2.6.: Long distance cortical connections closing the PTF ring. Comparison of the topography of the two rings (lateral and dorsal views), with superimposed major cortical fiber tracts (see text for details). Mapping of major long-distance fiber tracts on the 3D mask of the PTF ring (Figure 2.6A) and VSA ring (Figure 2.6B). Long-range connections on the VSA ring and the PTF ring, mapped together (Figure 2.6C).

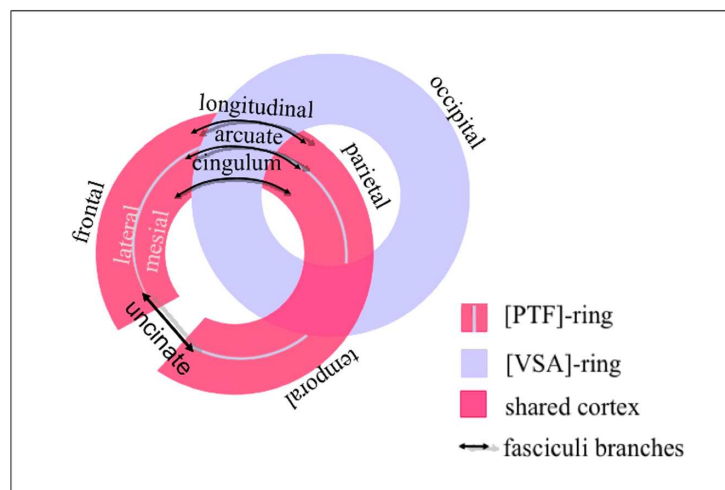


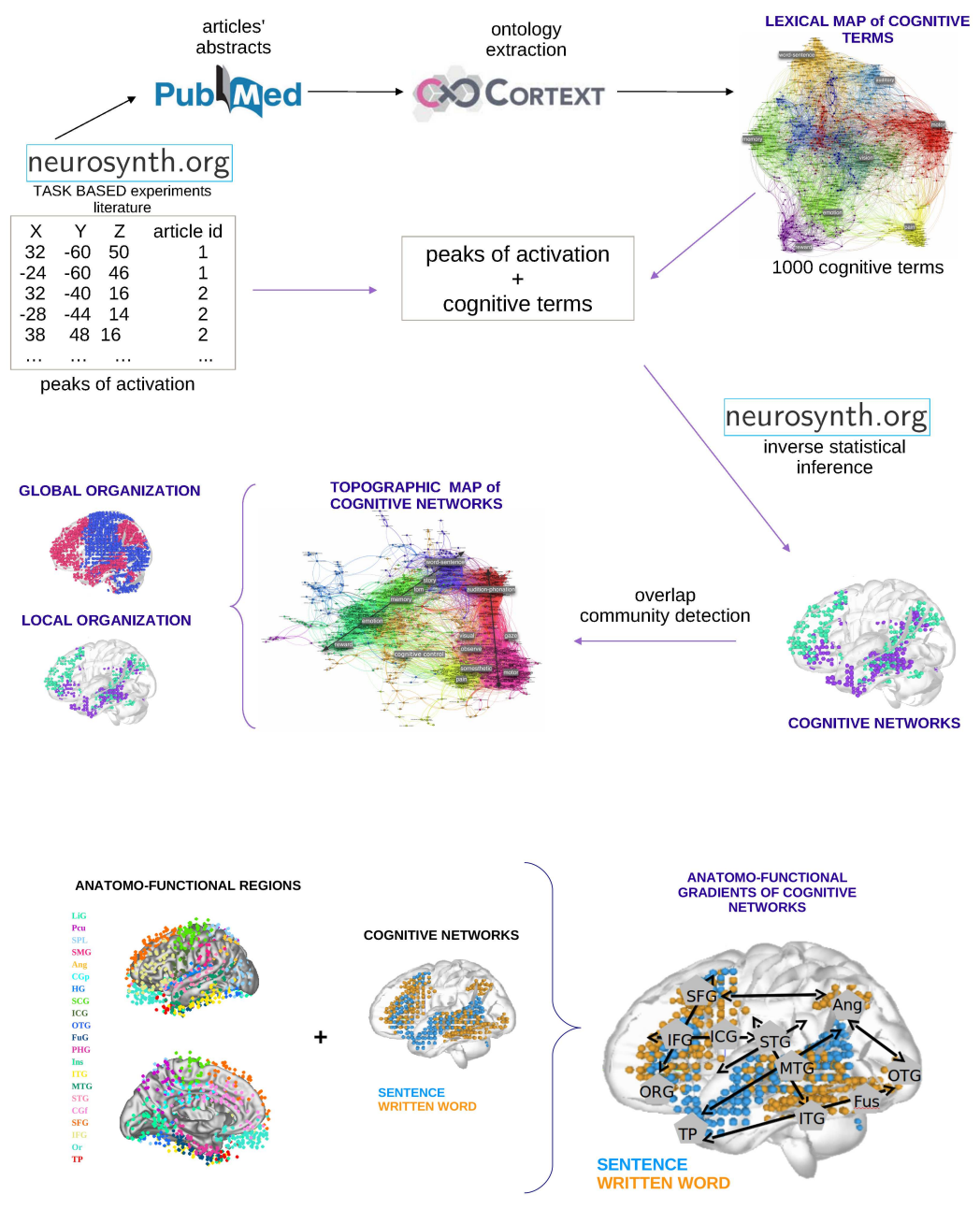
Fig. 2.7.: Intertwining scheme. Schematic representation of the principle of intertwining of the VSA ring and the PTF ring within each hemisphere, thanks to the major long-range tract fibers.

Gradients of cognitive networks across the cortical surface

In the previous chapter we interpreted a group of reproducible Resting State Networks based on their anatomo-functional characteristics. The comparison of these networks with Brodmann Areas, Task Based Networks and fibers tracts allowed us to reveal two large ensemble of regions differentiated by their cortical topography and by the type of cognitive functions implemented. In particular the latter difference lead us to oppose what we called the two rings VSA and PTF based on their preferred way of processing information: real-time, stimulus driven for VSA, multi-temporal, more spontaneous and internally driven for PTF.

In this chapter we investigate how cognitive networks are organized among them across the cortical mantle. To do so we used the *Neurosynth* database about fMRI literature connecting single task based studies to a set of peaks of activations. We used text mining algorithms to help extracting a cognitive ontology from the ensemble of abstracts belonging to the articles in the *Neurosynth* database. We used the *Neurosynth* statistical framework to evaluate a cognitive map for each of the cognitive term extracted. We finally studied the relations between the different cognitive maps evaluated, based 1) on their overlap across the cortical surface and 2) their mutual position with respect to a set of anatomo-functional landmarks. Figures 3.3, 3.4, 3.5-3.11 show the main results for this chapter. This work has been only partially published at the annual meeting of the *OHBM* held in *Seattle, USA in 2013 (Cioli et al.)*. The material contained in this chapter will be further structured to be published.

3.1 Graphical abstract



3.2 Abstract

In this chapter we investigate how cognitive networks are organized across cortical regions. Using the Neurosynth database, we first built a lexical map (graph) of all the cognitive categories (concerning e.g., sensory, motor, language, emotion, semantic and episodic memory) and their co-occurrences, and build a topographical map (graph) of all the overlaps between the corresponding cognitive networks. The list of cognitive tasks contained about 1000 cognitive terms. It represents a cognitive ontology extracted in a bottom-up fashion and provides a map of literature organization showing how researchers understand the relations between the cognitive categories. We built a graph of overlaps of the cognitive networks corresponding to these cognitive categories covering all the domains sensory-motor, language, emotional, vital needs, etc. At a global level we found that the main organization of cognitive networks (in term of overlaps) reproduces the two intertwined rings architecture, although they were obtained with a totally different method. Furthermore, this graph shows many overlaps between different cognitive networks revealing the continuity of underlying neural processes. We need anatomical landmarks more precise than the two rings to understand the organization of cognitive networks across the cortical surface. We interpret the overlaps and continuity between cognitive networks in the light of some known principles of the multi-scale anatomo-functional organization of the cerebral cortex. These principles will be very useful to interpret the gene expression results. Starting from these general organizational principles, we chose a set of 21 anatomo-functional regions, (1) forming like BAs a tessellation of the cortex covering the entire cortical surface without overlaps, (2) organized as Brodmann areas along the main cortical gradients, (3) directly comparable with the tessellation and the sampling proposed in the Allen atlas of genetic expression, (4) forming a more precise description of the dual ring architecture, (5) differentiated by a global sensory-motor or cognitive specialization. Cognitive networks are organized on the gradients formed within and between the 21 anatomo-functional cortical regions. Each anatomo-functional region represents a pole for specific groups of cognitive tasks. We propose a scheme to describe the organization of cognitive networks across the cortex. This scheme is determined by 1) poles of connections of cerebral regions with the other brain regions; 2) the functional gradients connecting these poles along parietal, frontal and temporal gradients. These results are fundamental to understand the work presented in Chapter 5 showing the correlation between gene expression and anatomo-functional regions. We found indeed that it was not possible to clearly relate the expression for a single gene with one anatomo-functional region and even less with a cognitive network but instead it was possible to relate in a robust way gradients of gene expression with gradients of anatomo-functional regions and then with gradients of cognitive networks.

3.3 Introduction

The systematic investigation of the human brain had a huge impulse 25 years ago with the development of the fMRI (functional Magnetic Resonance) technique. This technique is based on the fact that an increased neuronal activity is known to be associated to a local increased blood flow leading oxygen depleted blood to be replaced by oxygen rich blood. Exploiting the difference in magnetic properties between oxygen-rich and oxygen-depleted blood, the BOLD signal is then capable to measure the local consumption of oxygen corresponding to neuronal activity.

An fMRI experiment is performed asking participants to accomplish a specific task while monitoring their brain activity. A set of different subjects (~ 10) is usually analyzed in order to statistically determine the most activated locations in the brain. Each fMRI article is then characterized by two main aspects:

- the *description of the task* performed during the experiment, either sensorymotor (move an arm, painful stimuli) or cognitive (read something)
- *peaks of activation*: set of (x, y, z) coordinates indicating the locations in the brain which statistically displayed the maximum activation during the experiment

Since this method is completely non invasive and fMRI machines are present in almost all hospitals for diagnostic purposes this led to an always increasing proliferation of fMRI experiments: in 25 years more than 20.000 fMRI studies on human subjects have been published.

This big amount has been exploited in order to unify and corroborate results of many different studies on single cognitive task using the meta-analysis framework. This consists in collecting the bigger number of papers relevant to the study of one cognitive task and treat them as independent different trials of the same experiment in order to increase the size of the sample to perform statistics on. Meta-analysis works present two drawbacks: on one hand they are usually time consuming from the point of view of constituting significant databases of papers and extracting meaningful data from them; on the other hand the constitution of this databases is based on a priori classification of the literature by cognitive tasks.

In 2011 Tal Yarkoni developed the Neurosynth project representing an open-source framework allowing bottom-up retrieval, classification and meta-analysis of potentially all fMRI literature at the same time allowing the direct comparison of activations related to different cognitive tasks. In particular in this framework the automated meta-analysis is made possible by labeling every retrieved paper with 1) a set of words present in the text and relevant to the kind of cognitive task treated in the experiment and 2) the peaks of activations (x, y, z) (Talairach or MNI coordinates) reported. This procedure creates a database on

which statistical analysis can be performed and it addresses in particular the question: if a given cognitive term is considered which is the probability that a given region of the brain has been found to be activated throughout the all literature (retrieved)?

In this work we exploited and improved Neurosynth potentialities in order to tackle the problem so far not investigated of how the different networks involved in the large set of cognitive tasks so far explored in literature are topographically related among them.

3.3.1 fMRI: single study vs meta-analysis

The term meta analysis was coined by the statistician Gene V. Glass who formalized this framework starting from 1976 [100]. The aim of this statistical technique is to combine the findings from independent studies in order to test the robustness of the results shown in the literature or to discover new patterns. This method indeed allows to overcome biases due to single studies and to raise the prediction power resulting from a bigger number of trials.

A central issue in carrying out a worthwhile meta-analysis is represented by the selection of the papers to be used in such analysis; while a good meta-analyses aim for a complete coverage of all relevant studies existing in literature this is often not the case. For what regards fMRI studies the selection of the literature to be incorporated in meta-analysis turns out to be particularly central: in these studies scientists are concerned about identifying specific regions of the brain responsible for the performance of a given task; but if theoretically we can isolate a special task, especially when involving primary sensorymotor areas, it becomes more difficult when we consider more complex cognitive tasks. An example for a complex task can be the process of reading. During this task at least two processes are involved: 1) the perception of the text involving our visual system together with our primary visual cortex; 2) the process allowing to pass from letter perception to the identification of words. Moreover tasks and experiments protocols are not univocally defined; this point out two key points:

- classify cognitive tasks
- classify studies according cognitive task classification

3.3.2 Data-driven meta-analysis: the Neurosynth framework

fMRI meta-analysis studies are usually performed on databases of papers selected by single teams of research or via an effort of the community. These databases are created according to choices made by humans with their scientific background and beliefs and are often structured following a priori hierarchical classifications of cognitive tasks.

An example of this top-down approach is represented by the BrainMap project (<http://www.brainmap.org/>). This way to proceed can lead to biased analysis imposing the researcher point of view for example on the studies to be taken into account or the hierarchical organization of tasks used for to perform further studies.

In 2011 Tal Yarkoni developed the web-based project called Neurosynth described in [295] and available at <http://neurosynth.org>. Neurosynth is a completely automated framework to both retrieve data from and perform meta-analyses on fMRI available literature. Indeed choosing a cognitive term from the database allows first to select the subset of the literature citing the chosen term and second to perform a meta-analysis on the subset of articles selected. It can be described as a meta-analysis generator. Figure 3.1 shows an example of meta-analysis obtained for the cognitive term *emotion*.

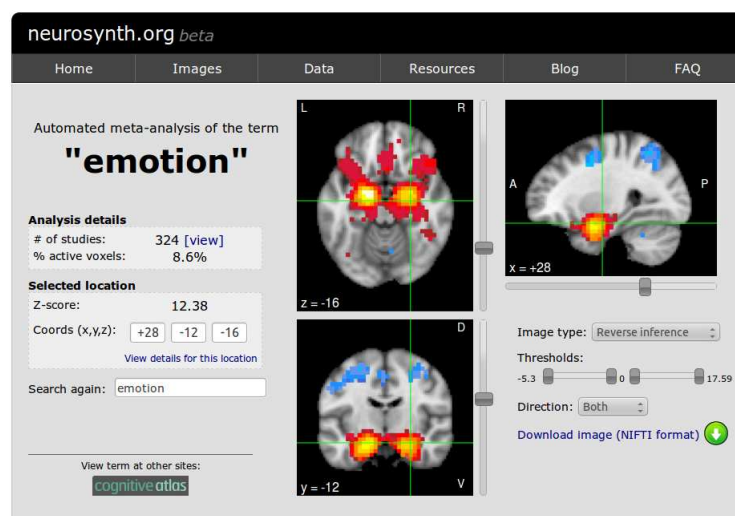


Fig. 3.1.: Neurosynth: Neurosynth webpage (<http://neurosynth.org>) displaying an example of automated meta-analysis performed for the term *emotion*. In particular the page displays the reverse inference map evaluated for the term based on 4939 papers 324 of which were associated to the term chosen.

The importance of this framework is its ability to retrieve virtually all the relevant articles about fMRI literature and to extract data from them (in particular the peaks of activation identified by the experiments). The method is then data driven allowing the generation of bottom-up ontologies of cognitive tasks on one hand and to define in a bottom-up fashion sets of article to be submitted to meta-analysis.

3.3.2.1 The double nature of cognitive terms

Each paper in Neurosynth framework is associated with a set of peaks of activations and a set of terms existing in the papers. In this framework terms have then a double nature:

¹*Talairach, MNI*: to reduce intersubject anatomical variability in human brain mapping studies, coordinates measured during experiments are mapped onto a standard brain; Talairach and MNI are the most used standard spaces.

³*Voxel*: volumetric pixel

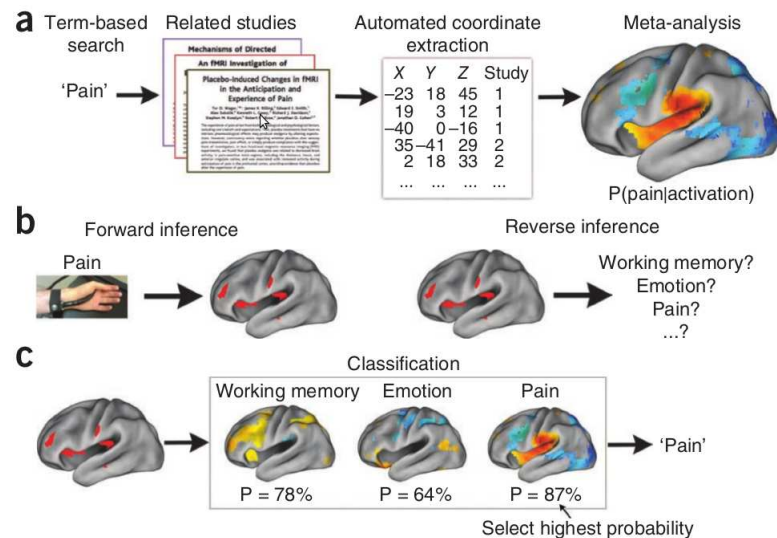


Fig. 3.2.: (source: [295]) *a) Neurosynth pipeline:* once selected a term to meta-analyze, Neurosynth identifies all the papers present in the database reporting the term chosen and the coordinates of peaks of activations present in those papers. The last step is to evaluate inference maps for the term chosen based on the papers selected. *b) Inference maps:* two different kind of statistical analysis can be performed using Neurosynth framework: it is possible to evaluate forward inference maps evaluating which brain regions are activated when a given term is present in the paper; or forward inference maps evaluating the probability that given a pattern of activations the term treated is the one chosen.

- *Lexical:* because of their meaning they stand for categories (i.e.: cognitive tasks) and they are the key to categorize papers according to different cognitive tasks
- *Topographical:* since they are associated with peaks of brain activation in each paper, they represent activations in the brain

The main goals of this work were two: first build a lexical map based on a bottom-up ontology of cognitive terms and understand the organization of the different subfields of the domain avoiding a prior, top-down categorization; second to build topographical maps of cognitive networks and study their mutual organization across the cortex.

3.4 Results

3.4.1 Lexical Map: 1000 cognitive terms

Using *PubMed* we first built the database containing the abstract for the 4939 (at the time of this work) fMRI articles contained in Neurosynth. We used the platform *CorText* (see section 3.5.2) to extract the most meaningful multigrams from the database of abstracts we had prepared. The analysis produced a list of about 10000 between mono and multi-terms. The list mainly contained multigrams related to four categories: cognitive tasks, experimental protocols, anatomical regions of the brain and cognitive disorders. We manually tagged

each terms according to these four categories (fundamental step in ontology extraction) and we worked on the list of cognitive tasks. The list of cognitive tasks contained about 1000 cognitive terms and it represents the cognitive ontology extracted in a bottom-up fashion, for the database analyzed.

To represent the relations between the terms of this ontology we built a co-occurrence graphs according to the similarity index proposed by *Weeds* and *Weir* [288]. We then applied several community detection algorithms to assess qualitatively the stability of the results respect to different clustering methods. We used *Gephi* (<http://gephi.org>) to represent the results. In Figure 3.3 we show the results obtained by applying the Louvain algorithm: this figure is interesting since it allows to have a synthetic view of how the fMRI scientific research is organized. Observing Figure 3.3 we can see how the overall structure of the graph is made of well defined but continuous clusters. We can qualitatively appreciate two kinds of clusters: more isolated clusters positioned at the periphery of the graph and linked mainly with one other; and clusters occupying a central position and connected to several communities. A peripheral position is occupied by the cluster labeled in Figure 3.3 as *Pain*. This cluster is the most isolated suggesting well defined and separated field of study. Its main connections are with the *Motor* and *Emotion* clusters. *Reward* community also tends to be isolated and essentially linked with the *Emotion* community. The *Memory* cluster is instead strongly linked with *Working Memory* related communities (not labeled, colored in blue and red at the center of the graph). The *Word and sentence* community is mainly connected to the *Auditory* cluster and the *Working Memory* one. Finally The *Motor cluster* is in continuity with the *Auditory* and the *Vision* ones via smaller clusters containing intermediate tasks such as *Motion Perception* (in dark green) or *Auditory Motion* (in light blue).

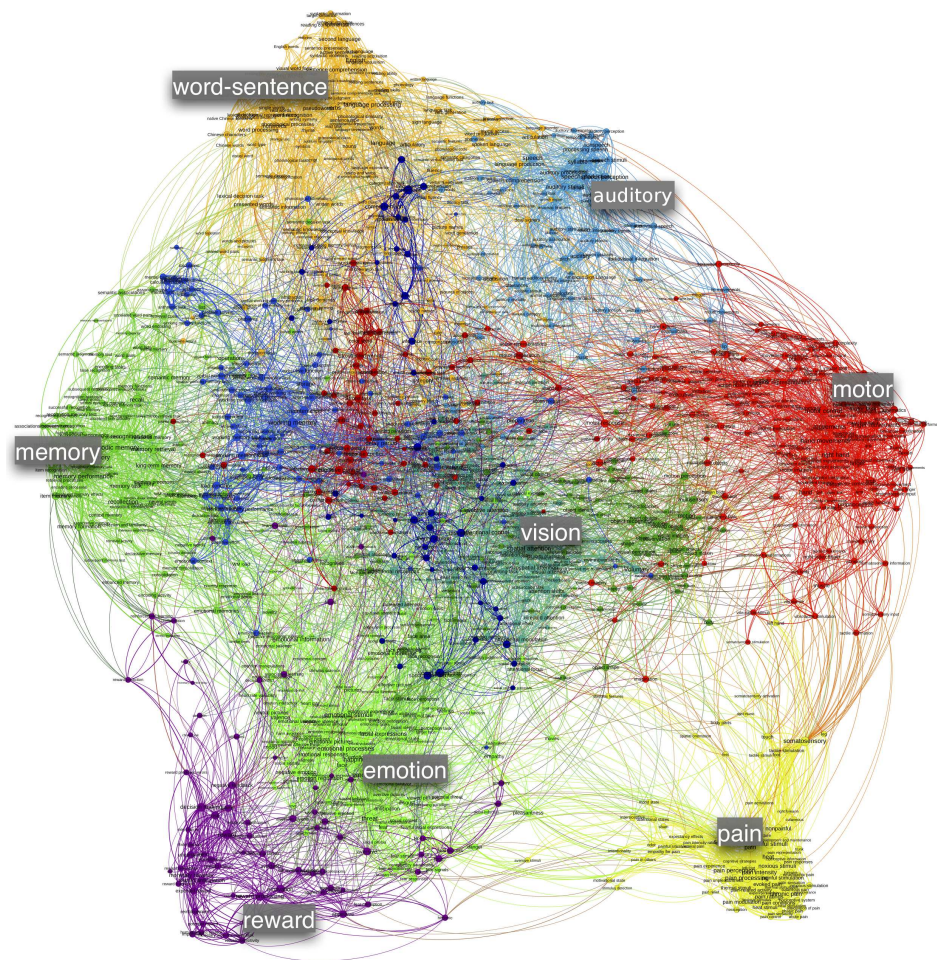


Fig. 3.3.: 1000 newly extracted terms - Lexical analysis: this figure shows the result of Louvain clustering method performed on the graph created using the co-occurrence measure described by eq. (3.3).

3.4.2 Topographic Map: 1000 cognitive categories

To study the cortical organization of cognitive networks across the cortex we needed to combine the new database of cognitive terms with the peaks of activations observed during experiments. To do so we used the Neurosynth framework and we chose to focus on reverse inference maps (see section 3.5.1). This choice was made to reduce as much as possible the overlap between maps belonging to different terms/cognitive tasks. The reverse inference map tells us indeed which is the probability that a specific task was performed given the activation of a voxel.

Once we had evaluated the reverse inference maps for each of the about 1000 cognitive terms, we transformed them into binary masks. We finally evaluated the amount of overlap (in number of voxels) between each pair of masks and we used this matrix as a base to perform community detection. The result is shown in the graph presented in Figure 3.4 where the cognitive terms are clustered by cognitive categories covering all the domains sensory-motor, language, emotional, vital needs, etc. The topographical analysis shows a new scenario compared to the lexical map of Figure 3.3. While the main clusters detected by the algorithm remain essentially the same, their overall organization is different. The clusters are in this case organized into two well shaped meta-clusters. At a global level we found that the two meta-clusters of cognitive networks (in term of overlaps) reproduces the two intertwined rings architecture, obtained with a totally different method (see Chapter 2): looking at the clusters composing the two meta-classes we see that they stand for sensorymotor and bimodal tasks (somatomotor, visual, auditory, speech as VSA), and more integrated cognitive tasks (emotion, memory, language) together with vital needs. Furthermore, this graph shows many overlaps between different cognitive networks revealing the continuity of underlying neural processes.

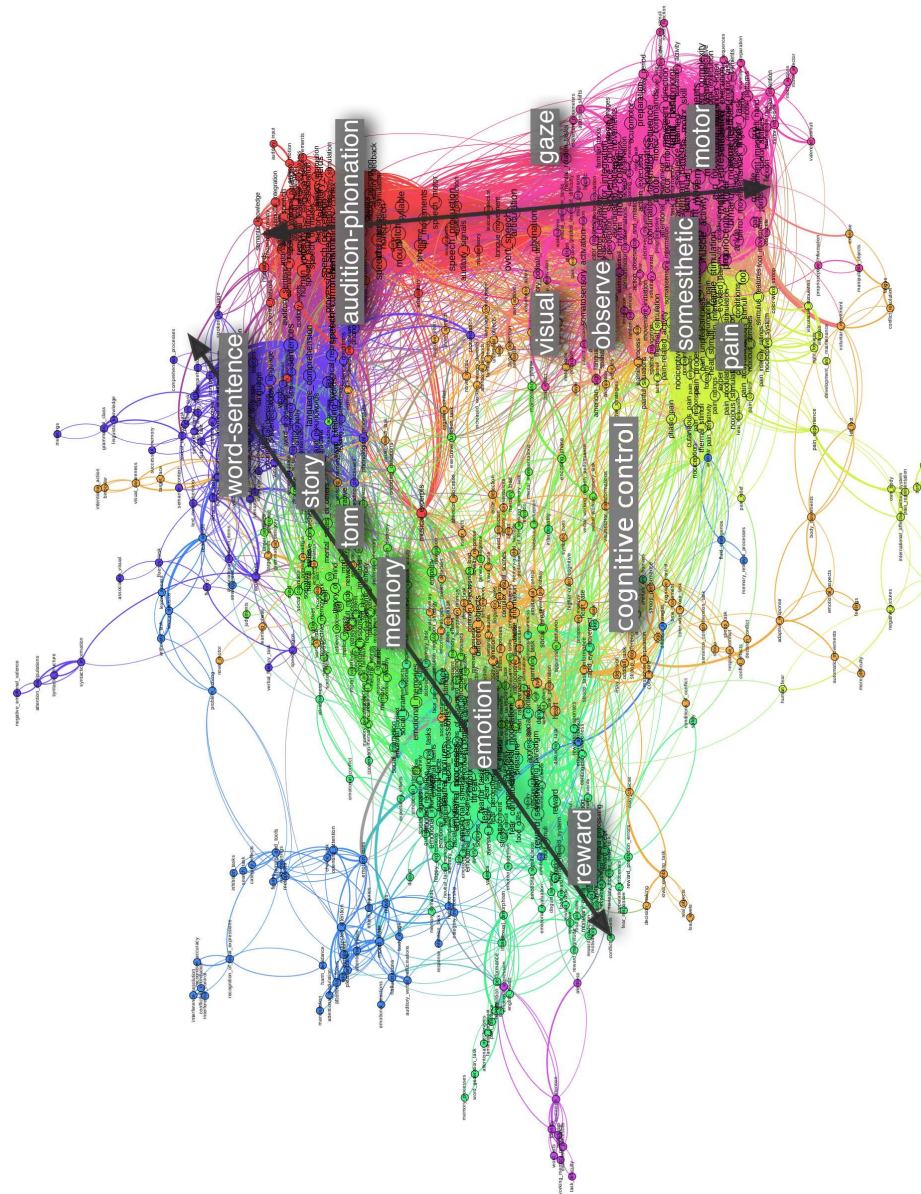


Fig. 3.4.: 1000 newly extracted terms - Topographical analysis: this figure shows the result of Louvain clustering method performed on the graph obtained using the measure (based on networks overlap) $A_i \cap A_j / A_i$ to quantify between terms similarity.

3.4.3 **Anatomo-functional gradients of cognitive tasks across the cortex**

3.4.3.1 **Principles of anatomo-functional organization of the cerebral cortex**

We need anatomical landmarks more precise than the two rings to understand the organization of cognitive networks across the cortical surface. We interpret the overlaps and continuity between cognitive networks in the light of some known principles of the multi-scale anatomo-functional organization of the cerebral cortex. Such principles have been detailed in the literature on unit recording and connective studies in primate performing sets of sensory-motor and cognitive tasks. A systematic review of the literature [32] proposed an integrated framework to relate the anatomy, the connections, the properties of neurons, and the organization of the sensory-motor and cognitive networks. These links will be very useful to interpret the gene expression results.

1. Cortical areas defined by their connections with other brain regions form functional poles: for example primary areas form visual, auditory, motor poles; other areas connected to other brain regions such as the hypothalamus, the hippocampus, the amygdala, form also functional poles more involved respectively in hormone controls, in episodic memory formation, in emotional arousal.
2. Cortical areas form continuous connective and functional maps organized by their main axes aligned with the main axes of the cortex: connections and functional properties change continuously within maps and between maps in a gradient like fashion. Many cortical areas are defined by their position on the main axes of the cerebral cortex, rostro-caudal (anterior-posterior) and dorso-ventral (superior-inferior): e.g., Dorsolateral frontal cortex, superior temporal area.
3. External and cortico-cortical connections form gradients generally aligned with the main sulci, along the antero-posterior and dorso-ventral axes of the cortex; for example, fronto-parietal connections are organized along anterior-posterior gradients, linking neuronal populations symmetrical with respect to the central sulcus (also shown in humans [261]).
4. Gradients of functional properties of neurons are organized along the connective gradients. Within each area, neurons have combinatorial tuning properties (for example visual, and tactile, and proprioceptive and visual); long distance connections between frontal and parietal connect neurons with similar sensory-motor tuning properties, but with different temporal properties (sustained activation characteristic of working memory in frontal areas).

5. Learning cognitive tasks at the neuronal level consist of aligning congruent tuning properties: for example a neuron tuned for a given position of the arm and tuned for a gaze position, will learn the motor direction aligning the initial position of the arm and the final position matching the gaze position. Consequently, different cognitive networks will spontaneously emerge through learning along gradients of combinatorial properties induced by gradients of connections.

3.4.3.2 Tessellation of the cortex: 21 anatomo-functional regions

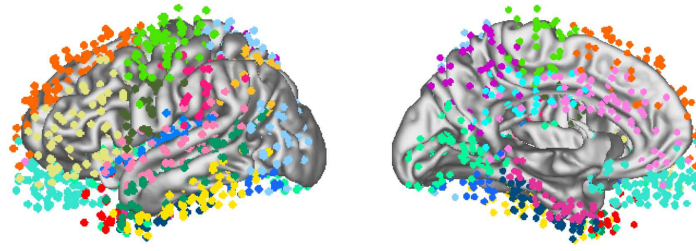
Starting from these general organizational principles, we chose a set of 21 anatomo-functional regions, as shown in Figure 3.5:

1. these regions form a tessellation of the cortex covering the entire cortical surface without overlaps (as BAs), organized along the main cortical gradients
2. these regions are organized along the main cortical gradients, rostral-caudal (or anterior-posterior), and rostral-ventral (superior-inferior)
3. these regions are directly comparable with the tessellation and the sampling proposed in the Allen atlas of gene expression
4. these regions match the dual ring architecture
5. these regions are characterized by a global sensory-motor or cognitive specialization

Most of the time different cognitive networks recruit several anatomically defined regions of the cortex. These regions are not necessarily contiguous across the cortical mantle. At the same time anatomically defined cortical regions can participate to the implementation of more than one cognitive task. This phenomenon is clear if for example we observe Figure 3.4 where the relation between cognitive networks is described starting from their overlap on the cortical surface.

The functional features of an anatomical region are based on the topology of its connectivity: the more a region have pathways of cortico-cortical connections with contiguous areas or long range connections with further regions, the larger will be the number of cognitive task it will be involved in.

To better describe this phenomenon we adopted a similar approach to the one used in section 2.4.3 where we compared and interpreted resting state networks with Brodmann Areas. Instead of Brodmann Areas we chose in the present case, a set of anatomo-functional regions. This set of anatomo-functional regions have like BAs the advantage of representing a tessellation of the cortical surface, namely they cover the entire cortical surface without



Label	Anatomical region	BA	Function
LiG	Lingual Gyrus, Cuneus	17,18,19 (medial part)	visual features
Pcu	Precuneus	7 (medial part)	recollection, retrieval
SPL	Superior Parietal Lobule	5,7 (lateral part)	visuomotor, visuospatial
SMG	Supramarginal Gyrus	40	tools manipulation
Ang	Angular Gyrus	39	visual interpretation
CGp	Cingular Gyrus (posterior)	23,31	social cognition
HG	Herschel Gyrus, Planum Temporale	41, 42, 22	auditory perception
SCG	Superior Post and Pre Central Gyrus	1, 2, 3, 4	hand, arm control
ICG	Inferior Post and Pre Central Gyrus	1, 2, 3, 4, 43	speech production
OTG	Occipito-Temporal Gyrus	37 (posterior)	shape recognition
FuG	Fusiform Gyrus	37 (anterior)	face recognition
PHG	Parahippocampal Gyrus	34	episodic memory, emotion
Ins	Insula	13, 16	pain, heat
ITG	Inferior Temporal Gyrus	20	lexicon, semantic memory
MTG	Medial Temporal Gyrus	21	sentence comprehension
STG	Superior Temporal Gyrus	22	speech comprehension
CGf	Cingular Gyrus (anterior)	24,32	cognitive strategies
SFG	Superior Frontal Gyrus	6,8,9	working memory, executive f
IFG	Inferior Frontal Gyrus	44, 45, 46	sentence production
Or	Orbital regions	10, 11, 12, 25, 27, 47	reward, motivation
TP	Temporal Pole	38	recall, emotion

Fig. 3.5.: The 21 anatomo-functional regions

overlaps. The anatomo-functional regions we chose were defined by grouping anatomical regions as described in the Allen Human Brain Atlas <http://casestudies.brain-map.org/ggb#section>. This choice was thought to favor a more direct comparison between cognitive tasks and gradients of gene expression as it will be discussed in Chapter 5. In Figure 3.5 the colored dots represent all the samples (MNI coordinates) for which the Allen Institute collected and analyzed the level of mRNA expression for the entire human genome across 6 adult brains. At this point of the work they will be just used as coordinates sampling anatomo-functional regions.

3.4.3.3 Main functional specialization of each anatomo-functional region

Once we had defined the anatomo-functional regions described in Figure 3.5 we evaluated the cognitive networks the most spatially correlated with each of them. To do so we used the platform *LinkRbrain* described in detail in Chapter 6 where the cognitive networks used

	Visual	Visuospatial Goal directed Tools	Calculus WM Executive	TOM Empathy Social	Recall Memory	DMN Self Introspection	Conflict	Reward Drive Valence	Emotion
SPL	High	High							
SMG		High							
Ang		High	High		High	High			
SFG		High	High	High	High				
Pcu			High	High	High	High			
CGp				High	High	High			
CGf					High	High	High	High	High
Or					High	High		High	High

Fig. 3.6.: This figure shows the main cognitive categories (columns) associated with the anatomofunctional regions(rows)

	Hand Motor skills	Speech production Phonation	Auditory perception	Speech perception Voice	Sentence comprehen sion	Semantic memory Lexicon	Face Object recognition	Episodic memory Retrieval	Emotion
SCG	High								
ICG	High	High							
HG		High	High	High					
STG		High	High	High	High				
MTG			High	High	High	High			
ITG						High	High	High	High
FuG						High	High	High	High
PHG						High	High	High	High

Fig. 3.7.: This figure shows the main cognitive categories (columns) associated with the anatomofunctional regions(rows)

as comparison are those determined in section 3.4.2 of the present chapter. In Figures 3.6 and 3.7 we show a qualitatively results obtained.

The cognitive tasks represented in the two figures are the most correlated to the ensemble of anatomo-functional regions presented in each figure. This choice was made to simplify the representation. These two figures elucidate how each anatomo-functional region represents a pole for specific groups of cognitive tasks (marked in dark red in Figures 3.6 and 3.7) while (in lighter red) they take part to the implementation of several groups.

3.4.3.4 Relation between gradients of anatomo-functional regions and gradients of cognitive tasks

Based on the spatial reference frame represented by the anatomo-functional regions described in Figure 3.5 we propose a global scheme to describe the organization of cognitive networks across the cortex. This scheme is determined by: 1) poles of connections of cerebral areas with the rest of nervous structures: the visual pole (LiG, OTG), the motor pole (SCG and ICG), the auditory pole (HG), the pole of vital functions linked to the Hypothalamus (Or), the pole of episodic memory (PHG) linked to the Hippocampus (HIP), the pole of emotional recruitment (TP) linked to the Amygdala (Amy); 2) functional gradients connecting these poles in correspondence of parietal, frontal and temporal regions.

Parietal regions organize functional gradients connecting visual, motor and auditory poles with functions such as visuo-guided movements or space representation. Temporal regions organize functional gradients between the visual and auditory poles, the hippocampal pole devoted to episodic memory, the amygdala pole related to emotions and the hypothalamic pole for vital functions. Interactions between these functional gradients result in learning cognitive functions such as language comprehension. Frontal regions organize functional gradients between the motor pole and the hypothalamic one. Learning on these gradients form cognitive functions such as planning, executive functions, or the temporal organization of sentences.

In the following we will detail these gradients. Since these results have been obtained using LinkRbrain in Chapter 6 based on the Neurosynth database all the references (often hundreds of references) are provided in the LinkRbrain website.

Central and parietal regions

The parietal posterior-anterior gradient: visuomotor integration connecting gaze, hand movement, and space

The parietal posterior-anterior gradient links visual regions (LiG,OTG) to superior motor areas commanding arm-and-hand movements (SCG: superior central gyrus) throughout superior parietal regions (SPL). This gradient (OTG-SPL-SCG) is illustrated in Figure 3.8 in relation with data from the neuroimaging literature extracted by Neurosynth and visualized by our platform LinkRbrain.

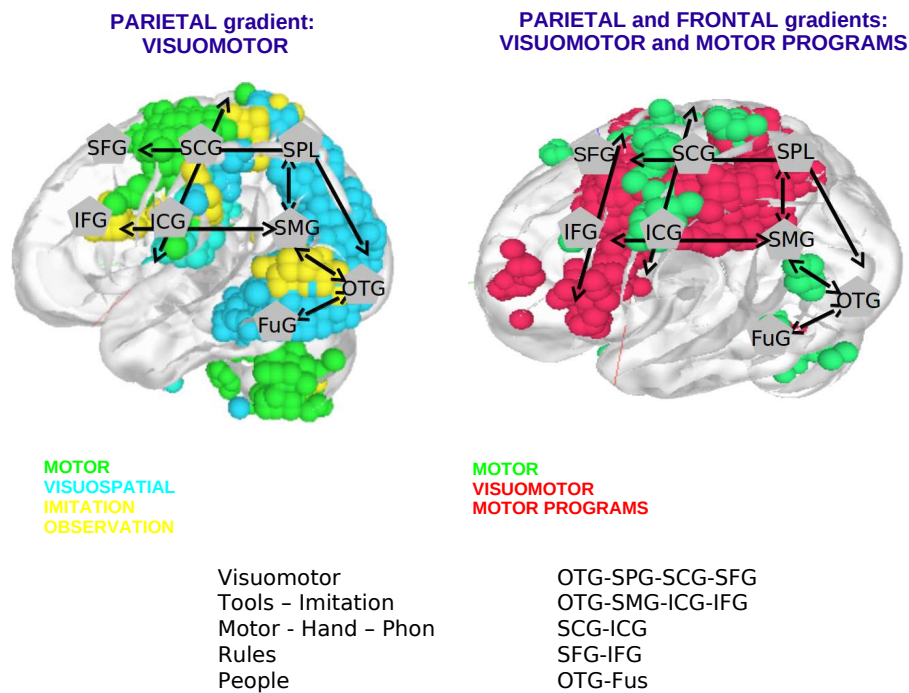


Fig. 3.8.: Parietal gradients

SPL: the Superior Parietal Lobule is connected both with LiG-OTG visual regions and to SCG motor regions: it can learn cognitive tasks implementing visuospatial and visuomotor integration. It can thus relate in a coherent way spatial visual information from LiG-OTG (depth cues, object motion, motion perception), gaze control (gaze, oculomotor, smooth pursuit, eye movement) to motor control for hands and arms (hand, arm, gesture, motor function, movement sequence) implemented in SCG. Visual, parietal and sensorymotor regions project toward the cerebellum that in return projects to the motor cortex. Cerebellum learns how to optimize the command of the movement to anticipate as best as possible the next movement. For example the cerebellum controls the body's muscles to maintain the equilibrium.

SCG: This region comprehends the superior parts of the precentral and postcentral gyri namely the superior portions of the primary motor and somatosensory cortices. These two regions are responsible respectively for motor control and somatosensory information pertaining on arms, hands and fingers. SCG directly project to the motor neurons of the spinal cord which implements the commands of the muscles. SCG regions are connected both to parietal regions on a parietal posterior-anterior gradient, and to frontal regions on a frontal anterior-posterior gradient. The parietal gradient to SCG allows to control movement of hand and fingers based on proprioceptive and tactile feedback received from somatosensory areas, and also from visual information received from SPL. The frontal gradient to SCG allows to control hand and finger movements based on goals, plans, and motor programs. The parietal and temporal gradients are reciprocally connected by connection symmetrical with respect to the central sulcus. As a consequence, proprioceptive information is related

to muscular contractions commands, tactile information is in relation with more integrated gestures (tactile feedback at the end of the gesture), and the visual information to sequences of gestures.

The parietal superior-inferior gradient: from visuomotor integration toward representation of interactions with objects and people

This gradient (OTG-SMG) is illustrated in Figure 3.8. The parietal gradient linking visual to motor areas in the superior part of the parietal lobe (SPL) is accompanied by a second visual to motor gradient in the inferior parietal regions, through the Angular Gyrus and the Supramarginal Gyrus. These two areas are particularly developed in humans and they are directly connected to frontal regions (BAs 44-45) supporting language. Superior and inferior parietal regions form a parietal superior-inferior gradient toward temporal regions involved in recognition (STG, FuG) and naming.

SMG The Supramarginal Gyrus on the parietal superior-inferior gradient toward temporal areas can integrate visuomotor information related to objects and people, together with the appropriate words. In relation with object recognition, it can learn codes representation of tools and manipulation. Since it is also in relation with recognition of human and human actions, it can learn interactions with people and objects (such as “give an object”, “indicate an object by pointing”, important for language learning by children).

Ang The Angular Gyrus, thanks to its connections, can integrate visuospatial relations in a scene with several persons, and anticipate their interactions. The relation with language regions allows to interpret these scenes in term of social relations. The Angular gyrus is also connected to the posterior and then the anterior cingulate regions, which represents intentions (forming the Default Mode Network). This network allows to decode interactions between people in the Angular Gyrus in term of intentions and mental state of others, in relation with memory and language.

Temporal regions

The temporal posterior-anterior gradients for people and emotion recognition

The temporal posterior-anterior gradients relate the occipital regions important for local visual feature extraction, the occipito-temporal regions (OTG) which integrate local features in global shapes, the Fusiform Gyrus (FuG) implementing face and object recognition, the parahippocampal (PHG) regions able to memorize particular faces (relation with the Hippocampus), toward the temporal pole (TP close to the amygdala (Amy) which amplifies the emotions related to faces (emotional recognition of facial expression). This gradient (OTG-FuG-TP) is illustrated in Figure 3.9 in relation with data from the neuroimaging literature extracted by Neurosynth and visualized by our platform LinkRbrain.

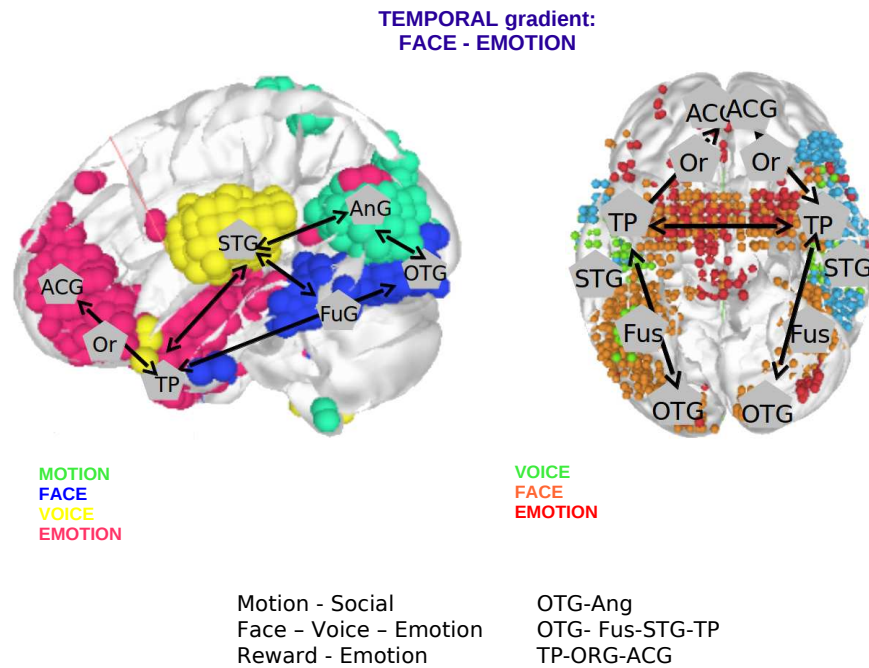


Fig. 3.9.: Temporal gradients

LiG: The primary and secondary visual areas correspond to the occipital Brodmann Areas 17, 18 and 19. The primary visual areas (BA 17) code for the local features of stimuli activating the retina: visual cues (motion, orientation, curvature, color), temporally and spatially repeated stimuli (checkerboard). Secondary areas extract coherent patterns associating local features, such as triangles, symmetries, multi-scale curvatures etc., and also code for saccades toward the most salient stimuli.

OTG: The Occipito-Temporal Gyrus integrates local features extracted from primary and secondary visual areas (LiG) in coherent shapes, as for example integrating multi-scale curvatures and colors necessary to detect eyes, mouth, head and body contours, or integrating local motions into biological movements to recognize facial expressions. These feature correlations performed in real-time generate perception of integrated shapes.

FuG: the Fusiform Gyrus is the next step along the temporal gradient: it can learn to integrate shapes in general categories such as faces, objects, places, etc.. It receives auditory information on voices from STG and can associate voice and face recognition, along with their expressions, in a coherent percept even if the person is not recognized as an individual.

PHG: The ParaHippocampal Gyrus, the next step in the gradient, can learn the recognition of a particular face, depending upon experience (episodic memory in relation with the Hippocampus). PHG can indeed associate all the simultaneous information present about a specific person, along with verbal information such as the name of the person..

TP: The temporal gradient continues till the temporal pole and the amygdala. The amygdala is responsible for emotional amplification when face traits, eye and mouth movements, respiration and the expression of the voice can be related with emotions such as joy, pain, fear, tenderness.

The temporal superior-inferior gradient between the auditory and the hippocampal poles, for language comprehension

The superior-inferior gradient of the temporal lobe organizes the different functions necessary for language comprehension and production. This gradient (STG-MTG-ITG) is illustrated in Figure 3.10 in relation with data from the neuroimaging literature extracted by Neurosynth and visualized by our platform LinkRbrain.

HG: Primary auditory regions are in the superior part of the temporal lobe in correspondence with the Sylvian fissure. These regions code for auditory cues like for example frequencies in a similar way to how primary visual regions code for visual cues. It is the first step of the temporal superior-inferior gradient for comprehension of language.

STG: the superior temporal gyrus is the next step of this temporal gradient. It receives the auditory features. It is also connected to the motor areas for phonation (ICG). This regions can thus process auditory information that the phonatory apparatus is able to produce, that are the phonemes, the sounds proper to a language. Phonemes are learnt thanks to the auditory-phonation loop in a similar way as visuo-motor information in parietal regions. This region is thus specialized to code for recognition and production of speech. It is indeed activated every time we perceive phonemic sounds even we do not understand the meaning.

MTG: the medial temporal gyrus is the next step of the temporal superior-inferior gradient. It is intermediate between STG coding for phonemes and the inferior temporal regions ITG, PHG specialized in memorization of word meaning. MTG can learn words as meaningful sequences of phonemes. MTG is also connected to inferior frontal regions producing structured sequences of phonemes and words. MTG can then participate to sentence recognition by decoding sequences of phonemes in meaningful words.

ITG: the inferior temporal gyrus is the next step of this temporal gradient, intermediate between the MTG processing sentences, breaking them down into words, and the hippocampal and parahippocampal regions performing memorization by auto-association. ITG allows to learn lexicon linking the words of the language to their meaning. In the left hemisphere ITG allows to learn categories and concepts associated with words. This region is strongly activated when performing categorization tasks.

PHG: this region is intermediate between ITG and the hippocampus in the temporal gradient. PHG facilitates the auto-associative memorization of words' meaning performed thanks to the hippocampus (episodic memory) and the recall of memory that can lead to sentence production. PHG is activated at the same time in relation with episodic memory and emotions. The memorization of the meaning is facilitated in presence of emotional arousal determined by the response of the amygdala.

Frontal regions

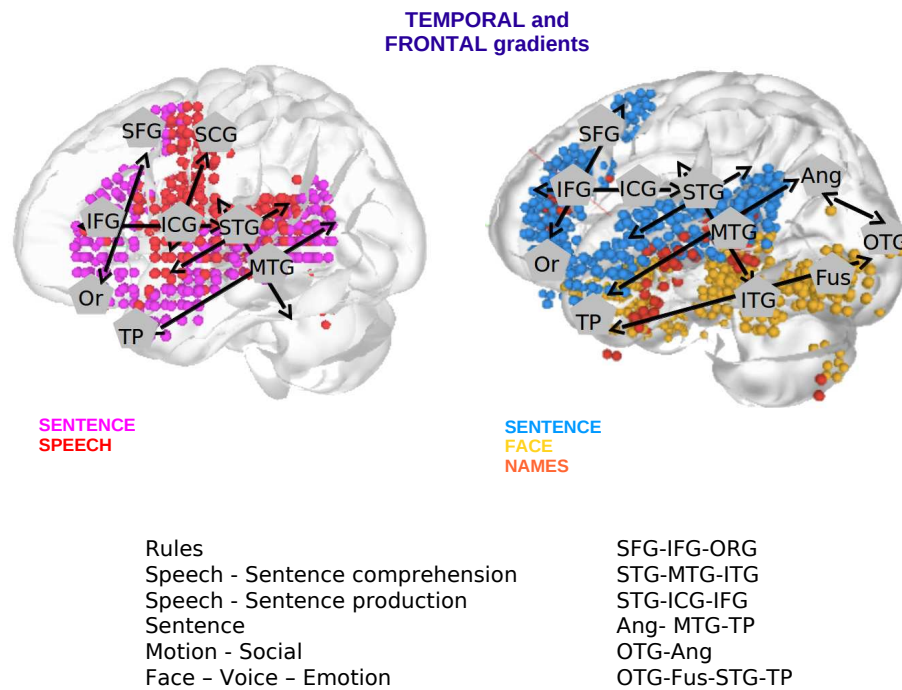


Fig. 3.10.: Frontal gradients

The frontal anterior-posterior gradient between vital functions and motor commands

The frontal anterior-posterior gradient (SFG) and its symmetry with the parietal posterior-anterior gradients (SPL), both converging on motor commands of the hand, is illustrated in Figure 3.8 (SFG-SCG-SPL). The frontal anterior-posterior gradient (IFG) and its relation with temporal regions, both converging on motor commands of phonation, is illustrated in Figure 3.10 (Or,IFG,ICG,STG).

Or: orbito-frontal regions which are connected with the hypothalamus can code for the satisfaction of vital needs (thirst, hunger, thermoregulation) in relations with specific neurohormones. They are also connected with the nucleus accumbens which is characterized by a strong dopaminergic innervation coding activated in reinforcement and reward expectation. Orbito-frontal regions are activated when expecting a reward (drive, motivation), either the satisfaction of vital needs or by secondary rewards. Gradients of connections are organized from this “hypothalamic” pole according to two directions: (1) the frontal antero-

posterior gradient (toward SFG and IFG and then SCG and ICG) can learn sequences of actions motivated by a goal, a reinforcement; (2) the temporal antero-posterior gradient (toward TP, PHG and Fus) can learn categories (objects, places, faces) associated to a reinforcement. Olfactory (orbito-frontal and temporal pole) and gustatory maps (Insula) are strongly interacting with the orbitofrontal regions. Food reinforcement are guided by smell and taste.

SFG: the Superior Frontal Regions are intermediate between the Or regions and the motor regions. This frontal antero-posterior gradient can learn sequences of motor commands and actions that allow to reach a goal or a reinforcement. This gradient is symmetrical to the parietal postero-anterior gradient which performs visuomotor integrations, and both gradients are connected together along this symmetry converging toward the motor regions to activate together the motor programs. SFG regions are characterized by working memory which both memorize previous sensorymotor events and anticipate next ones until the final reinforcement. SFG learns goal-directed sequences of actions adapted to each context and can form: (1) executive control of motor programs and plans (attention shift, switch task) (1) conditional rules of action guiding to the achievement of a goal, (2) inferences and hypotheses aimed to approach the goal; (3) sequences of actions hierarchically encapsulated in chunks; (3) calculation (arithmetic operation).

IFG The Inferior Frontal Gyrus learn sensorymotor actions, like SFG, but specialized for phonation due to its connections to ICG which controls the phonatory apparatus. IFG is connected with the temporal regions STG and MTG coding for words. IFG is also intermediate between Orbitofrontal regions and motor regions, along the frontal antero-posterior gradient. It can learn to produce a sequence of phonemes and words, that are sentences, in order to communicate recollections (stories), vital needs, social relations (social network), emotions. Similarly as SFG, it can generate sustained activities (working memory) which memorize temporarily the pronounced words and predict the next words. IFG can thus form: (1) control of sequences of words (2) conditional rules of word and phonemes (grammatical rule) (3) verbal inferences and hypotheses; (4) sequences of word hierarchically encapsulated in chunks (5) reasoning (mental operations). The frontal superior-inferior gradient between SFG and IFG relate plans and strategies to organization sentences and stories.

3.4.3.5 Relation between two intertwined rings and the 21 anatomo-functional regions

If we map on the brain cognitive networks associated with real time interactions (VSA: motion, oculomotor, motor, somatosensory, speech) and multi-temporal memory task (episodic memory, autobiographical memory, semantic memory and working memory) we obtain the two intertwined rings architecture (see bottom of in Figure 3.11). Since the topography of the two rings is well defined we can establish a direct relation between each ring and a

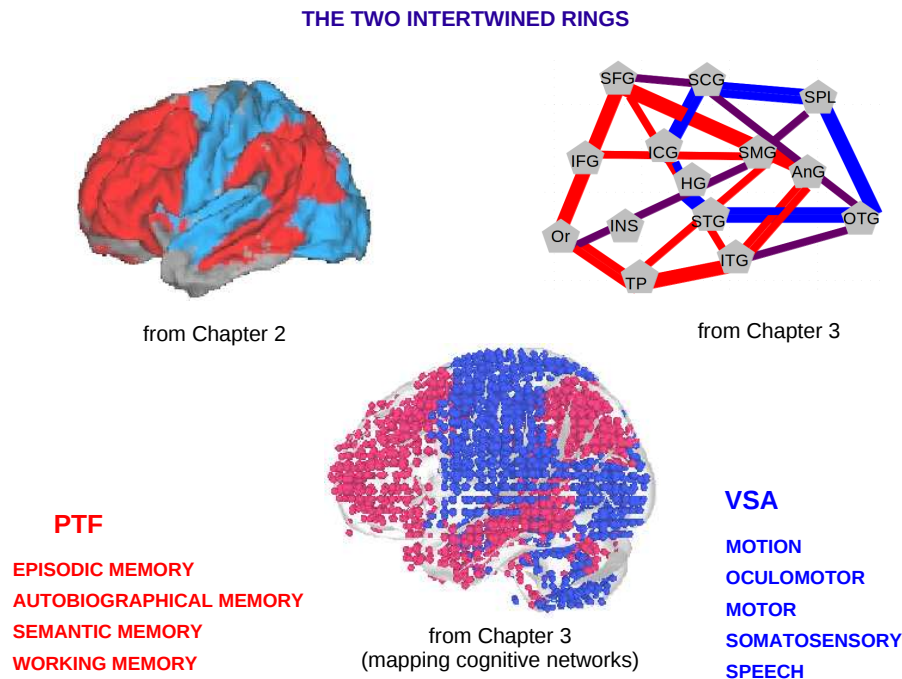


Fig. 3.11.: The two intertwined rings and the 21 anatomo-functional regions

subset of the 21 anatomo-functional regions as shown on the top-right of Figure 3.11. Each anatomo-functional region is assigned to one of the two rings.

3.5 Methods

The set of terms used to tag papers in Neurosynth have been retrieved based on simple frequency ranking methods. Moreover the frequency is evaluated based on the entire body of text of each paper contained in the database and it does not take into account (at least at the time of this work) multigrams such as *working memory task*. We wanted to improve the method for tagging papers focusing on three main points:

- frequency alone is not the best way to find the most representative terms for the experiment described in a paper
- terms represented by single words (e.g.: *memory*, *word*) are less specific than *multi-terms* (e.g.: *autobiographical memory*, *written word*) so that categories turn out to be broader (bigger number of paper related) tying together papers that should not be.
- terms present in sections like *Introduction* or *Conclusions* tend to related to the area of the topic treated but less specific of the particular cognitive task investigated.

Starting from these observations we decided to create a new set of terms to tag papers by:

- restricting our analysis only to the *Abstract* section
- preferring *multigrams* to monograms
- using text mining statistical methods to perform lexical extraction

3.5.1 Neurosynth: inverse inference maps

The Neurosynth database was composed of 4393 (at the time this work was developed) papers retrieved searching *PubMed* database for human fMRI studies. Every paper retrieved is associated with:

- *Peaks of activation*: x, y, z coordinates of the brain where a major activity has been detected during the experiments
- *Most frequent terms* appearing at least once in each section of the paper (e.g.: Introduction, Methods, Conclusions)

In order to perform statistical analysis peaks of activation that are usually reported as standard stereotactic coordinates x, y, z (Talairach or MNI¹) are converted if necessary in MNI standard space and then transformed in binary image masks in the following way [295]: starting from a standard map with $n_v = 231,202$ voxels³ corresponding to a single voxel size of $2\text{ mm} \times 2\text{ mm} \times 2\text{ mm}$, value of 1 assigned to each voxel if it turns out to be in a 10 mm radius from a peak reported in the article and 0 otherwise. For what regards terms the database is restricted to a list of $n_T = 10000$ terms; each paper is then associated with a binary vector indicating the terms present in a paper with a frequency exceeding a given threshold (usually $f = 0.001$). The Neurosynth database is then a 3-D meta-database where each paper i is univocally identified by:

- its *doi*: digital object identifier
- a binary mask of *activated voxels*: $A_i = (A_{ij})$ where $j \in [0, n_v]$
- a binary vectors of *present terms*: $T_i = (T_{ik})$ where $k \in [0, n_T]$

This structure permits to perform easily statistical analysis on the database (see Figure 3.2). The main tools developed are the so called inference maps (χ^2 test based) defined as follows [295]:

- *Forward inference map*: z-scores corresponding to the likelihood that a region will activate if a study uses a particular term (i.e., $P(\text{Activation}|\text{Term})$)

$$P(A_i = 1|T_k = 1) \quad (3.1)$$

- *Inverse inference map*: z-scores corresponding to the likelihood that a term is used in a study given the presence of reported activations. This map gives a more precise information about the possible identification of a cognitive task and a location/activation in the brain corresponding to the *specificity* criteria [295]. To be noticed that this kind of analysis is not addressable in single studies and that it will be the inference map we will refer to in the following of this work.

$$P(T_k = 1|A_i = 1) = \frac{P(A_i = 1|T_k = 1) \cdot P(T_k = 1)}{P(A_i)} \quad (3.2)$$

3.5.2 CorText: lexical extraction

The scientific tools we adopted in order to retrieve our new list of terms are those developed in the context of the *CorText* <http://www.cortext.net> project for *lexical extraction* purposes. In this frame work lexical extraction is performed using Natural Language Processing (NLP) tools [20] in order to automatically identify representative terms pertaining to a given corpus. For terms we mean this time not only single words but also multi-terms. This kind of analysis has been successfully used to produce multi-level (hierarchical) maps of scientific literature and its phylogenetic profile [49].

The core of lexical extraction proposed by *Cortext* is represented by NLP automatic multi-terms extraction; since this methods is not not powerful enough to recognize and extract only salient terms, NLP based extraction is enhanced using existing methods aiming to the extraction of relevant terms seen as those displaying both high *unithood* and high *termhood* [140]. The whole method can be split in two main methodological steps as in the following.

*Classical linguistic processes to define a set of candidate noun phrases*¹

This step exploits NLP to build the raw set of candidate multi-terms and it comprehends:

- *POS-tagging*: (Part-of-Speech Tagging) each term is tagged according to its grammatical nature: noun, adjective, verb, adverb and so on
- *Chunking*: tags are used to identify *noun phrases*¹

¹*Noun phrase*: a noun phrase can be minimally defined as a list of successive nouns and adjectives.

²*Hyphens*: punctuation mark (-) used to join words.

- *Normalizing*: orthographic differences are corrected between multi-terms respect to the presence/absence of hyphens² (e.g.: *single-strand polymer* and *single strand polymer* are put in the same class)
- *Stemming*: terms sharing same stem are gathered together (e.g.: singulars and plurals)

Statistical criteria to sort the list of candidate multi-terms

This step aims to refine NLP tools and it based on the observations that salient terms tend to appear more frequently and that longer phrases are more likely to be relevant (unithood) and that neutral terms may appear in any document of the corpus independently from the precise thematics addressed by the document (termhood).

- *Counting*: each multi-terms belonging to a given stemmed class is counted in the whole corpus of papers to obtain their frequency in the overall
- *C-value*: for each multi-stem is evaluated the corresponding C-value (unithood) according to [88]
- *Sorting*: the list of candidate multi-stems is ranked according to their unithood and reduced to the first N multi-stems in order of C-value.
- *Termhood θ* : for each term its termhood *theta* is evaluated and the list of terms is sorted according to this index [74]. The termhood *theta* of a multi-stem is the sum of the chi-square values it takes with every other classes in the list: irrelevant terms should have an unbiased distribution compared to other terms in the list. This allows to get rid of irrelevant multi-terms that may still be very frequent like: *review of literature* or *past articles*. This is a second order statistical analysis based on the co-occurrence matrix M between each item in the list

3.5.3 Cognitive terms: lexical and topographical similarity

In order to study the structure of the relations among terms according to both their double nature we described above we adopted two different similarity measures:

- *Lexical*: to establish the lexical similarity among terms due to their co-occurrence in papers we used the asymmetric measure proposed in [288]:

$$P_{ij} = \frac{\sum_k \min(M_{ik}, M_{jk})}{\sum_i M_{ik}} \quad \forall i, k \quad s.t. \quad M_{ik} > 0 \quad (3.3)$$

where M_{ij} represents the *mutual information* between the term i and j .

- *Topographic*: to establish the topographical similarity among terms due to activations in the cortex we used a measure based on the amount of voxels overlapping between the *inverse inference map* of terms i and the one of term j

$$P_{ij} \sim A_i \cap A_j \quad (3.4)$$

where A_i and A_j represent voxels activated in the *inverse inference maps* relatively to terms i and j .

3.6 Conclusions

We improved the potentialities of Neurosynth framework introducing a new way to tag papers based on computational linguistic tools. This permitted a more precise classification of the papers according to different cognitive tasks (increasing the power in discriminating papers) and a finer analysis of how networks activated by different cognitive tasks are disposed on the cortex surface. The observation of this global organization of cognitive tasks led to the conclusion that two big clusters of cognitive tasks: one related to sensory motor tasks (physical interaction with the external world) the other one related to mentalizing tasks (abstract representation of the external world and of the self). we deepened the analysis of the organization of these networks at a finer level. To do so we built a graph of topographical similitude among several hundreds of cognitive networks covering all the domains, sensory-motor, emotional, vital needs and cognitive. This analysis allowed not only to find again the ring organization but also to establish relations and continuity across different cognitive domains. We finally propose a global scheme to describe the organization of cognitive networks across the anatomo-functional regions of the cortex. This scheme is determined by: 1) poles of connections of cerebral areas with the rest of nervous structures; 2) functional gradients connecting these poles within parietal, frontal and temporal regions. These results are fundamental to understand the work presented in Chapter 5 showing the correlation between gene expression and anatomo-functional regions. We found indeed that it was not possible to clearly relate the expression for a single gene with one anatomo-functional region and even less with a cognitive network but instead it was possible to relate in a robust way gradients of gene expression with gradients of anatomo-functional regions and then with gradients of cognitive networks.

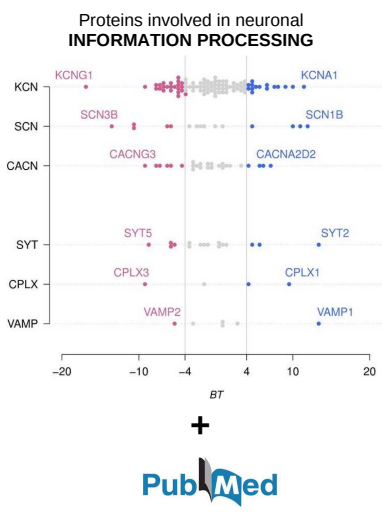
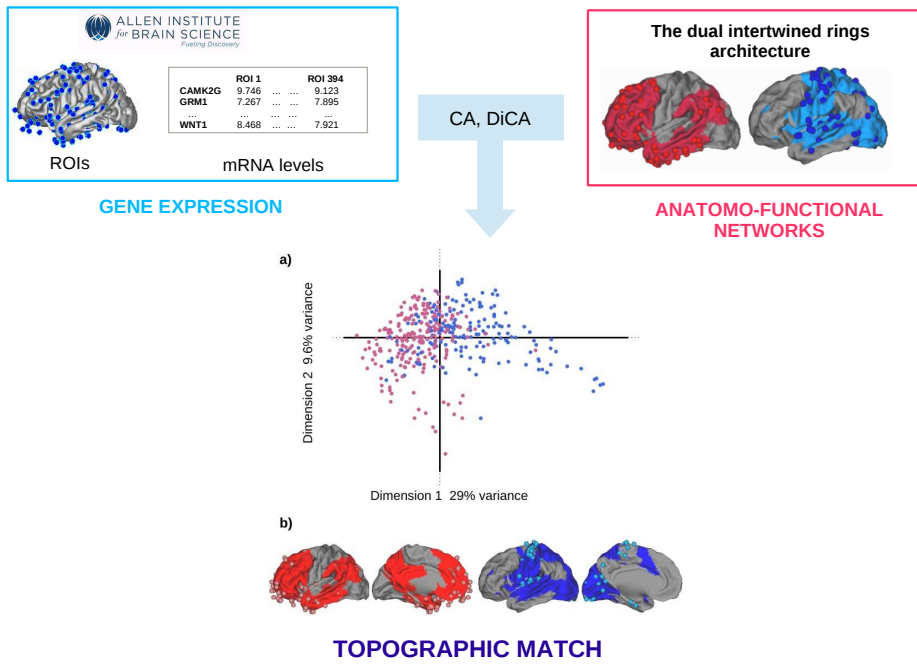
Part II

Cortical organization of gene expression in
relation with anatomo-functional networks

Cortical gene expression match the temporal properties of large-scale functional networks

In the previous chapters we studied the anatomo-functional organization of the cortical networks at two different scales: the global scale of the two intertwined rings architecture and the local scale describing the mutual organization of different cognitive networks as described in fMRI literature. We also introduced the parallel between the type of information processing performed at the level of cognitive networks and the one performed by the underlying neuronal networks. In this chapter we wanted to explore the link between cortical gene expression patterns and anatomo-functional regions. In particular we wanted to do that at the global spatial level represented by the two intertwined rings architecture. The first question we wanted to answer was: given the well defined anatomo-functional topography of the two rings VSA and PTF, is there a spatial match with cortical gradients of genes? The second question was if this topographic match does exist can we find a functional match between the information properties proper to the two different rings—real-time vs multi-temporal—and the one of the groups of genes possibly topographically related to these two ensembles of regions? To answer these questions we used the human brain transcriptome data provided by the Allen Institute. We studied these data in relation to the two intertwined rings architecture by means of multivariate statistical techniques such as Correspondence Analysis (CA) and Discriminant Correspondence Analysis (DiCA). Figures 4.2 and 4.9 show the main results of this work published in *Cioli et al., PLoSOne 2014*.

4.1 Graphical abstract



	VSA ring	PTF ring
Cortical topography		
Cognitive functions	Sensory-motor, uni and bi-modal	Memory, language and vital functions
Temporal information processing	Real time interactions	Multi-temporal integration
Potassium channels	KCNA1, KCNC1 High temporal precision	KCNG1 Modulation of K currents
Sodium channels	SCNA1, SCNB1 High temporal precision	SCNA3, SCNB3 Persistent currents, sustained activity
Calcium channels	CACNA2D2 Fast, stimulus driven release	CACNA1H Spontaneous release, Rhythms generation
Synaptotagmins	SYT2 Kiss and run, fast evoked release	SYT5, SYT9, SYT10 Spontaneous, slower release
Complexins	CPLX1 Stimulus driven control of release	CPLX3 Spontaneous release
Synaptobrevins	VAMP1 High frequency evoked release	VAMP2 Maintains the pool of available vesicles

FUNCTIONAL MATCH

4.2 Abstract

We explore the relationships between the cortex functional organization and genetic expression (as provided by the Allen Human Brain Atlas). Previous work suggests that functional cortical networks (resting state and task based) are organized as two large networks (differentiated by their preferred information processing mode) shaped like two rings. The first ring-Visual-SensorimotorAuditory (VSA)-comprises visual, auditory, somatosensory, and motor cortices that process real time world interactions. The second ring-Parieto-Temporo-Frontal (PTF)-comprises parietal, temporal, and frontal regions with networks dedicated to cognitive functions, emotions, biological needs, and internally driven rhythms. We found-with correspondence analysis-that the patterns of expression of the 938 genes most differentially expressed across the cortex organized the cortex into two sets of regions that match the two rings. We confirmed this result using discriminant correspondence analysis by showing that the genetic profiles of cortical regions can reliably predict to what ring these regions belong. We found that several of the proteins-coded by genes that most differentiate the rings-were involved in neuronal information processing such as ionic channels and neurotransmitter release. The systematic study of families of genes revealed specific proteins within families preferentially expressed in each ring. The results showed strong congruence between the preferential expression of subsets of genes, temporal properties of the proteins they code, and the preferred processing modes of the rings. Ionic channels and release-related proteins more expressed in the VSA ring favor temporal precision of fast evoked neural transmission (Sodium channels SCNA1, SCN1B1 potassium channel KCNA1, calcium channel CACNA2D2, Synaptotagmin SYT2, Complexin CPLX1, Synaptobrevin VAMP1). Conversely, genes expressed in the PTF ring favor slower, sustained, or rhythmic activation (Sodium channels SCNA3, SCN3B3, SCN9A potassium channels KCNF1, KCNG1) and facilitate spontaneous transmitter release (calcium channel CACNA1H, Synaptotagmins SYT5, Complexin CPLX3, and synaptobrevin VAMP2).

4.3 Introduction

In order to understand how the human cerebral cortex processes information we need to connect the anatomo-functional organization of the cortex (as described, e.g., in [85, 156, 189]) with the topographic organization of gene expressions [228, 233, 104]. To do so, several recent studies have analyzed-in species such as monkey, mouse, and human [117, 297, 106]-the pattern of genetic expression of cortical regions (e.g., visual or prefrontal cortices). These studies revealed that cortical regions differ in the genes that they express. This pattern can be seen, for example, in mouse brain atlases of gene expression [25, 89, 90, 107, 291]. In humans-because the strong constraints of postmortem genome-wide analysis

make the data hard to obtain-only very few studies [117, 101] have explored the systematic anatomic organization of genetic expression across the whole brain.

By contrast with this small number of genetic systematic analyses, there are several systematic analysis of anatomo-functional cortical networks and functional connectivity as revealed by brain imaging. Together these studies show (as supported by several meta-analyses) that the correlations between task based networks (TBN), resting state networks (RSN), and anatomical networks (AN) are particularly robust [156, 189, 292, 247]. So, both the cortical expression of genes and the functional networks have been explored, but no attempt has been made, so far, to relate the information processing performed by cortical functional networks and the specific cellular properties of proteins coded by genes expressed in these networks. In this paper, we focus on the functional differences observed at large scales between networks which directly process the interaction with the external world and networks which are more internally driven. This large scale functional dichotomy-taken into account also in [41, 42, 257, 214]-has been systematically analyzed and modeled in [189] where we showed that task TBNs, RSNs, and ANs could be integrated into a common model called the “dual intertwined ring architecture” (Figure 4.1). Although this architecture had not been previously discussed as such, most published results dealing with the organization of RSNs present patterns that are compatible with it [72, 296, 238].

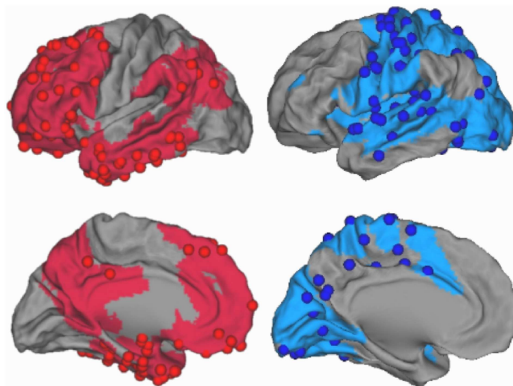


Fig. 4.1.: The two intertwined rings corresponding to different type of temporal processing. The VSA ring (in blue) corresponds to high fidelity evoked processing and the PTF ring (in red) corresponds to more spontaneous processing more independent of input action potentials timing (from [189]). Cortical regions sampled by the Allen Institute for Brain Sciences ([7]) are represented by spheres colored like their respective rings. Points in sulci are not visible.

According to this “dual ring” model, the human cerebral cortex comprises two large structures shaped like rings. The first ring-called the Visual-SensorimotorAuditory (VSA) ring- is continuous and forms a circle around parietal areas BA 39 and 40, whereas the second ring-called the Parieto-Temporo-Frontal (PTF) ring- is not fully continuous over the cortical mantle but is closed by long-range association fiber tracts (longitudinal parieto-frontal, arcuate, uncinata, and cingulum) that complete the intertwining. The two rings share a

set of common regions mostly localized along the precentral, intraparietal, and superior temporal sulci. The correlation of RSN and TBN as described in [156, 247] shows that VSA regions integrate various sources of auditory, visual, and somatomotor information together. VSA regions also perform bimodal interactions: between visual and motor (e.g., grasping, reaching, imitation) between auditory and somatomotor information (e.g., recognizing and producing phonemes) and between auditory and visual information (important for communication). All these functions imply strong real time constraints.

A similar comparison with RSNs and TBNs shows that the PTF ring implements at least four main groups of functions [156, 189, 247]: (1) biological regulation, olfaction, taste, and emotion which operate at different time scales, [156] (2) working memory and attention: planning and working memory (in the lateral frontal network of the PTF ring) which are based on the integration of information across time by sustained neuronal activations and are able to integrate in the same sequence, several sensory and motor events separated by long and variable delays (reviewed in [191, 93]), (3) self-referential functions and social cognition which require information to be integrated at different temporal scales from the past (memory), the present and the future [112, 217, 231, 232, 31] and (4) language which necessitates integration of information at different time scales (words, sentences, story) [19].

By contrast with the real-time information processing of the VSA ring, we propose that the functions implemented by PTF are produced by “multi-temporal integration” processes. The dual process that we postulate across the two rings (i.e., real-time and multi-temporal integration) is close to the dual process proposed in [92, 94] with both perception-action cycles and working memory (WM) processes. Evidence for this regional temporal specialization has also been found in experiments using single cell recording in non-human primates [194] and in empirically based mathematical models of the human cortex [148]. Furthermore, evidence from brain imaging and brain lesions indicates that spontaneous activity characterizes regions belonging to PTF. For example, in [217] the authors report from brain imaging experiments that regions corresponding to a large portion of PTF (specifically the “default mode network”) are spontaneously active even when no task is performed. Similarly patients affected by lesions within the dorsolateral prefrontal cortex suffer loss of spontaneous motor activity and spontaneous language production, a pattern often described as the “frontal syndrome” (see review in [191, 93, 176]).

The comparison of the sensorimotor and cognitive functions implemented by the two rings shows—in agreement with the literature cited above—that the two sets of functional networks differ essentially in the way they process information: The functional networks forming the VSA ring process real time information whereas the functional networks forming the PTF ring process multi-scale temporal information with a wider time range and also generate spontaneous activity. We expect that the difference between the processing modes of the rings will be reflected in the dynamics implemented in their populations of neurons. For ex-

ample, neuron activation can be evoked by incoming action potentials with high temporal precision or conversely spontaneous and more independent on timing of input action potential. High temporal precision and strongly input driven dynamics should be favored in the VSA ring while more spontaneous, sustained, and rhythmic activity should be favored in the PTF ring. These different types of information processing are likely to be implemented by families of proteins regulating ionic currents (i.e., potassium channels (KCNs), sodium channels (SCNs), and calcium channels (CACNs)) and neurotransmitter release (such as, e.g., synaptotagmins or synaptobrevins). We thus expect-in accordance with their information processing specialization revealed by brain imaging studies-to find differences in the expression of genes coding for ionic channels and transmitter release in the VSA and PTF rings.

In the present study, we explore the differential expression of genes into the two rings and the differential properties of related proteins critical for information processing. To estimate cortical genetic expression we used the Allen Human Brain Atlas (ABA) [133] of the human transcriptome-produced by the Allen Brain Institute-which provides microarray expression profiles of almost every gene of the human genome at hundreds of locations in the brain for two complete postmortem brains. Figure 4.1 shows the localization of ABA regions with respect to the two rings topography. In this paper:

(1) we used correspondence analysis (CA) to describe the pattern of expression of the 938 genes with the largest variance of expression (as in [117]) and found that the first dimension of this analysis opposes two large sets of regions; (2) we show that these two sets of regions representing the major source of genetic variation match the topography of the two rings; (3) we corroborate the results of (1) and (2) by showing that each cortical region can be reliably associated with one of the two rings based on its profile of genetic expression; (4) we show that genes are organized into two exclusive groups that reflect the functional opposition between the two rings; (5) we show that many proteins coded by genes that most differentiate between cortical regions belong to families of proteins involved in neuronal information processing such as ionic channels and neurotransmitter release; (6) we show that the systematic study of families of genes identified in (5) (e.g., ionic channels) reveals the proteins most expressed in each of the two rings; and (7) we show that the temporal properties and neural dynamics of these proteins closely correspond to the information processing differentiated in the two sets of functional networks.

To obtain these results we used multivariate analysis techniques. First, we used CA [284, 108, 290, 4, 3] to describe the patterns of genes expression over the cortex. This multivariate descriptive technique classifies the regions based exclusively on their expression profile and does not take into account their topographical position (e.g., if they belong to the VSA or PTF areas or not). Second, we used discriminant correspondence analysis (DiCA) [2]-a discriminant analysis method derived from CA-to quantitatively evaluate whether the differences in gene expression across cortical regions are informative enough to predict the

ring membership of these regions. We also used DiCA analysis to identify the genes that most contribute to the differentiation between the rings.

4.4 Materials and Methods

4.4.1 Data Base

The data used in this paper were obtained from the Allen Brain Atlas project [133]. We used for this study two postmortem brains (H0351.2001 and H0351.2002) that were sampled for (respectively) 946 and 896 distinct brain locations representing all structures within the brain in approximate proportion to the volumetric representation of each cortical, subcortical, cerebellar, and brain stem structures. From these two sets of regions, we selected the subsets of: (1) all 394 cortical regions in the first brain, and (2) all 337 cortical regions in the second brain. The genetic expression of the cortical regions was described by the subset of 938 genes selected in [117] for their ability to generate the largest differences among 56 groups of regions of the cortex. In this paper, we present only the analysis performed on Brain H0351.2001 because the analysis performed on Brain H0351.2002 provided highly similar results (the results for Brain H0351.2002, however, can be found in the Supporting Material).

4.4.2 Labeling of cortical regions by VSA or PTF rings

The 394 (for Brain H0351.2001) and 337 (for Brain H0351.2002) cortical regions used in this study were identified from their MNI (Montreal Neurological Institute; [78]) coordinates which were then used to assign each region to one of two groups of regions: ring VSA or ring PTF according to the labeling scheme described in [189].

4.4.3 Statistical Analysis I: Correspondence Analysis (CA)

In order to describe cortical genetic organization we used correspondence analysis (CA) [284, 108, 290, 4]. CA-a variant of principal component analysis (PCA)-is used when the data are non-negative numbers (as is the case here, see [3, 240]) and when the goal is to compare observations according to the relative distributions-as opposed to the absolute values-of a set of variables. Here, observations are brain regions and variables are genes, as measured by their expression values. To do so, for each region, the genetic expression values are scaled such that their sum is equal to one (this re-scaled vector of genetic values for a given observation is called a profile) and a generalized PCA (i.e., a generalized singular value decomposition, see, e.g., [284, 4, 13]) is then applied to the profile data matrix. This generalized PCA creates-from both observations and genes-a

new set of orthogonal variables, called factor scores (a.k.a. components or dimensions), that best represents the variability in the original data. Observations and variables are assigned scores- called factor scores-on the factors. These factor scores can be used to create (for both cortical regions and genes) maps in which the proximity between items reflects the similarity of their profiles. To better identify the genes consistently associated with a given dimension, we also computed bootstrap ratios (see [5, 154]). To do so, we generated 1,000 new bootstrapped samples by sampling with replacement from the set of cortical regions. The factor scores for the variables of each bootstrap sample were then computed as supplementary (a.k.a., “out of sample”) variables (this procedure is sometimes called “partial bootstrap,” see, e.g., [284]). For each gene, the mean and standard deviation of these factor scores were then computed and a statistic akin to Student’s t-called a bootstrap ratio (denoted BT, see, [154], for details)-was then computed by dividing the mean bootstrapped factor score of this gene by its standard deviation. By analogy with a t-statistic, a bootstrap ratio value of 2.00 will (roughly) correspond to a (un-corrected for multiple comparisons) p value of .05. Using a Bonferroni correction [1] for multiple testing for 938 comparisons (i.e., the number of genes) will give a corrected value of 3.90 that we rounded to 4.00. We used the implementation in the R programming language (R Development Core Team, 2013) of CA obtained from the packages ExPosition and InPosition (see [13] and <http://cran.r-project.org/web/packages/ExPosition/index.html>). We also used the R packages Hmisc (<http://cran.r-project.org/web/packages/Hmisc/index.htm>) and beeswarm (<http://cran.r-project.org/web/packages/beeswarm>).

4.4.4 Statistical Analysis II: Discriminant Correspondence Analysis (DiCA)

In order to test our hypothesis that the profile of genetic expression of a region depends upon its ring (i.e., VSA or PTF), we used discriminant correspondence analysis (DiCA)-a discriminant analysis version of CA [2]-to predict the regions’ ring from their gene expression profiles. We used the implementation of DiCA in the TExPosition/TInPosition packages (<http://cran.r-project.org/web/packages/TInPosition/index.html>; see also [13] and R Development Core Team, 2013). DiCA creates a matrix that represents each group (i.e., PTF and VSA) by the sum of its observations (for all the gene expressions). In our case, this matrix is a 2×938 (2×161 for the second pool of genes analyzed) data table that contains the sum of each gene expression level (columns) for each ring (rows). This data table is then analyzed by CA (this step solves the discriminant problem because CA computes factor scores that maximize the difference between rows). The original cortical regions are then projected as supplementary elements (a.k.a. “out of sample”) in the group factor space and the distance of each cortical region to each ring is also computed in this space [284]. Finally each cortical region is assigned to its closest ring. The quality of this assignment can be assessed by 1) a confusion matrix that shows for each ring the number of cortical regions of this ring assigned to this and the other ring and 2) by an

R^2 statistic computed as the ratio of the ring variance to the total variance of the cortical regions. A random effect confusion matrix is also computed using a leave one out cross-validation scheme: For each cortical region, the whole analysis is run without this region which is then projected (as a supplementary element) in the ring factor space and assigned to the closest ring. The quality (i.e., “significance”) of the R^2 is evaluated by computing a probability distribution under the null hypothesis with a permutation test: For 1,000 iterations, the labels of the cortical regions are shuffled and the R^2 is recomputed. In addition, a permutation test was also used to evaluate the null hypothesis of an overall effect and to identify significant components (see [13]). Also, the bootstrap resampling scheme used in CA (obtained by resampling the cortical regions with replacement) was also used in DiCA to compute bootstrap ratios for the genes and also to derive confidence intervals for the groups. An equivalent bootstrap resampling scheme was used to compute bootstrap ratios for the regions. To further assess the quality of the assignment model, we also used the model computed on one brain to assign to their rings the brain regions of the other brain.

4.5 Results

For this study, we replicated all results by performing the same analysis on two different postmortem brains for which a similar genome-wide analysis was performed. We found that the conclusions were highly similar (see also [117]), thus for simplicity we present in details only the results for Specimen H0351.2001. Complete results about Specimen H0351.2002 are reported in the Supporting Information.

4.5.1 Gene expression spontaneously separates the rings

We first performed a descriptive multivariate analysis of the topographic distribution of genetic expression over the cortical surface. This analysis can reveal if there is an underlying organization of these expressions. Specifically, we used CA (see Materials and Methods) to describe the relationships between 394 cortical regions and the expression of 938 genes that were selected by [117] because these genes had the largest variation in expression across the cortical surface (see Materials and Methods section). CA (a multivariate descriptive method) computes—without about using the a-priori information about ring membership—the similarity between cortical regions based on their profiles of genetic expression and represents the configuration of the similarity between these regions along dimensions (also called factors) that maximize the variance between these cortical regions. CA also represents, in the same space, the similarity of the genes derived from their profiles of expression over the regions (see [284]).

The analysis revealed that a large proportion (i.e., 47%) of the explained variance was concentrated on the first four dimensions that explained respectively: 29%, 9%, 5%, and 4%

($p < .001$, $.001$, $.001$, $.001$, respectively by permutation test) of the total variance. Figure 4.2A displays the map obtained by plotting the region factor scores for the first 2 dimensions of the analysis. This graph shows that there are two different sub-sets of cortical regions opposed on the first dimension. In Figure 4.2A, each region is represented by a dot colored according to its topographical membership to the VSA ring (in blue) or to the PTF ring (in red) to indicate if the two ring structure was related to the first dimension of CA. Figure 4.2A shows that PTF regions are clustered on the left side of Dimension 1 (negative factor scores), whereas most of the VSA regions are clustered along the right side of Dimension 1 (positive scores). When we plot the highly significant regions (using their bootstrap ratios, see Materials and Methods) on the cortical surface (Figure 4.2B) we find that the two sub-sets show a clear match between the first dimension and the PTF and VSA rings. This configuration of the regions on Dimension 1 indicates that the patterns of gene expressions spontaneously organize the cortical regions in two groups that closely correspond to the VSA and PTF rings (note that this result is obtained without using the information about the regions anatomical position or ring assignment). Thus, the functional model in two rings appears to be the primary source of cortical genetic variation.

This result is confirmed by a similar analysis performed on Brain H0351.2002. Here again, the first dimension of the CA clearly opposes two ensembles of regions that match the two rings (Figure A.1). Region factor scores for Dimensions 1 and 2 and region bootstrap ratios for Dimension 1-for Brains H0351.2001 and 2 - are reported as supporting material in Table A.1 and Table A.2.

4.5.2 Cortical gene expression predicts the assignment of cortical regions to the rings

In the previous section, we showed that the first dimension of CA identified two distinct subsets of cortical regions. These subsets closely match the PTF and VSA rings. The large proportion of variance explained by Dimension 1 of the CA indicates that the different profiles of genetic expression are associated with different rings, but is this large association strong enough to actually predict the ring membership of cortical regions? For the present analysis, we labeled each cortical region according to its membership to the PTF or VSA rings (following the scheme described in [189]) and used a discriminant analysis version of CA- DiCA-to assign each region to a ring. To assign a region to its ring, DiCA combines the values of gene expression to create new optimal dimensions that best discriminate these two groups of regions and also identify the genes responsible for this separation.

With two groups, DiCA extracts only one dimension. In addition to separating the two a priori groups (PTF and VSA, see Figure 4.3 for Brain H0351.2001 and Figure A.2 for Brain H0351.2002), DiCA also provides information on the assignment- predicted from gene expressions-of the cortical regions to these groups.

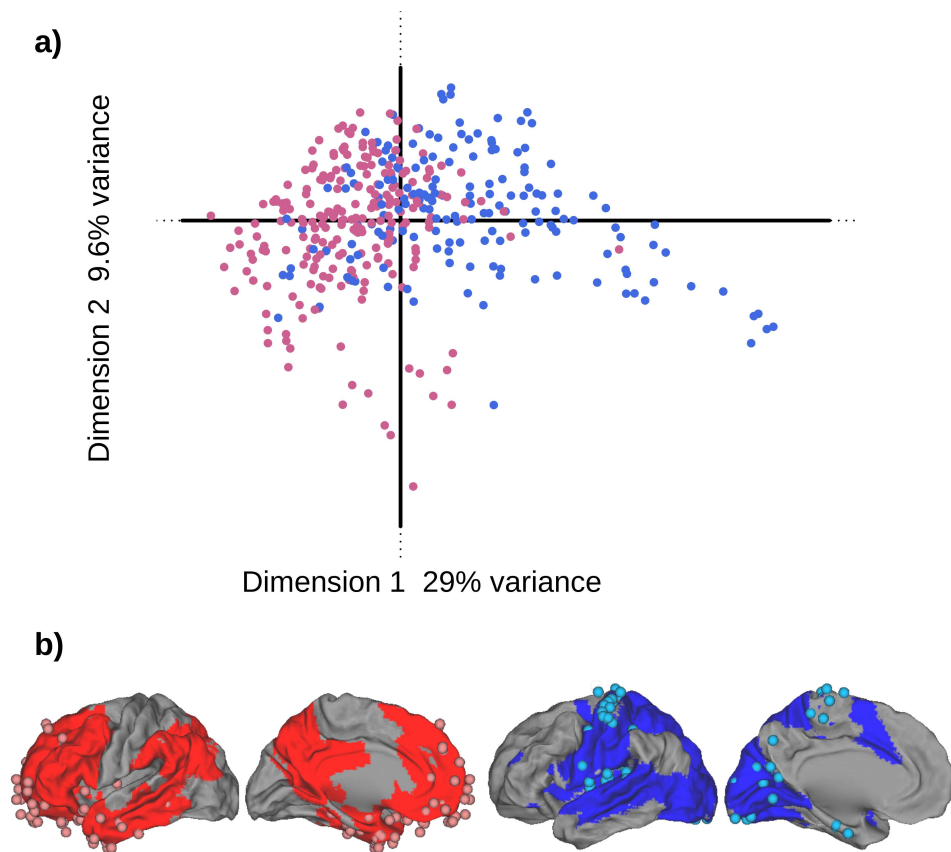


Fig. 4.2.: Differential distribution of gene expression: CA analysis. a) Dimensions 1 and 2 as extracted by a CA performed on the 394 regions and the 938 genes. The dots represent the factor scores for the regions; each dot is colored in red or blue depending on the represented region localization within (respectively) PTF or VSA. The eigenvalue of Dimension 1 ($\lambda_1 = 4.59^{-03}$) represents 29% of the total variance. The eigenvalue of Dimension 2 ($\lambda_2 = 1.51^{-03}$) represents 9% of the total variance. b) The localization of the cortical regions on the brain with PTF and VSA rings colored in, respectively, dark red and dark blue. Light red dots represent regions with significant negative factor scores ($BT < -2.00$) whereas light blue dots represent regions with significant positive factor scores ($BT > 2.00$).

As can be seen in Table A.3, 320 out of the 394 cortical regions were correctly classified (i.e., 81%, $p < .0001$ by Binomial test; for Brain H0351.2002, cf. Table A.4, we found 315 out of 337 regions correctly classified, or 93%, $p < .001$, by Binomial test). To insure that this performance was genuine, we also used a random effect model based on a leave one out procedure (see Materials and Methods section, see, also results in Table A.5 for Brain H0351.2001) and found that we could then correctly assign 319 out of 394 regions (i.e., 81%, $p < .0001$ by Binomial test, for Brain H0351.2002, cf. Table A.6, we found 313 out of 337 regions correctly classified or 93%, $p < .001$, by Binomial test). All these results clearly confirm that the genetic profile of a cortical region can determine its localization within one of the two functional rings.

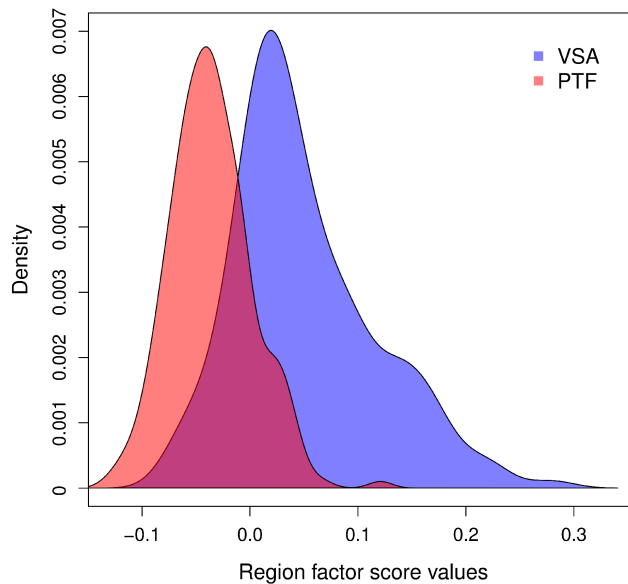


Fig. 4.3.: DiCA analysis: regions factor scores histogram. We plot the histogram of the factor score values-obtained for the 394 regions by the DiCA analysis-as a function of the number of regions a priori assigned to the VSA (blue) or the PTF (red) ring.

4.5.3 Correlation between gene expressions

To better understand the organization of the genes between and within the rings (along the first dimension), we computed the correlations (across the regions) between genes. To graphically represent these correlations we ordered the genes according to their position on Dimension 1 of the DiCA (see Table A.7) and colored the correlations according to their values (see Figure 4.6). As can be seen in Figure 4.6, the correlations (outside the diagonal) ranged from -0.89 to $+0.96$ and the genes were clearly organized into two exclusive blocks with genes positively correlated within each block and negatively correlated between blocks. This opposition reflects, at the gene level, the functional opposition between the two rings.

4.5.4 The proteins coded by genes most differentiated between cortical regions belong to families of proteins involved in neuronal information processing such as ionic channels and neurotransmitter release

In order to identify the genes important to discriminate between PTF and VSA rings, we also computed bootstrap ratios for the genes (see Figure 4.5, see also Table A.7 and Table A.8 for the complete list of genes and their bootstrap ratios for the two brains). Out of 938, we found that 650 (i.e., 69.2%) genes had a significant bootstrap ratio (BT) for the first dimension (a value of $BT > 4.00$ roughly corresponds to a Bonferroni/Sidak corrected value of $p = .05$ for 938 comparisons, see [1]).

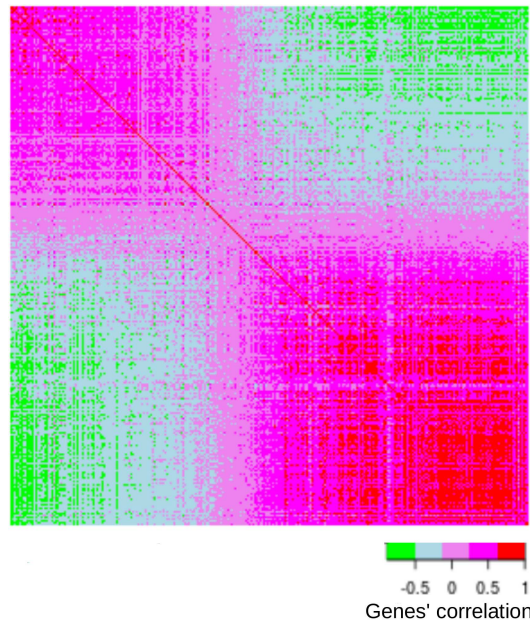


Fig. 4.4.: Heatmap representing the correlations between the 938 genes used in DiCA. The correlation coefficients between genes were computed using all 394 regions. The genes are ordered according to their positions on the dimension extracted by DiCA. Red to magenta colors denote strong positive correlations whereas green denotes a strong negative correlation. The genes are clearly organized into two blocks that are related to the gene differential expression for the two rings.

Among the genes that mostly differentiate between the two rings, we found genes that code for proteins important for neuronal functions such as ionic channels, neurotransmitter release, receptors, cytoskeleton, transcription factors, and cellular recognition. Specifically, associated with the VSA ring, we found genes coding for sodium channels isoforms such as *SCN1A* ($BT = 15.81$) and *SCN1B* ($BT = 16.54$) and genes coding for potassium channels isoforms such as *KCNA1* ($BT = 14.98$). By contrast, associated with the PTF ring, we found *KCNG1* ($BT = -14.06$) that codes for a potassium channel, and *CACNA1H* ($BT = -10.13$) a gene that encodes syntaxin-1A/Ca(v)3.2 T-type calcium channel. Along the same lines, we found strongly associated with VSA, genes encoding for proteins implied in neurotransmitter release such as *SYT2* ($BT = 13.58$), *CPLX1* coding for Complexin 1 ($BT = 12.42$) that influences the fast kinetics of cellular recognition release (i.e., “kiss-and-run”). We found also *VAMP1* encoding for Vesicle Associated Membrane Protein ($BT = 17.12$) strongly associated with the VSA ring and important for maintaining the pool of vesicles for high frequency stimulus driven release.

Among the other families identified by their high bootstrap ratios we also found glutamate receptors (*GPRIN1*, $BT = -8.56$; *GRM1*, $BT = -7.78$), hormone receptors (*ESRRG*, $BT = 16.31$; *PMEPA1* $BT = 11.84$), neuropeptides (*GRP*, $BT = -9.45$; *TAC1*, $BT = -7.66$), kinases (*PLCD4*, $BT = -15.40$; *PRKDCCD*, $BT = -11.44$), transcription and growth factors (*EGFR*, $BT = 15.29$; *ASCL2*, $BT = 11.54$), genes implicated

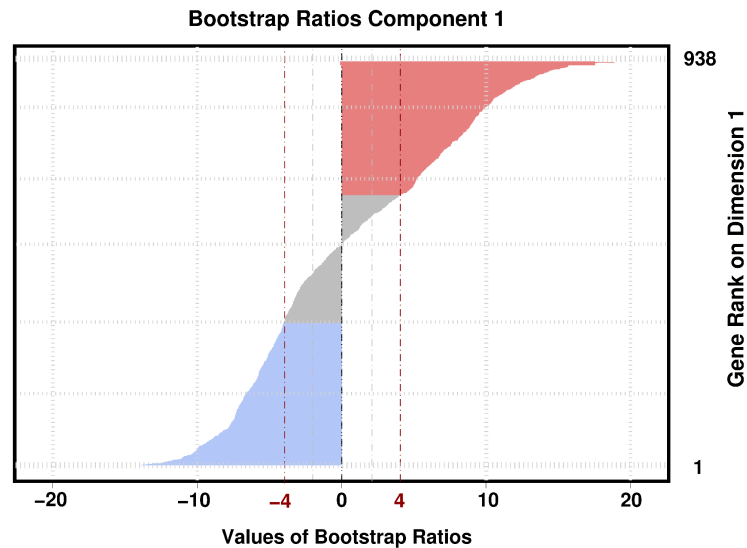


Fig. 4.5.: Bootstrap ratios for the genes for the Dimension extracted by DiCA. A very large proportion (i.e., 66.5%) of the genes are significant with $|BT| > 4.00$. This indicates that the expression of most genes differ significantly between regions.

in cell communication (SSTR1, $BT = -9.63$; CORT, $BT = -9.29$) and associated to cytoskeleton (RPGR, $BT = 12.42$; CORO1A, $BT = -8.13$).

4.5.5 Determination of genes the most expressed in VSA and PTF for the ionic channels and transmitter release functional classes

Among the most extreme genes (i.e., the genes most important for the opposition between VSA and PTF) revealed by our analysis, we found, in particular, genes coding for proteins responsible for two classes of neuronal functions that are directly implicated in the shaping of neuronal dynamics and with specifically known time properties: ionic channels and neurotransmitter release. Genes coding for proteins responsible for these two classes of neuronal functions appear to be distributed on both the VSA and PTF regions. To better understand the characteristics of this distribution and the specific connection with either VSA or PTF regions, we performed a systematic analysis on these two groups of genes. Table 4.1 shows the 6 families of genes pertaining to these two classes of neuronal functions for a total of 161 genes. Table 4.1 also lists the number of genes per family and the number of genes per class.

We first verified that this pool of 161 genes was able to discriminate regions belonging to the two rings. To do so we used these 161 genes to perform a DiCA predicting the ring membership of the 394 regions from Brain H0351.2001. Results (Table A.9) indicate that DiCA correctly predicts the ring membership of 324 out of these 394 regions (82%, $p < .0001$ by binomial test). As we did for the set of 938 genes, to insure that this performance

Neuronal function class	Family name	Family symbol	N genes per family	N genes per neuronal function class
Ionic channels	Potassium channels	KCN	94	135
	Sodium channels	SCN	15	
	Calcium channels	CACN	26	
Neurotransmitter release	Synaptotagmins	SYT	16	26
	Complexins	CPLX	6	
	Synaptobrevins	VAMP	4	

In the analysis of the genes the most differentially expressed on the cortex we found genes belonging to ionic channels and neurotransmitter release neuronal function classes. In particular these genes belong to six families of genes (KCN, SCN, CACN, SYT, CPLX, and VAMP). The members of these six families (when we take all the members for each family) sum up to a total of 161 genes. The table gives the number of genes per family and the number of genes per class.

doi:10.1371/journal.pone.0115913.t001

Tab. 4.1.: The 161 genes coding for proteins forming ionic channels or involved in neurotransmitter release.

was genuine, we also used a random effect model based on a leave one out procedure (see Materials and Methods section, see, also results in Table A.10) and found that we could then correctly assign 321 out of 394 regions (i.e., 81%, $p < .0001$ by binomial test). For Brain H0351.2002 (cf. Table A.11 and Table A.12) we found, for the fixed and random effects, values of (respectively) 306 and 305 (out of 337) correctly classified regions (91% and 90%).

To further assess the predictive quality of the DiCA model, we also used the model derived on one brain to predict the ring assignment of the regions from the other brain (i.e., a “one brain left out” scheme). Doing so, we were able to correctly assign 287 regions out of 394 for Brain H0351.2001 (i.e., 73%, $p < .0001$ by Binomial test) and 288 regions out of 337 for Brain H0351.2002 (i.e., 85%, $p < .0001$ by Binomial test). Figure 4.6 shows the results for the bootstrap analysis separating, on each row, the results pertaining to a single family. Represented in blue are genes with significant positive bootstrap ratios ($BT > 4.00$, indicating a preferential expression in VSA) while in red are genes with significant negative bootstrap ratios ($BT < -4.00$, indicating a preferential expression in PTF). For each family, extreme genes (i.e., best predictors) are labeled.

Similar results for Brain H0351.2002 are reported in Figure A.3. It is interesting to note that, for each family, extreme genes are essentially the same in both brains (see Table A.13 for a complete list of bootstrap ratios). To better quantify the reproducibility of the results of the DiCA in the second brain we plotted against each other the gene factor scores obtained by the DiCA analysis of Brains H0351.2001 and H0351.2002. Figure 4.7 illustrates the high correlation between the results of these two brains ($r = .90$, $r^2 = .81$, $p < .001$). Moreover we found that, for each family under investigation, the most significant PTF or VSA genes extracted by their bootstrap ratios were the same in almost all cases (compare Figure 4.6 with Figure A.3). When this was not the case, the genes that had an extreme bootstrap ratio for the first brain had the second most extreme bootstrap ratio for the second and were still highly significant.

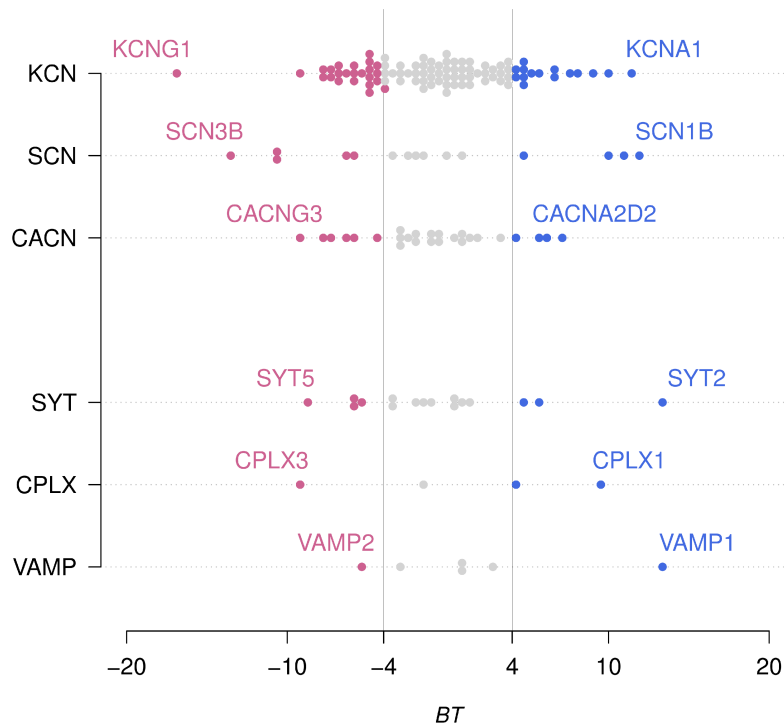


Fig. 4.6.: Map of the bootstrap ratios for the 161 genes, analyzed with DiCA, grouped per family and per class of neuronal function. In blue are represented genes with significant positive bootstrap ratios ($BT > 4.00$) associated with the VSA ring and in red genes with significant negative bootstrap ratios ($BT < -4.00$) associated with the PTF ring. For each family, extreme genes are identified. These genes are the most preferentially expressed in either VSA or PTF.

The most characteristic temporal properties associated to the extreme genes (i.e., preferentially expressed in one of the two rings) coding for ionic channels and transmitter release proteins are detailed in the discussion. The families belonging to the ionic channels neuronal function class present a similar characteristic: their members are spread from extreme VSA to extreme PTF and comprise two groups of genes, which discriminate strongly between the VSA and PTF regions. In particular, extreme members of the sodium channel (SCN) family have some of the highest bootstrap ratios. For the sodium channels family on the VSA side, we found SCN1B ($BT = 12.10$) and SCN1A ($BT = 11.17$) while on the other extreme preferentially expressed in the PTF ring (and not present in the 938 genes) we found SCN3B ($BT = -13.55$) and SCN3A ($BT = -10.62$). To illustrate the relation between a high bootstrap ratio and the cortical distribution for a gene (preferential distribution on a ring) we show two examples in Figure 4.8.

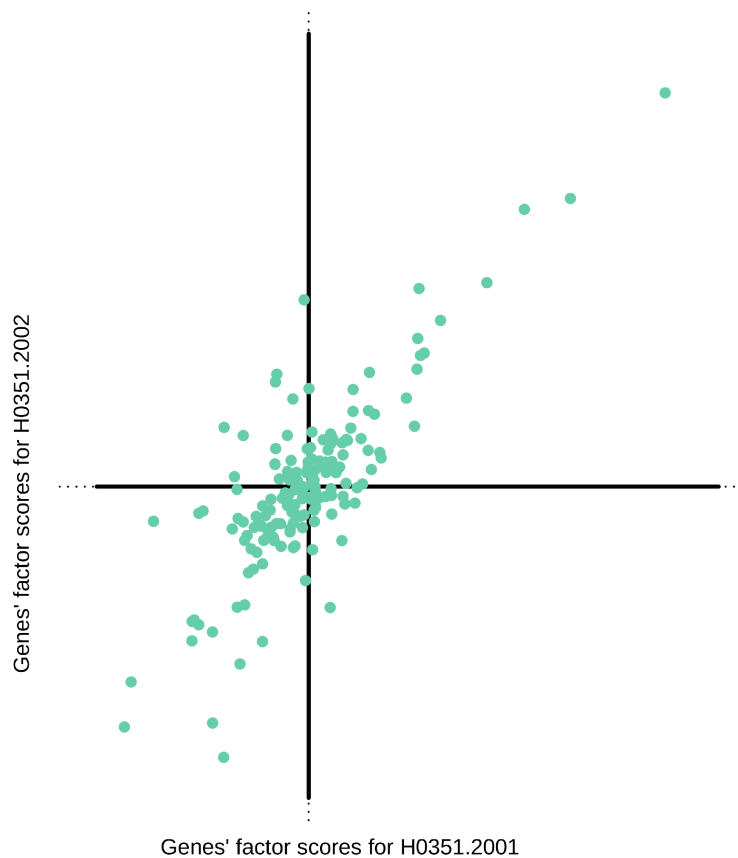


Fig. 4.7.: Scatter plot of the gene factor scores of the discriminant dimension extracted by the DiCA analyses performed on the 161 genes measured on Specimens H0352001 (horizontal) and H0352002 of ABA. Each dot represents one of the 161 genes. The coefficient of correlation is equal to .90 ($r^2 = .81, p < .001$).

Figure 4.8 shows the extreme members belonging to the SCN family (i.e., SCN1A and SCN1B vs. SCN3A and SCN3B). For the potassium channel family we found, with the highest bootstrap ratio in VSA, KCNA1 ($BT = 11.49$) and on the other side we found KCNG1 ($BT = -16.80$). For the calcium channel family, CACNA2D2 had the highest bootstrap ratio in the VSA ring ($BT = 7.12$) while CACNG3 had the highest bootstrap ratio in the PTF ring ($BT = -9.20$). For the synaptotagmin family we found, on the VSA side, SYT2 with an extremely high boot ratio ($BT = 13.49$). By contrast, on the PTF side we found SYT5 ($BT = -8.52$). For the complexin family, on the VSA extreme, we found CPLX1 ($BT = 9.29$). Conversely, on the PTF side we found as the most extreme gene CPLX3 ($BT = -9.37$). Finally, for the VAMP family we found VAMP1 preferentially expressed in the VSA ring with a $BT = 13.53$ while VAMP2 was preferentially expressed in the PTF ring with a $BT = -5.38$.

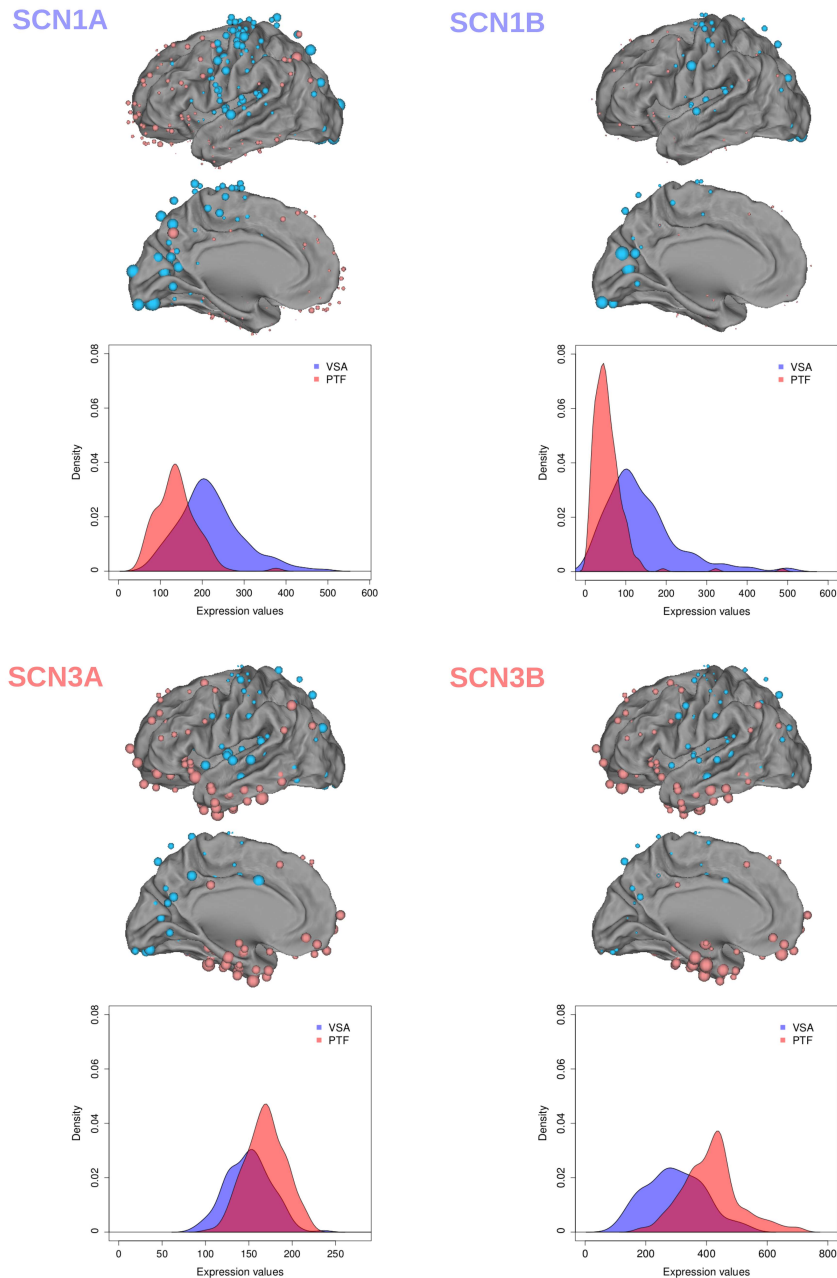


Fig. 4.8.: Example of cortical mapping of gene expression with extreme bootstrap ratios in PTF or VSA. Top. Cortical mapping of the expression of the 4 SCN genes with the highest bootstrap ratios in PTF or VSA: each dot represents one of the 394 cortical regions used in the analysis. The color depends upon the a priori assignment of each region the VSA-ring (in blue) to the PTF-ring (in red). The size of a dot is proportional to the expression of the gene under consideration for the cortical region represented by this dot. Bottom. For each gene, we plot the histogram of the number of regions as a function of gene expression intensities for the VSA (blue) and PTF (red) rings.

4.6 Discussion

In this paper we correlated the topographic organization of gene expressions with the anatomo-functional organization of the cerebral cortex. To evaluate gene expression we

used the Allen Human Brain Atlas [133] of the whole transcriptome because these data constitute the unique set that covers the entire cortex for 21,000 genes. We first focused our analysis on the subset of 938 genes that were selected in [117] because they had the largest variance of expression over the cortex. This first analysis revealed some families of genes important for basic neuronal information processing. We then decided to specifically analyze two classes of genes: 1) genes coding for ionic channels and 2) genes coding for proteins involved in transmitter release. For the cognitive networks, we used a model-called the dual intertwined rings architecture [189]-that integrates in a common framework large cognitive [156], resting state [292, 247], anatomical networks, and functional connectivity. Most published results dealing with the organization of RSNs present patterns that are compatible with this model [85, 72, 296, 272, 239]. According to the two-ring model, the cortex is organized in two main regions called the VSA and PTF rings that mainly differ in the temporal integration of the information that they process: The VSA ring comprises brain regions involved in immediate real-time information processing of sensory, motor, and bimodal information, whereas the PTF ring integrates systems dedicated to multi-temporal processes (e.g., language, episodic memory, social interactions, self) with systems dedicated to emotions, basic biological needs, and rhythms. Evidence for this regional temporal specialization has also been found in experiments using single cell recording in non-human primates [194] and in empirically based mathematical models of the human cortex [148].

Our first result indicates that the cortical organization in two rings constitutes the major source of genetic variation in the cortex. This result shows that cortical gene expression spontaneously organizes the cortex into two rings. This result extends a previous result [117] that showed-using a principal component analysis- that the opposition of primary vs associative regions was important for the organization of genetic expression, but in addition, the present results suggest that the cortex is organized as a two-rings topography comprising two sets of functional regions differentiated by their genetic expression. A second result showed that the profiles of gene expression of a cortical region could reliably be used to assign this region to one ring. However, certain cortical regions were not correctly classified and, interestingly most of the ill-assigned regions were localized on the border between the two rings. The critical importance of the ring model is confirmed by the third result that shows that gene expression is strongly correlated within the two rings and anti-correlated between them.

We found in our first analysis using 938 genes that many proteins coded by genes that most differentiated between cortical regions belong to two classes of proteins involved in neuronal information processing namely ionic channels and neurotransmitter release. We then decided to specifically focus on the systematic study of these two families of genes comprising six families of genes (see Table 4.1). In the following section, we identify the genes with the highest bootstrap ratios (from the DiCA analysis) and discuss the cellular

properties controlled by these genes in relation with the type of information processing performed by the two rings (see Figure 4.9 for a summary of this section).

4.6.1 Sodium and potassium channels

The sodium (SCN) and the potassium (KCN) channel families are distributed in the two rings. In fact, SCN and KCN family members turn out to be spread ranging from extremely PTF to extremely VSA expression with high bootstrap ratios on both sides. In the SCN family, we found the highest bootstrap ratios on the VSA side for SCN1A ($BT = 11.17$) and SCN1B ($BT = 12.10$). The sodium channel, voltage-gated Nav1.1, is essential for the generation and propagation of action potentials, with a large alpha subunit encoded by SCN1A, and smaller beta subunits, encoded by SCN1B, important for its fast inactivation kinetics [39]. These two subunits play a critical role in the temporal precision of neuronal information processing. For the highest expression of K channels in VSA, we found KCNA1 ($BT = 11.49$). This gene codes for a subunit responsible for currents Kv1.1, which, in turn, play a major role in maintaining action potential temporal precision: This gene is expressed in neurons that fire temporally precise action potentials [98], in particular for processing rapid acoustic stimuli, animal vocalizations, human speech [130], sound localization (which depends on timing occurring within a submillisecond epoch) [143]. This potassium channel subunit is important for regulating a tight input-output correspondence and temporal synchrony [8]. We thus found, more expressed in the VSA ring, genes (SCNA1, SCNB1, KCNA1) which control the temporal precision of neuronal activation, and these ionic channel properties match the data-driven, real-time information processing in the VSA ring underlying sensorimotor interactions. Conversely, on the PTF side, we found for sodium channels an overexpression of both SCN3A ($BT = -10.62$) and SCN3B ($BT = -13.55$) (alpha and beta subunits of Nav1.3). The beta3-subunit influences the temporal properties of sodium channels in such a way that they stay open and active for a longer time [56], and favor persistent sodium currents and sustained activation of the neuron. [216, 9, 77, 55]. The next gene with the highest bootstrap ratio, SCN9A ($BT = -10.66$) codes for sodium channels Nav1.9 and contributes also to foster a persistent sodium current [270]. For the KCN family, more expressed on the PTF side, we found the genes KCNF1 (Kv5.1, $BT = -6.25$) and KCNG1 (Kv6.1, $BT = -16.80$) that code for proteins that are electrically silent Kv (KvS) potassium subunits which modulate the Kv2.1 channel, the major delayed rectifier channel expressed in most cortical pyramidal neurons, and slow its activation, inactivation and deactivation kinetics (reviewed in [152, 24]). We found other genes overexpressed in the PTF ring-such as KCNMB4 ($BT = -9.21$)-which have similar effects. We found also KCNN3 ($BT = -6.56$) which induces a sustained activation of dopamine neurons [249], KCNJ1 ($BT = -7.51$) [12] which generates rhythmic activation and spontaneous activity, and KCNA4 ($BT = -7.17$) which regulates long term circadian rhythms [105]. We thus found, more expressed in the PTF ring, genes which facilitate persistent currents (SCN3A and SCN3B), prolonged

effects of input activities, (KCNF1, KCNG1, KCNMB4, KCNN3), and spontaneous and rhythmic activation (KCNJ1, KCNA4): All these temporal neuronal properties match the multi-temporal processing in the PTF ring, contrasting with the high precision timing control of SCN1A, SCN1B and KCNA1 in the VSA ring. However, the precise role of these genes in the different regions of the PTF ring remains to be elucidated.

4.6.2 Calcium channels

We found also calcium channels with a preferential distribution either in the VSA or the PTF ring. Calcium (Ca²⁺) channels initiate release of neurotransmitters at synapses, from the timescale of milliseconds to minutes, in response to the frequency of action potentials [40]. Mostly expressed in the VSA ring we found CACNA2D2 ($BT = 7.16$). This subunit causes faster activation and inactivation kinetics [155] of calcium channels and drive exocytosis with an increased release probability, making synapses more efficient at driving neurotransmitter release [125]. Mutations of CACNA2D2 result in slow inactivation of calcium channels and a prolonged calcium entry during depolarization [75]. The control of input/output timing and quantification of evoked transmitter release is requested for data-driven real-time processing in the VSA ring underlying sensorimotor functions. Conversely, on the PTF side, we found CACNA1H ($BT = -7.71$). This gene encodes a syntaxin-1A/Cav3.2 T-type calcium channel which controls low threshold exocytosis in an action potential-independent manner [289, 46], and can trigger the release of neurotransmitters at rest. This produces low-threshold burst of action potentials for the genesis of neuronal rhythms. Similarly, CACNG3 strongly expressed on PTF ($BT = -9.20$) shows multiple long-lived components [241] which can facilitate prolonged activation of neurons. The spontaneous, prolonged, or rhythmic release, matches the multi-temporal processing in the PTF ring for vital needs, memory, and language, compared to the high fidelity evoked processing in the VSA ring.

4.6.3 Synaptotagmins

Central synapses operate neurotransmission in several modes: synchronous/fast neurotransmission- neurotransmitters release is tightly coupled to action potentials-and spontaneous neurotransmission where small amounts of neurotransmitter are released without being evoked by an action potential [47]. Synaptotagmins (SYTs) are abundant membrane proteins [192, 251], with at least 16 isoforms in mammals, which influence the kinetics of exocytotic fusion pores and the choice of release mode between full-fusion and “kiss-and-run” (partial fusion) of vesicles with the presynaptic membrane [192, 114, 299]. Kiss-and-run allows neurons to respond to high-frequency inputs mediating tight millisecond coupling of an action potential to neurotransmitter release [251]. The synaptotagmin most strongly associated to VSA is SYT2 ($BT = 13.49$) which controls the kiss-and-run behavior of vesicles and temporal accuracy of transmitter release [299, 150] for example in the auditory sys-

tem or the neuromuscular junction. The kiss-and-run mode of SYT2 matches the real-time data-driven processing mode of VSA.

By contrast, we found more expressed in the PTF ring, the synaptotagmin V. SYT5 ($BT = -8.52$) which promotes the fusion of vesicles with a slower binding and is targeted to dense-core vesicles (821) that undergo Calcium-dependent exocytosis of various neurohormones and neuropeptides. The SYT5 preferred expression in the PTF ring is compatible with the multi-temporal processing mode of the PTF ring and contrasts with other synaptotagmins (e.g., SYT2) which favor high temporal precision in response to evoked stimuli (SYT2) and are therefore more expressed in VSA.

4.6.4 Complexins

We also studied the complexin (CPLX) family whose members assist synaptotagmin by activating and/or clamping the core fusion machinery of exocytosis of vesicles controlling either spontaneous or evoked neurotransmitter release [134, 139, 35]. In the complexin family, we found that CPLX1 ($BT = 9.29$) was strongly expressed in the VSA ring. CPLX1 is important for the tight time coupling (of the order of a millisecond) of the action potential to neurotransmitter release [293] while suppressing spontaneous synaptic vesicle exocytosis driven by low levels of endogenous neural activity [181]. Here again, a fast evoked release mechanism matches the real-time processing mode of the VSA ring. Conversely, on the PTF side, we found as the most extreme gene CPLX3 ($BT = -9.37$), which is an activator of spontaneous exocytosis [293]. Furthermore, the molecular structural differences between Complexins 1 and 3 have been studied in relation with their two different functional roles, where the C-terminal sequence of CPLX1 facilitates evoked release whereas the C-terminal sequence of CPLX3 facilitates spontaneous release. The preferential expression of CPLX1 and CPLX3, which induces either evoked or spontaneous release, matches both the real-time data-driven processing in VSA and the goal-driven multi-temporal integration in PTF that is based on more spontaneous activation.

4.6.5 Synaptobrevins

Our results also show a differential expression of synaptobrevins (VAMP vesicle associated membrane protein) in VSA or PTF. This protein family plays an important role in vesicle docking and maintenance controlling the rate of release. VAMP1 ($BT = 13.53$) gene is strongly expressed in the VSA ring—a pattern consistent with previous results showing that these proteins are important for the fast processing of sensory stimuli such as auditory stimuli [91]. Results have shown that VAMP1 (Synaptobrevin 1) is more important for evoked release [300], while Synaptobrevin 2 (VAMP2, $BT = -5.38$) seems to have a more general role in maintaining a pool of available vesicles. Here again this differentiation matches the importance of precise control of evoked release in the VSA ring.

In summary (see Figure 4.9), our results showed co-expression in VSA of a set of genes which favor high temporal precision of fast evoked neural transmission: Sodium channels SCNA1, SCNB1 and potassium channels KCNA1, and proteins facilitating fast evoked transmitter release: calcium channels CACNA2D2, Synaptotagmin SYT2, Complexin CPLX1, Synaptobrevin VAMP1. Conversely the results showed in PTF co-expression of a set of genes responsible for slower, sustained, or rhythmic activation: Sodium channels SCNA3, SCNB3, SCN9A potassium channels KCNF1, KCNG1, KCNMB4, KCNJ1, KCNA4, KCNN3 together with genes that facilitate spontaneous transmitter release: calcium channel CACNA1H, Synaptotagmin SYT5, Complexin CPLX3, and Synaptobrevin VAMP2. The results showed that there is a strong congruence between the preferential expression of a subset of genes, the temporal properties of the proteins that they code, and the temporal processing modes of the two rings underlying their sensorimotor and cognitive functions.

4.7 Conclusions

The expression of the 938 genes most differentially expressed across the cortex organized the cortex into two sets of regions (called rings) that match two- previously described-large scale human functional cortical networks. The first ring processes real time sensory-motor information whereas the second ring processes multi-scale temporal information such as language, memory, or vital rhythms. The systematic study of families of genes coding for ionic channels and transmitter release proteins showed strong congruence between the preferential expression of genes, the temporal properties of the proteins they code at the cell level, and the temporal processing modes of these two large scale networks.

4.8 Remark: Regions are organized according to gradients based on their gene expression profile

In the work presented in this chapter, we showed how the 1000 genes the most differentially expressed across the cortex are organized in two main groups whose profiles match the two intertwined rings architecture. As already shown if we evaluate the pairwise correlation between these 1000 genes and we order the results according to their bootstrap ratio, we obtain two anticorrelated blocks of genes. Observing the values of correlation we see that PTF genes tend to have more similar profiles with high correlation between most of the genes. VSA genes are strongly correlated but by smaller blocks: this is coherent with the fact that VSA is made of highly differentiated cortices that treat different kind of stimuli.

The second figure presented (not included in the article) is the correlation between the cortical regions given their gene profiles. The interest of this figure resides in the contrast with the previous one: while the 1000 genes are overall neatly opposed into two blocks, the re-

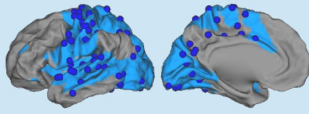
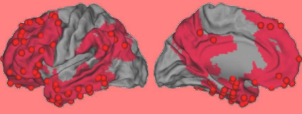
	VSA ring	PTF ring
Cortical topography		
Cognitive functions	Sensory-motor, uni and bi-modal	Memory, language and vital functions
Temporal information processing	Real time interactions	Multi-temporal integration
Potassium channels	KCNA1, KCNC1 High temporal precision	KCNG1 Modulation of K currents
Sodium channels	SCNA1, SCNB1 High temporal precision	SCNA3, SCNB3 Persistent currents, sustained activity
Calcium channels	CACNA2D2 Fast, stimulus driven release	CACNA1H Spontaneous release, Rhythms generation
Synaptotagmins	SYT2 Kiss and run, fast evoked release	SYT5, SYT9, SYT10 Spontaneous, slower release
Complexins	CPLX1 Stimulus driven control of release	CPLX3 Spontaneous release
Synaptobrevins	VAMP1 High frequency evoked release	VAMP2 Maintains the pool of available vesicles

Fig. 4.9.: Summary of the temporal properties of proteins that most differentiate between the two rings and their correspondence with the preferred information processing modes of the rings.

gions based on their gene profile are organized as a gradient, apart from the extreme groups of regions that are highly correlated among them and strongly anticorrelated between the two rings.

This result is interesting since it gives us a better idea of the gradient organization of genes' expression and show the continuity of gene organization across the cortex. This result obtained with the genes which differentiate the most 56 regions of the cortex elucidates how gene expression gradients follow primarily the large scale anatomo-functional organization in two rings.

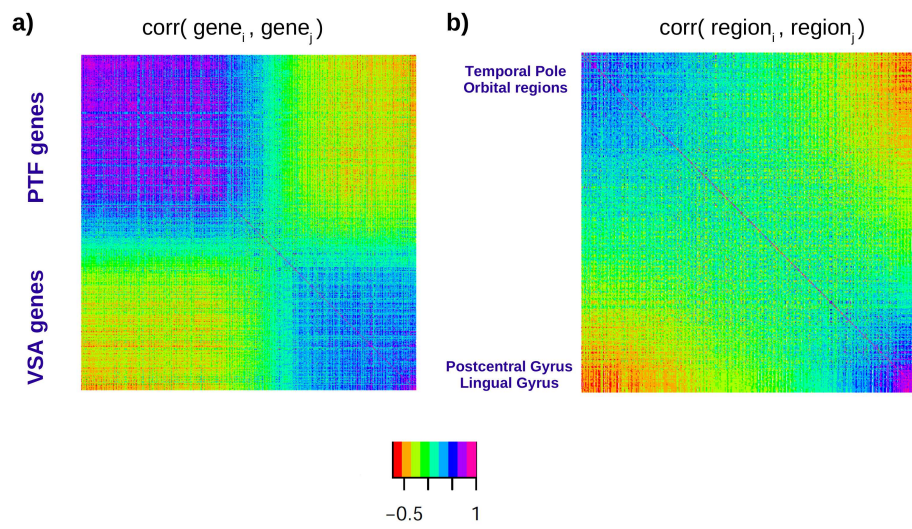


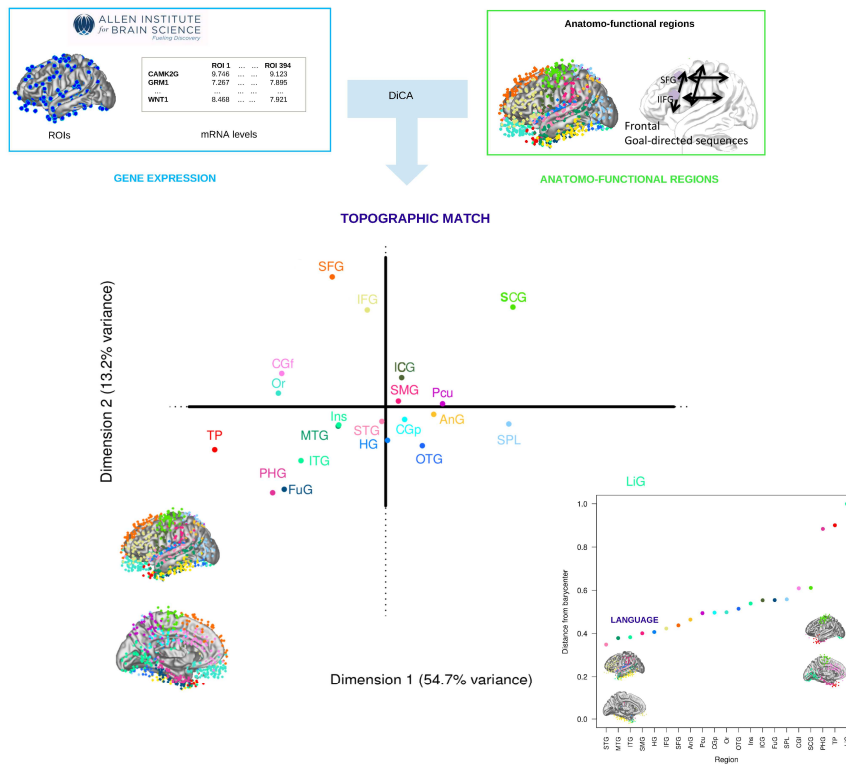
Fig. 4.10.: Genes correlation versus regions correlation

Gradients of synaptic genes properties across cognitive networks

In the previous chapter we studied the link between the topographic organization of the 1000 genes the most differentiated across the human cortex and the global anatomo-functional organization of cortical networks called the two intertwined rings architecture. We found that these genes are organized mainly according to two opposed anatomical gradients and that these two gradients match closely the topography of the two intertwined rings. Moreover studying the distribution of 163 genes known to be involved in shaping the way neuron process information (ionic channels, neurotransmitter release), we found also a functional match: proteins more expressed in a given ring tend to favor neuronal dynamics coherent with the preferred way of processing information of that ring. In this chapter we wanted to study the relation between cortical gradients of gene expression and anatomo-functional cortical networks a finer scale. The interest was to go closer to the spatial scale of cognitive networks to study if it exists a relation between cognitive functions and groups of genes. Since cognitive functions often overlap among them we chose to define a set of disjoint anatomo-functional regions based on the Allen Institute anatomical labels (see also section 3.4.3.2). We used this time the entire set of genes measured by the Allen Institute. We studied these data in relation to the anatomo-functional cortical regions by means of multivariate statistical technique called Discriminant Correspondence Analysis (DiCA). For completeness to better understand the overall picture we also studied gene expression in relation to the entire set of cerebral structures. To draw a link between genes' pole of expression and anatomo-functional regions this time at the functional level we focused the analysis of the results on three class of genes: genes involved in information processing, genes participating to memory formation (short term and long term) and genes taking part to networks genesis. We finally propose four multi-scale scenarios to describe and interpret the relation between synaptic properties of genes and functional specialization of cortical regions for those groups of genes and regions that our analysis revealed as spatially correlated.

Figures 5.3, 5.4, 5.14-5.16 show the main results of this work in course of submission (*Cioli et al.*).

5.1 Graphical abstract



<p>VisuoMotor</p>	<p>SCN1A,SCN1B KCNA1 CACNA2D2 Highly precise</p>	<p>SYT2 Kiss and run CPLX1 Stimulus evoked</p>	<p>GRIN2A :NR2A Shorter activity Less plastic</p>	<p>CaMK2G Actin sheets Adjustements</p>		
<p>Temporal Recognition</p>	<p>SCN3A,SCN3B KCG1 CACNA1H persistent</p>	<p>SYT5 Full fusion CPLX3 spontaneous</p>	<p>GRIN2B:NR2B Longer activity More plastic GRIN3B Slow maturation</p>	<p>CaMK2D Actin bundling Strong memory CaMK4</p>	<p>ACTR3 Branched actin network</p>	
<p>Frontal Goal-directed sequences</p>	<p>KCNA5, KCNS3 KCNN2,KCNJ8 Control Working memory</p>	<p>SYT5 Full fusion CPLX3 spontaneous</p>	<p>NR2B Working Memory ADRA1B,ADRA1D HTR1E, CHRN4 Modulation</p>	<p>CaMK1G Persist hours Act on tubulins</p>	<p>ACTN2 Actin bundling Spine length density</p>	<p>TUBA4, TUBB3 TUBB4A, TUBB4B Axo-dendritic network remodeling</p>
	<p>Ionic channel Transmission</p>	<p>Complexin Synaptotagmin Action</p>	<p>Glu NMDA receptor Association</p>	<p>CaMK Short-term memory</p>	<p>Actin Long-term memory</p>	<p>Tubulin Long-term memory and development</p>

5.2 Abstract

We explore the relationships between the brain anatomo-functional organization (with particular focus on the cerebral cortex) and gene expression (as provided by the Allen Human Brain Atlas). Previous studies showed that different cerebral structures and cortical areas present characteristic gene expression. However what is poorly understood is the relation between the functional role of proteins and gene expression at the synaptic level, and the functional specialization of brain networks at the sensory motor and cognitive levels.

We found-with discriminant correspondence analysis-that the patterns of expression of about 21000 genes oppose 1) regions of the cerebral cortex to brainstem and cerebellum 2) cerebral and cerebellar cortices to brainstem regions.

We found-with discriminant correspondence analysis-that the patterns of expression of about 14000 genes highly expressed in cortical regions oppose: 1) sensorymotor and bimodal regions (VSA: Visual-Somatic-Auditory regions) on one side, with higher associative areas (PTF: Parieto-Temporo-Frontal) on the other side; 2) dorsal versus ventral regions: frontal versus temporal regions (on the PTF side), and somatomotor versus occipital visual regions (on the VSA side). Moreover regions that are involved in supporting the functionalities of language are the less differentiated based on their gene expression profile.

We focused on the results for families of proteins involved in fundamental neuronal functions: 1) information processing (ionic channels, neurotransmission (pre and post-synaptic part), neuromodulation), 2) short-term memory formation (Calcium Calmodulin kinase dynamics), 3) long-term memory formation (actin and tubulin remodeling) and 4) network genesis and maintenance (cell-cell communication and growth factors). The systematic study of these families of genes revealed specific proteins within families preferentially expressed in different anatomo-functional regions of the brain and of the cortex. The results showed strong spatial congruence between the preferential expression of subsets of genes and specific anatomo-functional regions; and a functional congruence between the cellular properties of the proteins they code, and the cognitive functions implemented in these regions.

Short-term and long term memory involves a cascade of transformation: glutamate NMDA receptor activation signaling co-occurrence of inputs, calcium inflow prolonged by CaMK auto-phosphorylation producing a short term memory, and actin polymerization increasing the spine surface for long-term memory encoding. The expression of genes coding for these 3 families of proteins is highest in the cerebral cortex, with a differential distribution of subunits in the cortical regions. The glutamate receptor NR2B responsible of sustained activities of working memory and strong plasticity is higher in cognitive regions PTF; NR2A which produces shorter activation and limits plasticity is higher in sensorymotor VSA regions; GRIN3A, which delay maturation is more expressed in PTF. The CaMK isoforms CaMK2D higher in cognitive regions PTF and CaMK2G higher in sensorymotor regions VSA produce two modes of actin polymerization, with CaMK2D favoring strong

consolidation. There is also a contrast between temporal and frontal regions. CaMK1G in frontal regions produces longer duration of short term memory than CaMK4 in temporal regions. Genes coding for proteins regulating the actin network, are either more expressed in the frontal regions (ACTN2 gene coding for alpha-actinin2), or in the temporal regions (actin-related protein ACTR3) suggesting different mode of long-term memory encoding. Furthermore, genes coding for alpha and beta tubulin, which regulate the microtubule dynamics, and thus axon and dendrites growth, are also more expressed in the frontal regions where very slow maturation allows for learning-dependent network remodeling. Finally our results show an high expression in temporal regions of the gene coding for the transcription factor FOXP2, the related growth factor receptor c-MET and proteins related to the retinoic acid, which together control the development and homeostasis of cortical temporal regions, specialized for language comprehension.

5.3 Introduction

A key step in understanding how the human cerebral cortex processes and stores information is to connect the anatomo-functional organization of the cortex (as described, e.g., in [85, 156, 189]) with the topographic organization of gene expressions [228, 233, 104]. Processing and storage of information depend at the same time upon (1) the structure of cerebral networks (cerebral cortex, cerebellum, basal ganglia, as seen in brain imaging studies) and the ensemble of proteins that control the functioning of the networks at the synaptic and neuronal level (as seen in genetic studies).

Several studies [156, 189, 292, 247] have analyzed the large organization of cognitive networks with a topographical organization which is related both to Brodmann areas and cortico-cortical connections between these areas (for example temporo-frontal networks for language processing, or fronto-parietal networks for executive functions).

Systematic genetic studies of the human brain [117] reveal similarities and differences between the genetic expression in cerebral regions (cerebral cortex, cerebellum, hippocampus, etc), and between different areas of the cerebral cortex. Previous studies showed that different cerebral structures present characteristic genetic expression differentiating them, and that this is true also for different areas of the cerebral cortex. Furthermore, it appears that genetic expression is more similar within cerebral cortical regions and dissimilar between the cerebral cortex and the other structures.

However what is poorly understood is the relation between the functional role of proteins and gene expression at the synaptic level, and the functional specialization of brain networks at the sensory motor and cognitive levels.

We have previously shown [48] that genetic expression across the cortex is organized primarily according to two large set of regions known to deal respectively with sensory motor information and regions implementing higher cognitive functions such as language and

memory. We also showed that families of proteins involved in information processing and neurotransmitter release have differential expression in these two sets of regions, and that functional properties of different members of these families match the functional properties of cognitive networks which have a similar topographic organization across the cortex. In particular it was shown that proteins controlling precise evoked synaptic release are more important in regions processing real time sensory motor information, while proteins involved in favoring spontaneous release are preferentially expressed in associative regions generating autonomous activation as in language production or memory recall. Similarly temporal properties of ionic channels match this dual topographical organization: ionic channels in sensory motor regions are characterized by high temporal precision with high fidelity with respect to the input while ionic channels in associative regions display a more modulatory role and favor sustained activation like persistent sodium channels.

In this study we want to extend the relation between the synaptic functions of proteins and the functional specialization at the cerebral and cortical networks. We explored the topographical relation between these networks and the expression of genes. We first explored this relation for cerebral networks (cerebral cortex, cerebellum, basal ganglia and hippocampus), and then we performed a similar analysis at the level of different regions of the cerebral cortex implementing different cognitive functions.

To do so we conducted multivariate statistical analysis aimed to find the relation between particular cerebral and cortical regions, and groups of genes more expressed in these regions. This analysis revealed the genes the most differentially expressed across regions.

In order to better understand the link between the synaptic role of these genes, and the cognitive functions implemented in these regions, we focused on 8 groups of families of synaptic proteins important for information processing, short and long term memory formation and network genesis and maintenance. These families of proteins are: (1) ionic channels, (2) neurotransmitter release machinery, (3) gaba and glutamate receptors (4) neuromodulators, (5) CAMKs and PRKCs important for short term memory, (6) cytoskeleton proteins like actin and tubulin important for long term memory, (7) axon guidance and cell-cell recognition proteins (such as SEMAs, EPHs and CLECs), and (8) growth factor (such as FGFs, EGFs), important for building neuronal networks.

A central role in the construction and functioning of these networks is played by synapses and the proteins who take part to synaptic life. Indeed synaptic functioning depends upon different families of protein playing in different types of processes: proteins involved in information processing such as ionic channels (SCNs, KCNs, CACNs, HCNs) [39, 40] and neurotransmitter release machinery (SYTs, VAMPs, CPLXs) [47, 299, 293], GABA and glutamate receptors [96, 280, 279], neuromodulator receptors (DRDs, HTRs, CHRs, ADRs), proteins responsible for short term memory (CAMKs and PRKCs) [171, 286, 285, 177], cytoskeleton proteins involved in long term memory such as actin and tubulin (ACTs, ACTNs, ACTRs, TUBs) [184, 204, 126], and axon guidance and cell-cell recognition pro-

teins (such as SEMAs, EPHs and CLECs) [201, 206] proteins involved in networks genesis and homeostasis such as growth factors (EGFs,FGFs) [58, 53].

The data used in this study are the transcriptome data of the human brain as produced by the Allen Institute for Brain Science for six hemispheres brains. The statistical method we used was a Discriminant Correspondence Analysis (DiCA) applied at two levels of brain organization: cerebral regions (cerebral cortex, cerebellum, basal ganglia and hippocampus) and cortical regions only.

5.4 Materials and Methods

5.4.1 Data Base

The data used in this paper were obtained from the Allen Brain Atlas project [133]. We used for this study six postmortem half brains that were sampled for a total of 2691 distinct brain locations representing all structures within the brain in approximate proportion to the volumetric representation of each cortical, subcortical, cerebellar, and brain stem structures. Of these 2691 regions 1322 samples were cortical. We analyzed the six half brain together as part of an average brain using the profile of expression for: 1) all the genes analyzed in the Allen data base (29175 genes and non assigned probes) when studying the entire set of 32 brain regions; 2) all the genes displaying an average ≥ 4 (log2) across cortical areas on at least one of the six brains (14575 genes) when studying the set of 21 anatomo-functional regions.

5.4.2 Anatomo-functional regions

To perform our analyses we chose a set of anatomo-functional regions (see Figure 3.5) defined by grouping the samples based on their anatomical labels as described in the Allen Human Brain Atlas http://casestudies.brain-map.org/ggb#section_explorer. The choice of these anatomo-functional regions was made for three main reasons: 1) like Brodman Areas they represent a tessellation of the cortex; 2) they are well characterized on both the anatomical and the functional level allowing to interpret the results in term of cognitive tasks; 3) they maximize the homogeneity for the number of samples across the different brains for each.

5.4.3 Statistical Analysis: Discriminant Correspondence Analysis (DiCA)

In order to study the relation between the cerebral and cortical anatomo-functional regions chosen and the organization of gene expression we used discriminant correspondence analysis (DiCA), a discriminant analysis version of CA [2]. This choice was made since DiCA allow to contrast among them the anatomo-functional regions based on their gene expression profiles. We used the implementation of DiCA in the TExPosition/TInPosition packages (<http://cran.r-project.org/web/packages/TInPosition/index.html>; see also [13] and R Development Core Team, 2013). DiCA creates a matrix that represents each group (e.g., LiG, IFG, SFG) by the sum of its observations (for all the gene expressions). In our case, we analyzed two matrices using this same technique: a first matrix for the 32 cerebral regions was 32×29175 (about 21000 genes); a second matrix for the cortical regions was 21×14575 . These data tables contain the sum of each gene expression level (columns) for each ring (rows). This data table is then analyzed by CA (this step solves the discriminant problem because CA computes factor scores that maximize the difference between rows). The original cortical regions are then projected as supplementary elements (a.k.a. “out of sample”) in the group factor space and the distance of each cortical region to each ring is also computed in this space [284]. Finally each cortical region is assigned to its closest anatomo-functional region. The quality of this assignment can be assessed by an R^2 statistic computed as the ratio of the anatomo-functional region variance to the total variance of the cortical regions. The quality (i.e., “significance”) of the R^2 is evaluated by computing a probability distribution under the null hypothesis with a permutation test: for 1,000 iterations, the labels of the cortical regions are shuffled and the R^2 is recomputed. In addition, a permutation test was also used to evaluate the null hypothesis of an overall effect and to identify significant components (see [13]). Also, the bootstrap resampling scheme used in CA (obtained by resampling the cortical regions with replacement) was also used in DiCA to compute bootstrap ratios for the genes and also to derive confidence intervals for the groups. An equivalent bootstrap resampling scheme was used to compute bootstrap ratios for the regions.

5.5 Results

We are interested in understanding the relation between the topographical organization of gene expression and the anatomo-functional architecture of the brain. We want to better understand which are differences and similarities of distinct anatomo-functional regions based on their gene expression and which genes are important to draw these differences. We focused on genes which have known roles in basic synaptic functions (information processing, memory formation and networks genesis) to see if they are differentially expressed in different regions in relation with their sensorymotor or cognitive function.

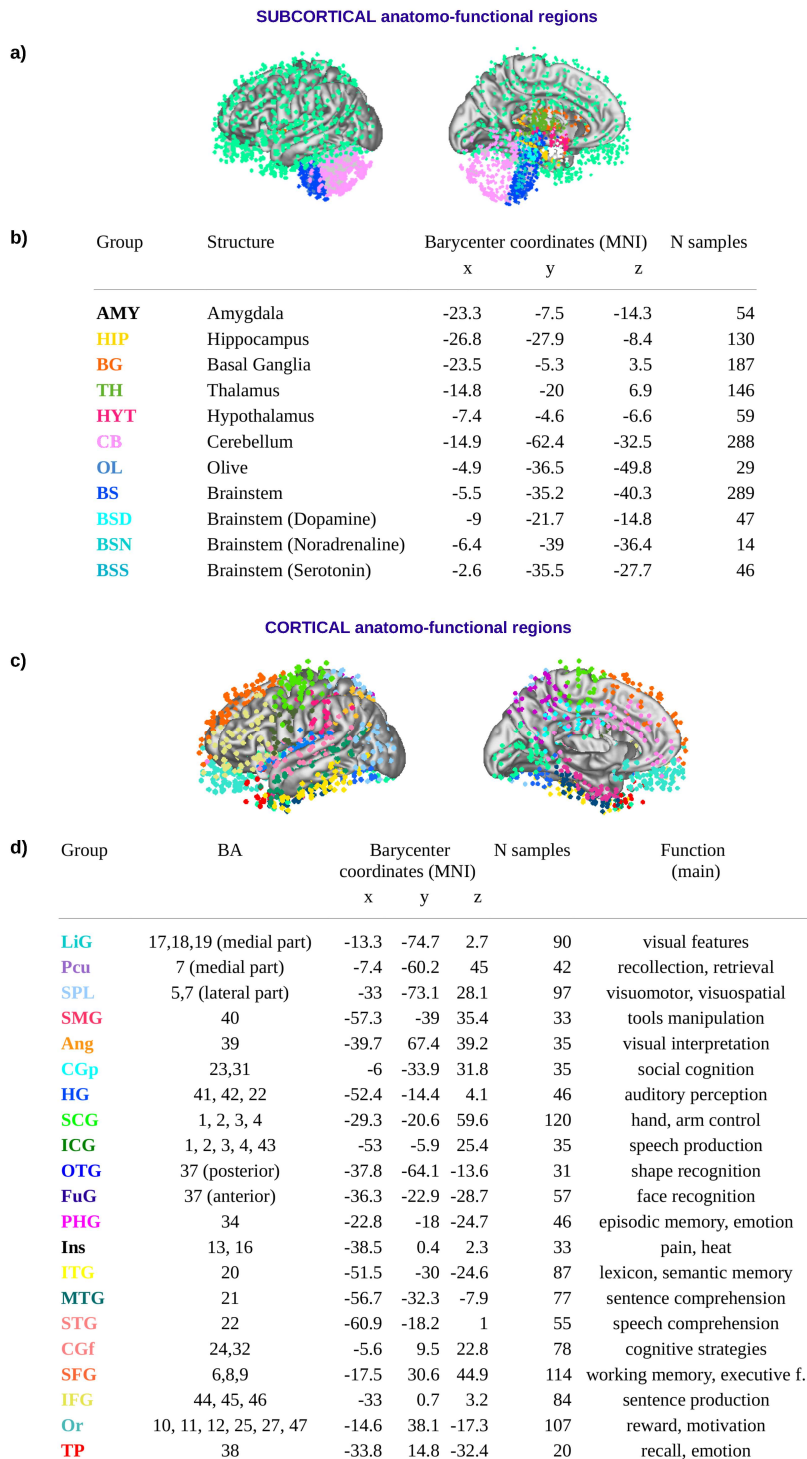


Fig. 5.1.: Cerebral and cortical anatomo-functional regions: definition. We defined two sets of anatomo-functional regions by grouping ABA anatomical labels: **a)-b)** 11 subcortical regions (in green all the cortical samples as opposed to subcortical regions) and **c)-d)** 21 cortical regions. The colored dots represent all the samples for the six brains as provided in the Allen database. The interest of this choice is to have a set of regions anatomically and functionally well characterized and representing a tessellation of the cortex.

In the following, we call cerebral regions the main neuronal structures of the human brain: cerebellum (cortex and nuclei), basal ganglia, hippocampus, cerebral cortex, etc...; we call cortical regions Brodmann areas or groups of Brodmann areas. Cerebral networks relate cerebral regions, and cortical networks relate cortical regions via axonic connections. These regions are anatomo-functional in the sense that they are both defined (1) by their structure (neurons ensemble forming a repeated texture such as the cortical column, with their connections) and (2) by their sensorymotor or cognitive specialization.

To carry our study we determined 11 anatomo-functional cerebral regions based on the anatomical labels of samples proposed in the ABA as described in Figures 5.1.a and b. We decided to keep separated samples for the brainstem nuclei which synthesize specific neuromodulators, since they are highly differentiated in molecular terms: the Substantia Nigra producing dopamine (BSD: BrainStemDopamine), the Raphe nuclei producing serotonin (BSS: BrainStemSerotonin) and the locus coeruleus producing norepinephrine (BSN: BrainStemNorepinephrin). The cerebral cortex was instead divided in 21 anatomo-functional regions based on the conjunction of anatomic, functional and cognitive criteria: (1) grouping of anatomical label as by the ABA in relation with Brodmann Areas (BA) and (2) grouping by their sensorimotor and cognitive specialization, as described in [156, 189]. This grouping is shown in Figures 5.1.c and d.

Our interest being in determining the relations between the anatomo-functional regions chosen and the genes that most differentiate them, the natural choice was to use the multivariate statistical technique called Discriminant Correspondence Analysis (DiCA). The interest of this analysis is to force the difference between a priori groups –cerebral and cortical regions in our case– based on the variables describing them, the genes' expression profiles.

5.5.1 Single gene expression profiles

It is possible for each gene to reveal differences in expression, both across cerebral region and cortical regions. We have illustrated two examples of cerebral and cortical distribution of gene expression in Figures 5.2.a and b (the genes represented are SATB2 and DRD1 respectively). This figure shows typical profiles where there are two superimposed distributions: one relative to subcortical regions and one relative to cortical regions. These two distributions reveal how differences between subcortical and cortical regions are much stronger than differences between cortical regions. Cortical regions indeed tend to remain grouped.

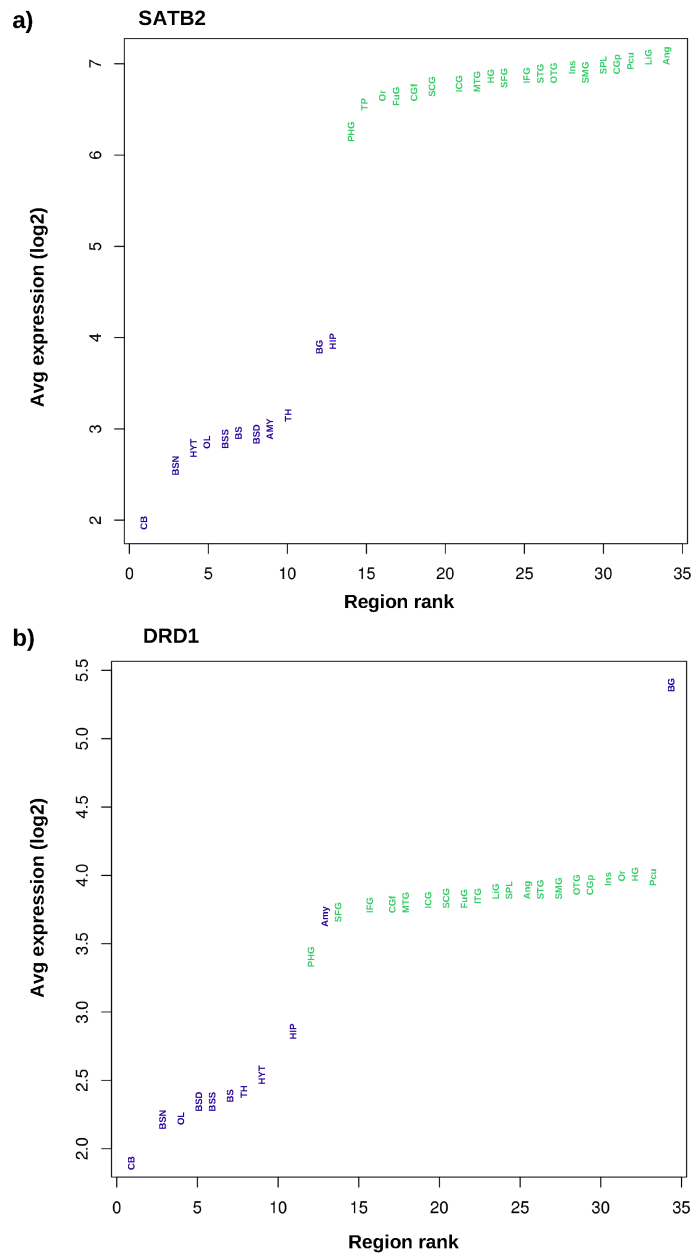


Fig. 5.2.: Expression profiles across cerebral regions: SATB2 and DRD1. Average expression for each of the 32 cerebral regions defined in 5.1 (ranked by level of expression) for genes SATB2 and DRD1. In green are represented the anatomo-functional cortical regions in blue the subcortical regions. It is evident how cortical regions have among them an homogeneous gene expression if compared with the rest of the cortical regions. Nonetheless if we observe the order of cortical regions it appears to be anatomically sound. SATB2 is a transcription factor heavily implicated in the genesis of cortical microcircuitry (see for example [165, 7]). Its profile of expression tells that in the adult it preserve a role eminently in cortical regions. DRD1 is a dopamine receptor well known to be strongly expressed in basal ganglia as also its profile of expression shows.

5.5.2 Organization of brain regions by gene expression

We first studied the organization of all the 32 anatomo-funcntional regions (11 cerebral and 21 cortical regions, 5.1) with respect to their gene expression. To do so we applied a

DiCA analysis to the table describing the amount of expression for 2691 samples (of the 32 brain regions) times 29175 genes and probes (21000 genes). This table is the result of the union of the table of expression for the six left hemispheres studied by the AI. Details about samples per brain and per group are given in the Supplementary Material. The first two dimensions of the analysis explain together 75.3% – 41.1% and 34.2% respectively, $p < 0.01$ – of the total variance of the data. Figure 5.3 shows the bootstraps for the cerebral regions as seen by the first two dimensions of the analysis. The first dimension tells us that the regions with the most different genetic expression are altogether the cortical regions (cerebral cortex) versus the regions of the cerebellar cortex and the brain stem. These results also show that cortical areas are homogeneous in term of gene expression if compared to other cerebral regions. This result means that there are genes which are mostly expressed across cortical areas, and genes mostly expressed across brain stem and cerebellar regions. The first component also tells that brain stem and cerebellar cortex share in part similar genetic expression, so there are genes mainly expressed in both the brainstem and in the cerebellar cortex. Basal ganglia, hippocampus, amygdala and hypothalamus are more central and form a bridge between the cortical regions and brainstem plus cerebellar regions in a gradient-like fashion. The second dimension instead point out the differences between the brainstem on one side and cerebral and cerebellar cortices on the other side. The second dimension suggest the existence of a pool of genes shared between the cerebral cortex and the cerebellar cortex. Basal ganglia, hippocampus, amygdala and hypothalamus are again more central, and forma bridge connecting the two cortices (cerebral and cerebellar) and brainstem regions also in a gradient-like fashion.

Basal ganglia, hippocampus and amygdala are opposed to brain stem regions on the third dimension extracted by the analysis (accounting for the 7% of the total variance, $p < 0.01$). The fourth dimension – accounting for the 4.6% of the total variance, $p < 0.01$ – opposes basal ganglia and hippocampus. Finally thalamus and hypothalamus are opposed to the brain stem and the visual part of the cortex on the sixth dimension (2.5% of the total variance, $p < 0.01$). Interestingly the fifth and the sixth (3% of the total variance, $p < 0.01$) dimension plotted together reveal an organization of the cortical regions similar to the main axes obtained when focusing on the cerebral cortex: the two intertwined architecture as described in [189]. The first six dimensions extracted by the analysis explain together the 92.4% of the total variance of the data and indeed they carry all the main information about brain regions organization based on their genetic profile. If we evaluate the distance of each cerebral region from the barycenter of the regions' factor scores we find that the cerebellar cortex is the structure the most genetically differentiated. The other regions instead are organized according to a gradient that goes from the olive – the second structure the most differentiated – to the brainstem regions and the rest of subcortical anatomic-functional regions (Basal Gnaglia, amygdala, hippocampus) up to the cortical ones.

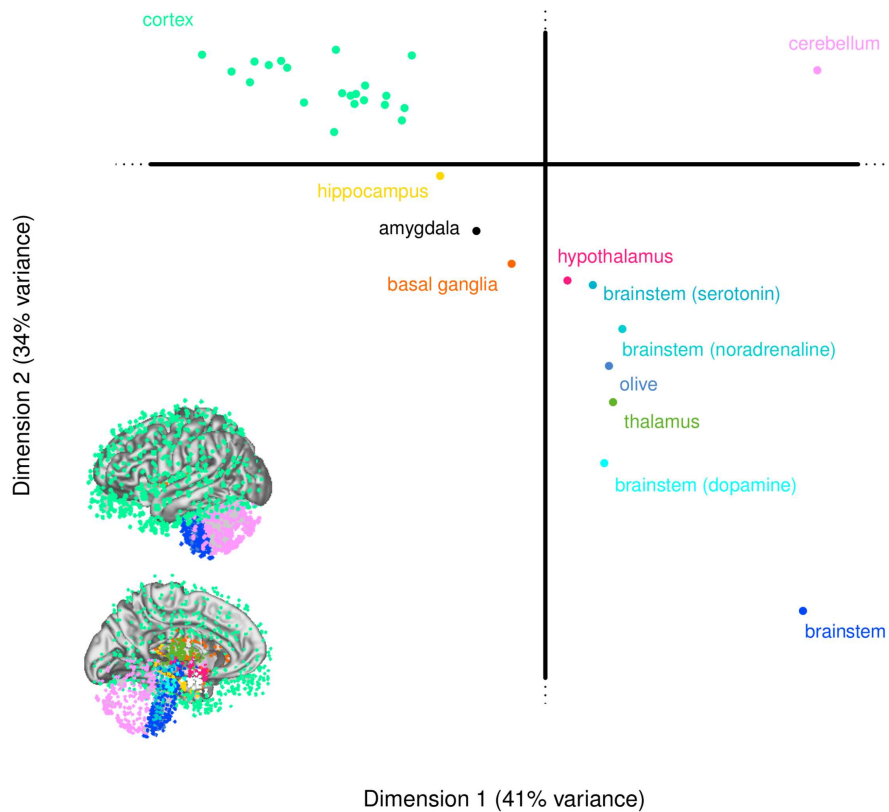


Fig. 5.3.: Cerebral regions' organization based on gene expression: DiCA analysis. Dimensions 1 and 2 as extracted by a DiCA performed on the 32 cerebral regions and the 29175 genes. The dots represent the bootstrap ratios for the barycenter of each cerebral region. The eigenvalue of Dimension 1 ($\lambda_1 = 3.09^{-03}$) represents 41% of the total variance, The eigenvalue of Dimension 2 ($\lambda_2 = 2.57^{-03}$) represents 34% of the total variance.

5.5.3 Organization of cortical regions by gene expression

Given the homogeneity of the genetic expression across the cortical regions, we tried to maximize the chance to see differences among the different anotomo-funcntional regions. To do so we reduced the analyzed table to the 1322 samples (corresponding to the 21 anatomo-fucntional cortical regions) and to 14575 genes. The genes were chosen as the genes (not probes) having an average of expression of at least 4 (\log_2) across the cortical samples for at least one brain. The first two dimensions of the DiCA (see Figure 5.4.a) account together for the 67.9% of the total variance – 54.7% and 13.2% respectively and $p < 0.01$. The organization of the genetic expression is mainly developed along the first axis, following the anatomo-fucntional organization previously described as the dual intertwined rings, with two directions, one grouping the sensorymotor and bimodal regions in the VSA direction (the VSA: Visual-Somatic-Auditory regions), and one grouping higher associative areas in the PTF direction (PTF: Parieto-Temporo-Frontal). The second dimension instead represents a dorso-ventral axis opposing frontal and temporal regions on the PTF side, and opposing somatomotor regions to occipital visual regions on the VSA side.

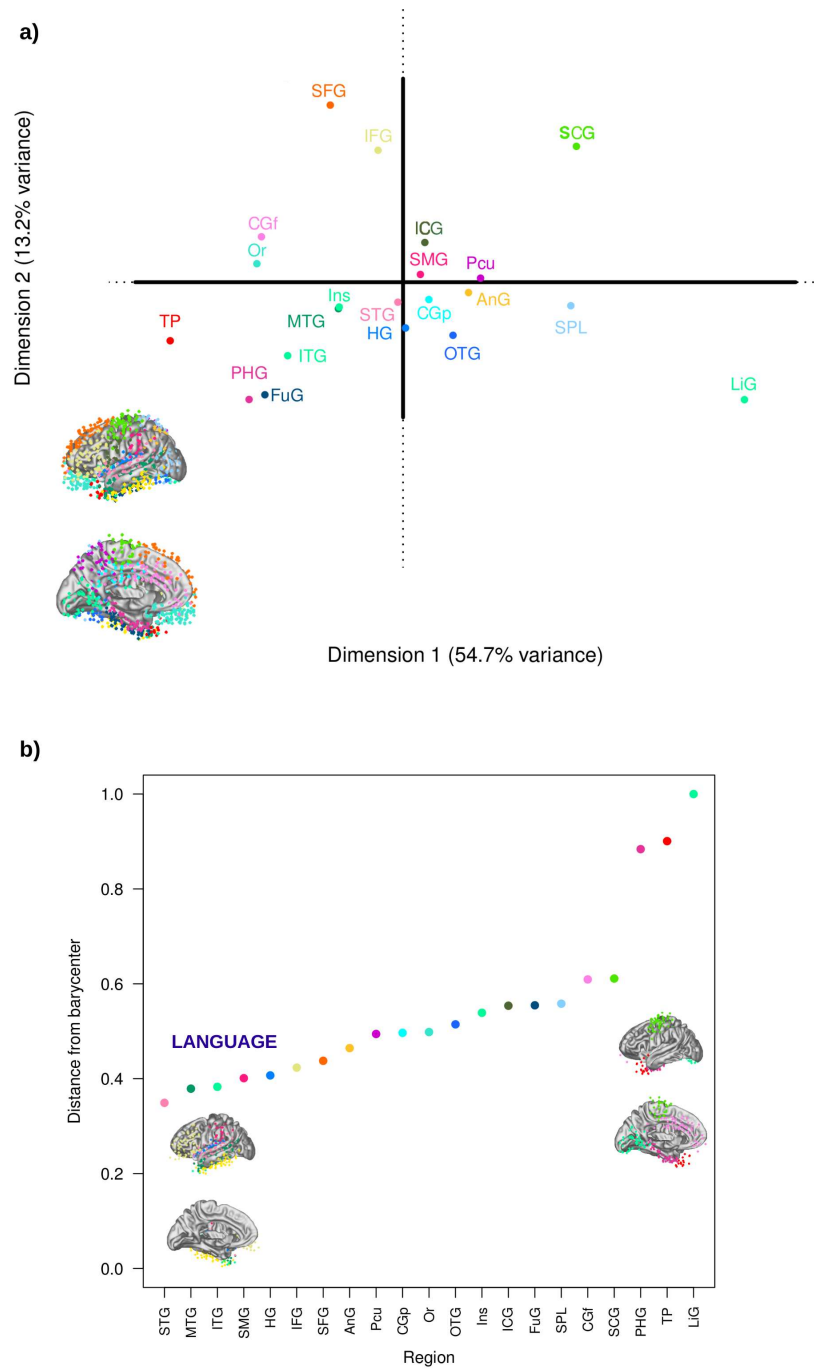


Fig. 5.4.: Cortical regions' organization based on gene expression: DiCA analysis. **a)** Dimensions 1 and 2 as extracted by a DiCA performed on the 21 cerebral regions and the 14575 genes. The dots represent the bootstrap ratios for the barycenter of each anato-functional cortical region. The eigenvalue of Dimension 1 ($\lambda_1 = 2.24^{-04}$) represents 55% of the total variance, The eigenvalue of Dimension 2 ($\lambda_2 = 5.38^{-05}$) represents 13% of the total variance. **b)** Distance from the barycenter of the regions' factor score whole space: regions are ranked based on their distance from the barycenter. Anato-functional regions implicated in language functionalities are the closest to the barycenter (less differentiated).

It is interesting to notice the genetic proximity of cortical regions in relation with their topographical proximity: for example, superior frontal regions and inferior frontal regions, which have a topographical continuity, have very similar genetic profiles. The results reveal the central genetic position occupied by the regions STG, PL, MTG, SMG, that are all involved in supporting the functionalities of language. Regions supporting language – one of the most distinctive cognitive functions for the human species – seem to be characterized by an average genetic profile. Visual regions on the VSA side, and parahippocampal regions on the PTF side, are the regions that present the most differentiated genetic profiles. The eigenvalues relative to the first and second dimension are 1 and 2: this tells us that there are significant differences between the genetic expression of different anatomic-functional regions, but it also explains that there are not regions expressing pool of genes on an exclusive way. The genetic differences between regions are indeed organized in gradients. The different anatomic-functional cortical regions all express the same genes but present different stoichiometry. There are no specific genes associated exclusively to any specific group of anatomic-functional regions and To be sure that these findings were not merely the results of the projection on the first two dimensions extracted by DiCA, we evaluated the distance of each region from the barycenter in the complete space of regions' factor scores. Figure 5.4.b shows for all the anatomic-functional regions, the distances – normalized to the maximum – from the barycenter of the whole factor scores space. The extreme position of visual regions (maximum), temporal regions and parahippocampal regions confirm that they are the most differentiated. The gradient followed by the other cortical regions confirms their relative homogeneity. The identity of the regions representing the minima – closer to the barycenter – tells us that indeed anatomic-functional regions supporting language's functionalities are those with the most average genetic profile. Finally the opposition of region further or closer to the factor scores' space barycenter represent an opposition of evolutionarily newer regions versus more ancient ones.

5.5.4 Differential expression of genes in families involved in information processing and memory formation

In Figures 5.5-5.12, we plot the bootstrap obtained for the genes of 8 groups of families of synaptic proteins (cerebral and cortical distributions): (1) ionic channels, (2) neurotransmitter release machinery, and (3) gaba and glutamate receptor known to be important in information processing, (4) neuromodulators and (5) CAMKs important for short term memory, (6) cytoskeleton proteins actin and tubulin important for long term memory, (7) axon guidance and cell-cell recognition proteins (such as semaphorins and ephrins), and (8) growth factor (such as FGF, EGF), important for building neuronal networks. For each family of genes only the isoforms which have a bootstrap greater than 5 ($BT > |5|$) on at least one of the two first dimensions were plotted. Moreover only the names of genes with the most extreme bootstrap – following a convex hull – are shown for readability purpose. The

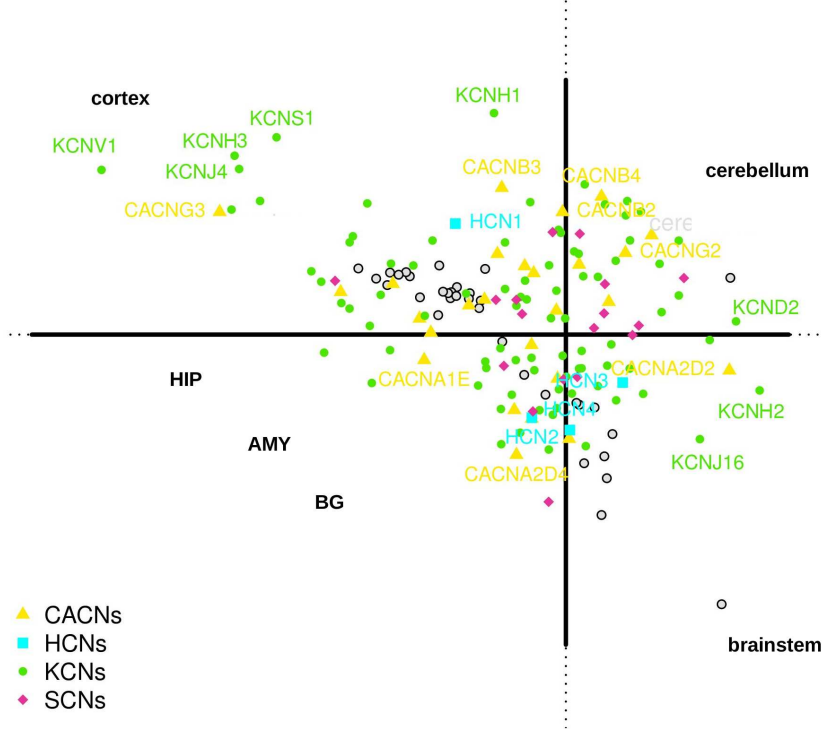
complete results are reported in table TS. On the same graphs are also shown the bootstrap obtained for the regions.

5.5.4.1 Ionic Channels

The results on the cortical expression of genes coding for ionic channels confirm the results previously obtained (Figure 5.5.b). The members of the channel families, potassium, sodium and calcium channel families are spread on all cortical regions from extreme VSA to extreme PTF. They comprise two groups of genes, which discriminate strongly between the VSA and PTF regions. For the sodium channels family on the VSA side, we found SCN1B and SCN1A while on the other extreme preferentially expressed in the PTF ring we found SCN3B and SCN3A. For the potassium channel family we found, with the highest bootstrap ratio in VSA, KCNA1 and on the other side we found KCNG1. For the calcium channel family, CACNA2D2 had the highest bootstrap ratio in the VSA ring while CACNG3 had the highest bootstrap ratio in the PTF ring. The present results complete this picture with a differential expression on the dorsolateral Fronto-temporal axis, in particular for potassium channels: KCNN2 (calcium dependent) and KCNJ8 are more expressed in the frontal regions; KCNA3 and KCNA5 are also more expressed in the frontal regions, while KCNA4 is more expressed in the temporal regions. The distribution on all the cerebral regions (5.5.a)) shows that ionic channels are distributed with a similar density in all cerebral regions. CACNG3 which had the highest bootstrap ratio in the PTF ring is concentrated on the cerebral cortex, and CACNA2D2 which has the highest cortical expression in VSA, is even highest in the cerebellum and the brainstem. Certain channels like CACNB2, B3 and B4 are shared by the two cortices, cerebral and cerebellar. A similar distribution is seen for HCN1, while HCN2,3,4 are overexpressed in the brain stem.

Ionic channels

a) Cerebral distribution



b) Cortical distribution

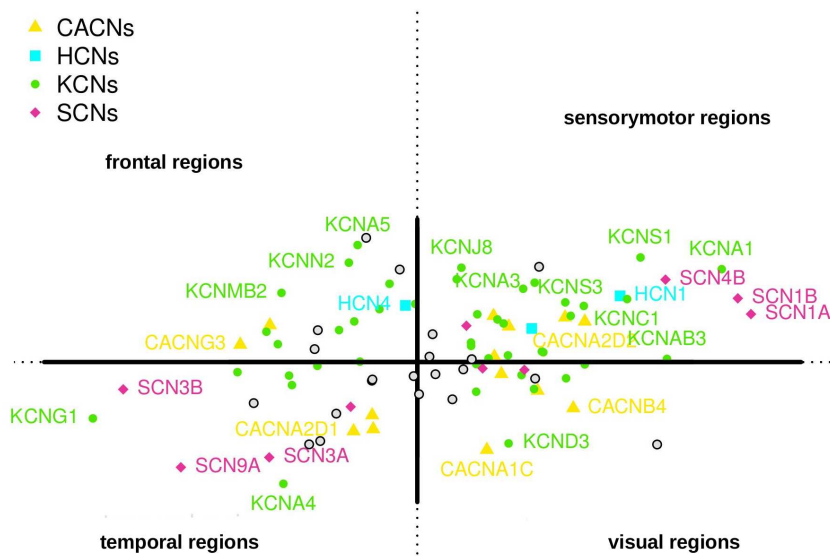


Fig. 5.5.: Ionic channels: cerebral **a)** and cortical **b)** distribution. In each figure are plotted the bootstrap ratios relative to the first two dimensions extracted by DiCA analysis (see Figure 5.3). Only genes which obtained a bootstrap ≥ 5 (corresponding to $p < 0.01$, Bonferroni corrected) on at least one dimension were plotted. For sake of clarity only the names of the most extreme genes are shown.

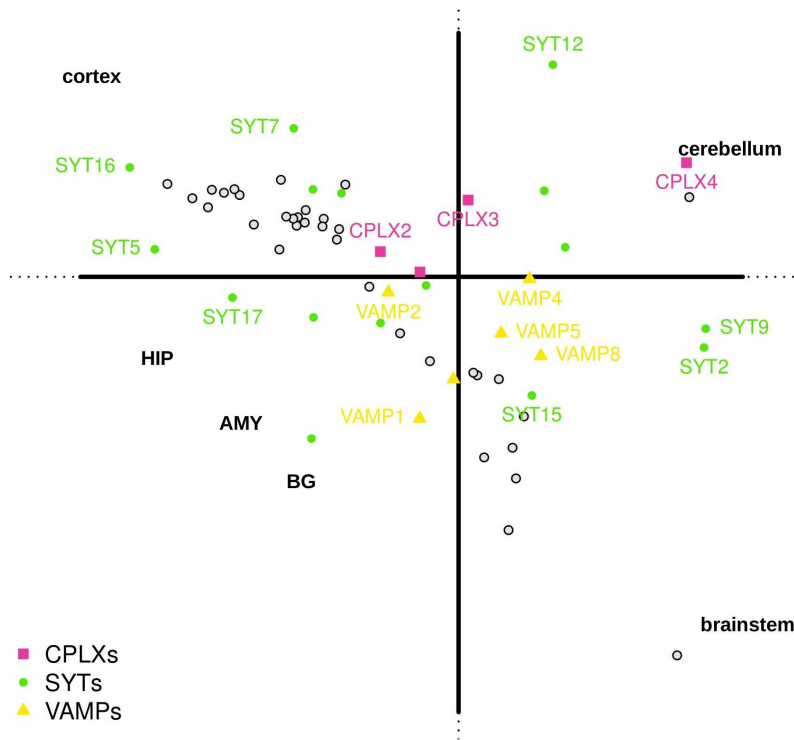
5.5.4.2 Neurotransmitter release

Similarly, we find similar results as in the previous paper for the genes coding for proteins involved in the presynaptic release machinery (Figure 5.6.b). For the synaptotagmin family we found, on the VSA side, SYT2 with an extremely high boot ratio. By contrast, on the PTF side we found SYT17 and SYT5. For the complexin family, on the VSA extreme, we found CPLX1. Conversely, on the PTF side we found as the most extreme gene CPLX3. Finally, for the VAMP family we found VAMP1 preferentially expressed in the VSA ring while VAMP2 was preferentially expressed in the PTF ring. When we extend to the distribution on all cerebral region 5.6.a), we see that the genes coding for synaptotagmin the most expressed in PTF (SYT17, SYT5) are shared between the cerebral cortex the hippocampus the amygdala and the basal ganglia; and the gene of the family the more expressed in VSA is higher in the brain stem and cerebellum.

While synaptotagmins are distributed across all cerebral regions, complexins, are more characteristic of the cerebral and cerebellar cortices (CPLX4 exclusively cerebellar) cortices, and synaptobrevins of the subcortical structures altogether.

Neurotransmitter release

a) Cerebral distribution



b) Cortical distribution

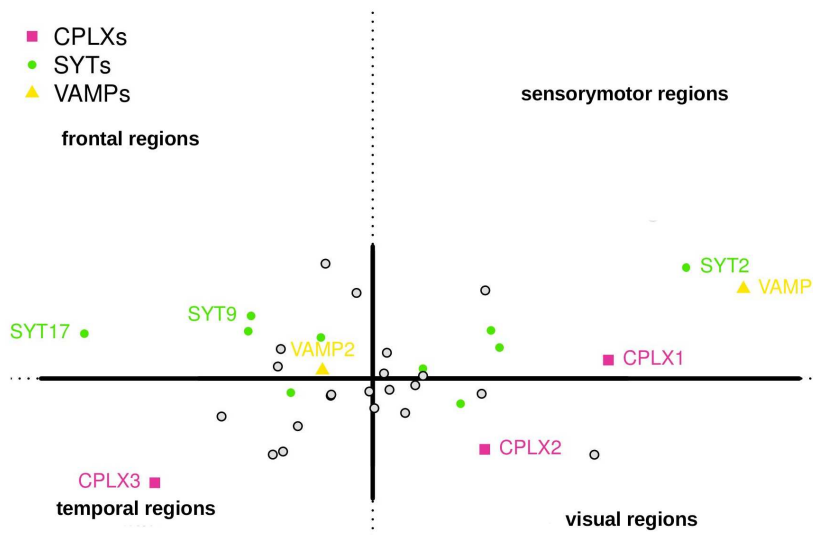


Fig. 5.6.: Neurotransmitter release: cerebral **a)** and cortical **b)** distribution. In each figure are plotted the bootstrap ratios relative to the first two dimensions extracted by DiCA analysis (see Figure 5.3). Only genes which obtained a bootstrap ≥ 5 (corresponding to $p < 0.01$, Bonferroni corrected) on at least one dimension were plotted. For sake of clarity only the names of the most extreme genes are shown.

5.5.4.3 Neurotransmitter receptors: GABA and Glutamate receptors

Most of the receptors for the inhibitory neurotransmitter GABA (13 out of 21 subunits have a $BT > |5|$) have their pole of expression in the cortical regions (e.g., GABRA4, GABRA2). GABRA5 and GABRA3 are characteristic of the cerebral cortex together with hippocampal and parahippocampal regions (Figure 5.7.a). These two genes are also the highest expressed genes in PTF (Figure 5.7.b). GABRD shared between cortical and cerebellar regions, but not with subcortical and brainstem structures (Figure 5.7.a), is strongly expressed in VSA (Figure 5.7.b). GABRA6 is expressed in the cerebellar cortex. Finally GABRQ is the isoform with the pole the closest to the brain stem. GABA receptors are distributed across all cortical structures but with a bias toward brain regions undergoing strong plasticity processes.

The glutamate NMDA receptor (NMDAR) is very important for controlling synaptic plasticity: calcium flux through NMDARs is increased when there is a co-occurrence of presynaptic activation (release of glutamate) and post synaptic activation (depolarization). These NMDA receptors have a higher distribution in the cerebral and cerebellar cortices, and subcortical cerebral regions proximal to the cerebral cortex (hippocampus, amygdala, basal ganglia). They are distributed in close relation of the adaptive plastic capacities of these different regions. The family of NMDA receptors (all the 6 subunits have a $BT > |5|$) for the neurotransmitter glutamate has a similar distribution of the isoforms of GABA receptors. The pole of expression of GRIN2A, GRIN2B and GRIN3A corresponds to the cortical regions and the hippocampus. Within the cortical regions, GRIN2B are more expressed in PTF, while GRIN2A is more expressed in VSA. Among the the genes coding for NMDA glutamate receptor family, the most extreme gene preferentially expressed in PTF is GRIN3A. By contrast GRIN2C is essentially expressed in the cerebellar cortex.

Another family with a similar distribution is the family of kainate glutamate receptors. The members of this family (4 out of 5 subunits have a $BT > |5|$) have indeed their maximal expression across the cortical regions, cerebellar cortex and the hippocampus, amygdala and basal ganglia regions. On the other hand GRIKs are different from the precedent two families since they always have their minima in correspondence of the brainstem and thalamic or hypothalamic regions. All the 4 subunits of the AMPA glutamate receptor have a $BT > |5|$. Three among them have their maxima of expression across the cortical regions (e.g., GRIA2) while one of them has the pole of its distribution in cerebellar regions (GRIA4). The GRIA family appears to have a preferential distribution shared between cerebral and cerebellar cortices.

Finally the family of metabotropic glutamate receptors is distributed either in cortical regions and proximal subcortical regions, hippocampus, amygdala-basal ganglia (GRM5 and GRM7), either in the cerebellum (GRM1, GRM4). Within the cortical regions, the most extreme gene is GRM1 preferentially expressed in the PTF ring.

Neurotransmitter receptors

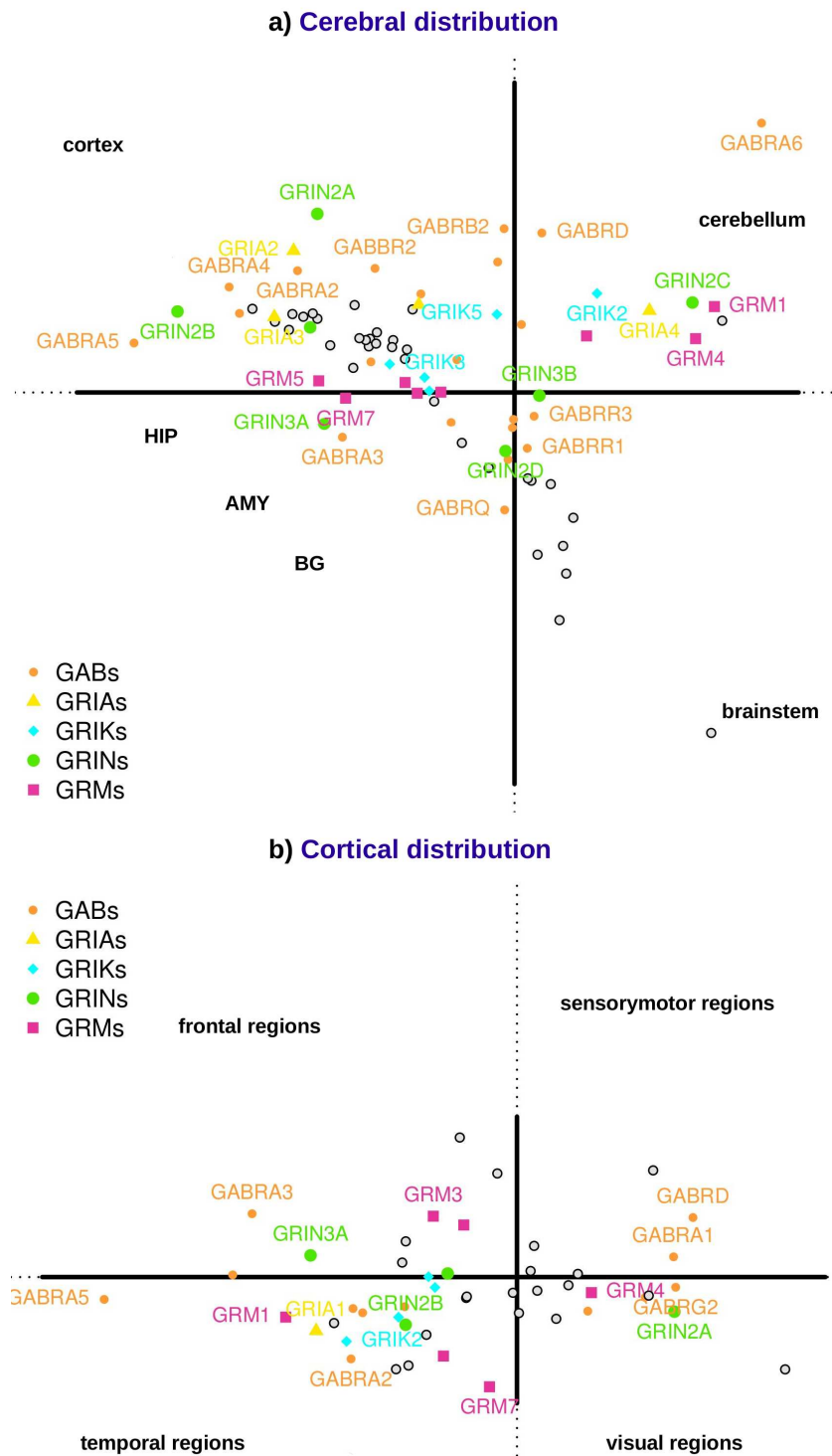


Fig. 5.7.: Neurotransmitter receptors: cerebral **a)** and cortical **b)** distribution. In each figure are plotted the bootstrap ratios relative to the first two dimensions extracted by DiCA analysis (see Figure 5.3). Only genes which obtained a bootstrap ≥ 5 (corresponding to $p < 0.01$, Bonferroni corrected) on at least one dimension were plotted. For sake of clarity only the names of the most extreme genes are shown.

5.5.4.4 Neuromodulators receptors: Serotonin, Dopamine, Norepinephrine

Neuromodulators Serotonin, Dopamine and Norepinephrine (adrenergic receptor) produced by brain stem nuclei have a strong and prolonged modulatory influence on synaptic transmission, modifying the spatial and temporal propagation of signals. Their synaptic effects depend strongly upon the receptor subtypes which is expressed.

The differentially expressed subtypes of dopamine receptors (3 out of 5 have a $BT > |5|$) have their maximal expression across cortical regions and the basal ganglia, hippocampus and amygdala, and their absolute minima in the cerebellum (Figure 5.8.a). The isoform DRD1 is highly expressed in the cortex, DRD3 in the basal ganglia and DRD2 in the brain-stem, consistently with known results on the distribution of dopamine receptors. DRD5 is expressed both in in the cortex and in basal ganglia. Within the cortical regions (Figure 5.7.b), DRD5 has a higher expression in PTF. The differentially expressed subtypes of adrenergic receptors (7 out of 9 have a $BT > |5|$) have a similar distribution. ADRA1B has the highest expression in cortical regions. Within cortical regions, ADRA1B is highly expressed in PTF, together with ADRB2, while ADRB1 is more expressed in VSA. A specific subtype, ADRA1D has an high expression in the frontal regions. A similar distribution is presented by serotonin receptors (19 out of 21 have a $BT > |5|$) with four subtypes highly expressed in cortical regions (HT3B, HTR2A, HTR1A and HTR1F). For HTR1A and HTR1F highly expressed in the cerebral cortex, we found that HTR1A is referentially expressed in PTF, and HTR1F preferentially expressed in VSA. HTR5A is shared between cortical areas and cerebellum, and within cortical regions is preferentially expressed in frontal regions. Finally acetylcholine receptors (17 out of 21 isoforms have a $BT > |5|$) are distributed across all cerebral regions. Muscarinic receptors are preferentially expressed in the cortex (CHRM1, CHRM3) hippocampus, amygdala and basal ganglia. Different isoforms of nicotinic receptors present their maxima in all the different cerebral regions: CHRNA7 cerebral cortex and hippocampus, CHRNA10 in the cerebellum.

Neuromodulators receptors

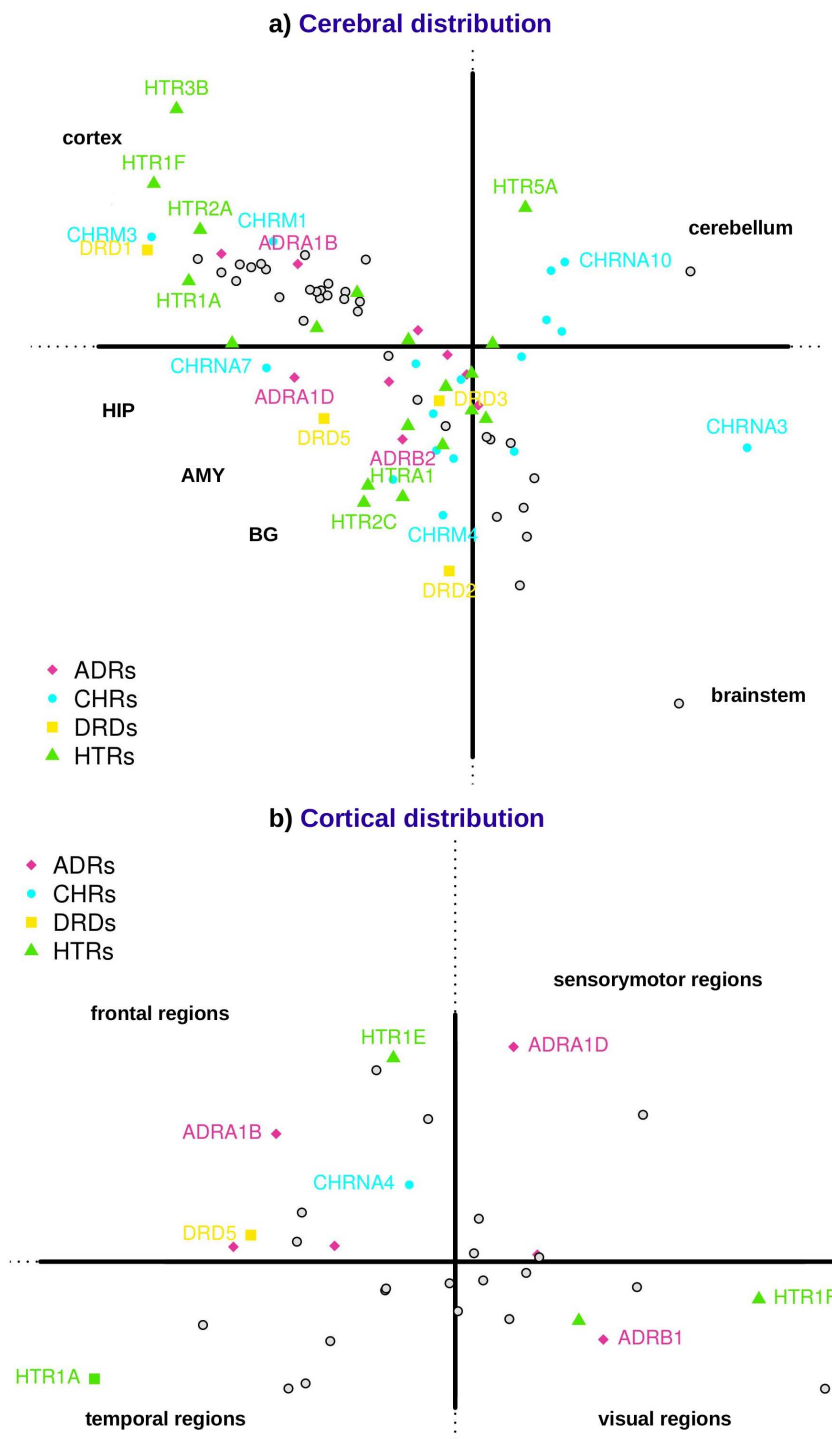


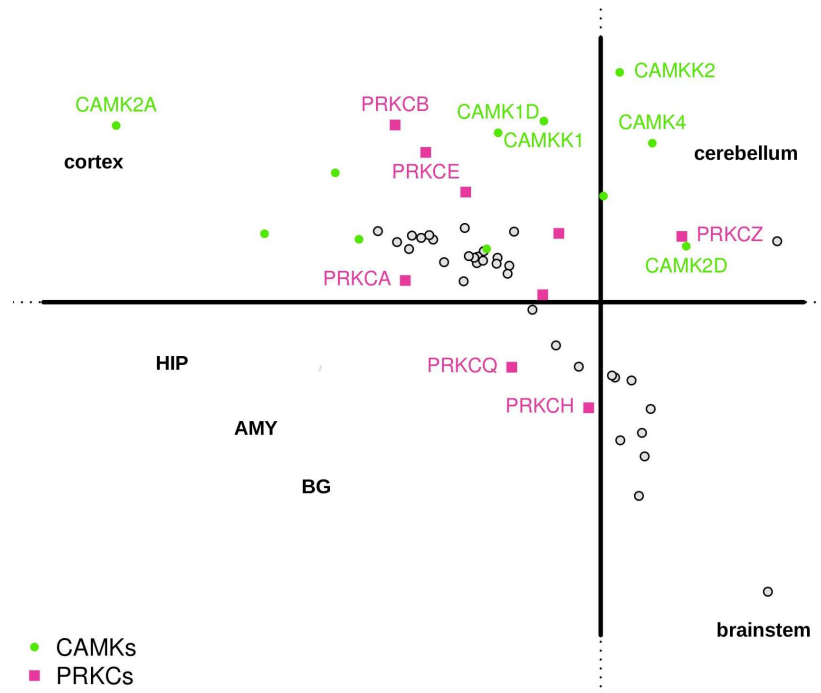
Fig. 5.8.: Neuromodulators receptors: cerebral **a)** and cortical **b)** distribution. In each figure are plotted the bootstrap ratios relative to the first two dimensions extracted by DiCA analysis (see Figure 5.3). Only genes which obtained a bootstrap ≥ 5 (corresponding to $p < 0.01$, Bonferroni corrected) on at least one dimension were plotted. For sake of clarity only the names of the most extreme genes are shown.

5.5.4.5 Short-term memory: CaMK and PKC

Short term memory is regulated by persistent CaMK autophosphorylation which follows transient elevations of intracellular calcium, with variable durations. This process can mediate long-term memory formation : CaMKII regulate the reorganization of the actin cytoskeleton at synapses, leading to a long-term activity-dependent increases in synaptic efficacy. Results show that the different members of the CaMK families are overexpressed mainly in the cerebral and in the cerebellar cortex, which have a major role in learning and memory (Figure 5.9.a). CaMK2A is essentially expressed in the cerebral cortex, and CaMK4 is strongly expressed in the cerebellum. Furthermore different members of the CAMK families are differentially distributed in different cortical regions, such as CaMK2G and CaMK2D (Figure 5.9.b): CaMK2G is more expressed in the VSA ring, more related to sensory-motor interactions, and CaMK2G in the PTF ring, more related to episodic memory and language. Results reveal also that CaMK4 and CaMK1 are differentially expressed on the frontal-temporal axis: within the Cortex, CaMK4 is more expressed in the temporal regions, and CaMK1G is more expressed in frontal regions. Protein kinase C (PKC) is also activated by calcium, and PKC family members phosphorylate a wide variety of protein targets involved in memory acquisition. While CAMKs are mostly expressed in cerebral and cerebellar cortices, PKCs extend to hippocampal, amygdala, basal ganglia and brain stem regions. When zooming on the different isoforms in the cerebral cortex, results show that PRKCG and PKRCD are more expressed in the PTF regions, and PRKCA in VSA regions.

Short term memory

a) Cerebral distribution



b) Cortical distribution

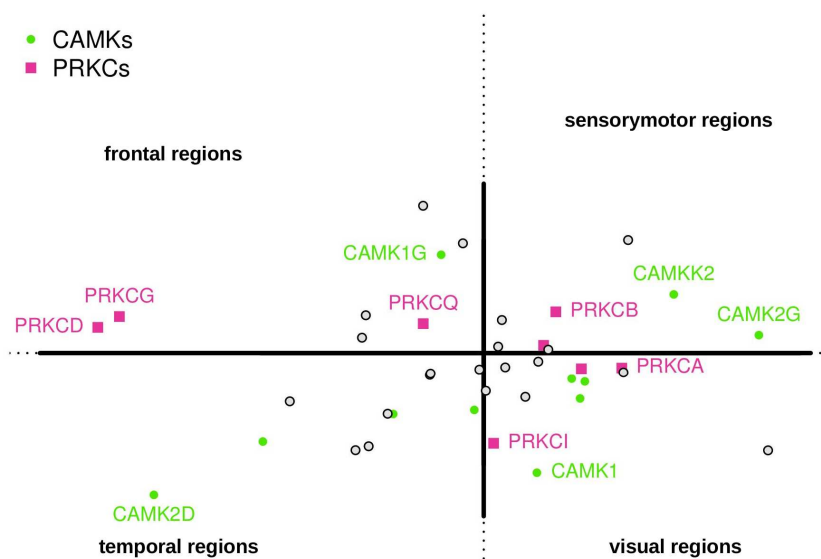


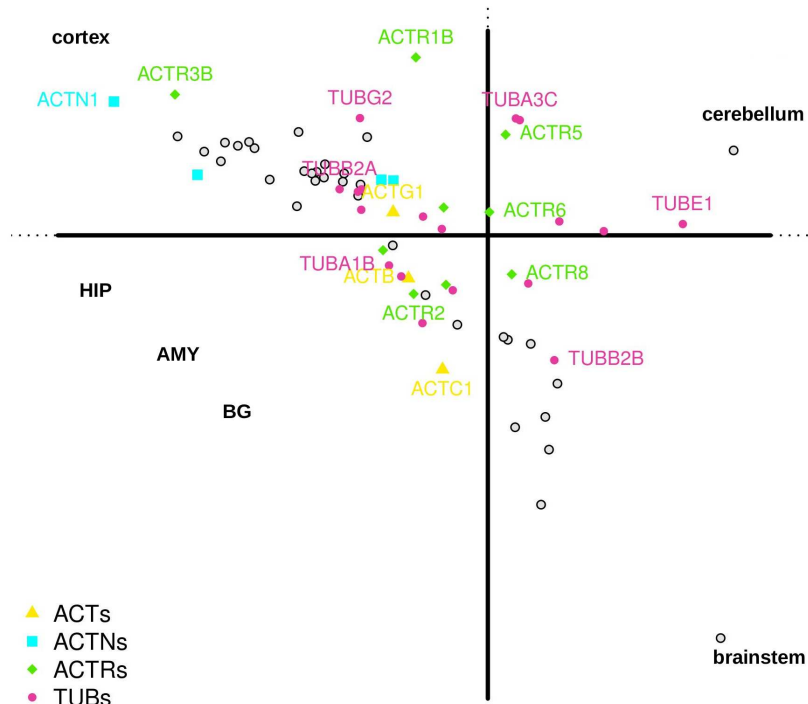
Fig. 5.9.: Short term memory: cerebral **a)** and cortical **b)** distribution. In each figure are plotted the bootstrap ratios relative to the first two dimensions extracted by DiCA analysis (see Figure 5.3). Only genes which obtained a bootstrap ≥ 5 (corresponding to $p < 0.01$, Bonferroni corrected) on at least one dimension were plotted. For sake of clarity only the names of the most extreme genes are shown.

5.5.4.6 Cytoskeleton Actin and Tubulin: Long-term memory

Long term memory formation is produced by actin polymerization, the key process responsible of spine enlargement which increases the synaptic efficacy. Tubulins, and microtubule polymers into which they incorporate, is critical for development of axons and dendrites, and activity-dependent remodeling of axons and dendrites can implement diverse forms of long-term memory. All the different isoform of the actual protein actin (ACTs) have a BT>|5| and appear to be distributed across all the cerebral structure with a weaker expression in the cerebellum respect to all the other regions. The actinin family (coded by ACTN gene) control the shape of spine. They have a global preferential expression in cortical areas (Figure 5.10.b), in particular ACTN1 (all isoforms have a BT>|5|). Alpha-actinin isoforms are differentially expressed in the cortical regions, with alpha-actinin2 (coded by ACTN2 gene) more expressed in the frontal cortex. The ACTR family (9 out of 10 isoforms have a BT>|5|) is part of the complex Arp2/3 which shape the actin network underlying synaptic efficacy. Isoforms are also distributed across cerebral and cortical regions (Figure 5.10.a) with ACTR3B maximum in cortex, ACTR2 maximum in hippocampus, basal ganglia-amygdala and brainstem. Results reveal that actin-related proteins ACTR3, ACTR3B and ACTR3C, have higher expression in the temporal regions. The family of tubulin (19 out of 21 isoforms have a BT>|5|) appears to be distributed across all the cerebral regions with some isoform preferentially expressed in the cerebral cortex as TUBB2A or having its maxima in the cerebellum or brains stem structures. Differential distribution in the cortical regions show that beta-tubulin TUBB (TUBB, TUBB2A, TUBB3A, TUBB3) and alpha-tubulin genes (TUBA1A) are more expressed in PTF regions, and within PTF, they have an high expression in the frontal regions, while other isoforms (such as TUBD1, TUBF1 are more expressed in VSA

Long term memory

a) Cerebral distribution



b) Cortical distribution

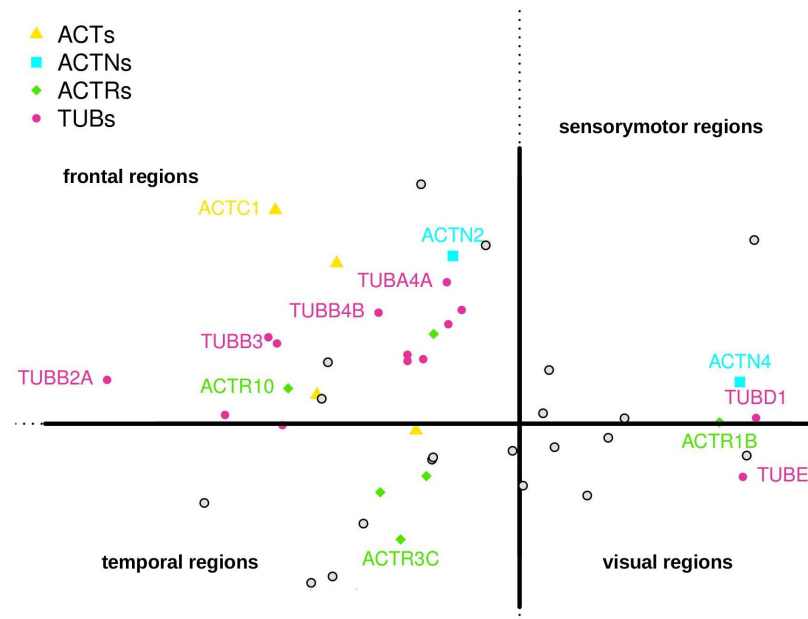


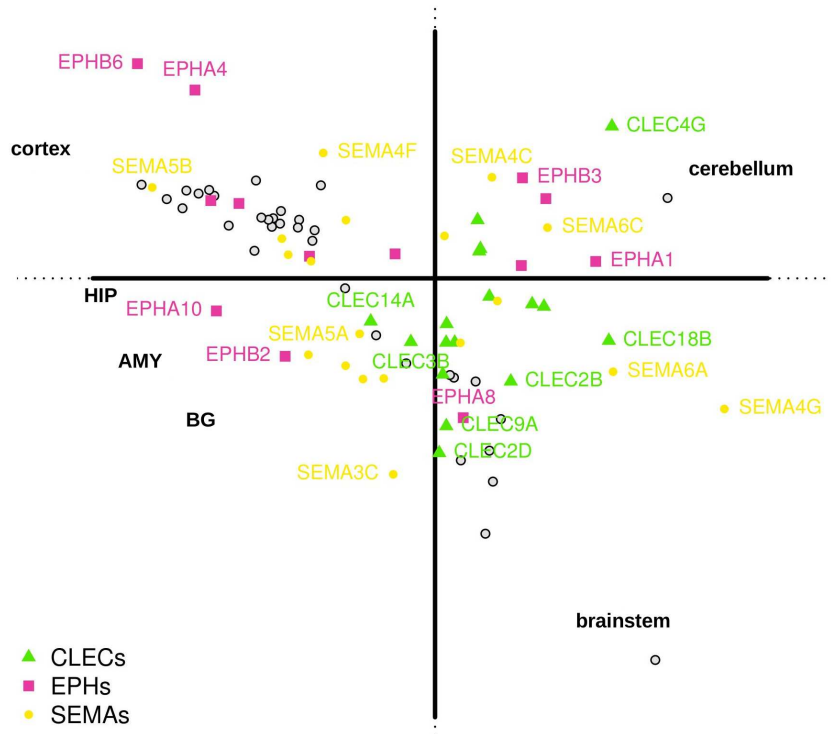
Fig. 5.10.: Long term memory: cerebral **a)** and cortical **b)** distribution. In each figure are plotted the bootstrap ratios relative to the first two dimensions extracted by DiCA analysis (see Figure 5.3). Only genes which obtained a bootstrap ≥ 5 (corresponding to $p < 0.01$, Bonferroni corrected) on at least one dimension were plotted. For sake of clarity only the names of the most extreme genes are shown.

5.5.4.7 Semaphorin, Ephrin C-Lectin Cell Cell attachment

Genes coding for protein sets on the neuronal surface, such as semaphorin, ephrin, c-lectin guide neuronal migration and synapses formation. That are found expressed in adults with a role in homeostasis of the resulting networks and long term changes of synaptic strength. The distribution of the ephrin family EPH (10 out of 14 isoforms have a $BT > |5|$) shows that the most polarized genes are in the cortical regions (e.g., EPHB6, EPHA4) followed by cerebellar regions (e.g., EPHB3) and hippocampal-amygdala-basal ganglia regions (EPHB2) (Figure 5.11.a). Only EPHA8 has a distribution maximal across brainstem regions. Within cortical regions (Figure 5.11.b), Ephrin are preferentially expressed on PTF (EPHA4, EPHA5), with a differential expression on temporal (EPHA3) and frontal regions (EPHB3). The semaphorin family SEMA (17 out of 20 isoforms have a $BT > |5|$) is characterized by a more uniform distribution of all its isoforms across all the cerebral regions. Semaphorins isoforms are differentially expressed in cortical regions, in particular in temporal regions (SEMA5B), with SEM4A and SEMA3D more in the temporal regions of PTF. The C-Lectin family CLEC (10 out of 27 isoforms of have a $BT > |5|$) have a complementary distribution with respect to the Ephrins. None of these isoforms appear to be polarized in correspondence of the cortical regions. CLECs have mainly poles in correspondence of the brainstem, thalamic and hypothalamic regions, also in basal ganglia (e.g., CLEC2D) and/or cerebellar regions (e.g., CLEC2B, CLEC18B). Ephrin, Semaphorins, and C-Lectin isoforms could thus control different types of homeostasis and activity-depedent synaptic rearrangement in different cerebral and cortical regions.

Cell-cell interaction

a) Cerebral distribution



b) Cortical distribution

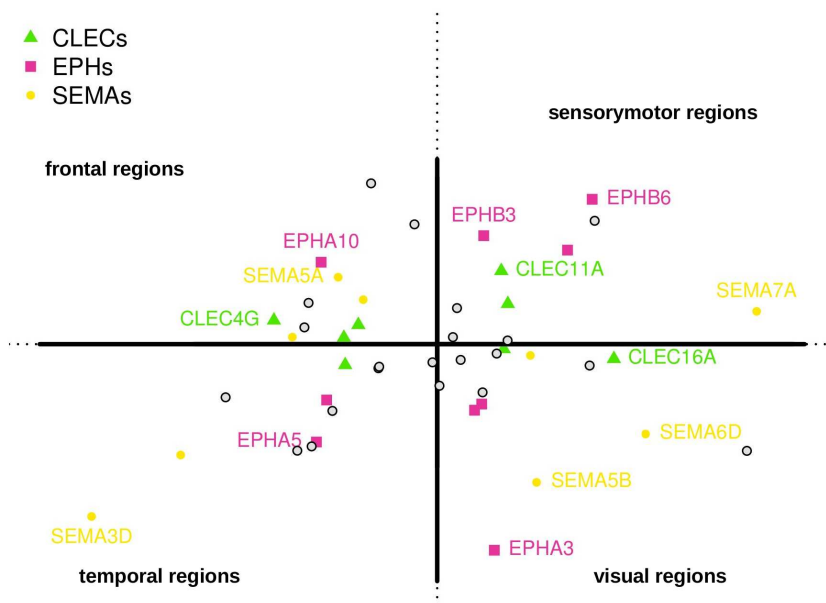


Fig. 5.11.: Cell-cell interaction: cerebral **a)** and cortical **b)** distribution. In each figure are plotted the bootstrap ratios relative to the first two dimensions extracted by DiCA analysis (see Figure 5.3). Only genes which obtained a bootstrap ≥ 5 (corresponding to $p < 0.01$, Bonferroni corrected) on at least one dimension were plotted. For sake of clarity only the names of the most extreme genes are shown.

5.5.4.8 Growth factors and Transcription factors: FGF, EGF, HGF, FOXP2

The fibroblast growth factor family (FGF) influences all phases of fetal and embryonic development and has a key role in specification and growth rates of brain regions and cortical areas. FGF isoforms in adults are also differentially expressed and can be important for neuronal and synaptic homeostasis while maintaining cortical layer structure. Our results (Figure 5.12.a) show that FGF isoforms are differentially expressed in all the different brain regions (cerebral and cerebellar cortex): for example FGF12 and FGF 18 in the cerebral cortex, FGF5 and FGF9 in the cerebellum, FGF1 in brainstem regions. FGF isoforms are also differentially expressed within cortical regions (Figure 5.12.b): FGF2 is more expressed in PTF, and FGF9 in VSA. FGF receptors are also differentially expressed, as FGFR1 in frontal regions. Our results show an overexpression in temporal regions of 2 genes which have been involved in language disorders and autism, and codes for strongly related proteins: the gene coding for the transcription factor FOXP2, and the gene coding for the growth factor receptor c-MET which has a particularly high level of expression in the temporal regions and occipital regions.

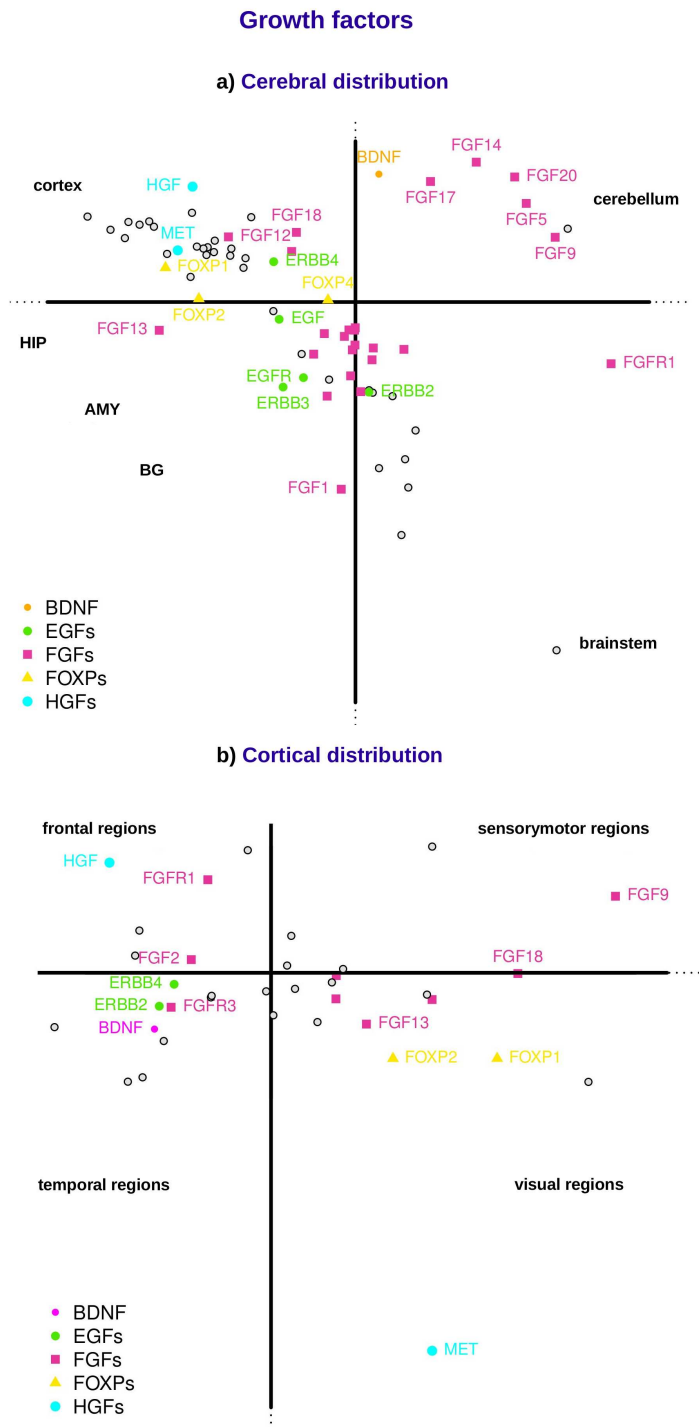


Fig. 5.12.: Growth factors: cerebral **a)** and cortical **b)** distribution. In each figure are plotted the bootstrap ratios relative to the first two dimensions extracted by DiCA analysis (see Figure 5.3). Only genes which obtained a bootstrap ≥ 5 (corresponding to $p < 0.01$, Bonferroni corrected) on at least one dimension were plotted. For sake of clarity only the names of the most extreme genes are shown.

5.5.5 Gradients of gene expression in the cerebral cortex

In Figure 5.13, we illustrate the example of the CAMK family to show that, for most of the explored families: i) all members of the family are highly expressed across all the cortical regions; ii) each member have a particular gradient of expression across different regions. In particular here we showed in panel a) only CAMK members with a gradient of expression across different regions. CAMK2B display an homogeneous distribution across all the cortical regions. CAMK2G presents instead a gradient that goes from visual and motor regions (VSA) to frontal and temporal regions (PTF). The CAMK2D present a gradient pattern symmetric with respect to CAMK2G. There is a similar contrast between CAMK1G, more expressed in the frontal regions, and CAMK4, more expressed in the temporal regions. The cortex is merely homogeneous with subtle gradients changing the stoichiometry of genetic expression across regions. The cortical adaptive property combines the capacities of a generic pool of genes expressed in synapses, and a local specialization finely tuning genetic stoichiometry.

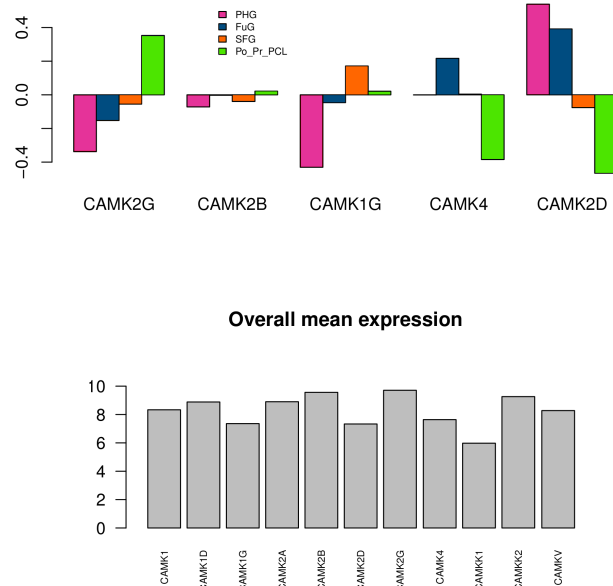


Fig. 5.13.: CaMKs family: differential distribution. Top panel: gradient of distribution of CAMK isoforms across four cortical regions. Different members show different cortical gradients. Bottom panel: average value of expression for CAMK isoforms evaluated across all cortical regions.

In Figure 5.14, we display the gradient patterns for genes the most differentiated across the cortex as given by bootstrap analysis. We chose the most extreme genes to compare their different gradients across the cortex. For each gene we sort the expression from the strongest to the smallest across the cortical regions. This figure shows that eight gradients of gene expression across the cortical regions. These eight profiles are extracted from the DiCA analysis and correspond to groups of genes which present significant bootstraps (only on the first dimensions, positive or negative, only on the second dimension positive or negative,

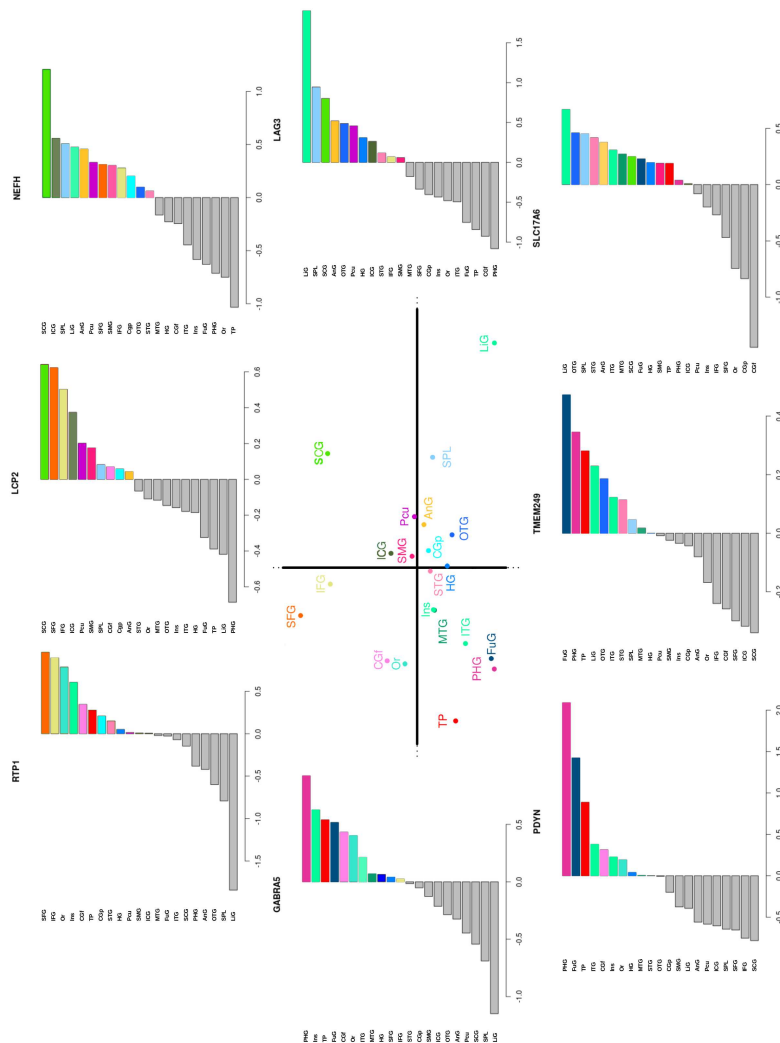


Fig. 5.14.: Cortical gradients of gene expression. Eight prototypical types of gene expression gradients corresponding to eight main directions defined in the space of Dimension 1 and 2 extracted by DiCA. For each direction we chose an extreme gene (in term of bootstrap ratio) and we plotted for each anoto-mo-functional region its deviation from the average gene expression.

both on the first and on the second positive/positive, negative/ negative) Each gene has regions of maximal expression but it is expressed also across the rest of the cortical regions with a smaller level. Isoforms with a significant bootstrap are characterized by gradient distributions. The quadrants on the two main axes, inform us about the pole of expression of this gradients. The larger the bootstrap absolute value in a given direction, the more polarized the gene’s distribution. So we have a palette of gradients that are ordered by the two main axes. The most representative patterns oppose VSA vs PTF regions (on the first dimension) and visual vs motor, and frontal vs temporal regions (on the second dimension). The maximum for PTF genes is in temporal and frontal regions with minimum in visual and motor region. Expression in STG and SMG is intermediate. Genes with a maximum in VSA has a gradient that is symmetric to the previous one, with a maximum in visuo-motor regions and minimum in frontal and temporal regions. Sensory-motor speech regions such

STG are intermediate once again. The other two gradients oppose frontal vs temporal regions.

5.6 Discussion

The main goals of this paper were three: first to study the relation between cortical gene expression and anatomo-functional regions used as proxy of sensory-motor and cognitive networks (as detected by brain imaging studies); second to study the distribution of family members for groups of genes known to be involved at the synaptic level in information processing, memory formation (short term and long term) and network genesis and maintenance; third to draw a link between specific protein functions at the neuronal level and cognitive function of the regions where these proteins are preferentially expressed. To do so we first studied the gene expression across all cerebral regions reported in the ABA. We grouped the anatomical regions into 32 groups corresponding to 21 cortical anatomo-functional regions and 11 main sub-cortical cerebral structures. We analyzed the table for the expression of 21000 genes across the 32 cerebral regions using a DiCA in order to maximize the differences between gene profiles associated to the 32 groups. Similarly we did for the table for the expression of 14000 genes (genes with average expression ≥ 4 across cortical samples) across the 21 anatomo-functional cortical regions.

5.6.1 Main axes of gene expression in cerebral regions and cortical regions

The results of DiCA show a double organization of gene expression patterns: one across the whole brain and one at the level of the cerebral cortex.

5.6.1.1 Cerebral regions

The first two dimensions extracted by the analysis (Figure 5.3) confirm the results obtained from the Allen Brain Institute and presented in <http://casestudies.brain-map.org/ggb>. The first two dimension show the existence of four main groups of regions: the cortical regions of the cerebral cortex (21 anatomo-functional regions), the cerebellar cortex, the brainstem regions and a set of cerebral regions including hippocampus, amygdala and basal ganglia. This latter set of regions is topographically and phylogenetically close to the cerebral cortex.

The first dimension opposes cerebral cortical regions to the cerebellar cortex and to the brain stem. The first dimension indeed tells that the genetic profiles of cortical regions are very similar among them and at the same time very different from the one of cerebellar and brainstem regions. Moreover cerebellar and brainstem regions share more similarities among them that with cortical regions. The set of cerebral regions proximal to the cerebral

cortex (hippocampus, amygdala and basal ganglia) are intermediate between the cortical ones and the brainstem ones. These results tell that genetic differences are mainly related to structure, textures and microcircuits [242]. Indeed all the cortical regions share similar neuronal textures of neurons and local circuits, the cortical columns. Within this prototypical local circuits, there are local cytoarchitectonic variations between sensory, motor and associative areas. Similar neural circuitry should involve similar synaptic operations implying similar genes expressed.

The second dimension opposes the cerebral and cerebellar cortex with the brainstem nuclei. The subcortical cerebral regions proximal to the cortex (hippocampus, amygdala, basal ganglia) are intermediate. While they are opposed by their local texture (on the first axis), the cerebral and cerebellar cortex share a strong similarity in their capacity of plasticity. The intermediate cerebral regions proximal to the cortex (hippocampus, amygdala, basal ganglia) have also a high degree of plasticity. By contrast, the brain stem nuclei are much less plastic. The second axis which organize the distribution of gene expression across cerebral regions can thus be interpreted as a “plasticity axis”, opposing regions with higher and lower degrees of plasticity.

Finally if we take into account the first six significant component extracted by the analysis we find a hierarchical organization of the differences characterizing gene expression across the different cerebral structures: the first dimension discriminates between the different neuronal textures and microcircuits of cerebral regions (neuronal microcircuits of cerebral cortex, cerebellar cortex, subcortical regions proximal to the cortex, and brainstem nuclei); the second dimension discriminates regions with respect to their level of plasticity (synaptic remodeling for learning and memory); the following significant dimensions extracted by the analysis (3-6) highlight the differences between hippocampus, amygdala and basal ganglia, and finally they reveal the main organization of cortical regions, with the VSA and PTF group of cortical regions, in a global cortical architecture with two intertwined rings as described in [48].

5.6.1.2 Cortical regions

Differences of expression between cortical areas are weaker than differences between different cerebral structures as shown in Figures 5.2.a and b. To magnify these differences we analyzed only the 14000 genes with a sufficient cortical expression on at least one brain. The technique used was again DiCA to force differences between the genetic profiles for the 21 cortical anatomo-functional regions defined in 5.1. The first dimension extracted by the analysis confirms the opposition between regions belonging to VSA and PTF ensembles as previously shown in [48] where the patterns of expression of the genes most differentially expressed across the cortex organized the cortex into two sets of regions that match the two rings. The second dimension extracted by the analysis opposes genetic profiles for dorsal versus ventral regions of the cerebral cortex: opposition between frontal (dorsal) and

temporal (ventral) regions, and between central motor (dorsal) and occipital visual regions (ventral). This axis opposes two types of functions: the dorsal cortical areas control the temporal organization of actions: motor actions in the central part, sensorymotor coordination in the parietal part (perception of body and motor control), and sequences of actions and planification in the more frontal parts. By contrast, the occipital and temporal regions are more specialized in perception of the outside world (exteroceptive perception, auditory and visual), recognition of categories (faces, places, etc), comprehension and memorization of categories, scenes and events.

5.6.2 Neoteny of language regions

The regions appearing in Figure 5.4.a as the most differentiated given their gene expression profiles are the visuo-motor regions on the VSA side and the parahippocampal gyrus (PHG) and the temporal pole (TP) on the PTF side. The anatomo-functional regions matching with language cognitive network result instead as the less differentiated in term of gene profiles. These results are corroborated by Figure 5.4.b where we evaluated the distance—in the space of regions' factor scores—from the barycenter of the whole space for each of the 21 anatomo-functional regions. These results confirm that the most differentiated regions (further from the barycenter) are the visual regions, the temporal pole and the parahippocampal cortex; while the less differentiated are anatomo-functional regions composing the cognitive network supporting language. Cortical regions of language (BAs 21, 22, 44, 45, 39, 40), which are newest in evolution, are the less specialized in term of gene expression. This suggests that the new regions subserving language are less structured and more flexible thus facilitating the largest range of learning and memory processes. Since speech and language regions are largely interfaced, language associates real-time processing of information (BA 22), categorization of words with their meaning stored in long-term semantic memory (BA 21), short-term and working memory to decode word sequences (BA 44, BA 45). This could help to understand the difficulties faced by scientists to find an extensive genetic specialization for language [116]: language learning thus appear as a generic cortical process. This result is consistent with the very prolonged neoteny of cortical maturation [97] characterizing language regions. In human evolution, prolongation of infant characteristics, or neoteny, has been proposed as a possible mechanism that contributed to the rise of many human-specific features, including an increase in brain size and the emergence of human-specific cognitive traits. The human brain transcriptome is dramatically remodeled during postnatal development with developmental changes in the human brain delayed relatively to other primates. This delay is not uniform across the human transcriptome but affects a specific subset of genes [250]. Recent findings from developmental neuroimaging studies suggest that the enhancement of cognitive processes during development may be the result of a fine-tuning of the structural and functional organization of brain with maturation. The developmental trajectory of large-scale structural brain networks indicates early maturation of primary sensorimotor regions and protracted development of higher order

association and paralimbic regions [147]. The diversification within families is the key of diversification of temporal properties related to different cognitive functions. The trend is consistent with evolutionary studies [225, 76]: first classes of proteins appeared very early in evolution as for example the apparition of CamK in choanoflagellates or NMDA receptors in cnidarians. Conversely the evolution in mammals, primates and humans are mostly related to differentiation within families. We know that the evolution of the two rings in primates result in the strong extension of PTF in human this influencing short and long term memory, language, autobiographical and episodic memory, theory of mind. We can then hypothesize that there is a differentiation of the topography of gene expression which is specific to human brain. This is also confirmed by comparison of mammals by the Allen Institute [297, 117] showing that there is a differentiation in the topography of gene expression across different mammals.

5.6.3 Gradients of gene expression

Figures 5.2.a and b show the double organization of gene expression, with differential distributions at two levels: the level of cerebral regions and the level of cortical regions. So there are genes important for the cerebral cortex as a whole and genes differentially expressed across the cortex (but not necessarily over-expressed on the cortex respect to the other cerebral structures) important for the finer differentiation of cortical areas. We can divide genes well expressed on the cortex into two ensembles: genes which have a flat distribution and genes which present differential distribution according to well characterized gradients. Genes with a flat distribution (the majority) play the same role everywhere. Genes with a differential distribution present maxima in well defined anatomo-functional regions as well as minima. Their stoichiometry is then unbalanced across different areas. This property suggests for these genes specific cellular roles carried out to support specific anatomo-functional needs of the area of high expression. Figure 5.14 shows that gene expression is organized in continuous gradients, with several possible prototypical profiles organized along the two main axes of the cortical gene distribution: the VSA-PTF axis and the dorsal-ventral (fronto-temporal) axis. The eight prototypical profiles are organized from the higher region of expression, specific for each gene, in one of the eight sectors determined by the two axes. The gradients are rather symmetrical for symmetrical sectors. However, there is a majority of genes with gradients organized according to the two rings, VSA and PTF.

The DiCA results on the cerebral and cortical regions do not show proximity between cortical regions and cerebral regions which have a topological relation: for example between parahippocampal area and hippocampus. What is emerging from the map shown in Figure 5.4.a—and coherent with results presented in [117]— is that similarities of genetic expression between cortical regions is primarily related to anatomical proximity within cortical regions. The organization of functional networks organized by long distance cortical con-

nections is another organizing principle but it seems less important [222]. For example temporal regions ITG, MTG and STG which are contiguous share strong gene expression similarities while they take part to different cognitive functions: STG is part of the cognitive network supporting speech functions while MTG and ITG are part of the language and memory networks. By contrast the frontal region IFG while it participates with the temporal region ITG to the language network, has a different genetic profile as shown by the opposition to all the temporal regions on the second dimension.

5.6.4 Multiscale anatomo-functional congruence

Since our results reveal the name of genes the more differentially expressed across cortical regions we will now focus on the functional properties of some of the extreme genes in the selected families.

We have extended the same analysis on 32 between subcortical and cortical regions, and on eight groups of families of synaptic proteins: (1) ionic channels, (2) neurotransmitter release machinery, and (3) gaba and glutamate receptors known to be important in information processing; (4) neuromodulator receptors, (5) CAMKs and PRKCs important for short term memory; (6) cytoskeleton proteins actin and tubulin important for long term memory; (7) axon guidance and cell-cell recognition proteins (such as semaphorins and ephrins), and (8) growth factor (such as FGF, EGF), important for neuronal networks genesis and maintenance. We focused the analysis of the results for these eight groups of families of genes central for the main synaptic functions. Our analysis gives at the same time information about which are the genes associated with the dimensions extracted and the level of significance for this association (Bootstrap technique). In Figures 5.5-5.12 are presented the results for these groups of families. Since the analysis reveals both the isoforms/subunits the most differentially expressed with their preferred region of expression, we can evaluate from the literature how isoforms/subunits properties within each family are related to the anatomo-functional properties of these cerebral and cortical regions. We wanted to know if it is possible to generalize the coherence of that we discovered for information processing properties between ionic channel and release-related proteins, and VSA-PTF specialization for temporal integration. We were interested to see if this congruence can also be observed for short-term processes (neuromodulator, CaMK), long-term memory processes (cytoskeleton proteins tubulin and actin), and networks genesis and homeostasis (semaphorins, ephrins, growth factors). As it will be described in details in the next sections Figure 5.15 shows that there is a strong congruence between the functional properties of proteins coded by genes maximally expressed in the different cortical regions and the specialization of information processing and memory formation in these cortical regions. This figure synthesizes the results for three sets of cognitive networks (parietal, temporal and frontal) and six families of genes coding from proteins mainly involved in the memory cascade. Figure 5.16 illustrates the coherence obtained in VSA and PTF regions between

three proteins involved in the memory cascade: with two subunits of NMDA receptor related to two isoforms of CAMKII generating two different types of actin polymerization in VSA and PTF (details in the following sections).



Fig. 5.15.: The differential stoichiometry of cortical synapses: this figure synthesizes the main results obtained showing the congruence between the main functional properties involved in the memory cascade, for three sets of anatomo-functional regions in parietal, frontal and temporal lobes.

The analysis presented in sections 5.6.4.1-5.6.4.5 are coherent with the results presented in Chapter 4. They can thus be skipped without loss of information.

5.6.4.1 Sodium and potassium channels

The sodium (SCN) and the potassium (KCN) channel families are distributed in the two rings. In fact, SCN and KCN family members turn out to be spread ranging from extremely PTF to extremely VSA expression with high bootstrap ratios on both sides. In the SCN family, we found the highest bootstrap ratios on the VSA side for SCN1A and SCN1B. The

sodium channel, voltage-gated Nav1.1, is essential for the generation and propagation of action potentials, with a large alpha subunit encoded by SCN1A, and smaller beta subunits, encoded by SCN1B, important for its fast inactivation kinetics [39]. These two subunits play a critical role in the temporal precision of neuronal information processing. For the highest expression of K channels in VSA, we found KCNA1. This gene codes for a subunit responsible for currents Kv1.1, which, in turn, play a major role in maintaining action potential temporal precision. This gene is expressed in neurons that fire temporally precise action potentials [98], in particular for processing rapid acoustic stimuli, animal vocalizations, human speech [130], sound localization (which depends on timing occurring within a submillisecond epoch) [143]. This potassium channel subunit is important for regulating a tight input-output correspondence and temporal synchrony [8]. We thus found, more expressed in the VSA ring, genes (SCNA1, SCNB1, KCNA1) which control the temporal precision of neuronal activation, and these ionic channel properties match the data-driven, real-time information processing in the VSA ring underlying sensorimotor interactions. Conversely, on the PTF side, we found for sodium channels an overexpression of both SCN3A and SCN3B (alpha and beta subunits of Nav1.3). The beta3-subunit influences the temporal properties of sodium channels in such a way that they stay open and active for a longer time [56], and favor persistent sodium currents and sustained activation of the neuron. [216, 9, 77, 55]. The next gene with the highest bootstrap ratio, SCN9A codes for sodium channels Nav1.9 and contributes also to foster a persistent sodium current [270]. For the KCN family, more expressed on the PTF side, we found the genes KCNF1 (Kv5.1) and KCNG1 (Kv6.1) that code for proteins that are electrically silent Kv (KvS) potassium subunits which modulate the Kv2.1 channel, the major delayed rectifier channel expressed in most cortical pyramidal neurons, and slow its activation, inactivation and deactivation kinetics (reviewed in [152, 24]). We found other genes preferentially expressed in the PTF ring-such as KCNMB4-which have similar effects. We found also KCNN3 which induces a sustained activation of dopamine neurons [249], KCNJ1 [12] which generates rhythmic activation and spontaneous activity, and KCNA4 which regulates long term circadian rhythms [105]. We thus found, more expressed in the PTF ring, genes which facilitate persistent currents (SCN3A and SCN3B), prolonged effects of input activities, (KCNF1, KCNG1, KCNMB4, KCNN3), and spontaneous and rhythmic activation (KCNJ1, KCNA4): All these temporal neuronal properties match the multi-temporal processing in the PTF ring, contrasting with the high precision timing control of SCN1A, SCN1B and KCNA1 in the VSA ring. However, the precise role of these genes in the different regions of the PTF ring remains to be elucidated.

5.6.4.2 Calcium channels

We found also calcium channels with a preferential distribution either in the VSA or the PTF ring. calcium (Ca²⁺) channels initiate release of neurotransmitters at synapses, from the timescale of milliseconds to minutes, in response to the frequency of action potentials

[40]. Mostly expressed in the VSA ring we found CACNA2D2. This subunit causes faster activation and inactivation kinetics [155] of calcium channels and drive exocytosis with an increased release probability, making synapses more efficient at driving neurotransmitter release [125]. Mutations of CACNA2D2 result in slow inactivation of calcium channels and a prolonged calcium entry during depolarization [75]. The control of input/output timing and quantification of evoked transmitter release is requested for data-driven real-time processing in the VSA ring underlying sensorimotor functions. Conversely, on the PTF side, we found CACNA1H. This gene encodes a syntaxin-1A/Cav3.2 T-type calcium channel which controls low-threshold exocytosis in an action potential-independent manner [289, 46], and can trigger the release of neurotransmitters at rest. This produces low-threshold burst of action potentials for the genesis of neuronal rhythms. Similarly, CACNG3 strongly expressed on PTF shows multiple long-lived components [241] which can facilitate prolonged activation of neurons. The spontaneous, prolonged, or rhythmic release, matches the multi-temporal processing in the PTF ring for vital needs, memory, and language, compared to the high fidelity evoked processing in the VSA ring.

5.6.4.3 Synaptotagmins

Central synapses operate neurotransmission in several modes: synchronous/fast neurotransmission- neurotransmitters release is tightly coupled to action potentials- and spontaneous neurotransmission where small amounts of neurotransmitter are released without being evoked by an action potential [47]. Synaptotagmins (SYTs) are abundant membrane proteins [192, 251], with at least 16 isoforms in mammals, which influence the kinetics of exocytotic fusion pores and the choice of release mode between full-fusion and “kiss-and-run” (partial fusion) of vesicles with the presynaptic membrane [192, 114, 299]. Kiss-and-run allows neurons to respond to high-frequency inputs mediating tight millisecond coupling of an action potential to neurotransmitter release [251]. The synaptotagmin most strongly associated to VSA is SYT2 which controls the kiss-and-run behavior of vesicles and temporal accuracy of transmitter release [299, 150] for example in the auditory system or the neuromuscular junction. The kiss-and-run mode of SYT2 matches the real-time data-driven processing mode of VSA.

By contrast, we found more expressed in the PTF ring, the synaptotagmin V. SYT5 which promotes the fusion of vesicles with a slower binding and is targeted to dense-core vesicles that undergo calcium-dependent exocytosis of various neurohormones and neuropeptides. The SYT5 preferred expression in the PTF ring is compatible with the multi-temporal processing mode of the PTF ring and contrasts with other synaptotagmins (e.g., SYT2) which favor high temporal precision in response to evoked stimuli (SYT2) and are therefore more expressed in VSA.

5.6.4.4 Complexins

We also studied the complexin (CPLX) family whose members assist synaptotagmin by activating and/or clamping the core fusion machinery of exocytosis of vesicles controlling either spontaneous or evoked neurotransmitter release [134, 139, 35]. In the complexin family, we found that CPLX1 was strongly expressed in the VSA ring. CPLX1 is important for the tight time coupling (of the order of a millisecond) of the action potential to neurotransmitter release [293] while suppressing spontaneous synaptic vesicle exocytosis driven by low levels of endogenous neural activity [181]. Here again, a fast evoked release mechanism matches the real-time processing mode of the VSA ring. Conversely, on the PTF side, we found as the most extreme gene CPLX3, which is an activator of spontaneous exocytosis [293]. Furthermore, the molecular structural differences between Complexins 1 and 3 have been studied in relation with their two different functional roles, where the C-terminal sequence of CPLX1 facilitates evoked release whereas the C-terminal sequence of CPLX3 facilitates spontaneous release. The preferential expression of CPLX1 and CPLX3, which induces either evoked or spontaneous release, matches both the real-time data-driven processing in VSA and the goal-driven multi-temporal integration in PTF that is based on more spontaneous activation.

5.6.4.5 Synaptobrevins

Our results also show a differential expression of synaptobrevins (VAMP vesicle-associated membrane protein) in VSA or PTF. This protein family plays an important role in vesicle docking and maintenance controlling the rate of release. VAMP1 gene is strongly expressed in the VSA ring—a pattern consistent with previous results showing that these proteins are important for the fast processing of sensory stimuli such as auditory stimuli [91]. Results have shown that VAMP1 (Synaptobrevin 1) is more important for evoked release [300], while Synaptobrevin 2 (VAMP2) seems to have a more general role in maintaining a pool of available vesicles. Here again this differentiation matches the importance of precise control of evoked release in the VSA ring.

5.6.4.6 Glutamate receptors

The glutamate NMDA receptor (NMDAR) is very important for controlling synaptic plasticity and memory. The NMDA receptor increases its opening to the calcium flux when there is simultaneously a presynaptic release of glutamate (presynaptic activation) and a post-synaptic depolarization (post synaptic activation). The postsynaptic calcium inflow produces a cascade of events: CaMK autophosphorylation (short term memory) and actin polymerization (long-term memory). The molecular ensemble NMDAR-CaMK-actin implements an Hebbian learning mechanism at the synaptic level. The precise NMDAR properties are critically dependent upon the proportion of its subunits [96]: NR2A coded by GRIN2A gene, NR2B coded by GRIN2B. The proportion of these subunits changes with

maturation. Whereas NR2B is predominant in the early postnatal brain, the number of NR2A subunits grows, and eventually NR2A subunits outnumber NR2B. This is called the NR2B-NR2A developmental switch, with kinetics changes: greater ratios of the NR2B subunit leads to NMDA receptors which remain open longer compared to those with more NR2A. This may in part account for greater memory abilities in the immediate postnatal period compared to late in life. As the brain ages, the ratio of NR2A/NR2B in the brain increases over time. The ratio of synaptic NR2B over NR2A controls spine motility and synaptogenesis [96]: the C-terminus of NR2B binds to CaMKII favoring synapse formation and maturation. Conversely, the C-terminus of NR2A limits the development of synapse number and spine growth. CaMKII binding to GluN2B is critical during memory consolidation [113] in robust forms of long-term memories. The maintenance of synaptic strength properties is due to the CaMKII/NMDAR complex [227]. Our results reveal that, compared to other cerebral structures, the expression of the genes GRIN2A and GRIN2B coding for subunits NR2A and NR2B expression is highest in the cerebral cortex. This is consistent with the property of the cerebral cortex to implement Hebbian learning mechanisms at the synaptic level in all cortical regions. Our results also reveals a differential distribution of subunits in the cortical regions: NR2A is preferentially expressed in VSA, and so the NR2A/NR2B ratio is higher in VSA, and the NR2B/NR2A ratio is higher in PTF. The higher NR2B/NR2A ratio in PTF that we find in relation with multi-temporal integration is consistent with the specific role of NR2B in generating persistent firing during working memory [278]. Neurons in the primate dorsolateral prefrontal cortex (dlPFC) generate persistent firing in the absence of sensory stimulation. Persistent firing arises from recurrent excitation within a layer III dlPFC network underlying working memory and containing NMDA NR2B subunits [278]. Recurrent excitatory, and persistent firing requires NMDA NR2B stimulation. The slower kinetics of NR2B are optimal for prolonged network firing. Our results also show that the dopamine receptor DRD5 is more expressed in PTF regions. DRD5 receptor activation elicits a bidirectional long-term plasticity of NMDA receptor-mediated synaptic currents depending upon the NR2A/B subunit composition, resulting in a decrease in the NR2A/NR2B ratio of subunit composition [60]. Persistent firing patterns is affected by prior experience in selective neuronal populations. Furthermore, high expression of NR2B subunit enhances forms of memories specific to PTF such as social recognition. By contrast, high expression of the NR2A subunit impairs long-term social recognition and olfactory memory [131, 54]. PTF is strongly influenced by the hypothalamus, and several hormones play a role in the learning of social recognition including estrogen, oxytocin and arginine vasopressin. Similarly, NR2B expression favors long-term rhythms in the supraoptic nucleus of the hypothalamus which synthesize the peptide hormones vasopressin and oxytocin, and produces burst firing patterns which maximize hormone release, while NR2A is weakly expressed [67]. Consistently with our results showing a preferential expression of NR2A in VSA, NR2A subunit seems important for learning in visual and motor regions [45, 208]. Visual experience modify the NR2A subunit composition of NMDARs, and these changes in turn modify the properties of synap-

tic plasticity in the visual cortex, and for motor learning [163]. Our results also reveal that among the NMDA glutamate receptor family, the most extreme gene preferentially expressed in PTF is GRIN3A. Also in this case this result concord with previous results: GRIN3A which codes for GluN3A plays a role in differential maturation of human cortex by inhibiting activity-dependent stabilization of synapses [103, 118]. GluN3A has been suggested as a molecular brake controlling the extent and timing of synapse maturation [144]. We can interpret this result by considering that this gene is delaying maturation of PTF with respect to VSA [103], during the developmental period where the plasticity of VSA is privileged [118]. Furthermore this gene is human-specific, and diverge between humans and chimpanzee: GRIN2C and GRIN3A are the most diverged Glutamate receptor genes [103]. We also found that GRIN2C and GRIN3A are the two of the NMDA receptor family which are the most expressed in PTF. NR2C receptors coded by GRIN2C prolong the duration of calcium influx during dendritic spiking and generate plateau potentials in basal dendrites of layer 5 pyramidal neurons in the mouse prefrontal cortex [203]. This process facilitate multi-temporal integration in PTF compared to real-time integration in VSA. In the amygdala, NMDA receptors subunits N2C are critical for the acquisition, retention, and extinction of classically conditioned fear responses which is a memory process characteristics of PTF [202]. We also found that in the family of glutamate metabotropic receptors, the most extreme gene is GRM1 and it is preferentially expressed in the PTF ring. GRM1 is involved in the dynamic regulation of calcium and in the control of short term synaptic plasticity [52]. We can interpret these results by the fact that this type of short term memory is important in multi-temporal integration in PTF ring as seen in language and memory.

5.6.4.7 GABA receptors

Our results reveal that the subunit alpha5 of the GABA receptor is more expressed in PTF. The subunit GABAR alpha5 coded by the gene GABRA5 generates a tonic inhibitory conductance [36, 237]. It provides an homeostatic regulation of neuronal excitability [26]. The persistent inhibitory activity raises the threshold for induction of long-term potentiation in a highly specific band of stimulation frequencies (10-20 Hz) and modify the strength of synaptic plasticity [182]; GABAR α 5 receptor activity sets the threshold for long-term potentiation and constrains long-term memory. The high expression of GABRA5 in PTF is consistent with a role of prolonged inhibitory to control short-term memory.

Excess of inhibition in Down syndrome produce synaptic plasticity deficits that may be a primary mechanism contributing to learning and memory impairments [211]. Inverse agonists selective for the α 5-subunit containing receptor, initially developed as cognitive enhancers for treatment of memory impairments, proved to be very efficient in reversing learning and memory deficits in a Down syndrome mouse model with altered GABAergic transmission. Chronic treatment with α 5IA increased IEGs expression, particularly of c-

Fos and Arc genes, alongside signaling cascades that are critical for memory consolidation and cognition [211, 183, 27].

5.6.4.8 Neuromodulators: serotonin receptors

Neuromodulators serotonin, dopamine and norepinephrine (interacting with adrenergic receptor) produced by brain stem nuclei have a strong and prolonged modulatory influence on synaptic transmission, modifying the spatial and temporal propagation of signals. Their synaptic effects depend strongly upon the receptor isoform which is expressed. Many results in literature show that the different serotonin receptors are differentially expressed in the different cortical regions. In our results, HTR receptor results show the highest bootstrap ratios for HTR1A and HTR7 in PTF and for HTR1F in VSA. Consistently HTR1A is known to play a role in motivation, emotions, mood and circadian rhythms as well as vital functions (feeding, sexual, thermoregulation) [229, 230], and HTR7 has a role in learning and memory [186], in sleep and circadian rhythms (e.g. through the modulation of neurons in the suprachiasmatic nucleus). On the other hand in VSA, HTR1F is known for their analgesic properties to calm migraines and pain, that can be interpreted as an inhibitory role on sensory transmission [160]. These results are consistent with a dual role of serotonin due to receptor distribution: in VSA, serotonin control sensory perception, inhibiting painful messages, while in PTF it controls circadian rhythms, vital function emotion and mood, in concordance with the functional specialization of VSA and PTF.

5.6.4.9 Calcium calmodulin kinases

Previous results have shown that many intracellular responses to elevated calcium involved in learning and memory are mediated by CaM kinases (CaMKs), a family of protein kinases whose activities are initially modulated by binding Ca²⁺/calmodulin and subsequently by protein phosphorylation (see reviews [285, 286, 177]). Transient elevations of intracellular calcium can result in prolonged CaMKII autonomous activity which can be dictated by the frequency of Ca²⁺ oscillations [62]. This mechanism is thought to be critical in potentiation of synaptic transmission with variable durations, relating short-term and long term memories [171, 172]. LTP triggers high-frequency calcium pulses that result in the activation of CaMKII which acts as a molecular switch because it remains active for a long time after the return to basal calcium levels.

Our results show that the different members of the CaMK family are highly expressed in the cerebral cortex, which has a major role in learning and memory, and subserve different forms of short term memories in different cortical regions. CaMKs are a key family for synaptic plasticity and all its members have their pole of expression in correspondence of the cerebral or cerebellar cortices or across the two of them. Our results show that different members of the CaMK families are distributed in different cortical regions. Our results reveal that two isoforms, CaMK2G and CaMK2D are differentially expressed, CaMK2G

in the VSA regions more related to sensorymotor interactions, and CaMK2D in the PTF regions, more related to episodic memory, recall and language. Our results reveal also that CaMK4 and CaMK1 are also differentially expressed on the frontal to temporal axis: CaMK4 is more expressed in the temporal regions and CaMK1G is more expressed in frontal regions.

Previous results have shown that members of the CaMK cascade—CaMKK (A,B), CaMKI (A,B,D,G) and CaMK4 have very different modes of regulation by phosphorylation. For example, CaMK2B, (e.g., bound to F-actin) regulates synaptic transmission quite differently than the CaMK2A isoform and bundles F-actin to promote isoform-specific neurite outgrowth and maintain dendritic spines; the ratio of CaMK2A/CaMK2B in neurons is modulated by prolonged neuronal activity that may be important in adaptation during synaptic homeostasis—increased activity favors CaMK2A whereas decreased activity enhances CaMK2B. Our results revealed the overexpression of CaMK2D in PTF and CaMK2G in VSA. The high expression of CaMK2D in PTF regions can be related with results demonstrating that *Camk2D* expression is specifically induced after strong training, during strong memory consolidation [82], and in more persistent forms of memory (for example, novel object recognition task in mice). Only strong training induced a long-lasting memory, and an increase in histone acetylation, which is specific molecular signature of enduring memories: histone acetylation occurs at a specific promoter region of the *Camk2d* gene. Then the differential expression of CaMK2D in PTF regions can be related to the property of this protein to facilitate long-lasting memories. Our results suggest that the storage of memories in synaptic weights, implemented by the actin cytoskeleton of spines may be quite different depending in VSA (with CaMK2G) and PTF (CaMK2D). Indeed previous results have shown that different types of CaMK2-actin interactions mediated by the different isoforms, and that CaMK2 isoform composition differentially impacts the formation and maintenance of the actin cytoskeleton responsible of long term memory. The CaMK2D isoform produces tightly packed 3D actin bundles while in contrast the CaMK2G isoform produced loosely associated large sheet-like structures [123]. These first type of memory storage could be well adapted to all-or-none long-lasting memories of events (in PTF), and the second type to memorize fine tuning of sensory-motor adaptation (in VSA). Our results also show that, within cortical regions, CaMK4 is more expressed in the temporal regions, and CaMK1G is more expressed in frontal regions. Previous results have shown that CaMK1 and CaMK4 have an “activation loop” phosphorylation site that is absent in CaMK2. CaMK1 and CaMK4 are fully activated by CaMKK-mediated phosphorylation [255], but with two different time constants: CaMKK-mediated phosphorylation/activation of CaMKIV appears to last for only a few minutes, while CaMK1 phosphorylation can persist up to an hour or more. These properties could differentiate two typical duration of short term memories, lasting few minutes in temporal regions (like integration of words in sentences), and lasting hours in the frontal regions (like working memory in planning). Previous results have shown that CaMK1 mediates calcium signal-induced neurite out-

growth through activation of microtubule affinity-regulating and accelerated the rate of axon formation. We have consistently found an high expression of CaMK1G and of a set of tubulin isoforms in frontal regions: this co-expression can facilitate activity-dependent axonal remodeling in frontal regions. Our results also shows that CaMK4 is more highly expressed in the cerebellum and in cortical temporal regions. Previous results have shown that CaMK4 enhances early synaptic potentiation by activating new protein synthesis [263], and induces development of dendrites and spines, by phosphorylation of the CREB transcription factor (cAMP-responsive element binding protein), which plays key roles in the induction LTP (hippocampus, cortex), and in the cerebellar LTD. Our results suggest that the two CaMK, CaMK1G and CaMK4 could induce two types of remodeling, CaMK1G via tubulin in frontal regions, and CaMK4 via protein synthesis leading to dendrite remodeling in temporal regions. In Figure 5.16 are summarized the main results found in this subsection.

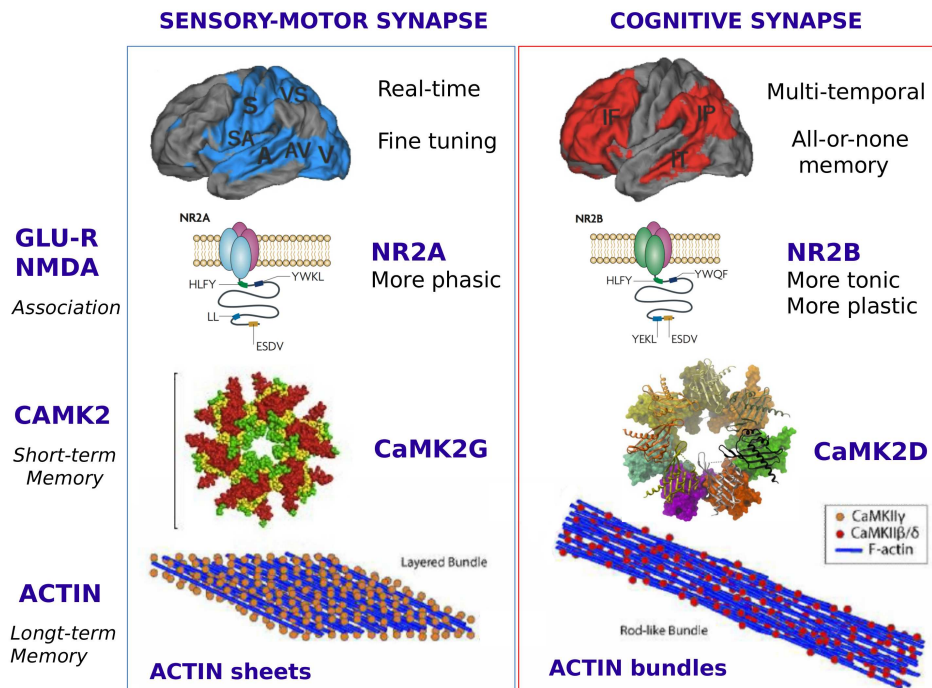


Fig. 5.16.: Results show two main variants of memory cascades congruent with two type of processing in the two rings VSA and PTF. In VSA processing information in real time the glutamate receptor NMDA is mainly represented by the NR2A subunit which is phasic; calcium inflow activates the CAMK2G isoform which produces polymerization of actin as sheets. Conversely in the PTF ring processing multi-temporal information, the glutamate receptor NMDA is mainly represented by the NR2B subunit which is more tonic and more plastic; calcium inflow activates the CAMK2D isoform which produces polymerization of actin as bundles. These two cascades could be related to two types of short term and long term memory, adjustments in VSA and all-or-none memorization in PTF.

5.6.4.10 Protein Kinases C enzymes

Protein kinase C (PKC) is a family protein kinases composed of at least 12 isoforms that can be activated by calcium and second messenger diacylglycerol. PKC family members phosphorylate a wide variety of protein targets and are involved in diverse cellular signaling pathways in development (cell growth, differentiation, apoptosis, transformation), and in memory acquisition and maintenance [252, 69]. Indeed, protein kinase C targets NMDA receptors and regulate their synaptic accumulation [167]. Our results show that PRKCG are more expressed in the PTF regions, and PKRCB is more expressed in frontal regions. This is consistent with previous results showing that PKCG is important for persistent forms of spatial memories [51], and PKCB is important for consolidation of fear conditioning [287]. Our results suggest that PKC isoforms (PKC delta, gamma, beta and alpha) should be specific of different types of learning and memories along the VSA-PTF and temporo-frontal gradients, in synergy with the different isoforms of CaMK.

5.6.4.11 Actin, actinin and actin-related genes

Actin, and actin-related proteins play a fundamental role in long-term memory formation. Actin polymerization is the key factor responsible of spine enlargement which increases the synaptic efficacy [184, 204, 126]. Actin-regulating proteins maintain the balance between F-actin assembly and disassembly that is needed to stabilize mature dendritic spines, and how changes in their activities may lead to rapid remodeling of dendritic spines responsible of long-term memory [210]. We have focused on two subfamilies, actinin and actin-related proteins ARP. Our results show that alpha-actinin (coded by ACTN gene) is differentially expressed in the cortex, and that alpha-actinin2 (coded by ACTN2 gene) is more expressed in the frontal cortex. Previous results have shown that α -actinin stabilize the supra-structure of the actin cytoskeleton by bundling F-actin and linking F-actin to the Post Synaptic Density and to the membrane [141]. Actinin 2 control the shape of spines and increases the length and density of dendritic protrusions [122]. Furthermore it influences the function of several proteins related to synaptic strength, including NMDAR, CaMK2, and spine associated GTPase [132, 132]. α -actinin 2 links NMDAR receptor and Ca(2+)-activated K(+) channel potassium channels KCNN2 (or SK2) to the actin cytoskeleton [175]. This set of specific properties could be a way to modulate specific form of short term and long term plasticity in the frontal cortex where we show the high expression of alpha-actnin2, together with KCNN2. Our results also reveal that actin-related proteins ACTR3, ACTR3B and ACTR3C, have higher expression in Temporal regions. ACTR genes encode actin-related proteins ARP which are important to shape the spine actin network underlying synaptic efficacy, as component of the Arp2/3 complex which mediates the formation of branched actin networks [126]. ARP3 also controls spine density. Our result suggest that the activity-dependent remodelling of the actin network in dendritic spines (actin branch-

ing made by Arp2/3 proteins) could be different in the cortical regions, producing different forms of long-term memory.

5.6.4.12 Tubulins

Tubulins, and microtubule polymers into which they incorporate, is critical for development of axons and dendrites, and activity-dependent remodeling of axons and dendrites can implement diverse forms of long-term memory. The tubulin gene family is mainly expressed during cortical development with a specific spatial and temporal expression pattern. Members of this family encode dimeric proteins consisting of two closely related subunits (A and B), representing the major constituents of microtubules. Microtubules are essential components of axon guidance machinery [259]. Our results show that, in the adult brain, beta-tubulin TUBB (TUBB, TUBB2A, TUBB3A, TUBB3) and α tubulin genes (TUBA1A) are more expressed in PTF and more particularly in the frontal cortex; other isoforms (such as TUBD1, TUBF1 are more expressed in VSA Previous results have confirmed the “multi-tubulin” hypothesis, which postulates that different tubulin isotypes may be required for specialized cellular functions in both the embryo and adult [259]. Results have shown that mutations in these α/β -tubulin genes (TUBA1A,, TUBB2A, TUBB2B, TUBB3, and TUBB) might alter the dynamic properties and functions of microtubules. Tubulin isotypes show intrinsic differences in the rates of microtubule assembly and the frequency of growth and shortening events, suggesting that cells can regulate microtubule dynamics by controlling the relative amounts of different tubulin isotypes [259]: TUBB3 heterodimers were considerably more dynamic and spent less time in paused states than those composed of TUBB2 or TUBB4. Our results suggest that microtubules dynamics could play a specific role in specific types of memory formation in the frontal PTF regions, as determined by different types of tubulin codes due to genetic overexpression of different forms of tubulins in these regions. The regionalization of microtubules isoforms can also be related to the differential development of cortical areas, gyri and sulci [223, 43, 57], which are particularly important for human cognition. Genetic variations affecting beta-tubulin genes expressed at high levels in the brain (TUBB2B, TUBB3, TUBB, TUBB4A, TUBB2A, TUBA1A and TUBB3) have been linked with malformations of cortical development: polymicrogyria, microlissencephaly and corpus callosum agenesis, with aberrations in the trajectories of commissural projection neurons.

5.6.4.13 Semaphorins

Semaphorins play an important role in axon guidance and growth by triggering dynamic rearrangements of the actin cytoskeleton in the neuronal growth cone. Some of these guidance molecules are persistently expressed after axonal pathfinding and target recognition are completed, for controlling synaptogenesis, axon pruning, elimination of synaptic connections and maturation of dendritic spines [201]; in adult these proteins regulate synaptic

physiology, neuronal excitability, synaptic plasticity and homeostasis [206, 264], suggesting that semaphorins function as coordinators of both structural and functional neuronal plasticity. Semaphorin 5B (Sema5B) control synapse number, and a size of presynaptic and postsynaptic compartments. Our results show that semaphorins isoforms are differentially expressed in different cortical regions. This suggests that several semaphorins isoforms could control different types of activity-depedent synaptic rearrangement and homeostasis in different cortical regions.

5.6.4.14 Ephrins

Eph/ephrin mediate contact-dependent cell-cell communication, and regulate a variety of biological processes during embryonic development including cell migration, guidance of axon growth cones, and formation of tissue boundaries [168]. Eph receptors and their surface associated ligands, ephrins can initiate new synaptic contacts, recruit and stabilize glutamate receptors and regulate dendritic spine morphology. Evidence now suggests that the same proteins that function early in development to regulate synapse formation may help to maintain and/or regulate the function and plasticity of mature synapses [127]. Our results reveal the differential expression of genes coding for different members of the ephrin family both in the VSA-PTF axis and in the temporo-frontal axis. Like for semaphorins, several sephrin isoforms could thus control different types of activity-dependent synaptic rearrangement and homeostasis in different cortical regions. Ephrins and semaphorins provides a regional control of synaptic processes, where each cortical region can modulate learning and memory processes depending upon its position along the VSA-PTF and Temporo-frontal axis.

5.6.4.15 Growth factors: FGF

The fibroblast growth factor family (FGF) influences all phases of fetal and embryonic development and has a key role in specification of brain regions and cortical areas. During brain development, FGF isoforms control neural cell migration which leads to the proper whole brain structural organization. FGF specifically promote excitatory or inhibitory synapse formation, respectively, and regulate the proper excitatory/inhibitory balance [58]: FGF in adults are differentially expressed and can be important for neuronal and synaptic homeostasis [53, 164]. Individual members of the diverse Fgf gene family differentially regulate global as well as regional cortical growth rates while maintaining cortical layer structure, influencing the size and position of cortical gyri. For example FGF2 influences the overall size and shape of the cortex and induces the formation of prominent, bilateral gyri and sulci in the rostrolateral neocortex [220]. Our results show a preferential distribution of FGF isoforms in different brain structures (cerebral and cerebellar cortex) as well as in cortical regions (VSA-PTF). These results suggest that FGF isoforms also participate

in a local control of synaptic homeostasis which may control specific forms of excitatory-inhibitory dynamics and memory formation in different cortical regions.

5.6.5 Transcription factor FOXP2 and growth factor MET: language and autism

Our results show an high expression in temporal regions of the transcription factor FOXP2 and the growth factor receptor c-MET. Furthermore, several genes highly expressed in temporal regions, such as CYP26B1, code for protein related to the retinoic acid which is strongly related to FOXP2 and MET. Our results are highly consistent with previous results on the combined expression of MET and FOXP2 in temporal regions. These results provide a link between the cellular role of FOXP2, MET and retinoic acid, their preferred expression, and the specialization for language comprehension of cortical temporal regions. FOXP2 drives neuronal differentiation by interacting with retinoic acid signaling pathways, regulated by genes such as CYP26B1 which behave as morphogens [65, 119]. The MET gene code for c-Met, also called hepatocyte growth factor receptor (HGFR). MET activates a wide range of different cellular signaling pathways, involved in proliferation, motility, migration, axon terminal outgrowth, synaptogenesis and control of spine head volume [136, 135]. Within the temporal lobe, the pattern of MET expression is highly complementary to the expression pattern of FOXP2. Low MET expression has been implicated in autism, with reduced levels of MET protein expression in the mature temporal cortex of subjects with ASD [193, 136, 135]. MET signaling is involved in the development of forebrain circuits controlling social and emotional behaviors that are atypical in autism spectrum disorders (ASD). Brain imaging results show that the MET gene is a potent modulator of key social brain circuitry in children and adolescents with and without ASD [224]. MET risk genotype produces atypical fMRI activation and deactivation patterns to social stimuli (i.e., emotional faces), as well as reduced structural connectivity in temporo-parietal regions known to have high MET expression, and these effects were more pronounced in individuals with ASD.

5.7 Conclusions

The patterns of expression of the human genome across cerebral areas are mainly dictated by anatomical and cytoarchitectural constraints. Differential gene expression across the cerebral cortex also follows anatomy and cytoarchitectonic more than functional specialization. The cortical regions with the most distinctive patterns of gene expression are also the more phylogenetically ancient namely visual and motor areas on the VSA side and parahippocampal and temporal pole regions on the PTF side. Regions implicated in the implementation of language result instead the most average regions in term of gene expression. The systematic study of families of genes coding for proteins covering central roles in

synaptic activity (information processing, neurotransmission, short and long term memory, networks genesis and homeostasis) showed strong congruence between the preferential expression of genes, the cellular properties of the proteins they code at the cellular level, and the cognitive function implemented in anatomic-functional regions (of preferential expression).

5.8 Remark I: The anatomic-functional synapse: multiscale scenarios in different cortical regions

Beyond this paper it is interesting to ask the question of the functional coherence of synapses within cortical regions taking into account the specialization of different genes isoforms and subunits. The exposed results are similar to the results exposed in the discussion of the paper but re-assembled by large anatomic-functional networks and not by families of proteins (all families participating in each networks but with different stoichiometry). It is just another way to read 5.15: it was read by columns in the paper and here we will read it by rows. It will be then be possible to skip this section which it is just a supplementary point of view of the same results. Interesting mainly to describe the “anatomic-functional synapses” specific of each cortical region.

We focus on four sensory-motor and cognitive functions, involving four different cortical regions (and networks) both on the PTF-VSA axis and the temporo-frontal axis:

1. *Perform a visuomotor task involving cortical motor, visual and parietal visuomotor regions (e.g., catch a ball)*
2. *Memorize-recognize faces and events, involving temporal fusiform and parahippocampal regions (e.g., meeting a new friend)*
3. *Produce a goal-directed sequence of actions, involving superior frontal regions (e.g., go to school)*
4. *Produce sentences, involving a network with three components: audition-phonation, temporal and frontal regions*

The four networks share similar types of neurons and microcircuits (6 layers micro-columns). Most of the genes of the “cortical pool” coexist in these neurons to guarantee basic information processing and memory formation (short and long-term), based on the eight basic synaptic processes: 1) ionic channels for information processing, both with highly precise channels such as SCN1A, SCN1B, KCNA1, and slow, more persistent channels such as SCN3A and SCN3B; 2) neurotransmitter release machinery, with synaptotagmins and

complexin, which can be either very precise and reactive, or more spontaneous; 3) gaba and glutamate receptors with NMDA receptors NR2B producing long lasting activations, or NR2A more phasic, their ratio depending upon maturation; 4) neuromodulators such as serotonin HTR1A,HTR1F, dopamine DRD1,DRD5 or adrenergic receptors ADRA1D, ADRA1B with different possible modulations of information processing and short-term memory; 5) CAMKs important for short term memory, with either CAMK2D or CAMK2G, producing different forms of actin polymerization remodeling dendritic spines, or CAMK1 and CaMK4 playing on different long term neuronal effects; 6) cytoskeleton proteins such as actinin ACTN, and actin-related protein ACTR producing different types of actin networks in remodeling spines and tubulin isoforms combinations producing different tubulin dynamics also important for dendritic-axonal network remodeling in long term memory; 7) axon guidance and cell-cell recognition proteins (such as semaphorins and ephrins), controlling different homeostatic regulation in different regions of the cortical network; 8) growth factor (such as FGF, EGF), important for building and maintaining neuronal networks with control of specialized protein machinery in different parts of the network.

5.8.1 Perform a visuomotor task: cortical motor, visual and parietal visuomotor regions

We focus on motor, visual and visuomotor networks performing visuomotor coordination and control (for ex catch a ball). The cortical network involves the primary visual regions, with high spatial and temporal precision, the primary motor regions controlling the motoneurons of the spinal cord , together with a parietal visuomotor network relating both types of information in a very precise temporal relation. This network is also strongly connected with the cerebellum which learns fast and precise movements. At the synaptic level, our results suggest that synapses in these regions have three main congruent properties: (1) stimulus-driven temporal precision; (2) massive learning during the first year of life , to acquire the basic visuomotor repertoire; (3) progressive adjustment of synaptic strength to increase the speed and precision of visuomotor skills.

1. *Stimulus-driven temporal precision is important for fast real-time interactions between the image of the ball and the control of the hand muscles that will catch the ball:* it is guaranteed by the size of cortico-spinal axons which are myelinated, and by the proteins controlling precise information processing. For the myelination process and large axonal diameters, we found an high expression of specific proteins controlling myelination, and proteins of neurofilaments controlling sizes such as NEFH, NEFM, NEFL. For the high temporal stimulus-driven precision, we found ionic channels highly expressed such as SCN1A, SCN1B, KCNA1, which can perform millisecond control of information processing. We found also precise stimulus-driven release machinery with synaptotagmin SYT2, which effect kiss-and-run type of release, and Complexin 1 which control the precise timing of the vesicle release.

2. *Massive learning during the first year of life to acquire the basic visuomotor repertoire*: we found that the NMDA receptor NR2A is overexpressed in the motor and visual regions of the cortex. The NR2A/NR2B switch control the maturation of learning processes. First NR2B produces long-lasting collective activation of the networks which facilitate the learning of the basic visuomotor repertoire during the first year of life; then the NR2A is more expressed, both inducing more temporal precision and limiting the plasticity of the synapses.
3. *Progressive adjustment of synaptic strength to increase the speed and precision of visuomotor skills*: we found an overexpression of CaMK2G isoform which control the short-term memory and the remodeling of the actin cytoskeleton of dendritic spines. The CaMK2G isoform produced loosely associated large sheet-like actin structures (contrary to CaMK2D which produces tightly packed 3D actin bundles). These sheet-like actin structures could favor a progressive adjustment of synaptic strength rather than a fast remodeling, and thus result in a progressive improvement of visuomotor skills.

5.8.2 Memorize-recognize faces and events: temporal fusiform and parahippocampal regions

We focus on temporal networks for Recognition of a new face and memorizing an event (e.g., meeting a new friend). The cortical network involves a bottom-up flow from sensory visual and auditory regions, via the fusiform regions (specialized in face processing) and temporal areas BA 20 (specialized in forming categories repertoire). This network is strongly related with the hippocampus, important to store new information on persons, places, scenes and events, and with the amygdala important for the emotional amplification of events; it involves also a top-down flow from hypothalamus (specialized in vital program and rhythms). At the synaptic level, we found a striking opposition between gene expression in PHG region and gene expression in visuomotor regions. Our results suggest that synapses in these regions have three main congruent properties: (1) spontaneous activity rather than stimulus-driven temporal precision; (2) memorization of persons and events throughout the life opposed to the massive learning during the first year of life; (3) strong and rapid all-or-none modification of synaptic strength to store the representation of a new person or an event (rather than a progressive adjustment of synaptic weight); these strong all-or-none changes can be amplified by modulatory effect of hormones related to vital program and needs.

1. *Spontaneous activity rather than stimulus-driven temporal precision*: we found ionic channels highly expressed such as SCN3A and SCN3B which facilitates prolonged neuronal activation (rather than temporal precision). We found also more prolonged release with synaptotagmin SYT5; moreover we found the high expression of Com-

plexin 3 (CPLX3) which produces spontaneous transmitter release (opposite effect of complexin 1 which prevents spontaneous release). PHG can thus be spontaneously activated by recall from memories stored in spines configurations.

2. *Memorization of persons and events throughout life opposed to the massive learning during the first year of life:* contrary to motor regions, there is no NR2A/NR2B switch to limit the prolonged activity of neurons ; the NR2B can produce both prolonged activation and strong plasticity throughout life.
3. *Strong and rapid (all-or-none) modification of synaptic strength to store the representation of a new person or event* We found an overexpression of CaMK2D isoform which control the short-term memory and the remodeling of the actin cytoskeleton of dendritic spines: CaMK2D produces tightly packed 3D actin bundles (contrary to CaMK2G isoform which produce loosely associated large sheet-like structures in VSA regions). Our results also reveal higher expression in temporal regions of specific actin-related proteins (ACTR3, ACTR3B and ACTR3C), which are important to shape the formation of branched actin networks. The mode of actin polymerization could favor a fast and permanent remodeling of spines to store new persons and events in an all-or-not fashion. We also found in this region a high expression of neuropeptides receptors related to vital programs, consistently with the importance of vital programs or emotional amplification for long-term memory formation.

5.8.3 Produce goal-directed sequences of actions: superior frontal regions

We focus on frontal networks for producing goal-directed sequence of actions and sets, for example going to school and learning a set of new acquisitions. The cortical frontal network is related to cortical regions controlling motor behavior, to parietal regions processing sensory multimodal information, and to orbitofrontal and cingulate regions activated by vital programs, reward, drives, motivation. This frontal network is strongly related to the basal ganglia, and influenced by neuromodulatory systems: Dopamine, originating in the ventral tegmental area (VTA), Norepinephrin originating in the locus coeruleus (LC), serotonin in the raphe nuclei and acetylcholine in the septum. At the synaptic level, we found that frontal regions have intermediate gene expression between temporal and motor regions Our results suggest that synapses in these regions have six main congruent properties: (1) fine regulation of the phasic-tonic dynamics of working memory by glutamate NMDA NR2B receptors properties with a large repertoire of potassium channels; (2) very slow adaptive building of the frontal neural network in relation with learning throughout life; (3) strong modulatory effects on working memory of all neuromodulators, dopamine, norepinephrine, serotonin, acetylcholine which interact at the receptor level with NMDA receptors; (4) autonomous activation of CaMK1 which can persist hours; (5) strong re-

modeling of the neural network by learning due to the adaptive regulation of both tubulin dynamics (axon, dendrites), and actin dynamics (spine shapes); (6) extension and new connections of human frontal network by growth factors and cell-cell recognition molecules which regulate a new set of cognitive functions in human.

1. *Fine regulation of the phasic-tonic dynamics of working memory with NR2B receptors and a large repertoire of potassium channels:* a key feature of neuron in the dorsolateral prefrontal cortex (dlPFC) is the adaptive generation of persistent firing. Persistent firing arises from recurrent excitation within a layer III dlPFC network underlying working memory and containing NMDA NR2B subunits. The slower kinetics of NR2B are optimal for prolonged network firing. The higher NR2B/NR2A ratio in PTF in general, and particularly in frontal region, is consistent with the specific role of NR2B in generating persistent firing during working memory in the absence of sensory stimulation, depending upon prior experience in selective neuronal populations. Our results reveals a repertoire of potassium channels which are highly expressed in the frontal regions: KCNA5, (KCNA4 is higher in temporal regions), KCNS3 (KCNS1 is higher in motor regions), KCNN2, KCNJ8. KCNN2 (small conductance Ca²⁺ activated K⁺ channels SK) are expressed at high levels in brain regions critical for learning and memory. SK channels regulate cellular mechanisms of memory encoding. Most of these channels also regulate short-term activations of neurons: KCNN channels regulate sustained activation of dopamine neurons, KCNJ generate rhythmic activation and spontaneous activity, KCNA regulates long term circadian rhythms. These results suggest that the specific repertoire of potassium channels in frontal regions can control the subtle dynamics of sustained and phasic activation subserving working memory, in relation with previous learning episodes.
2. *Very slow adaptive building of the frontal neural network in relation with learning throughout life:* our results also reveal that among the NMDA glutamate receptor family, the most extreme gene preferentially expressed in PTF is GRIN3A which control the differential maturation of human cortex by inhibiting activity- dependent stabilization of synapses, as a molecular brake controlling the extent and timing of synapse maturation. This gene expression can produce a slow maturation of PTF, which allows to adapt the building of the local neural network (axon, dendrites) to the learning experience throughout life.
3. *Strong modulatory effects on working memory of all neuromodulators, dopamine, norepinephrine, serotonin, acetylcholine which interact with NMDA receptor at the receptor level:* our results show that several isoforms of modulator receptors are overexpressed in the frontal regions: dopamine (DRD5), Norepinephrin (ADRA1B, ADRA1D) , acetylcholine (CHRN4), serotonin (HTR1E) GRIN2B are modulated by dopamine, norepinephrin, serotonin and acetylcholine receptors. Numerous studies have shown that Dopamine receptors have extensive functional interaction with

NMDA receptor. Dopamine and glutamate extensively interact in the striatum, nucleus accumbens, hippocampus and prefrontal cortex, to regulate reinforcement, attention and working memory. At the postsynaptic level, the two receptors interact locally through Dopamine/NMDA receptor complex. DRD5 which is highly expressed in the frontal regions elicits a bidirectional long-term plasticity of NMDA receptor-mediated synaptic currents resulting in a decrease in the NR2A/NR2B ratio and keeping the high plasticity of NR2B channel. Norepinephrin play a powerful role in regulating the working memory and attention functions of the prefrontal cortex (PFC) The dorsolateral prefrontal cortex (dlPFC) working memory is significantly modulated both by dopamine (DA) and norepinephrine (NE). Dopamine receptors and adrenergic receptors co-localize in PFC dendrite. Working memory performance is a function of both dopamine and Norepinephrin concentrations.

4. *Autonomous activation of CaMK1 which can persist hours:* our results show that CaMK1G is highly expressed in frontal regions while CaMK4 is more expressed in temporal regions, CaMK1 phosphorylation in frontal regions can persist up to an hour or more, while CaMK4 activation in temporal regions can persist autonomously during minutes). These properties could differentiate two typical duration of short term memories, lasting few minutes in temporal regions (like integration of words in sentences), and lasting hours in the frontal regions (like working memory in planification).

5. *Strong remodeling of the neural network by learning due to the adaptive regulation of both tubulin dynamics that change neurites (axon, dendrites), and actin dynamics that change spine shapes:* our results show that alpha-actinin2 (coded by ACTN2 gene) is more expressed in the frontal cortex. Actinin 2 control the shape of spines by bundling F-actin and increases the length and density of dendritic protrusions. Furthermore it influences the localization and function of several proteins related to synaptic strength, including NMDAR, CaMKII, and spine associated GTPase, and KCNN2 (or SK2), also strongly expressed in frontal regions. Furthermore our results reveal that a set of tubulin isoforms are highly expressed in frontal regions (TUBA4A, TUBB4B, TUBB4A, TUBB4B, TUBB3). These Tubulin isotypes show intrinsic differences in the rates of microtubule assembly and the frequency of growth and shortening events, suggesting that cells can regulate microtubule dynamics by controlling the relative amounts of different tubulin isotypes: TUBB3 heterodimers were considerably more dynamic and spent less time in paused states than those composed of TUBB4. We know that local frontal networks are modified throughout life. Our results suggest that the adaptive control of microtubules dynamics could modify local frontal networks, including dendrites and axons, depending upon learning experience. Learning and memory formation in the frontal PTF regions, could profoundly remodel the local frontal networks. Previous results have shown that

CaMK1 mediates calcium signal-induced neurite outgrowth through activation of microtubule affinity-regulating and accelerated the rate of axon formation. Our results show that both CaMK1G and Tubulins are also more expressed in PTF regions : this co-expression can facilitate activity-dependent remodeling of neural networks, including dendrites and axons, in frontal regions in relation with learning experience throughout life.

6. *Extension and new connections of human frontal network by growth factors and cell-cell recognition molecules which regulate a new set of cognitive functions in human:* our results show that some growth factors, such as HGF, or growth factor receptors, such as FGFR1 are overexpressed in frontal regions. Individual members of the diverse Fgf gene family differentially regulate global as well as regional cortical growth rates while maintaining cortical layer structure, influencing the size and position of cortical gyri. FGF2 influences the overall size and shape in the rostrolateral neocortex and FGFR2 is involved in the development of frontal brain regions. The growth factor c-MET (the HGF receptor) is highly expressed in the temporal regions, and within the temporal lobe, the pattern of MET expression is highly complementary to the expression pattern of FOXP2 involved in the development of language network. Conversely, our results show that the growth factor HGF is highly expressed in frontal regions. This fronto-temporal complementarity could be important to develop specific fronto-parietal networks important for language production and for social behaviors. These growth factor could play a role in the homeostatic control of frontal network activity and plasticity, together with cell-cell recognition molecules overexpressed in frontal regions: such as Ephrins EphB2, EphB3, EphB6.

5.8.4 Produce sentences: network relating audition-phonation, temporal and frontal regions

The cortical network for language associate 3 subnetworks which are both strongly related together, and each one is related to one of the previous networks, visuomotor, temporal and frontal. The cortical network for speech comprehension-production reproduce the properties of the visuomotor network in central, parietal, and precentral cortical regions: it involves the primary auditory regions, following the auditory information with high spatial and temporal precision, the primary motor regions controlling the motoneurons of the spinal cord for phonation , together with a parieto-temporal audition-phonation network relating both types of information. This network is also strongly related with the cerebellum which helps learning fast and precise movements. The temporal network for recognition of words reproduces the temporal network for face and event recognition: it involves a bottom-up flow from auditory regions and temporal areas BA22, 21 and 20 (specialized in categories recognition); it involves also a top-down flow from hypothalamus hippocampus, important to store new information. The frontal network for producing sentences repro-

duces the frontal network for producing goal-directed sequences of actions: it is related to cortical regions controlling phonation, to sensory multimodal information processed by parietal and temporal regions, and with orbitofrontal and cingulate regions activated by vital programs, reward, drives, motivation. It is strongly related to the basal ganglia, and influenced by neuromodulatory systems: dopamine, which originates in the ventral tegmental area (VTA), norepinephrine which originates in the locus coeruleus (LC), serotonin in raphe nuclei and acetylcholine in the septum.

The synaptic properties of the language network are a synthesis of all the adaptive synaptic properties observed in the 3 previous networks (visuomotor, temporal and frontal) but less differentiated and closer to the barycenter. The neurons in the audition-phonation network (speech network) which learn the phonemes are equipped with some specific synaptic real-time properties close to those of the “visuomotor” network: - stimulus-driven temporal precision, - massive learning during the first year of life of the basic audition-phonation repertoire, and - progressive adjustment of synaptic strength to increase the speed and precision of audition-phonation skills. The neurons in the temporal regions of language which learn to recognize words are equipped with some specific synaptic properties close to the temporal network for recognition of person, places and event: 1) spontaneous activity rather than stimulus-driven temporal precision; 2) memorization of words at throughout life opposed to the massive learning during the first and second year of life; 3) strong and rapid all-or-none modification of synaptic strength to store these words rather than a progressive adjustment of synaptic weights; these strong changes can be amplified by the modulatory effect of hormones (vital program and needs). The neurons in the frontal regions of language which learn to produce a sequence of words are equipped with some specific synaptic properties close to the frontal network producing goal-directed sequences of actions :

1. Fine regulation of the phasic-tonic dynamics of working memory by NR2B receptor with a large repertoire of potassium channels, - very slow adaptive building of the frontal neural network in relation with learning throughout life (GRIN3A) - strong modulatory effects on working memory of all neuromodulators, dopamine, norepinephrine, serotonin, acetylcholine which interact at the receptor level with NMDA receptors; - autonomous activation of CaMK1 that can persist hours; - strong remodeling of the neural network by learning due to the adaptive regulation of both tubulin dynamics (axon, dendrites remodeling), and actin dynamics (spine remodeling) - extension and new connections of human frontal network by growth factors and cell-cell recognition molecules which regulate a new set of cognitive functions in human (temporal MET-HGFR and frontal HGF)

The anatomo-functional regions matching with language cognitive networks result instead as the less differentiated in terms of gene profiles: it associates all the adaptive generic properties of proteins in the “cortical synapse”, while keeping specific synaptic properties in the network formed by audition-phonation, temporal and frontal language regions. This

suggest that the new regions subserving language are equipped with a maximal number of proteins that can facilitate the largest range of learning and memory processes. This could help to understand the difficulties faced by scientists to find specific genes for language: cortical regions implementing language functionalities are the less differentiated in term of gene expression; they can be thought of as average cortical areas.

5.9 Remark II: Synaptic proteins evolution and the tethering hypothesis

Chapters 4 and 5 revealed three main results: 1) different isoforms/subunits belonging to the same family of proteins are differentially expressed across different anatomic-functional regions (e.g., rings, ITG, SFG, PHG); 2) there is a coherence between functionalities of the regions of expression at the cognitive level and properties of isoform/subunits at the cellular level; 3) anatomic-functional regions are linked by gradients of gene expression outsourcing from well characterized poles of gene expression: the most ancient parts of the cortex present indeed the most differentiated gene profiles while the most recent areas and in particular regions implicated in language are the most undifferentiated (have an average profile) such as regions subserving language. Taken together these findings are coherent with results and hypotheses about the evolution of the vertebrate nervous system and the anatomic-functional evolution of the human cortex coming from the fields of evolutionary molecular biology and phylogenetics.

Evolution of synaptic proteins

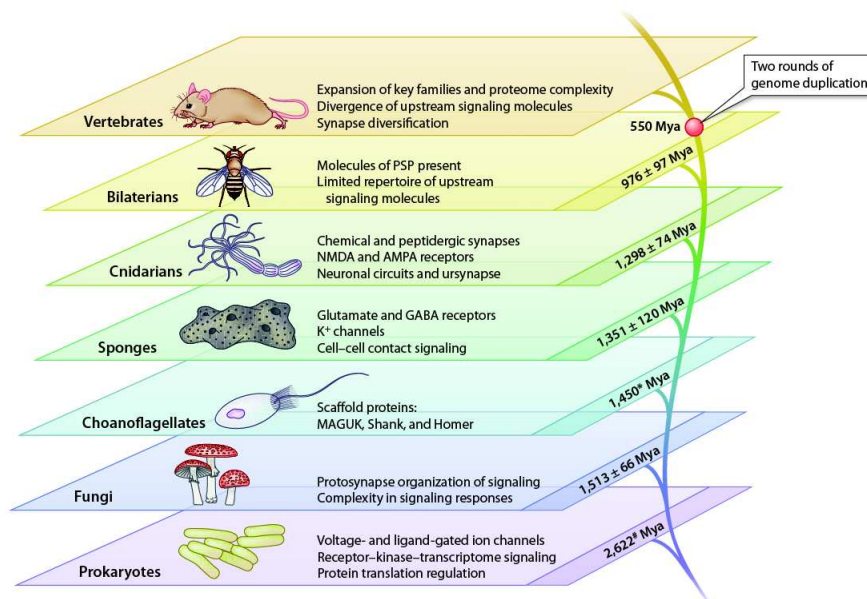


Fig. 5.17.: Source: [76]. Cladogram of taxonomic groups and origins of synaptic components

It seems [76, 225] in fact that genomic duplication—which took place 550 Mya, before the appearance of the complex nervous systems owned by vertebrates— favored the expansion of key families of proteins to the creation of new ones (see Figure 5.17).

According to the model proposed in [76, 225], mammalian synapse has evolved from a common invertebrate protosynapse and the family expansion with consequence enlargement of synaptic pool was determinant for its combinatorial potentiality to give birth to a huge number of possible synaptic and neuronal types. These findings and hypotheses elucidate our results telling that different anatomo-functional regions are characterized by a different combination of isoforms/subunits for given set of families (see Figures 4.9, 5.15, 5.16).

Anatomo-functional evolution of the cortex and the tethering hypothesis

The evolution of families of proteins would have then progressed in parallel with the complexification of vertebrate nervous system and in particular the transformation of the anatomo-functional organization of the cortex. Figure 5.18 shows the cladogram for the evolution of the anatomo-functional organization of the cortex in mammals starting from the common ancestor. In particular the figure shows how visual (in blue), somatosensory (in red), auditory (in yellow) and multimodal regions (in green) maps are organized across the different species. They correspond to the main poles of what we called VSA ring. The organization of VSA subregions is similar across species and associative regions tend to be interspersed between them bridging and combining different sources of information. Going from the common ancestor towards monkeys, associative regions tend to grow in size in parietal, temporal and frontal areas.

In humans compared to chimpanzee we see the development of regions devoted to language around auditory and phonatory regions in strong relation with associative parietal, frontal and temporal areas. It is interesting to think about the evolution of the organization of cortical maps and areas and the results reported in Figure 5.4 where we showed how all the anatomo-functional regions participating to the functional network implementing language turn out to be the less differentiated from a genetic point of view.

Trying to explain the emergence and dominance of associative cortices in humans, Buckner in [29] reviews the so called tethering hypothesis. According to this hypothesis, the expansion of the cortex happened while the poles of gene expression remained unvaried. This would have let the new areas of the cortex free from the strong molecular constraints imposed by genetic gradients determining the formation of sensorimotor maps. These new areas (interspersed between sensorimotor areas) freed at the same time from strong molecular constraints and external sensory activity, started to connect to one another emerging as association cortex resulting in human cognition. This hypothesis goes in the same direction as our results suggesting how more modern cortical areas and in particular those implementing language functionalities (see Figure 5.4), are less characterized having an

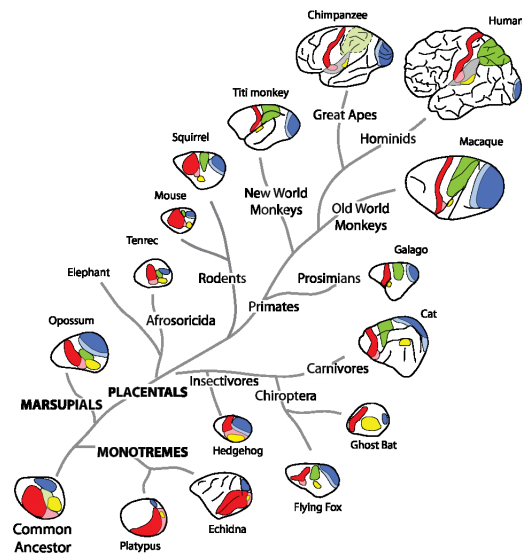


Fig. 5.18.: Source: <http://krubitzer.faculty.ucdavis.edu/>. Phylogenetic relationships of mammals and their basic plan of cortical organization. In red is represented the primary somatosensory area, in pink the second somatosensory area, in green the posterior parietal cortex, in dark blue the primary visual area, in light blue secondary visual area, in yellow auditory cortex

average profile in term of gene expression. The characteristic of these regions of having a less structured gene/cytoarchitectonic specialization could explain the extraordinary ability to process and store the most large diversity of language signals.

Part III

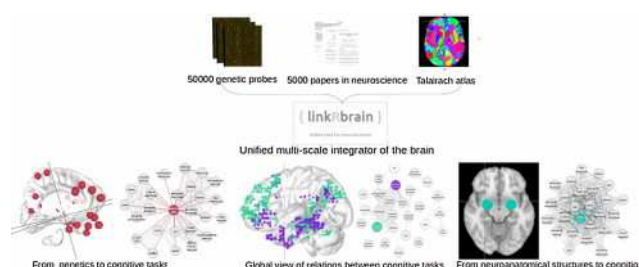
Tools development

LinkRbrain: a web-based platform to analyze spatial correlation of gene expression and cognitive networks

In the first part of this dissertation we presented our studies aiming to better understand the anatomo-functional organization of the human cortex at both a global (the two intertwined rings architecture) and a local scale (gradients of cognitive tasks). In the second part we related this multi-scale architecture with the cortical organization of genes' gradients of expression at both the topographic (spatial match) and the functional level (functional coherence).

In this chapter we present a web based platform thought to allow the interaction between different set of cerebral anatomo-functional data and transcriptomic data. In particular we integrated in the platform the cognitive networks as derived in Chapter 3 and the gene expression data provided by the Allen Institute. The platform can be found at the address <http://www.linkrbrain.org>. This work was published in Mesmoudi *et al.*, *Journal of Neuroscience Methods* 2015.

6.1 Graphical abstract



6.2 Abstract

Background: LinkRbrain is an open-access web platform for multi-scale data integration and visualization of human brain data. This platform integrates anatomical, functional, and genetic knowledge produced by the scientific community.

New method: The linkRbrain platform has two major components: (1) a data aggregation component that integrates multiple open databases into a single platform with a unified representation; and (2) a website that provides fast multi-scale integration and visualization of these data and makes the results immediately available.

Results: LinkRbrain allows users to visualize functional networks or/and genetic expression over a standard brain template (MNI152). Interrelationships between these components based on topographical overlap are displayed using relational graphs. Moreover, linkRbrain enables comparison of new experimental results with previous published works.

Comparison with existing methods: Previous tools and studies illustrate the opportunities of data mining across multiple tiers of neuroscience and genetic information. However, a global systematic approach is still missing to gather cognitive, topographical, and genetic knowledge in a common framework in order to facilitate their visualization, comparison, and integration.

Conclusions: LinkRbrain is an efficient open-access tool that affords an integrative understanding of human brain function.

6.3 Introduction

Sensorimotor and cognitive processing in humans is dependent on the anatomical and functional organization of the brain [86, 156, 189]. Numerous studies have been conducted that focus on a single level of brain organization such as the anatomical [38], the functional [23] or the genetic level [117]. However to really understand the emergence of human cognition, it is necessary to investigate the relationships between these different scales and study the brain as a complex system. The main challenge is thus the integration of available multi-scale knowledge about brain function. Previous studies have tried to link the expression of certain genes with specific cognitive functions [297, 106, 117, 99]. In parallel, fMRI studies have related brain hemodynamic activity to cognitive and sensorimotor function. Manual and automated meta-analysis of large databases of neuroscientific papers have integrated results into synthetic representations (BrainMap [157] and NeuroSynth [294], respectively). These methods are based on extraction of fMRI activation peaks (i.e. coordinates) as reported in published articles. They support construction of probabilistic maps of specific cognitive functions.

To visualize and analyze the complex convolutions of the cerebral cortex, the Caret platform provides a powerful approach to quantitatively represent both the consistency and variability in the pattern of convolutions and functional activation from any given task. This tool also allows supports comparisons across species and evaluation of candidate homologies between cortical areas or functionally delineated regions [268].

Brainscanner was developed in order to analyze abstracts from scientific papers published in peer-reviewed journals. It measures lexical associations between neuroscientific concepts, then extracts relationships between brain structures, functions, and diseases (Voytek and Voytek, 2010). Other tools such as the Genetic Association Database (GAD) [14], GeneCard [226], and GeneBank [18] collect, standardize, and archive valuable genetic information. The GeneMANIA tool can be used to find other genes that are related to a set of input genes, based on a very large set of functional association data such as protein and genetic interactions, pathways, co-expression, co-localization and protein domain similarity [283].

Recently, the Allen Institute for Brain Science (ABI) released an open access database called the “Allen Human Brain Atlas” [133] that contains expression data for 21,000 different genes across 1000 brain regions.

In addition, the Neuroscience Information Framework (NIF) [6] provides a unified portal to several neuroscience databases, facilitating access to existing knowledge from neuroimaging, neuroanatomy, cognitive, and genetics databases.

These tools illustrate the opportunities for data mining across multiple sources of neuroscience and genetic information. However, the field is currently lacking a global systematic approach for gathering cognitive, topographical, and genetic knowledge in a common framework that can facilitate visualization, comparison, and integration.

In order to take on the challenge of integrating cognitive, genetic, and anatomical knowledge about brain function, we developed the linkRbrain platform ¹. This platform (1) accumulates information from several databases, and (2) integrates these multi-scale data into a common framework so that every point in the brain is characterized by a cognitive profile, a gene expression profile, and a neuroanatomical label. Thus, linkRbrain systematically links: (1) a set of activation peaks over the brain to a set of cognitive labels; (2) a genetic expression profile to a set of cognitive labels; and (3) a set of cognitive labels or genetic expression profile to neuroanatomical labels.

The linkRbrain platform provides brain mapping and relational graphs comprising current available information on brain activity, genetic expression and cognitive functions. This integrative platform is available to the whole community, through an open collaborative website.

¹www.linkrbrain.org

6.4 Data sources

Functional MRI data. LinkRbrain relies on the database of activation peaks generated by the Neurosynth framework [294]. The version of the database used in linkRbrain contains 194,387 activation peaks automatically extracted from over 5000 published neuroimaging papers, with roughly 140,974 coordinates correctly labeled in Talairach or MNI [256, 78].

Article abstracts. In order to extract the terms used by authors to describe cognitive tasks in a bottom-up manner, we used the abstracts and titles of over 5000 neuroimaging articles contained in the Neurosynth database.

Gene expression data. The Allen Human Brain Atlas (ABA) [133] produced by the Allen Brain Institute (ABI) provides microarray expression profiles of almost every gene in the human genome at hundreds of locations in the brain. Two complete postmortem brains (H0351.2001 and H0351.2002) are available. Genetic profiles of the two brains are highly compatible [117]. LinkRbrain used the H0351.2001 ABA, which reports the genetic profiles for a set of 947 samples, representing the structures within the human brain in approximate proportion to the volumetric representation of each cortical, subcortical, cerebellar, and brain stem structure. This first version of linkRbrain supports visualization of about 21,000 genes expression profiles (as studied in [117]) across the complete set of 947 brain regions.

The H0351.2001 ABA dataset contains about 451 cortical and 496 subcortical regions. To avoid driving results that could be induced by the over-sampling of the subcortical structure, the first version of linkRbrain focuses exclusively on human cortical organization. Hence, the graphs used to quantify gene/cognition overlap and gene/gene overlap take into account only the cortical samples (451 regions).

Neuroanatomical data. We used the 3D Talairach Atlas [159] to label neuroanatomical structures. This atlas was created from the reference images using resampling following the x and y axis and nearest neighbor interpolation in the z direction. The 3D Talairach Atlas is available as a NIFTI image “Talairach.nii”, where every voxel refers to one of the area labels.

6.5 Methods

6.5.1 Text mining

Two types of relations link the sensorimotor/cognitive tasks. First, lexical relations can be directly extracted from the text of articles, thereby providing an overview of the relations between cognitive domains as conceptualized by the scientific community as a whole. Second, topographical relations can be estimated by quantifying the spatial overlap between task-related activations for different functions. In this work, we focus on topographical relations between cognitive networks, genetic expression profiles, and neuroanatomical structures.

Cognitive task labels. We used the lexical extraction capabilities of the CorText platform to identify a set of pertinent terms. Text processing involves both grammatical ² and statistical [140, 88] phases to automatically extract candidate n-grams (also called multi-tems). ³ We analyzed the textual content found in titles and abstracts of the 5000 papers within Neurosynth (corpus). The most pertinent noun phrases in our corpus were then curated by a neuroscientist who manually selected the 300 most frequent sensorimotor/cognitive tasks (e.g. spatial working memory, emotional facial expressions)

Linking activation peaks and task labels. Neurosynth data and software ⁴ were used to generate a meta-analytic reverse inference map [295, 209] for each of the previously extracted n-grams. This map quantifies the degree to which each brain region is preferentially activated in studies tagged with a particular sensorimotor/cognitive task label.

6.5.2 From probes to expression of genes

Genetic expression profiles of the H0351.2001 Atlas were published by ABI as a matrix of 58000 *probes* \times 947 *regions* of the brain, and includes a list of correspondences between probes and genes [133]. The final expression profile of every gene was computed by averaging the corresponding probes.

6.5.3 Topographical distances

The topographical overlap among cognitive activations, between cognitive activations and gene expression regions, or between cognitive activations/gene expression regions and anatomical structure of brain, is expressed as a distance based on a correlation metric. Each network (corresponding to a cognitive task, gene expression region, or anatomical structures of brain) is a set of points or nodes. Let two nodes (sets of weighted points) A and B :

$$A = \{(M_i, \mu_i) \mid i \in \llbracket 1, m \rrbracket\} \quad B = \{(N_j, \nu_j) \mid j \in \llbracket 1, n \rrbracket\}$$

where μ_i and ν_j are the weights of M_i and N_j respectively. The weights express statistical or genetic expressions values related to the activation peaks or cortical regions respectively.

The correlation score (cor) between the nodes A and B was defined by the formula:

$$cor(A, B) = \sum_{d(M_i, N_j) \leq r} \mu_i \cdot \nu_j \frac{d(M_i, N_j)}{r}$$

where r is the reference radius (10mm in this case, consistent with the meta-analysis), and $d(M_i, N_j)$ is the distance between two points M_i and N_j . The overlap between the two nodes A and B , was obtained by normalizing the correlation score with their autocorrelation. This overlap was based on the RV coefficient (Robert and Escoufier, 1976):

$$s(A, B) = \frac{cor(A, B)}{\sqrt{cor(A, A) \cdot cor(A, B)}}$$

6.5.4 Visualization

All the activation peaks extracted from the literature [294, 295], the gene expressions regions [133], or anatomical structures of brain [159] are plotted on a 3D and 2D reconstructed brain from the T1-weighted MNI152 [78]. 3D visualization allows a global localization of studied networks or regions of brain, while 2D visualization allows more precise location of various anatomical structures of the brain.

6.5.4.1 Visualization of activation peaks

We use the MAP inference procedure to generate sensorimotor/cognitive networks from the activation peaks [294]. To better illustrate the spatial distribution and overlapping, only one color was assigned to each network. Every task can be represented in two different ways: as spheres, or as a continuous surface.

Figure 6.1 illustrates the spatial distribution of the networks involved in a sensorimotor transformation relevant to speech: the relation between a sound and the motor production of this sound by speech. The observation of this graph suggests a relation between the networks specialized in syllable production, sensory tone processing, and motor control of the lips.



Fig. 6.1.: Mapping of the networks corresponding to the cognitive functions “syllables production”, “pure tone” and “lips movement” in blue, red, and green respectively. On the right side we represent the activated regions by spheres, whereas on the left side we display these networks as a continuous surface.

6.5.4.2 Visualization of expression genes regions

For each gene, we identified 451 regions of cortical and 496 subcortical regions of gene expression. In this version of linkRbrain, we focused on the cortical region to evaluate the overlap between task-based networks and genetic expression profiles. Plane visualization is anyway available for all the 947 regions that cover the cortical and subcortical brain regions. The expression of each of the 21,000 genes is represented by spheres located at each of the 947 brain samples; the diameter of each sphere is proportional to the intensity of expression of the given gene at this position in the brain (see Figure 6.2 and Figure 6.3).

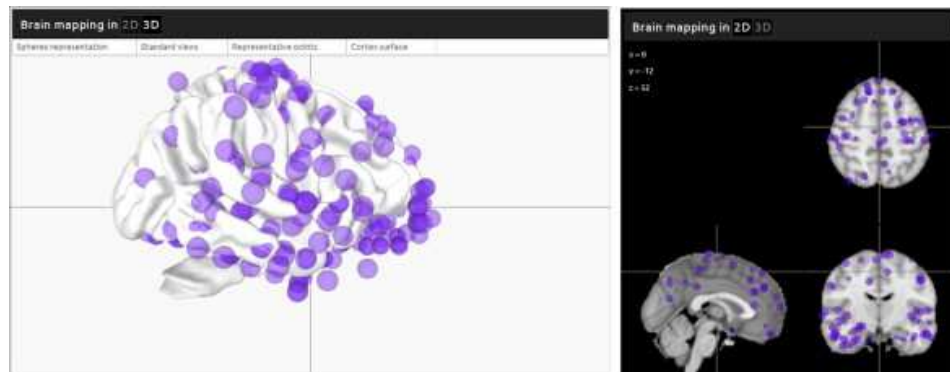


Fig. 6.2.: 3D and 2D mapping of the expression profile across the 947 brain regions for the Microtubule-associated Protein Tau (MAPT) gene. Each region is represented by a sphere whose diameter is proportional to the expression intensity at the specific region.

6.5.4.3 Visualization of user results

LinkRbrain users can visualize and correlate their neuroimaging results with the sensorimotor/cognitive networks, neuroanatomical regions, or genetic expression regions by loading a NIFTI file or MNI coordinates (using NIFTI files, input coordinate, or text files option). Moreover, by using the input coordinate or text file options, the user can (1) quickly and easily compare the expression among several genes by mapping only the cortex regions

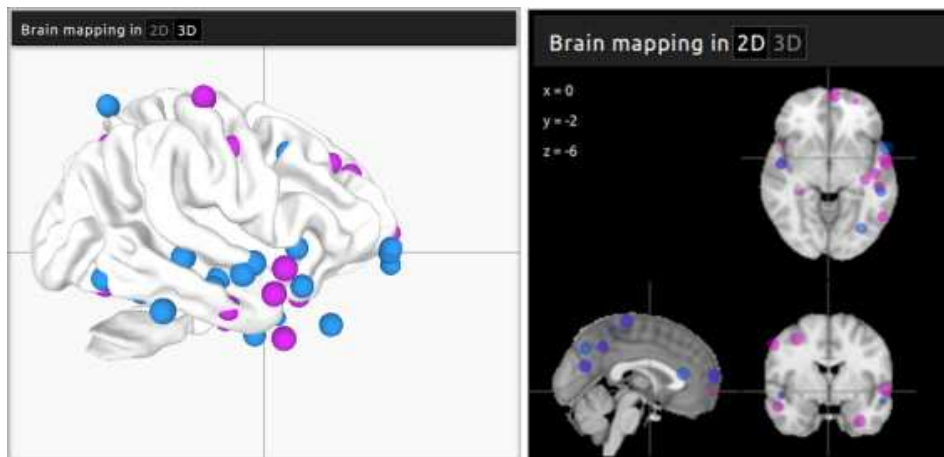


Fig. 6.3.: 3D and 2D mapping of the regions of maximal expression for Microtubule-associated protein tau (MAPT) and Myelin basic protein (MBP) genes. Each region is represented by a sphere colored in blue or magenta to indicate MAPT or MBP expression respectively.

where they are the most expressed, and (2) upload her genetic results or a specific probe from the ABA dataset to correlate it with sensorimotor/cognitive networks.

6.5.4.4 Graph-based visualization of correlations

The topographical overlaps (i.e. correlations) between selected task(s), gene(s), or neuroanatomical regions (current node) and the other cognitive tasks, genes, or neuroanatomical regions (nodes) can be represented as a graph. The graph is computed using the force-directed layout algorithm (Fruchterman and Reingold, 1991). Figure 6.6 shows two types of links: (1) colored links connect the current node to another node and reveal that an overlap exists between these two nodes; (2) grey links express the overlap between the other nodes without involving the current node. The thickness of the link is proportional to the magnitude of the correlation (overlap).

6.5.4.5 Visualization of correlations with identified neuroanatomical structures

To identify the regions involved in cognitive activation or genetic expression regions, linkR-brain quantified the overlap (i.e. correlations) between this input and the structures of brain identified in the Talairach atlas. These results can be represented as colored regions in the brain, or a graph with cognitive activation or genetic expression regions (see Figure 6.5).

6.6 LinkRbrain as a multi-scale, integrative explorer

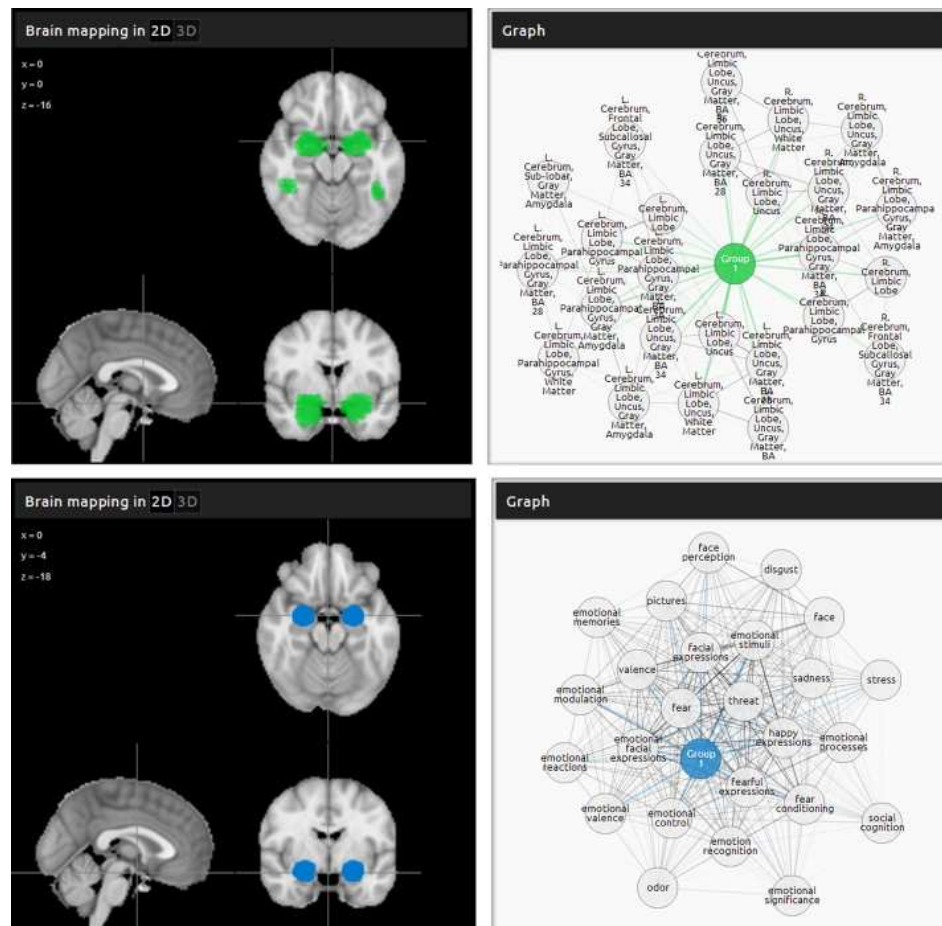


Fig. 6.4.: 2D mapping of the cognitive network “facial expression” in green. The corresponding graph shows the neuroanatomical regions involved in this network (overlap). In the bottom, 2D mapping of the neuroanatomical region called “Amygdala” in blue. The corresponding graph shows the sensorimotor/cognitive task-based networks that are localized in this region.

6.6.1 From cognitive functions to functional-anatomical architecture

To separately assess the performance of linkRbrain as an exploratory tool at the cognitive and the topographical scales, and as an integrated multiscale tool, we used the example of the model called “the dual intertwined ring architecture” [189]. This model originated from a systematic analysis of anatomical, resting-state (RSN), and task based networks (TBN). According to this model, the human cerebral cortex comprises two large ensembles shaped like two rings. The first ring, called the Visual–Sensorimotor–Auditory ring (VSA ring), comprises visual, auditory, somatosensory and motor cortices, including intermediate bimodal regions. The second ring, called the Parieto–Temporo–Frontal ring (PTF ring), comprises parietal, temporal, and frontal regions. The VSA ring is continuous and forms a circle around the parietal areas BA 39 and 40, whereas the PTF ring, which is not fully continuous over the cortical mantle, is closed by the long-range association fiber tracts

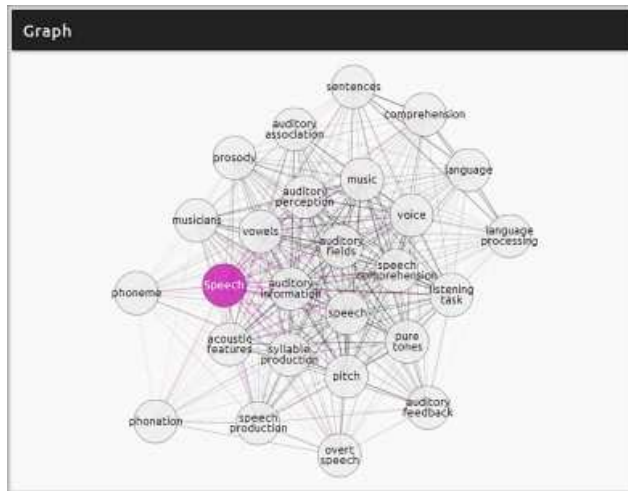


Fig. 6.5.: The graph shows the topographical similarities (overlap) between “speech function” (nodes in magenta) and the 300 cognitive tasks. Only the most highly correlated tasks (25) are represented. The magenta links connect “speech” network with similar tasks. The gray links connect tasks with each others.

(longitudinal parieto-frontal, arcuate, uncinata, and cingulum) that complete the intertwining. The two rings share a set of common regions mostly localized along the precentral, intraparietal, and superior temporal sulci.

Based on the overlap between the resting state networks and different areas and cortices, we can infer that the first ring (VSA ring) links various sources of auditory, visual and somatomotor information together and to control actual behavior. These interactions are important, not only within each modality, but also for all of their bimodal interactions: between visual and motor (e.g., grasping, reaching, imitation), between auditory and somatomotor information (e.g., recognizing and producing phonemes) and between auditory and visual information (important for communication). To illustrate these functional interactions, we used linkRbrain to build the VSA ring by plotting on the brain the task based networks (TBN) corresponding to these modalities (visual, auditory, and motor) and bimodal interactions (motor–visual, visual–auditory, etc). As shown in Figure 6.6, we plot in blue the activations corresponding to: motor function, pictures, hand gestures, limb, somatomotor stimulation, auditory, etc. These networks are activated when we directly stimulated the visual, motor and auditory cortices. In addition, to obtain the bimodal interactions, we plot activations corresponding to speech, oculomotor, etc.

The PTF ring (in red) interfaces systems dedicated to higher cognitive functions with systems dedicated to emotions, biological needs and rhythms. In Figure 6.6 we showed that the PTF ring (in red) was reconstructed functionally by plotting the activations peaks corresponding to functions such as recollection, autobiographical memory, semantic memory, working memory, episodic memory, etc.

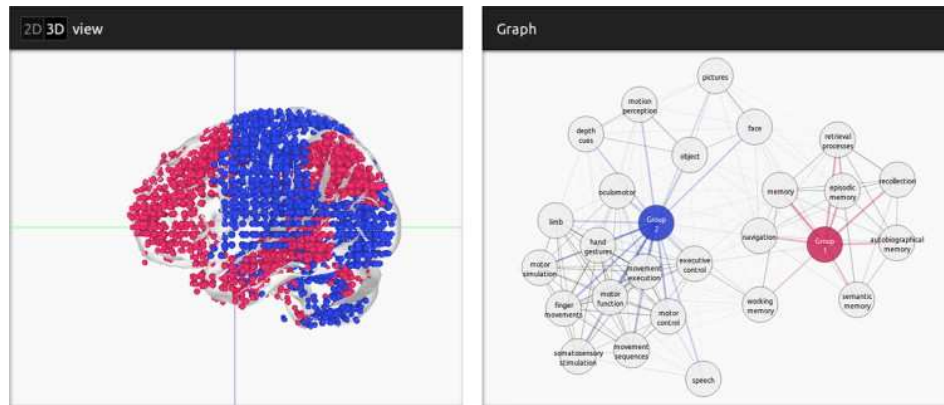


Fig. 6.6.: Mapping of the cognitive and sensorimotor functions related to the VSA ring (in blue), and some cognitive functions that reconstruct the PTF ring (in red). The corresponding graph shows these functions and confirm the topographical similarities (overlap) between VSA/PTF (in blue/red respectively) and the 300 tasks. The blue/red links connect VSA/PTF rings (respectively) with similar tasks. The gray links connect tasks with each other.

6.6.2 From genetic expression to cognitive functions

As explained previously the linkRbrain platform computes the topographical overlap on the brain between different cognitive activations, gene expression regions, or between cognitive activations and gene expression regions. This topographical overlap is based on a correlation metric, and is represented by linkRbrain as a graph of topographical correlations. To illustrate these correlations, we compare the gene expression profiles of the Oxytocin receptor (OXTR) [111, 128], and the Dopamine D5 Receptor (DRD5) [158, 253] (see Figure 6.7). Results show large overlaps, with an important difference: DRD5 is more highly expressed in the anterior cingulate cortex, and OXTR is more highly expressed in the medial anterior temporal pole. To compare the differential spatial correlations (overlap) with cognitive tasks, linkRbrain provides the graphs of topographical similarities. This graph is obtained from the correlation between regions of expression of the OXTR and DRD5 genes and all the activations corresponding to the 300 cognitives tasks extracted from the 5000 neuro-cognitive papers. We see that both regions of gene expression are related to Reward, but OXTR expression is more strongly associated with overlapping emotional networks, and in particular facial expression (important for social interaction), while DRD5 is more related to autobiographical memory, self, and interoceptive awareness. These results obtained from the overlap between genetic expressions and cognitive networks, are confirmed by the literature. In fact, several studies suggest a modulatory role of oxytocin on amygdala responses to facial expressions [68, 169] (see Figure 6.4). Conversely, other studies implicate dopaminergic pathways in regulation of neuronal systems associated with reward sensitivity, self-control, and interoceptive awareness [276].

6.7 LinkRbrain as comparator of brain networks of cognitive functions

The cognitive functions “speech” and “sentences” are considered as two distinct functions. The “speech” function is related to word production, syllables, and/or vowels production and/or recognition [235, 195], while the “sentences” function is concerned with the meaning of sequences of words. This function is related to language comprehension and memory [115, 265]. Thus, all of these cognitive differences should be topographically reflected. In Figure 6.8, by plotting the networks corresponding to the functions “speech” and “sentences” (colored in purple and magenta respectively), we notice: (1) the “V” shape that characterize these two functions, with a temporal and a frontal component; and (2) despite the proximity of these functions, their topographies are clearly different. In the corresponding graph generated by linkRbrain two sets of the interactions with the other cognitives functions emerge. The first one is related to the “speech” functions (connected to the purple node) with functions such as: vowels, syllables production, etc. The second set is related to the “sentences” function (connected to the magenta node) and represents cognitive functions that topographically overlap with “sentences”, such as: speech comprehension, language processing, etc.

6.8 LinkRbrain as a comparator of user results with the literature

Laird et al. reconstructed 20 intrinsic connectivity networks (ICN) from the BrainMap database which archived the peak coordinates and metadata associated with 8637 functional brain imaging experiments [156]. These experiments were extracted from 1840 publications that reported 69,481 activation locations across 31,724 subjects. The masks of these 20 ICN.5 Based on [156], we used the ICN7 as example which include dorsolateral prefrontal (BA 46) and posterior parietal cortices (BA 7). ICN7 involve visuospatial processing and reasoning, with a strong weighting for tasks such as the mental rotation, and counting or calculation.

Based on correlations between the ICN7 image and each cognitive network in the linkRbrain database (see Section 3), we produced a proximity graph. According to the graph of topographical proximities (see Figure 6.9), the volume analyzed corresponds to cognitive functions such as oculomotor, visuospatial working memory, saccades, anti-saccades, arithmetic operation and mental calculation. Theses functions extracted by linkRbrain are quite similar with those described in Laird et al. (2011).

6.9 Conclusion

The number of shared fMRI databases and genetic studies is continuously increasing thanks to the collective efforts of the scientific community. In this work we exploited several new open access databases, extending their value by integrating them in a common framework: a multi-scale data integrator. In fact, with the linkRbrain platform we can: (1) integrate anatomical, functional, and genetic knowledge, (2) visualize and compare functional networks and/or genetic expression, and (3) make sense of new experimental results produced by the community by comparing them with previously published work. In the future, we will extend the linkRbrain platform to include: (1) the new NeuroSynth database with 9721 studies, (2) fiber tracts data, to extend the present integration of multiscale data, and (3) new data coming from the community of users to extend and improve the existing database of cognitive task networks.

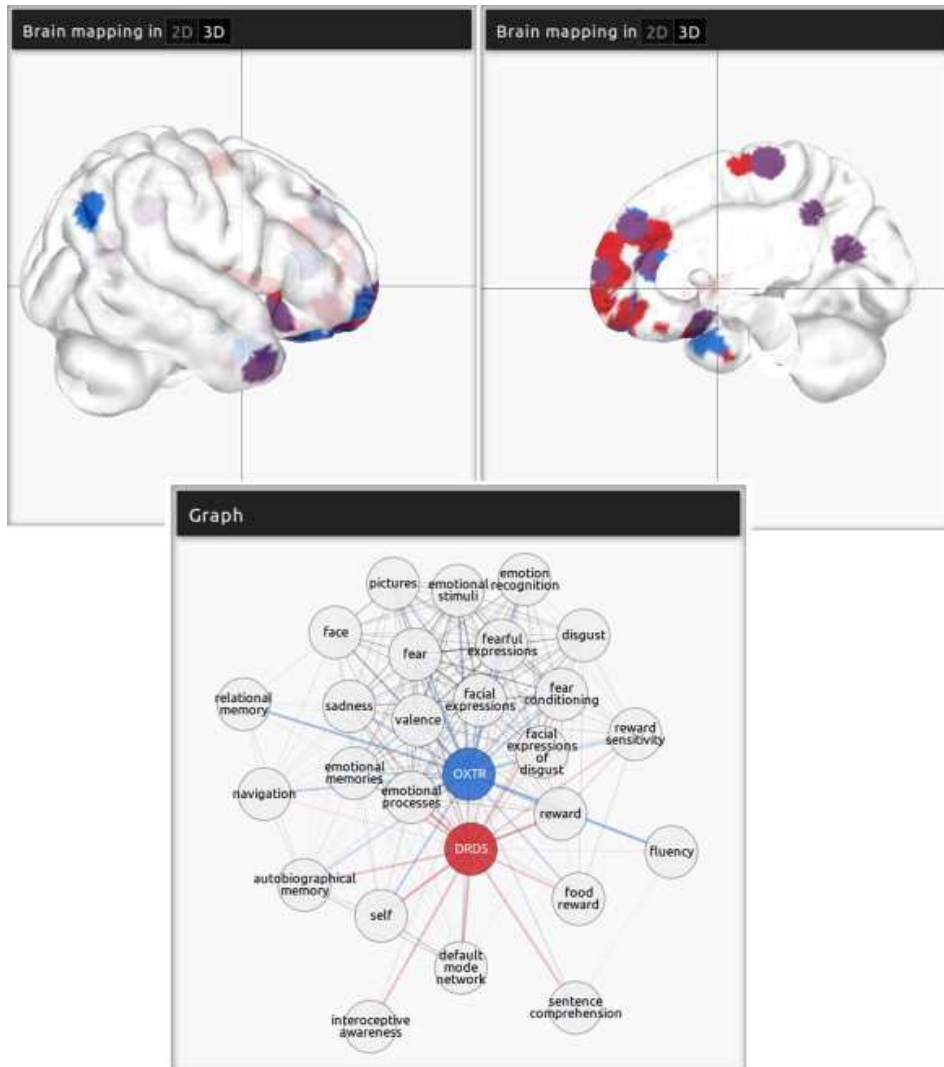


Fig. 6.7.: Mapping of the regions where the genes coding for oxytocin receptor (OXTR) and dopamine receptor D5 (DRD5) (in blue and red, respectively) are the most expressed. The regions in purple represent the overlap between the two gene expressions. The corresponding graph shows the sensorimotor/cognitive task-based networks that are localized in the same regions where the genes OXTR and DRD5 are most strongly expressed. Red links connect the DRD5 expressions with the topographically nearest tasks, whereas the blue links connect the OXTR expressions with the topographically nearest tasks. The gray links connect tasks with each other on the basis of their topographical overlaps.

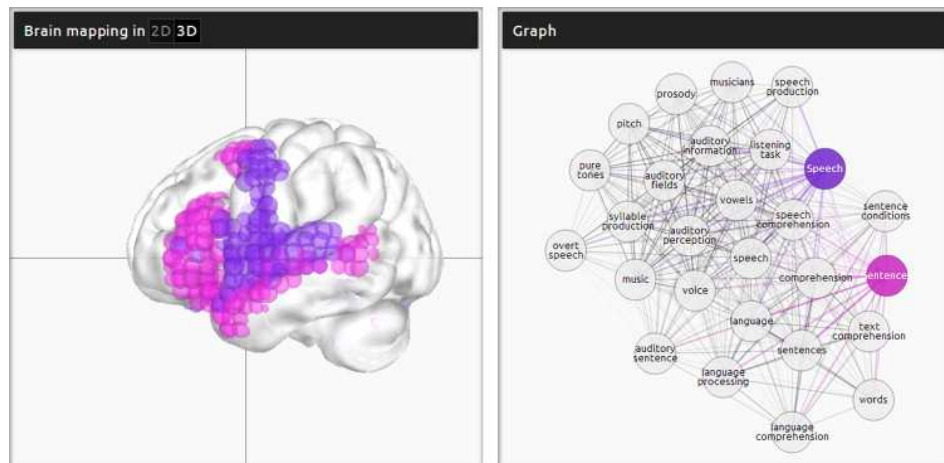


Fig. 6.8.: Mapping of the networks corresponding to the cognitive functions “speech” and “sentences” in purple and magenta respectively. The corresponding graph shows the topographical similarities (overlap) between the “speech” and “sentences” functions (respectively in purple and magenta) and the 300 cognitive tasks. The “purple/magenta” links connect “speech/sente-nces” networks (respectively) with similar tasks. The gray links connect tasks with each other.

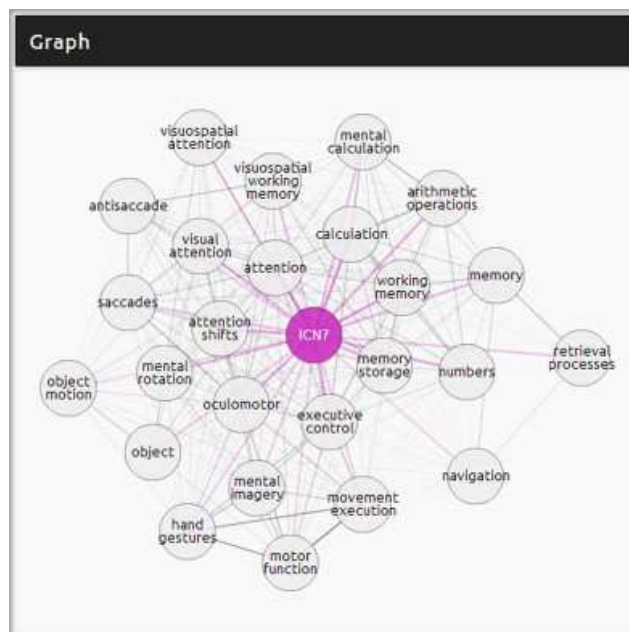


Fig. 6.9.: The graph shows the topographical similarities (overlap) between the ICN7 network (colored nodes) and the 300 cognitive tasks. The colored links connect ICN7 network with similar tasks. The gray links connect the cognitive tasks with each other.

Conclusions and future work

7.1 Conclusions

In Chapter 2 we elaborated an anatomo-functional model of the human cortex—called the two intertwined rings architecture – allowing a multi-scale interpretation of the cortical organization in terms of anatomo-functional and information processing. The first ring forms a continuous ensemble and includes visual, somatic, and auditory cortices, with interspersed bimodal cortices (auditory-visual, visual- somatic and auditory-somatic, abbreviated as VSA ring). The second ring integrates distant parietal, temporal and frontal regions (PTF ring) through a network of association fiber tracts which closes the ring anatomically and ensures a functional continuity within the ring. The PTF ring relates association cortices specialized in attention, language and working memory, to the networks involved in motivation and biological regulation and rhythms. This dual intertwined architecture suggests a dual integrative process: the VSA ring performs fast real-time multimodal integration of sensorimotor information whereas the PTF ring performs multi-temporal integration (i.e., relates past, present, and future representations at different temporal scales). This model is important to relate cerebral activity at the cortical level with the one at the neuronal level, where proteins and their interactions determine time-scale of the different activities.

In Chapter 3 we adopted a meta-analytic approach to make sense of the cortical organization of anatomo-functional networks implementing cognitive functions. In particular we extracted in a bottom-up fashion a cognitive ontology based on Neurosynth database of more than 4000 fMRI papers. Based on the co-occurrences of the ontology terms in abstracts, we were able to produce a map describing the relation between the different cognitive areas studied in the fMRI scientific community (modulo the papers contained in the Neurosynth database). Coupling the cognitive ontology with the peaks of activation associated to each article in the database we were able to get a map of similarity for the different cognitive tasks based on the amount of overlap on the cortical surface. The map obtained revealed a global organization for the cognitive tasks consistent with the two intertwined rings architecture described in Chapter 2. Moreover this map can reveal at a finer scale the similarities between each couple of cognitive tasks. We finally introduced a set of anatomo-functional cortical regions to be used as landmarks to describe this cognitive organization at a finer level.

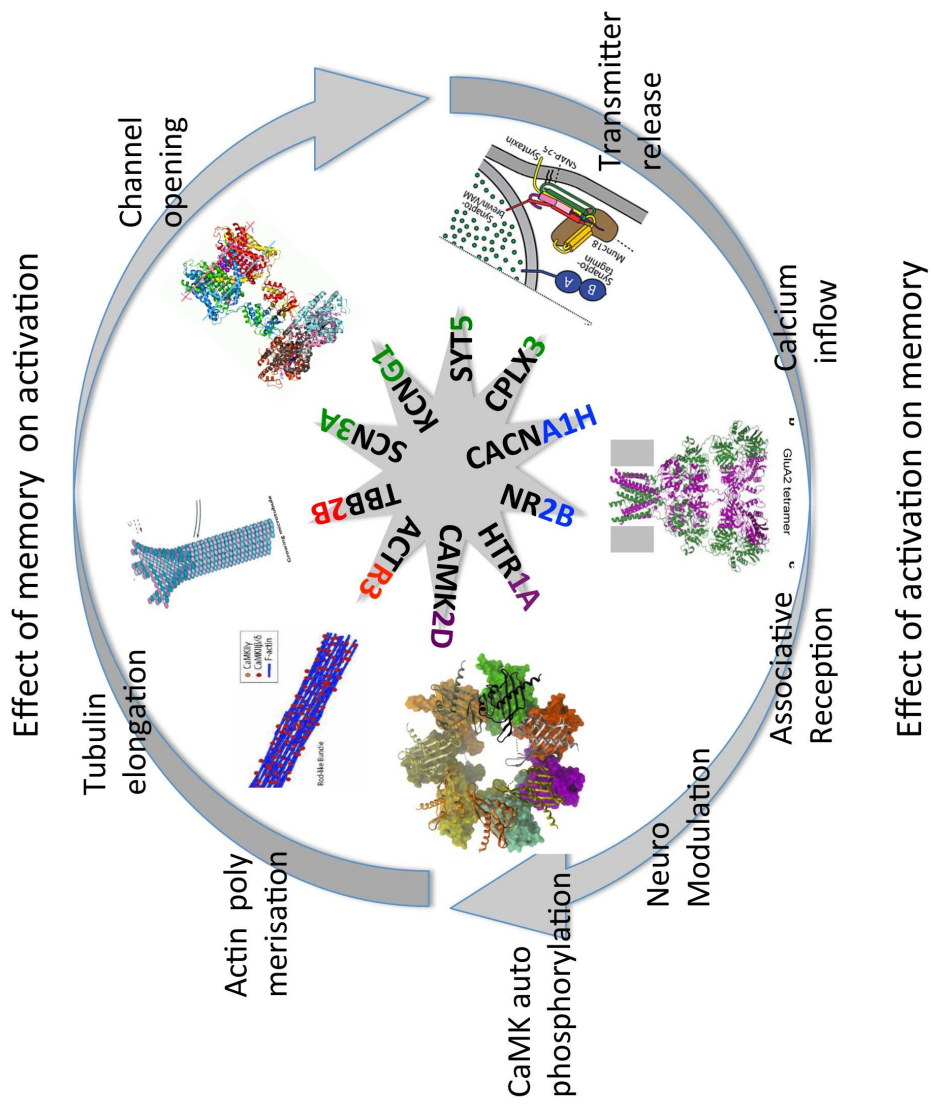
In Chapter 4 we drew a link between the anatomo-functional organization of the cortex and the cortical distribution of gene expression for the 1000 genes the most differentially expressed across the cortex. We showed that the gene expression is primarily organized according to the two intertwined rings architecture. Genes profiles follow indeed two main gradients showing strong correlation among them if their pole of expression is in the same ring and strongly anti-correlated if their poles are in opposite rings. We showed that genes implied in information processing and neurotransmitter release are among the genes the most important for the regional opposition between the two rings. The study of the whole families for genes coding for ionic channels subunits (SCNs, KCNs, CACNs) and synaptic proteins involved in neurotransmitter release (SYTs, CPLXs, VAMPs) showed that different subunits and isoforms of a same family have a differential expression across the two rings. Moreover subunits or isoform more expressed in VSA tend to favor evoked phasic activities presenting high-fidelity respect to real-time stimuli; while those more expressed in PTF tend to favor more sustained and spontaneous activity, less related to external stimuli. Finally we showed that while genes profile are either strongly correlated or anti-correlated presenting a block decomposition of the correlation matrix, regions differences are instead organized by a gradient.

In Chapter 5 we showed confirmed previous results about gene expression across different cerebral areas; we interpreted these differences as mainly related to the regional differences in texture/cytoarchitectonic. Results about cortical organization of gene expression follows primarily the two intertwined rings using the totality of genes expressed in the cortex. We showed the existence of a second gradient opposing ventral versus dorsal regions and in particular temporal versus frontal regions. We focused on the results for families of proteins involved in fundamental neuronal functions: 1) information processing (ionic channels, neurotransmission (pre and post-synaptic part), neuromodulation), 2) short-term memory formation (Calcium Calmodulin kinase dynamics), 3) long-term memory formation (actin and tubulin remodeling) and 4) network genesis and maintenance (cell-cell communication and growth factors). The systematic study of these families of genes revealed specific proteins within families preferentially expressed in different anatomo-functional regions of the brain and of the cortex. The results showed strong congruence between the preferential expression of subsets of genes, cellular properties of the proteins they code, and the cognitive functions implemented. These results point out to the existence of differential synapses whose composition in terms of proteins varies based on the anatomo-functional specialization of the region they belong to.

In Chapter 6 we presented a web based platform thought to gather and to compare data used or produced in the previous chapters. In particular the platform allows to integrate on a same spatial reference frame (MNI coordinates) anatomo-functional labels for the different areas of the brain (cortical and subcortical), to study the organization of cognitive

networks as described and derived in Chapter 3, to observe and correlate the expression of small groups of genes with cognitive networks.

In Figure 7.1 **a** and **b** we synthesized these results.



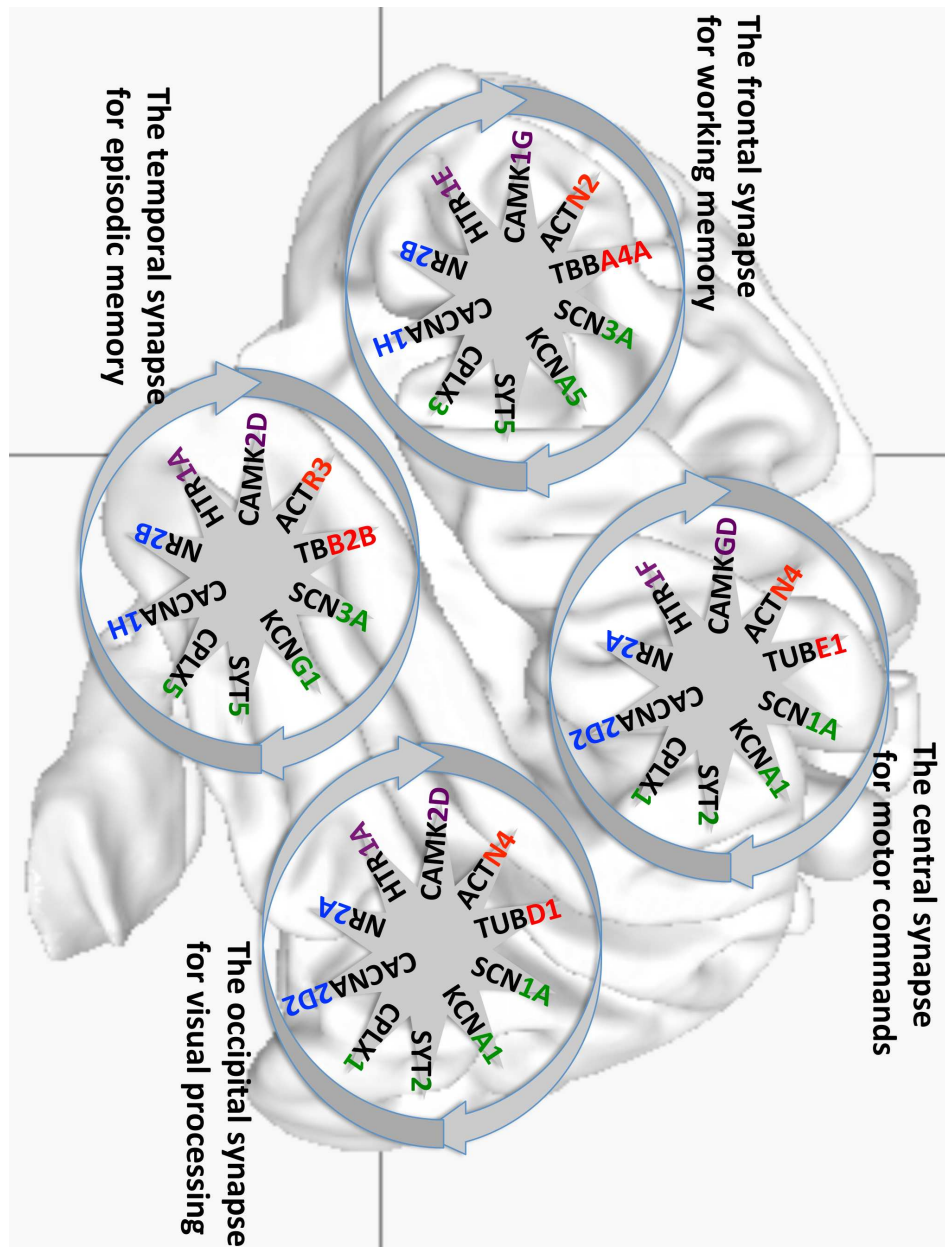


Fig. 7.1.: Figure a shows the memory cascade with different proteins which interact within each synapse with two symmetrical dynamics: the effect of activation on memory, and the effect on memory on activation. These proteins have several subunits and isoforms. Our results show that these subunits or isoform can be differentially expressed across different regions of the cerebral cortex. They form different synapses and memory cascades specialized by regions as shown in Figure b). The figure illustrates four types of synapses organized along the two main gradients of genetic expression (VSA-PTF and temporo-frontal): the congruence between the synapses and the functional specialization of the different anatomo-functional cortical regions are presented in Chapters 4 and 5.

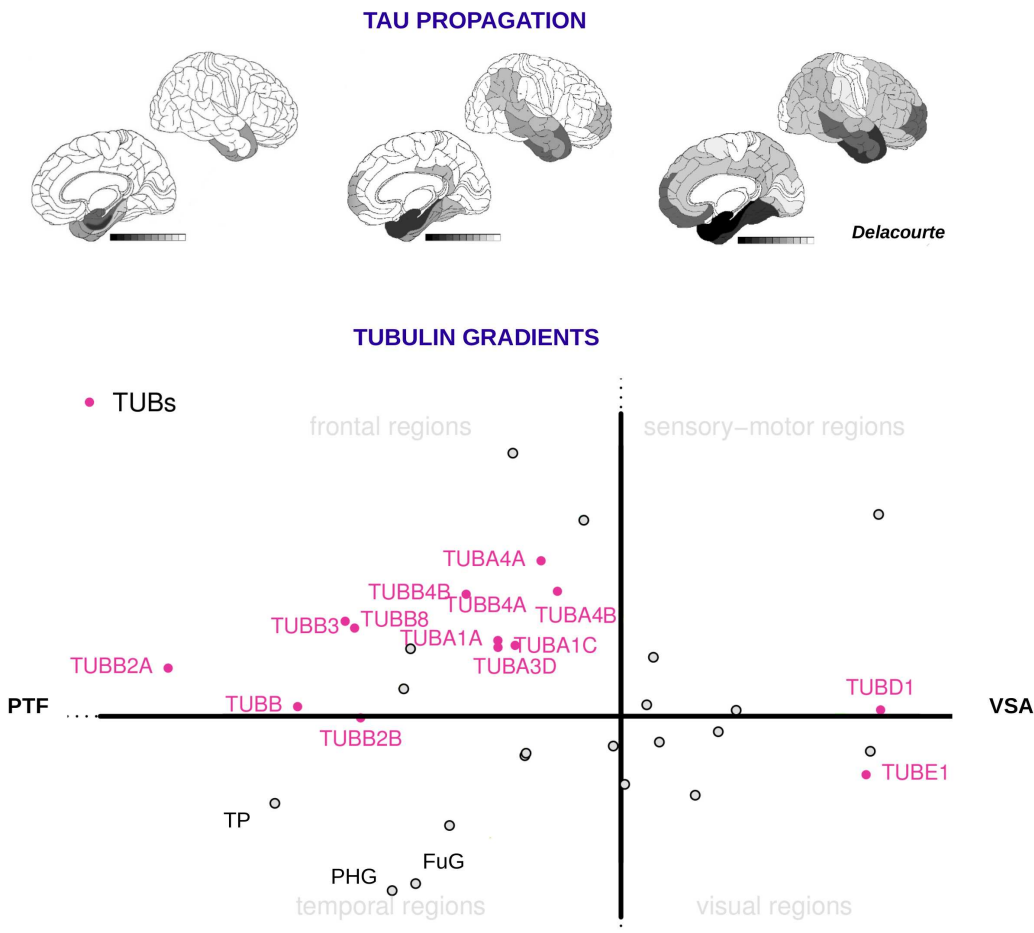


Fig. 7.2.: Protein Tau propagation patterns in AD and tubulin subunits cortical gradients

7.2 Future work

The results of the heuristic presented along this thesis allow at the same time: to draw links between functional properties of specific genes and their regions of maximal expression when genes' function is known; to suggest experimental hypotheses for genes with unknown cellular function but known topographic expression; to suggest pool of candidate genes for neurodegenerative and neuropsychiatric diseases known to perturb specific cognitive functions. In the following we will present three line of research that could benefit from this approach: the study of Alzheimer diseases, the study of Autism Spectrum Disorder and the models describing neuronal and cerebral functioning.

7.2.1 Alzheimer disease

A perspective work in the continuity of this thesis is to develop a general method to extract genes whose expression patterns follow precisely the propagation of a disease, and to focus on candidate genes coding for proteins favoring this propagation. Indeed our re-

sults suggest an hypothesis on the propagation of Alzheimer disease across cortical areas: the propagation of Alzheimer disease across areas follows not only neural connections but also genetic gradients. Among the genes whose gradients correlate with Alzheimer propagation pathway, there are some alpha-beta tubulin isoforms. One hypothesis is that the propagation of the pathology depends upon gene gradients that control the microtubule dynamics.

7.2.1.1 The propagation of Alzheimer disease across areas follows the main genetic gradients from the extreme pole of PTFregions (Parahippocampal Gyrus and Temporal pole) toward the more extreme pole of VSA regions (visual and motor areas)

In Alzheimer disease, researchers have found specific molecules which are dysfunctional, like beta-amyloid peptide and tau proteins which interacts with tubulin to stabilize microtubules (reviewed in [73]). They produce lesions at the neuronal level: Tau accumulate in the cell body of the neuron as neurofibrillary tangle, in the dendrites as neuropil threads, and in the axons forming the senile plaque. At the neuronal circuit level, these lesions produce losses of synapses and neurons. At the level of cortical networks, there is a progression of the tau pathology which involves specific networks from the entorhinal cortex, through the hippocampus, to the isocortex. At the psychological and clinical level, there are progressive deficits starting from memory losses to language alterations and then to sensorymotor dysfunctions.

It is interesting to see that the propagation of the pathology is similar to the PTF-VSA gradient which is the the major organizer of the differential gene expression in the cerebral cortex.

7.2.1.2 An example: alpha-beta tubulin subunits gradients across cortical regions

As an example of gradients of gene expression we can take the case of the tubulin family. In Alzheimer disease (AD), hyperphosphorylation of tau proteins results in microtubule destabilization and cytoskeletal abnormalities. a clear reduction in microtubules in pyramidal neurons in AD compared to controls [298, 34]. In normal cells, Tau stabilizes microtubules by binding at the interface between tubulin heterodimers [138, 137]: Alzheimer disease propagation is related to the instability of the tubulin controlled by the alpha-beta tubulin heterodimers. Tubulin dynamics is controlled by the different combinations of alpha and beta isotypes (the so-called tubulin code) representing the major constituents of microtubules (for ex TUBA4A, TUBB4B, TUBB4A, TUBB4B, TUBB3). These tubulin isoforms show intrinsic differences in the rates of microtubule assembly and the frequency

of growth and shortening events, suggesting that cells can regulate microtubule dynamics by controlling the relative amounts of different tubulin isoforms.

Our results (see Figure 7.2) show that the alpha-beta tubulin heterodimers are differentially expressed along the PTF-VSA gradient. A subset of tubulin isoforms (TUBB, TUBB2A, TUBB2B and TUBB3) are highly expressed in the extreme pole of PTF regions (PHG, temporal pole); among the different beta-isoforms, TUBB3 has a major role in the dynamic instability of the microtubule. Another subset (TUBB4A, TUBB4B, TUBA4A, TUBA4B) is more expressed in the frontal pole and could have different dynamics.

We propose in future work to develop a generic method which goes beyond the topographical correlations between gene expression and cortical regions, and also extract the genes which have gradients of expression similar to the pathway of propagation of a pathology across cortical and cerebral regions. Among these genes, we can select candidate genes which have specific cellular roles favoring cell dysfunctions in this pathology.

7.2.2 Autism Spectrum Disorder

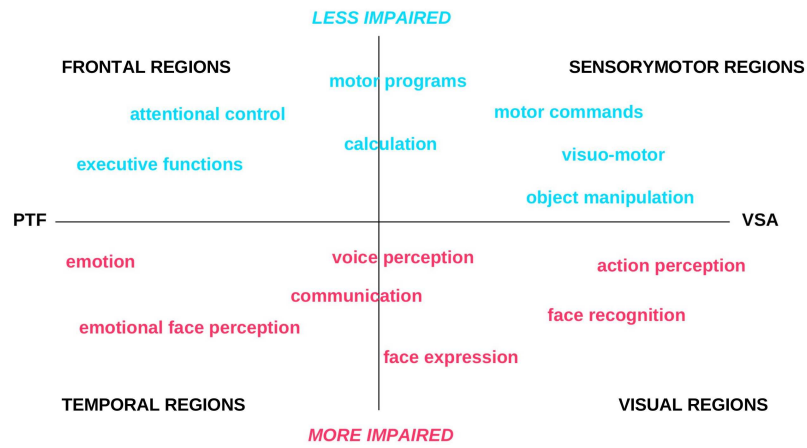
7.2.2.1 Relation between gradients of cognitive networks and gradients of gene expression

Our results for genes labeled as High Confidence in the SFARI database (www.gene.sfari.org/autdb/GS_Hom) show these genes as clustered in correspondence of the temporal pole (see Figure 7.3).

This result reveals that the different genes strongly involved in ASD are all maximally expressed in the occipital and temporal regions. Systematic meta-analysis of the fMRI literature shows that these anatomo-functional regions are implied in a set of tasks which can present difficulties for ASD children: visual motion processing, recognition of facial expression from motion, face and gaze focusing to extract their fine movements which are the basis of emotional facial expression, face recognition, auditory motion processing, interpretation of voice modulation, interpretation of others intentions (from the Parieto-temporal junction). It is interesting to see that these tasks form a continuum, with a gradient starting from the occipital areas toward the temporal pole and the regions close to the amygdala in relation with emotions. So there is a correlation between a set of genes potentially involved in ASD and a set of anatomo-functional regions involved in social behaviours and communication which are both organized along similar occipito-temporal gradients.

Furthermore at the network level, researchers found that there is a dysmaturation of cortical thickness in the temporal lobes and within these the fusiform and middle temporal gyri [221]. These brain regions are crucial to social cognition which is a specific cognitive deficits in ASD. The remaining question is to understand the functional role of the set of genes maximally expressed in the temporal pole. Previous systematic studies [262] showed

COGNITIVE FUNCTIONS AND AUTISM



GENES IMPLICATED IN ASD: CORTICAL DISTRIBUTION

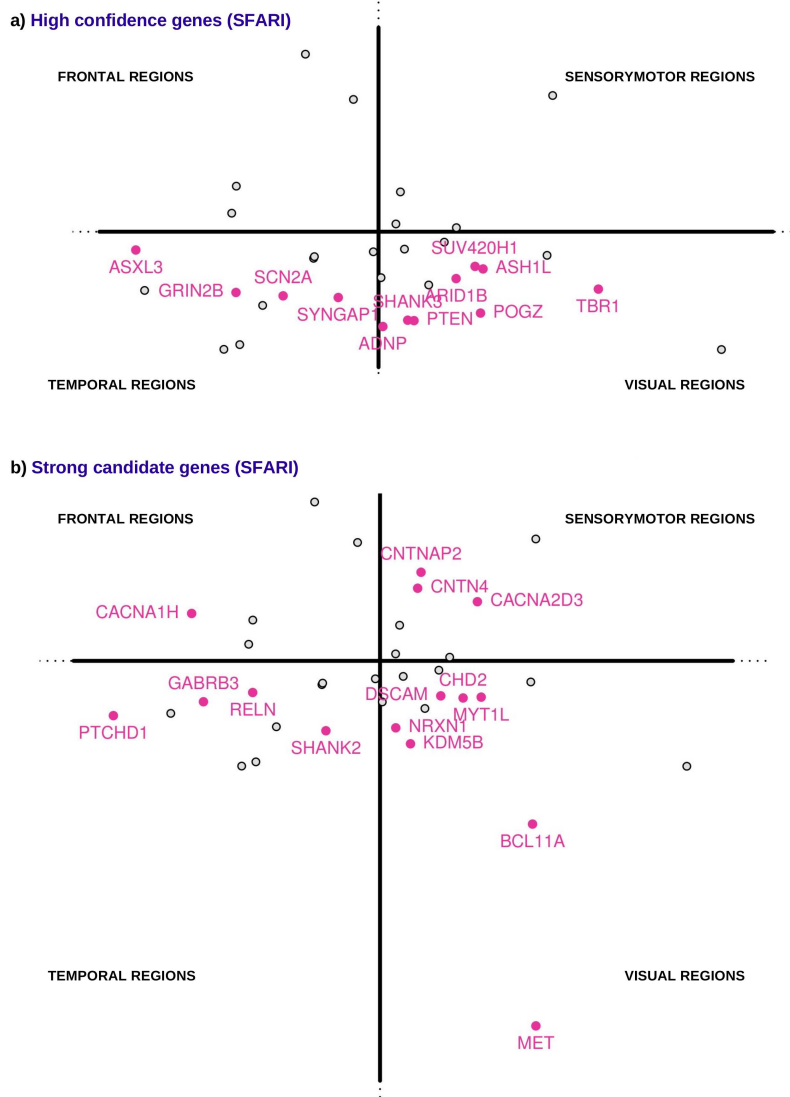


Fig. 7.3.: ASD: comparison of impaired cognitive networks and distribution for implicated genes

that the main category of genes associated with ASD is related to the development and function of neuronal circuits, and in synaptogenesis, such as, cell adhesion molecules which are major organizers of excitatory glutamatergic and inhibitory GABAergic synapses, and contribute to the activity-dependent formation of neuronal circuits. This set of genes is responsible after birth for synaptic homeostasis that allows neurons to maintain an optimal level of activity which plays an important role in the activity-dependent refinement of brain connections during development and the first years of life.

Furthermore, the genes the more expressed in the ventro-dorsal axis is MET (among the Strong Candidate genes, see Figure 7.3). MET signaling is involved in the development of forebrain circuits controlling social and emotional behaviors that are atypical in autism spectrum disorders (ASD). Brain imaging results show that the Met Receptor Tyrosine Kinase gene is a potent modulator of key social brain circuitry in children and adolescents with and without ASD [224]. MET risk genotype produced atypical fMRI activation and deactivation patterns to social stimuli (i.e., emotional faces). By contrast, the cognitive and sensorimotor functions subserved by dorsal frontal and parietal regions are less affected in ASD: e.g., visuomotor processing, motor skills, calculation, planning. The regions specialized in speech and language are intermediate. The gradient-type relation between regions involved in social behaviours and regions involved in language may also be related to gradients of gene expression, FOXP2 involved in language and c-MET involved in social cognition. A perspective of future work in the continuity of this thesis is to correlate gradients of cognitive networks and gradients of gene expression. It could help to better understand the variety of cognitive and sensorymotor symptoms in ASD, related to a variety of genetic deficits.

7.2.3 Models

A future perspective of this work is to adapt functional models of neurons and neural nets to specific anatomo-functional regions (such as parietal regions involved in visuomotor processing, frontal regions involved in working memory, temporal regions involved in sentence comprehension) by taking into account regional parameters based on proteins properties differentially expressed. We will illustrate these regional adaptations in four examples of well-known models: 1) models of neural computation based on temporal properties of ionic channels (see [11]), 2) model of generation of sustained activation for working memory by recurrent excitation due to temporal properties of NMDA receptors [277, 282, 281, 280], 3) models of transformation from short-term to long-term memory by the relation between CaMK autophosphorylation and actin polymerization [173, 172, 170], 4) models of the relation between network construction and plasticity related to the tubulin dynamics [33].

7.2.3.1 Model of neural computation based on temporal properties of ionic channels

The computational properties of neurons critically depend on the temporal properties of ionic channels (closing and opening times) via the Hodgkin–Huxley model [11]. We thus found, more expressed in the PTF ring, genes which facilitate persistent currents (SCN3A and SCN3B), prolonged effects of input activities, (KCNF1, KCNG1, KCNMB4, KCNN3), and spontaneous and rhythmic activation (KCNJ1, KCNA4). All these temporal neuronal properties match the multi-temporal processing in the PTF ring, contrasting with the stimulus-driven high precision timing control of SCN1A, SCN1B and KCNA1 in the VSA ring. Our results also reveal a set of potassium channels with a higher expression in the frontal cortex: KCNA5 (KCNA4 is more temporal), KCNS3 (KCNS1 is higher in motor regions), KCNN2, KCNJ8. KCNN2 (small conductance Ca²⁺-activated K⁺ channels SK which regulate cellular mechanisms of memory encoding). Most of these channels also regulate short-term activations of neurons: KCNN channels regulate sustained activation of dopamine neurons, KCNJ generate rhythmic activation and spontaneous activity, KCNA regulates long term circadian rhythms. These results suggest that the specific repertoire of potassium channels in frontal regions can control the subtle dynamics of sustained and phasic activations subserving working memory, in relation with previous learning episodes. We thus expect a gradient of computational properties along the anatomo-functional gradients, from phasic activities in VSA to sustained activities in PTF, and with a larger set of fine timing regulations from the temporal to the frontal regions.

7.2.3.2 Model of generation of sustained activation for working memory by recurrent excitation due to temporal properties of NMDA receptors

A model of neural net with lateral connections between units containing excitatory synapses modeling the the dual conductance and timing properties of NMDA NR2B receptors, produces a persistent activation [277, 282, 281, 280]. This makes a prototypical model of sustained firing in the dorsolateral prefrontal cortex (dlPFC) from recurrent excitation (within layer III of the frontal networks). The slower kinetics of NR2B are optimal for prolonged network firing, and is consistent with the specific role of NR2B in generating persistent firing during working memory in the absence of sensory stimulation, depending upon prior experience in selective neuronal populations. Our results show a NR2B/NR2A gradient from PTF to VSA regions. NR2A is preferentially expressed in VSA, and so the NR2A/NR2B ratio is higher in VSA, while the NR2B/NR2A ratio is higher in PTF. The introduction of a NR2B/NR2A gradient in the model will produce more sustained recurrent activations along the gradient from motor to frontal regions, from occipital to temporal regions.

7.2.3.3 Model of transformation from short-term to long-term memory by the relation between CaMK autophosphorylation and actin polymerization

LTP triggers high-frequency calcium pulses that result in the activation of CaMKII which acts as a molecular switch because it remains active for a long time after the return to basal calcium levels. Models introducing calcium inflow due to NMDAR opening and the autophosphorylation of CaMKII function as a bistable switch capable of short-term and long-term memory [173, 172, 170]. The binding of CaMKII to the NMDAR may act as a tag to organize the binding of further proteins that produce the synapse enlargement that underlies late LTP [173, 172, 170]. This mechanism is thought to be critical in potentiation of synaptic transmission with variable durations, relating short-term and long term memories [173, 172, 170]. Our results show that different members of the CAMK families are distributed in different cortical regions along the VSA-PTF gradients such as CaMK2G in the VSA regions more related to sensorymotor interactions, and CaMK2D in the PTF regions, more related to episodic memory, recall and language. Previous results have shown that CaMK2 isoform composition differentially impacts the formation and maintenance of the actin cytoskeleton responsible of long term memory. The CaMK2D isoform produces tightly packed 3D actin bundles while in contrast the CaMK2G isoform produced loosely associated large sheet-like structures. These first type of memory storage could be well adapted to all-or-none long-lasting memories of events (in PTF), and the second type to memorize fine tuning of sensory-motor adaptation (in VSA). The model of CaMK autophosphorylation and actin polymerization could be modulated along VSA to PTF gradients with different memorization dynamics, going from fine tuning in the extreme visual and motor regions of VSA to all-or-none memory in the extreme regions of PTF in the parahippocampal regions. Language regions could then cumulate both properties.

7.2.3.4 Model of the relation between network construction and plasticity related to the tubulin dynamics

Computer models of microtubule dynamics have provided the basis for many of the theories on the cellular mechanics of the microtubules, their polymerization kinetics, and the diffusion of tubulin and Tau [33]. The effects of tau concentration and the hydrolysis of GTP-tubulin to GDP-tubulin produces microtubule dynamic instability. Previous results have confirmed the “multi-tubulin” hypothesis, which postulates that different tubulin isotypes (TUBA1A, TUBB2A, TUBB2B, TUBB3, and TUBB) alter the dynamic properties and functions of microtubules. Tubulin isotypes show intrinsic differences in the rates of microtubule assembly and the frequency of growth and shortening events, suggesting that cells can regulate microtubule dynamics by controlling the relative amounts of different tubulin isotypes. TUBB3 heterodimers are considerably more dynamic and spent less time in paused states than those composed of TUBB2 or TUBB4. Our results shows the highest expression of alpha and beta tubulin subunits, in extreme PTF (PHG, temporal pole) for a

subset of subunits, and in frontal regions for an other subset. These tubulin codes could be integrated in the model to modulate the dynamic instability along the gradient from VSA to PTF, and from temporal to frontal regions.

Bibliography

- [1]H. Abdi. “Bonferroni and Sidak corrections for multiple comparisons”. In: *Encyclopedia of Measurement and Statistics*. 2007, 103–107 (cit. on pp. 88, 92).
- [2]H. Abdi. “Discriminant correspondence analysis”. In: *Encyclopedia of Research Design*. 2007, 270–275 (cit. on pp. 86, 88, 113).
- [3]H. Abdi and M. Béra. “Correspondence Analysis”. In: *Encyclopedia of Social Network Analysis and Mining*. 2014, pp. 275–284 (cit. on pp. 86, 87).
- [4]H. Abdi and L. J. Williams. “Correspondence Analysis”. In: *Encyclopedia of Research Design*. 2010, pp. 267–278 (cit. on pp. 86, 87).
- [5]H. Abdi, J. P. Dunlop, and L. J. Williams. “How to compute reliability estimates and display confidence and tolerance intervals for pattern classifiers using the Bootstrap and 3-way multi-dimensional scaling (DISTATIS)”. In: *Neuroimage* 45.1 (2009), pp. 89–95 (cit. on p. 88).
- [6]H. Akil, M.E. Martone, and D.C. Van Essen. “Challenges and opportunities in mining neuroscience data”. In: *Science* 331.6018 (2011). cited By 64, pp. 708–712 (cit. on p. 173).
- [7]E. A. Alcamo, L. Chirivella, M. Dautzenberg, et al. “Satb2 regulates callosal projection neuron identity in the developing cerebral cortex”. In: *Neuron* 57.3 (2008), pp. 364–377 (cit. on p. 116).
- [8]P. D. Allen and J. R. Ison. “Kcna1 Gene Deletion Lowers the Behavioral Sensitivity of Mice to Small Changes in Sound Location and Increases Asynchronous Brainstem Auditory Evoked Potentials But Does Not Affect Hearing Thresholds”. In: *Journal of Neuroscience* 32.7 (2012), pp. 2538–2543 (cit. on pp. 100, 145).
- [9]T. K. Aman, T. M. Grieco-Calub, C. Chen, et al. “Regulation of persistent Na current by interactions between beta subunits of voltage-gated Na channels”. In: *J. Neurosci.* 29.7 (2009), pp. 2027–2042 (cit. on pp. 100, 145).
- [10]J. R. Andrews-Hanna, J. S. Reidler, C. Huang, and R. L. Buckner. “Evidence for the default network’s role in spontaneous cognition”. In: *J. Neurophysiol.* 104.1 (2010), pp. 322–335 (cit. on p. 39).
- [11]M. A. Arbib, ed. *The Handbook of Brain Theory and Neural Networks*. USA: A Bradford Book, 2002 (cit. on pp. 196, 197).
- [12]M. L. Bacceti. “Pacemaker Neurons and the Development of Nociception”. In: *Neuroscientist* 20.3 (2014), pp. 197–202 (cit. on pp. 100, 145).

- [13]D. Beaton, C. R. Chin Fatt, and H. Abdi. “An ExPosition of multivariate analysis with the singular value decomposition in R”. In: *Computational Statistics & Data Analysis* 72 (2014), pp. 176–189 (cit. on pp. 87–89, 113).
- [14]K.G. Becker, K.C. Barnes, T.J. Bright, and S.A. Wang. “The Genetic Association Database [1]”. In: *Nature Genetics* 36.5 (2004). cited By 372, pp. 431–432 (cit. on p. 173).
- [15]C. F. Beckmann and S. M. Smith. “Probabilistic independent component analysis for functional magnetic resonance imaging”. In: *IEEE Trans Med Imaging* 23.2 (2004), pp. 137–152 (cit. on p. 38).
- [16]C. F. Beckmann and S. M. Smith. “Tensorial extensions of independent component analysis for multisubject fMRI analysis”. In: *Neuroimage* 25.1 (2005), pp. 294–311 (cit. on pp. 25, 39).
- [17]P. Bellec, P. Rosa-Neto, O. C. Lyttelton, H. Benali, and A. C. Evans. “Multi-level bootstrap analysis of stable clusters in resting-state fMRI”. In: *Neuroimage* 51.3 (2010), pp. 1126–1139 (cit. on p. 38).
- [18]D. A. Benson, I. Karsch-Mizrachi, D. J. Lipman, J. Ostell, and D. L. Wheeler. “GenBank”. In: *Nucleic Acids Res.* 33.Database issue (2005), pp. D34–38 (cit. on p. 173).
- [19]J. R. Binder, R. H. Desai, W. W. Graves, and L. L. Conant. “Where is the semantic system? A critical review and meta-analysis of 120 functional neuroimaging studies”. In: *Cereb. Cortex* 19.12 (2009), pp. 2767–2796 (cit. on pp. 24, 25, 41, 85).
- [20]S. Bird, E. Klein, and E. Loper. *Natural language processing with Python*. Beijing Cambridge Mass: O’Reilly, 2009 (cit. on p. 75).
- [21]B. Biswal, F. Z. Yetkin, V. M. Haughton, and J. S. Hyde. “Functional connectivity in the motor cortex of resting human brain using echo-planar MRI”. In: *Magn Reson Med* 34.4 (1995), pp. 537–541 (cit. on pp. 24, 38).
- [22]B. B. Biswal, J. Van Kylen, and J. S. Hyde. “Simultaneous assessment of flow and BOLD signals in resting-state functional connectivity maps”. In: *NMR Biomed* 10.4-5 (1997), pp. 165–170 (cit. on p. 24).
- [23]T. Blumensath, S. Jbabdi, M.F. Glasser, et al. “Spatially constrained hierarchical parcellation of the brain with resting-state fMRI”. In: *NeuroImage* 76 (2013). cited By 29, pp. 313–324 (cit. on p. 172).
- [24]E. Bocksteins and D. J. Snyders. “Electrically silent Kv subunits: their molecular and functional characteristics”. In: *Physiology (Bethesda)* 27.2 (2012), pp. 73–84 (cit. on pp. 100, 145).
- [25]J. W. Bohland, H. Bokil, S. D. Pathak, et al. “Clustering of spatial gene expression patterns in the mouse brain and comparison with classical neuroanatomy”. In: *Methods* 50.2 (2010), pp. 105–112 (cit. on p. 83).
- [26]R. P. Bonin, A. A. Zurek, J. Yu, D. A. Bayliss, and B. A. Orser. “Hyperpolarization-activated current (In) is reduced in hippocampal neurons from *Gabra5*^{-/-} mice”. In: *PLoS ONE* 8.3 (2013), e58679 (cit. on p. 149).
- [27]J. Braudeau, L. Dauphinot, A. Duchon, et al. “Chronic Treatment with a Promnesiant GABA-A $\hat{\pm}$ 5-Selective Inverse Agonist Increases Immediate Early Genes Expression during Memory Processing in Mice and Rectifies Their Expression Levels in a Down Syndrome Mouse Model”. In: *Adv Pharmacol Sci* 2011 (2011), p. 153218 (cit. on p. 150).

- [28]R. L. Buckner and D. C. Carroll. “Self-projection and the brain”. In: *Trends Cogn. Sci. (Regul. Ed.)* 11.2 (2007), pp. 49–57 (cit. on p. 41).
- [29]R. L. Buckner and F. M. Krienen. “The evolution of distributed association networks in the human brain”. In: *Trends Cogn. Sci. (Regul. Ed.)* 17.12 (2013), pp. 648–665 (cit. on p. 166).
- [30]R. L. Buckner, J. Sepulcre, T. Talukdar, et al. “Cortical hubs revealed by intrinsic functional connectivity: mapping, assessment of stability, and relation to Alzheimer’s disease”. In: *J. Neurosci.* 29.6 (2009), pp. 1860–1873 (cit. on pp. 24, 39, 41).
- [31]R. L. Buckner, J. R. Andrews-Hanna, and D. L. Schacter. “The brain’s default network: anatomy, function, and relevance to disease”. In: *Ann. N. Y. Acad. Sci.* 1124 (2008), pp. 1–38 (cit. on pp. 24, 25, 39, 41, 85).
- [32]Y. Burnod, P. Baraduc, A. Battaglia-Mayer, et al. “Parieto-frontal coding of reaching: an integrated framework”. In: *Exp Brain Res* 129.3 (1999), pp. 325–346 (cit. on p. 62).
- [33]G. A. Buxton, S. L. Siedlak, G. Perry, and M. A. Smith. “Mathematical modeling of microtubule dynamics: insights into physiology and disease”. In: *Prog. Neurobiol.* 92.4 (2010), pp. 478–483 (cit. on pp. 196, 198).
- [34]A. de Calignon, M. Polydoro, M. Suarez-Calvet, et al. “Propagation of tau pathology in a model of early Alzheimer’s disease”. In: *Neuron* 73.4 (2012), pp. 685–697 (cit. on p. 193).
- [35]P. Cao, X. Yang, and T. C. Sudhof. “Complexin activates exocytosis of distinct secretory vesicles controlled by different synaptotagmins”. In: *J. Neurosci.* 33.4 (2013), pp. 1714–1727 (cit. on pp. 102, 147).
- [36]V. B. Caraiscos, E. M. Elliott, K. E. You-Ten, et al. “Tonic inhibition in mouse hippocampal CA1 pyramidal neurons is mediated by alpha5 subunit-containing gamma-aminobutyric acid type A receptors”. In: *Proc. Natl. Acad. Sci. U.S.A.* 101.10 (2004), pp. 3662–3667 (cit. on p. 149).
- [37]M. Catani and M. Thiebaut de Schotten. “A diffusion tensor imaging tractography atlas for virtual in vivo dissections”. In: *Cortex* 44.8 (2008), pp. 1105–1132 (cit. on p. 39).
- [38]M. Catani, M. Thiebaut de Schotten, D. Slater, and F. Dell’Acqua. “Connectomic approaches before the connectome”. In: *NeuroImage* 80 (2013). cited By 16, pp. 2–13 (cit. on p. 172).
- [39]W. A. Catterall. “Structure and function of voltage-gated sodium channels at atomic resolution”. In: *Exp. Physiol.* 99.1 (2014), pp. 35–51 (cit. on pp. 100, 111, 145).
- [40]W. A. Catterall and A. P. Few. “Calcium channel regulation and presynaptic plasticity”. In: *Neuron* 59.6 (2008), pp. 882–901 (cit. on pp. 101, 111, 146).
- [41]F. Cauda, G. C. Geminiani, and A. Vercelli. “Evolutionary appearance of von Economo’s neurons in the mammalian cerebral cortex”. In: *Front Hum Neurosci* 8 (2014), p. 104 (cit. on p. 84).
- [42]F. Cauda, S. Palermo, T. Costa, et al. “Gray matter alterations in chronic pain: A network-oriented meta-analytic approach”. In: *Neuroimage Clin* 4 (2014), pp. 676–686 (cit. on p. 84).
- [43]G. Y. Cederquist, A. Luchniak, M. A. Tischfield, et al. “An inherited TUBB2B mutation alters a kinesin-binding site and causes polymicrogyria, CFEOM and axon dysinnervation”. In: *Hum. Mol. Genet.* 21.26 (2012), pp. 5484–5499 (cit. on p. 154).
- [44]C. Chang and G. H. Glover. “Time-frequency dynamics of resting-state brain connectivity measured with fMRI”. In: *Neuroimage* 50.1 (2010), pp. 81–98 (cit. on p. 40).

- [45]W. S. Chen and M. F. Bear. “Activity-dependent regulation of NR2B translation contributes to metaplasticity in mouse visual cortex”. In: *Neuropharmacology* 52.1 (2007), pp. 200–214 (cit. on p. 148).
- [46]E. Cheong and H. S. Shin. “T-type Ca²⁺ channels in normal and abnormal brain functions”. In: *Physiol. Rev.* 93.3 (2013), pp. 961–992 (cit. on pp. 101, 146).
- [47]C. Chung and J. Raingo. “Vesicle dynamics: how synaptic proteins regulate different modes of neurotransmission”. In: *J. Neurochem.* 126.2 (2013), pp. 146–154 (cit. on pp. 101, 111, 146).
- [48]C. Cioli, H. Abdi, D. Beaton, Y. Burnod, and S. Mesmoudi. “Mechanisms of CaMKII action in long-term potentiation”. In: *PLoS One* 9.12 (2014), e115913 (cit. on pp. 110, 140).
- [49]J. P. Cointet and D. Chavalarias. “Multi-level Science mapping with asymmetric co-occurrence analysis: Methodology and case study”. In: *Netw. Heterog. Media* 3.2 (2008), pp. 267–276 (cit. on p. 75).
- [50]C. Colantuoni, B. K. Lipska, T. Ye, et al. “Temporal dynamics and genetic control of transcription in the human prefrontal cortex”. In: *Nature* 478.7370 (2011), pp. 519–23 (cit. on p. 7).
- [51]P. J. Colombo, W. C. Wetsel, and M. Gallagher. “Spatial memory is related to hippocampal subcellular concentrations of calcium-dependent protein kinase C isoforms in young and aged rats”. In: *Proc. Natl. Acad. Sci. U.S.A.* 94.25 (1997), pp. 14195–14199 (cit. on p. 153).
- [52]K. E. Cosgrove, E. J. Galvan, G. Barrionuevo, and S.D. Meriney. “mGluRs modulate strength and timing of excitatory transmission in hippocampal area CA3”. In: *Mol Neurobiol.* 44.1 (2011), pp. 93–101 (cit. on p. 149).
- [53]V. Cuccioli, C. Bueno, R. Belvindrah, P. M. Lledo, and S. Martinez. “Attractive action of FGF-signaling contributes to the postnatal developing hippocampus”. In: *Hippocampus* 25.4 (2015), pp. 486–499 (cit. on pp. 112, 155).
- [54]Z. Cui, R. Feng, S. Jacobs, et al. “Increased NR2A:NR2B ratio compresses long-term depression range and constrains long-term memory”. In: *Sci Rep* 3 (2013), p. 1036 (cit. on p. 148).
- [55]T. R. Cummins, F. Aglieco, M. Renganathan, et al. “Nav1.3 sodium channels: rapid repriming and slow closed-state inactivation display quantitative differences after expression in a mammalian cell line and in spinal sensory neurons”. In: *J. Neurosci.* 21.16 (2001), pp. 5952–5961 (cit. on pp. 100, 145).
- [56]F. S. Cusdin, D. Nietlispach, J. Maman, et al. “The sodium channel beta3-subunit induces multiphasic gating in NaV1.3 and affects fast inactivation via distinct intracellular regions”. In: *J. Biol. Chem.* 285.43 (2010), pp. 33404–33412 (cit. on pp. 100, 145).
- [57]T. D. Cushion, A. R. Paciorkowski, D. T. Pilz, et al. “De novo mutations in the beta-tubulin gene TUBB2A cause simplified gyral patterning and infantile-onset epilepsy”. In: *Am. J. Hum. Genet.* 94.4 (2014), pp. 634–641 (cit. on p. 154).
- [58]A. Dabrowski, A. Terauchi, C. Strong, and H. Umemori. “Distinct sets of FGF receptors sculpt excitatory and inhibitory synaptogenesis”. In: *Development* 142.10 (2015), pp. 1818–1830 (cit. on pp. 112, 155).
- [59]J. S. Damoiseaux, S. A. Rombouts, F. Barkhof, et al. “Consistent resting-state networks across healthy subjects”. In: *Proc. Natl. Acad. Sci. U.S.A.* 103.37 (2006), pp. 13848–13853 (cit. on pp. 25, 38, 39).

- [60]O. David, I. Barrera, A. Chinnakkaruppan, et al. “Dopamine-induced tyrosine phosphorylation of NR2B (Tyr1472) is essential for ERK1/2 activation and processing of novel taste information”. In: *Front Mol Neurosci* 7 (2014), p. 66 (cit. on p. 148).
- [61]R. J. Davidson, G. E. Schwartz, and D. Shapiro, eds. *Consciousness and Self-Regulation*. Springer US, 1986 (cit. on p. 41).
- [62]P. De Koninck and H. Schulman. “Sensitivity of CaM kinase II to the frequency of Ca²⁺ oscillations”. In: *Science* 279.5348 (1998), pp. 227–230 (cit. on p. 150).
- [63]M. De Luca, C. F. Beckmann, N. De Stefano, P. M. Matthews, and S. M. Smith. “fMRI resting state networks define distinct modes of long-distance interactions in the human brain”. In: *Neuroimage* 29.4 (2006), pp. 1359–1367 (cit. on pp. 25, 38, 39).
- [64]J. Decety and J. A. Sommerville. “Shared representations between self and other: a social cognitive neuroscience view”. In: *Trends Cogn. Sci. (Regul. Ed.)* 7.12 (2003), pp. 527–533 (cit. on p. 41).
- [65]P. Devanna, J. Middelbeek, and S. C. Vernes. “FOXP2 drives neuronal differentiation by interacting with retinoic acid signaling pathways”. In: *Front Cell Neurosci* 8 (2014), p. 305 (cit. on p. 156).
- [66]E. W. Dickie, A. Tahmasebi, L. French, et al. “Global genetic variations predict brain response to faces”. In: *PLoS Genet.* 10.8 (2014), e1004523 (cit. on p. 5).
- [67]F. C. Doherty and C. D. Sladek. “NMDA receptor subunit expression in the supraoptic nucleus of adult rats: dominance of NR2B and NR2D”. In: *Brain Res.* 1388 (2011), pp. 89–99 (cit. on p. 148).
- [68]G. Domes, M. Heinrichs, J. Gläscher, et al. “Oxytocin Attenuates Amygdala Responses to Emotional Faces Regardless of Valence”. In: *Biological Psychiatry* 62.10 (2007). cited By 309, pp. 1187–1190 (cit. on p. 181).
- [69]C. Dong, D. W. Godwin, P. A. Brennan, and A. N. Hegde. “Protein kinase Calpha mediates a novel form of plasticity in the accessory olfactory bulb”. In: *Neuroscience* 163.3 (2009), pp. 811–824 (cit. on p. 153).
- [70]V. Doria, C. F. Beckmann, T. Arichi, et al. “Emergence of resting state networks in the preterm human brain”. In: *Proc. Natl. Acad. Sci. U.S.A.* 107.46 (2010), pp. 20015–20020 (cit. on p. 42).
- [71]N. U. Dosenbach, D. A. Fair, F. M. Miezin, et al. “Distinct brain networks for adaptive and stable task control in humans”. In: *Proc. Natl. Acad. Sci. U.S.A.* 104.26 (2007), pp. 11073–11078 (cit. on pp. 38, 39).
- [72]G. Doucet, M. Naveau, L. Petit, et al. “Brain activity at rest: a multiscale hierarchical functional organization”. In: *J. Neurophysiol.* 105.6 (2011), pp. 2753–2763 (cit. on pp. 24, 25, 39, 84, 99).
- [73]C. Duyckaerts, B. Delatour, and M. C. Potier. “Classification and basic pathology of Alzheimer disease”. In: *Acta Neuropathol.* 118.1 (2009), pp. 5–36 (cit. on pp. 3, 193).
- [74]N. J. van Eck and L. Waltman. *Text mining and visualization using VOSviewer*. 2011. eprint: [arXiv:1109.2058](https://arxiv.org/abs/1109.2058) (cit. on p. 76).
- [75]S. Edvardson, S. Oz, F. A. Abulhijaa, et al. “Early infantile epileptic encephalopathy associated with a high voltage gated calcium channelopathy”. In: *J. Med. Genet.* 50.2 (2013), pp. 118–123 (cit. on pp. 101, 146).

- [76]R. D. Emes and S. G. N. Grant. “Evolution of Synapse Complexity and Diversity”. In: *Annual Review of Neuroscience* 35.1 (2012), pp. 111–131 (cit. on pp. 142, 165, 166).
- [77]M. Estacion, A. Gasser, S. D. Dib-Hajj, and S. G. Waxman. “A sodium channel mutation linked to epilepsy increases ramp and persistent current of Nav1.3 and induces hyperexcitability in hippocampal neurons”. In: *Exp. Neurol.* 224.2 (2010), pp. 362–368 (cit. on pp. 100, 145).
- [78]A.C. Evans, D.L. Collins, S.R. Mills, et al. “3D statistical neuroanatomical models from 305 MRI volumes”. In: *1993 IEEE Conference Record Nuclear Science Symposium and Medical Imaging Conference*. IEEE, 1993 (cit. on pp. 87, 174, 176).
- [79]D. A. Fair, N. U. Dosenbach, J. A. Church, et al. “Development of distinct control networks through segregation and integration”. In: *Proc. Natl. Acad. Sci. U.S.A.* 104.33 (2007), pp. 13507–13512 (cit. on p. 42).
- [80]D. A. Fair, A. L. Cohen, J. D. Power, et al. “Functional brain networks develop from a “local to distributed” organization”. In: *PLoS Comput. Biol.* 5.5 (2009), e1000381 (cit. on p. 42).
- [81]D. A. Fair, A. L. Cohen, N. U. Dosenbach, et al. “The maturing architecture of the brain’s default network”. In: *Proc. Natl. Acad. Sci. U.S.A.* 105.10 (2008), pp. 4028–4032 (cit. on p. 42).
- [82]N. Federman, V. de la Fuente, G. Zalzman, et al. “Nuclear factor $\hat{\text{I}}^{\text{B}}$ -dependent histone acetylation is specifically involved in persistent forms of memory”. In: *J. Neurosci.* 33.17 (2013), pp. 7603–7614 (cit. on p. 151).
- [83]E. C. Ferstl and D. Y. von Cramon. “Time, space and emotion: fMRI reveals content-specific activation during text comprehension”. In: *Neurosci. Lett.* 427.3 (2007), pp. 159–164 (cit. on p. 42).
- [84]A. S. Fox, L. J. Chang, K. J. Gorgolewski, and T. Yarkoni. “Bridging psychology and genetics using large-scale spatial analysis of neuroimaging and neurogenetic data”. In: *bioRxiv* (2014) (cit. on p. 8).
- [85]M. D. Fox, M. Corbetta, A. Z. Snyder, J. L. Vincent, and M. E. Raichle. “Spontaneous neuronal activity distinguishes human dorsal and ventral attention systems”. In: *Proc. Natl. Acad. Sci. U.S.A.* 103.26 (2006), pp. 10046–10051 (cit. on pp. 25, 38, 39, 83, 99, 110).
- [86]M. D. Fox, A. Z. Snyder, J. L. Vincent, et al. “The human brain is intrinsically organized into dynamic, anticorrelated functional networks”. In: *Proc. Natl. Acad. Sci. U.S.A.* 102.27 (2005), pp. 9673–9678 (cit. on pp. 24, 39, 172).
- [87]P. Fransson, B. Skiold, S. Horsch, et al. “Resting-state networks in the infant brain”. In: *Proc. Natl. Acad. Sci. U.S.A.* 104.39 (2007), pp. 15531–15536 (cit. on p. 42).
- [88]K. Frantzi, S. Ananiadou, and H. Mima. “Automatic recognition of multi-word terms: the C-value/NC-value method”. In: *International Journal on Digital Libraries* 3.2 (2000), pp. 115–130 (cit. on pp. 76, 175).
- [89]L. French and P. Pavlidis. “Relationships between gene expression and brain wiring in the adult rodent brain”. In: *PLoS Comput. Biol.* 7.1 (2011), e1001049 (cit. on p. 83).
- [90]L. French, P. P. Tan, and P. Pavlidis. “Large-Scale Analysis of Gene Expression and Connectivity in the Rodent Brain: Insights through Data Integration”. In: *Front Neuroinform* 5 (2011), p. 12 (cit. on p. 83).

- [91]D. R. Friedland, R. Eernisse, and P. Popper. “Identification of a novel Vamp1 splice variant in the cochlear nucleus”. In: *Hear. Res.* 243.1-2 (2008), pp. 105–112 (cit. on pp. 102, 147).
- [92]J. M. Fuster. “The cognit: a network model of cortical representation”. In: *Int J Psychophysiol* 60.2 (2006), pp. 125–132 (cit. on pp. 41, 85).
- [93]J. M. Fuster. *The Prefrontal Cortex: Anatomy, Physiology, and Neuropsychology of the Frontal Lobe*. Raven Press, 1989 (cit. on pp. 41, 85).
- [94]J. M. Fuster and S. L. Bressler. “Cognit activation: a mechanism enabling temporal integration in working memory”. In: *Trends Cogn. Sci. (Regul. Ed.)* 16.4 (2012), pp. 207–218 (cit. on pp. 41, 85).
- [95]H. L. Gallagher and C. D. Frith. “Functional imaging of ‘theory of mind’”. In: *Trends Cogn. Sci. (Regul. Ed.)* 7.2 (2003), pp. 77–83 (cit. on p. 41).
- [96]A. C. Gambrell and A. Barria. “NMDA receptor subunit composition controls synaptogenesis and synapse stabilization”. In: *Proc. Natl. Acad. Sci. U.S.A.* 108.14 (2011), pp. 5855–5860 (cit. on pp. 111, 147, 148).
- [97]D. H. Geschwind and P. Rakic. “Cortical evolution: judge the brain by its cover”. In: *Neuron* 80.3 (2013), pp. 633–647 (cit. on p. 141).
- [98]J. X. Gittelman and B. L. Tempel. “Kv1.1-containing channels are critical for temporal precision during spike initiation”. In: *J. Neurophysiol.* 96.3 (2006), pp. 1203–1214 (cit. on pp. 100, 145).
- [99]D.C. Glahn, A.M. Winkler, P. Kochunov, et al. “Genetic control over the resting brain”. In: *Proceedings of the National Academy of Sciences of the United States of America* 107.3 (2010). cited By 121, pp. 1223–1228 (cit. on p. 172).
- [100]G. V. Glass. “Primary, Secondary, and Meta-Analysis of Research”. In: *Educ. Res.* 5.10 (1976), pp. 3–8 (cit. on p. 55).
- [101]P. Goel, A. Kuceyeski, E. LoCastro, and A. Raj. “Spatial patterns of genome-wide expression profiles reflect anatomic and fiber connectivity architecture of healthy human brain”. In: *Hum Brain Mapp* 35.8 (2014), pp. 4204–4218 (cit. on pp. 5, 84).
- [102]Y. Golland, S. Bentin, H. Gelbard, et al. “Extrinsic and intrinsic systems in the posterior cortex of the human brain revealed during natural sensory stimulation”. In: *Cereb. Cortex* 17.4 (2007), pp. 766–777 (cit. on p. 42).
- [103]H. Goto, K. Watanabe, N. Araragi, et al. “The identification and functional implications of human-specific “fixed” amino acid substitutions in the glutamate receptor family”. In: *BMC Evol. Biol.* 9 (2009), p. 224 (cit. on p. 149).
- [104]M. S. Goyal, M. Hawrylycz, J. A. Miller, A. Z. Snyder, and M. E. Raichle. “Aerobic glycolysis in the human brain is associated with development and neotenus gene expression”. In: *Cell Metab.* 19.1 (2014), pp. 49–57 (cit. on pp. 83, 110).
- [105]D. Granados-Fuentes, A. J. Norris, Y. Carrasquillo, J. M. Nerbonne, and E. D. Herzog. “I(A) channels encoded by Kv1.4 and Kv4.2 regulate neuronal firing in the suprachiasmatic nucleus and circadian rhythms in locomotor activity”. In: *J. Neurosci.* 32.29 (2012), pp. 10045–10052 (cit. on pp. 100, 145).
- [106]P. Grange, J. W. Bohland, B. W. Okaty, et al. “Cell-type-based model explaining coexpression patterns of genes in the brain”. In: *Proc. Natl. Acad. Sci. U.S.A.* 111.14 (2014), pp. 5397–5402 (cit. on pp. 83, 172).

- [107]Pascal Grange and Partha P. Mitra. *Statistical analysis of co-expression properties of sets of genes in the mouse brain*. 2011. eprint: [arXiv:1111.6200](https://arxiv.org/abs/1111.6200) (cit. on p. 83).
- [108]Michael Greenacre. *Theory and applications of correspondence analysis*. London Orlando, Fla: Academic Press, 1984 (cit. on pp. 86, 87).
- [109]M. D. Greicius, G. Srivastava, A. L. Reiss, and V. Menon. “Default-mode network activity distinguishes Alzheimer’s disease from healthy aging: evidence from functional MRI”. In: *Proc. Natl. Acad. Sci. U.S.A.* 101.13 (2004), pp. 4637–4642 (cit. on pp. 25, 39).
- [110]M. D. Greicius, B. Krasnow, A. L. Reiss, and V. Menon. “Functional connectivity in the resting brain: a network analysis of the default mode hypothesis”. In: *Proc. Natl. Acad. Sci. U.S.A.* 100.1 (2003), pp. 253–258 (cit. on pp. 25, 38, 39).
- [111]C. Grillon, M. Krimsky, D.R. Charney, et al. “Oxytocin increases anxiety to unpredictable threat”. In: *Molecular Psychiatry* 18.9 (2013). cited By 28, pp. 958–960 (cit. on p. 181).
- [112]D. A. Gusnard and M. E. Raichle. “Searching for a baseline: functional imaging and the resting human brain”. In: *Nat. Rev. Neurosci.* 2.10 (2001), pp. 685–694 (cit. on pp. 39, 41, 85).
- [113]A. R. Halt, R. F. Dallapiazza, Y. Zhou, et al. “CaMKII binding to GluN2B is critical during memory consolidation”. In: *EMBO J.* 31.5 (2012), pp. 1203–1216 (cit. on p. 148).
- [114]N. C. Harata, A. M. Aravanis, and R. W. Tsien. “Kiss-and-run and full-collapse fusion as modes of exo-endocytosis in neurosecretion”. In: *J. Neurochem.* 97.6 (2006), pp. 1546–1570 (cit. on pp. 101, 146).
- [115]L. Harris, A. Olson, and G. Humphreys. “The link between STM and sentence comprehension: a neuropsychological rehabilitation study”. In: *Neuropsychol Rehabil* 24.5 (2014), pp. 678–720 (cit. on p. 182).
- [116]M. D. Hauser, C. Yang, R. C. Berwick, et al. “The mystery of language evolution”. In: *Front Psychol* 5 (2014), p. 401 (cit. on p. 141).
- [117]M. J. Hawrylycz, E. S. Lein, A. L. Guillozet-Bongaarts, et al. “An anatomically comprehensive atlas of the adult human brain transcriptome”. In: *Nature* 489.7416 (2012), pp. 391–399 (cit. on pp. 5, 8, 9, 83, 84, 86, 87, 89, 99, 110, 142, 172, 174).
- [118]Maile A. Henson, Rylan S. Larsen, Shelikha N. Lawson, et al. “Genetic Deletion of NR3A Accelerates Glutamatergic Synapse Maturation”. In: *PLoS ONE* 7.8 (2012), e42327 (cit. on p. 149).
- [119]R. E. Hernandez, A. P. Putzke, J. P. Myers, L. Margaretha, and C. B. Moens. “Cyp26 enzymes generate the retinoic acid response pattern necessary for hindbrain development”. In: *Development* 134.1 (2007), pp. 177–187 (cit. on p. 156).
- [120]D. P. Hibar, J. L. Stein, M. E. Renteria, et al. “Common genetic variants influence human subcortical brain structures”. In: *Nature* 520.7546 (2015), pp. 224–229 (cit. on p. 4).
- [121]J. Hill, T. Inder, J. Neil, et al. “Similar patterns of cortical expansion during human development and evolution”. In: *Proc. Natl. Acad. Sci. U.S.A.* 107.29 (2010), pp. 13135–13140 (cit. on pp. 42, 43).
- [122]H. S. Hoe, J. Y. Lee, and D. T. Pak. “Combinatorial morphogenesis of dendritic spines and filopodia by SPAR and alpha-actinin2”. In: *Biochem. Biophys. Res. Commun.* 384.1 (2009), pp. 55–60 (cit. on p. 153).

- [123]L. Hoffman, M. M. Farley, and M. N. Waxham. “Calcium-calmodulin-dependent protein kinase II isoforms differentially impact the dynamics and structure of the actin cytoskeleton”. In: *Biochemistry* 52.7 (2013), pp. 1198–1207 (cit. on p. 151).
- [124]C. J. Honey, O. Sporns, L. Cammoun, et al. “Predicting human resting-state functional connectivity from structural connectivity”. In: *Proc. Natl. Acad. Sci. U.S.A.* 106.6 (2009), pp. 2035–2040 (cit. on p. 39).
- [125]M. B. Hoppa, B. Lana, W. Margas, A. C. Dolphin, and T. A. Ryan. “ $\hat{I}\pm 2\hat{I}$ ’ expression sets presynaptic calcium channel abundance and release probability”. In: *Nature* 486.7401 (2012), pp. 122–125 (cit. on pp. 101, 146).
- [126]P. Hotulainen and C. C. Hoogenraad. “Actin in dendritic spines: connecting dynamics to function”. In: *J. Cell Biol.* 189.4 (2010), pp. 619–629 (cit. on pp. 111, 153).
- [127]M. Hruska and M. B. Dalva. “Ephrin regulation of synapse formation, function and plasticity”. In: *Mol. Cell. Neurosci.* 50.1 (2012), pp. 35–44 (cit. on p. 155).
- [128]R. Hurlemann, A. Patin, O.A. Onur, et al. “Oxytocin enhances amygdala-dependent, socially reinforced learning and emotional empathy in humans”. In: *Journal of Neuroscience* 30.14 (2010). cited By 202, pp. 4999–5007 (cit. on p. 181).
- [129]R. M. Hutchison, J. P. Gallivan, J. C. Culham, et al. “Functional connectivity of the frontal eye fields in humans and macaque monkeys investigated with resting-state fMRI”. In: *J. Neurophysiol.* 107.9 (2012), pp. 2463–2474 (cit. on p. 43).
- [130]J. R. Ison and P. D. Allen. “Deficits in responding to brief noise offsets in *Kcna1 -/-* mice reveal a contribution of this gene to precise temporal processing seen previously only for stimulus onsets”. In: *J. Assoc. Res. Otolaryngol.* 13.3 (2012), pp. 351–358 (cit. on pp. 100, 145).
- [131]S. A. Jacobs and J. Z. Tsien. “Overexpression of the NR2A subunit in the forebrain impairs long-term social recognition and non-social olfactory memory”. In: *Genes Brain Behav.* 13.4 (2014), pp. 376–384 (cit. on p. 148).
- [132]N. Jalan-Sakrikar, R. K. Bartlett, A. J. Baucum, and R. J. Colbran. “Substrate-selective and calcium-independent activation of CaMKII by $\hat{I}\pm$ -actinin”. In: *J. Biol. Chem.* 287.19 (2012), pp. 15275–15283 (cit. on p. 153).
- [133]A. R. Jones, C. C. Overly, and S. M. Sunkin. “The Allen Brain Atlas: 5 years and beyond”. In: *Nat. Rev. Neurosci.* 10.11 (2009), pp. 821–828 (cit. on pp. 86, 87, 99, 112, 173–176).
- [134]R. A. Jorquera, S. Huntwork-Rodriguez, Y. Akbergenova, R. W. Cho, and J. T. Littleton. “Complexin controls spontaneous and evoked neurotransmitter release by regulating the timing and properties of synaptotagmin activity”. In: *J. Neurosci.* 32.50 (2012), pp. 18234–18245 (cit. on pp. 102, 147).
- [135]M. C. Judson, K. L. Eagleson, and P. Levitt. “A new synaptic player leading to autism risk: Met receptor tyrosine kinase”. In: *J Neurodev Disord* 3.3 (2011), pp. 282–292 (cit. on p. 156).
- [136]M. C. Judson, K. L. Eagleson, L. Wang, and P. Levitt. “Evidence of cell-nonautonomous changes in dendrite and dendritic spine morphology in the met-signaling-deficient mouse forebrain”. In: *J. Comp. Neurol.* 518.21 (2010), pp. 4463–4478 (cit. on p. 156).
- [137]H. Kadavath, M. Jaremko, ?. Jaremko, et al. “Folding of the Tau Protein on Microtubules”. In: *Angew. Chem. Int. Ed. Engl.* (2015) (cit. on p. 193).

- [138]H. Kadavath, R. V. Hofele, J. Biernat, et al. “Tau stabilizes microtubules by binding at the interface between tubulin heterodimers”. In: *Proc. Natl. Acad. Sci. U.S.A.* 112.24 (2015), pp. 7501–7506 (cit. on p. 193).
- [139]Y. J. Kaeser-Woo, X. Yang, and T. C. Sudhof. “C-Terminal Complexin Sequence Is Selectively Required for Clamping and Priming But Not for Ca²⁺ Triggering of Synaptic Exocytosis”. In: *Journal of Neuroscience* 32.8 (2012), pp. 2877–2885 (cit. on pp. 102, 147).
- [140]K. Kageura and B. Umino. “Methods of automatic term recognition: A review”. In: *Terminology* 3.2 (1996), pp. 259–289 (cit. on pp. 75, 175).
- [141]M. Kalinowska, A. E. Chavez, S. Lutz, et al. “Actinin-4 Governs Dendritic Spine Dynamics and Promotes Their Remodeling by Metabotropic Glutamate Receptors”. In: *J. Biol. Chem.* 290.26 (2015), pp. 15909–15920 (cit. on p. 153).
- [142]H. J. Kang, Y. I. Kawasaki, F. Cheng, et al. “Spatio-temporal transcriptome of the human brain”. In: *Nature* 478.7370 (2011), pp. 483–489 (cit. on p. 7).
- [143]A. Karcz, M. H. Hennig, C. A. Robbins, et al. “Low-voltage activated Kv1.1 subunits are crucial for the processing of sound source location in the lateral superior olive in mice”. In: *J. Physiol. (Lond.)* 589.Pt 5 (2011), pp. 1143–1157 (cit. on pp. 100, 145).
- [144]L. A. Kehoe, C. Bellone, M. De Roo, et al. “GluN3A promotes dendritic spine pruning and destabilization during postnatal development”. In: *J. Neurosci.* 34.28 (2014), pp. 9213–9221 (cit. on p. 149).
- [145]A. M. Kelly, A. Di Martino, L. Q. Uddin, et al. “Development of anterior cingulate functional connectivity from late childhood to early adulthood”. In: *Cereb. Cortex* 19.3 (2009), pp. 640–657 (cit. on p. 42).
- [146]C. Kelly, L. Q. Uddin, Z. Shehzad, et al. “Broca’s region: linking human brain functional connectivity data and non-human primate tracing anatomy studies”. In: *Eur. J. Neurosci.* 32.3 (2010), pp. 383–398 (cit. on pp. 39, 43).
- [147]B. S. Khundrakpam, A. Reid, J. Brauer, et al. “Developmental changes in organization of structural brain networks”. In: *Cereb. Cortex* 23.9 (2013), pp. 2072–2085 (cit. on p. 142).
- [148]S. J. Kiebel, J. Daunizeau, and K. J. Friston. “A hierarchy of time-scales and the brain”. In: *PLoS Comput. Biol.* 4.11 (2008), e1000209 (cit. on pp. 85, 99).
- [149]V. Kiviniemi, T. Vire, J. Remes, et al. “A sliding time-window ICA reveals spatial variability of the default mode network in time”. In: *Brain Connect* 1.4 (2011), pp. 339–347 (cit. on p. 40).
- [150]Olexiy Kochubey and Ralf Schneggenburger. “Synaptotagmin Increases the Dynamic Range of Synapses by Driving Ca²⁺-Evoked Release and by Clamping a Near-Linear Remaining Ca²⁺ Sensor”. In: *Neuron* 69.4 (2011), pp. 736–748 (cit. on pp. 101, 146).
- [151]C. K. Kovach, N. D. Daw, D. Rudrauf, et al. “Anterior prefrontal cortex contributes to action selection through tracking of recent reward trends”. In: *J. Neurosci.* 32.25 (2012), pp. 8434–8442 (cit. on p. 41).
- [152]J. W. Kramer, M. A. Post, A. M. Brown, and G. E. Kirsch. “Modulation of potassium channel gating by coexpression of Kv2.1 with regulatory Kv5.1 or Kv6.1 alpha-subunits”. In: *Am. J. Physiol.* 274.6 Pt 1 (1998), pp. C1501–1510 (cit. on pp. 100, 145).
- [153]D. J. Kravitz, K. S. Saleem, C. I. Baker, and M. Mishkin. “A new neural framework for visuospatial processing”. In: *Nat. Rev. Neurosci.* 12.4 (2011), pp. 217–230 (cit. on p. 42).

- [154]A. Krishnan, L. J. Williams, A. R. McIntosh, and H. Abdi. “Partial Least Squares (PLS) methods for neuroimaging: a tutorial and review”. In: *Neuroimage* 56.2 (2011), pp. 455–475 (cit. on p. 88).
- [155]L. Lacinova and N. Klugbauer. “Modulation of gating currents of the Ca(v)3.1 calcium channel by alpha 2 delta 2 and gamma 5 subunits”. In: *Arch. Biochem. Biophys.* 425.2 (2004), pp. 207–213 (cit. on pp. 101, 146).
- [156]A. R. Laird, P. M. Fox, S. B. Eickhoff, et al. “Behavioral interpretations of intrinsic connectivity networks”. In: *J Cogn Neurosci* 23.12 (2011), pp. 4022–4037 (cit. on pp. 24, 25, 28, 29, 38, 40, 41, 45, 83–85, 99, 110, 115, 172, 182).
- [157]A. R. Laird, J. L. Lancaster, and P. T. Fox. “BrainMap: the social evolution of a human brain mapping database”. In: *Neuroinformatics* 3.1 (2005), pp. 65–78 (cit. on pp. 6, 9, 172).
- [158]A. Lak, W.R. Stauffer, and W. Schultz. “Dopamine prediction error responses integrate subjective value from different reward dimensions”. In: *Proceedings of the National Academy of Sciences of the United States of America* 111.6 (2014). cited By 17, pp. 2343–2348 (cit. on p. 181).
- [159]J.L. Lancaster, M.G. Woldorff, L.M. Parsons, et al. “Automated Talairach Atlas labels for functional brain mapping”. In: *Human Brain Mapping* 10.3 (2000). cited By 1755, pp. 120–131 (cit. on pp. 174, 176).
- [160]L. Lanfumey and M. Hamon. “5-HT1 receptors”. In: *Curr Drug Targets CNS Neurol Disord* 3.1 (2004), pp. 1–10 (cit. on p. 150).
- [161]P. Latouche, E. Birmele, and C. Ambroise. “Variational Bayesian inference and complexity control for stochastic block models”. In: *Statistical Modelling* 12.1 (2012), pp. 93–115 (cit. on pp. 37, 44, 45).
- [162]M. H. Lee, C. D. Hacker, A. Z. Snyder, et al. “Clustering of resting state networks”. In: *PLoS ONE* 7.7 (2012), e40370 (cit. on pp. 25, 39).
- [163]J. Lemay-Clermont, C. Robitaille, Y. P. Auberson, G. Bureau, and M. Cyr. “Blockade of NMDA receptors 2A subunit in the dorsal striatum impairs the learning of a complex motor skill”. In: *Behav. Neurosci.* 125.5 (2011), pp. 714–723 (cit. on p. 149).
- [164]Y. Leng, Z. Wang, L. K. Tsai, et al. “FGF-21, a novel metabolic regulator, has a robust neuroprotective role and is markedly elevated in neurons by mood stabilizers”. In: *Mol. Psychiatry* 20.2 (2015), pp. 215–223 (cit. on p. 155).
- [165]D. P. Leone, K. Srinivasan, B. Chen, E. Alcamo, and S. K. McConnell. “The determination of projection neuron identity in the developing cerebral cortex”. In: *Curr. Opin. Neurobiol.* 18.1 (2008), pp. 28–35 (cit. on p. 116).
- [166]R. Li, K. Chen, A. S. Fleisher, et al. “Large-scale directional connections among multi resting-state neural networks in human brain: a functional MRI and Bayesian network modeling study”. In: *Neuroimage* 56.3 (2011), pp. 1035–1042 (cit. on p. 39).
- [167]G. Y. Liao, D. A. Wagner, M. H. Hsu, and J. P. Leonard. “Evidence for direct protein kinase-C mediated modulation of N-methyl-D-aspartate receptor current”. In: *Mol. Pharmacol.* 59.5 (2001), pp. 960–964 (cit. on p. 153).
- [168]E. M. Lisabeth, G. Falivelli, and E. B. Pasquale. “Eph receptor signaling and ephrins”. In: *Cold Spring Harb Perspect Biol* 5.9 (2013) (cit. on p. 155).

- [169]A. Lischke, M. Gamer, C. Berger, et al. “Oxytocin increases amygdala reactivity to threatening scenes in females”. In: *Psychoneuroendocrinology* 37.9 (2012). cited By 45, pp. 1431–1438 (cit. on p. 181).
- [170]J. Lisman and S. Raghavachari. “Biochemical principles underlying the stable maintenance of LTP by the CaMKII/NMDAR complex”. In: *Brain Res.* (2014) (cit. on pp. 196, 198).
- [171]J. Lisman, R. Yasuda, and S. Raghavachari. “Mechanisms of CaMKII action in long-term potentiation”. In: *Nat. Rev. Neurosci.* 13.3 (2012), pp. 169–182 (cit. on pp. 111, 150).
- [172]J. Lisman, H. Schulman, and H. Cline. “The molecular basis of CaMKII function in synaptic and behavioural memory”. In: *Nat. Rev. Neurosci.* 3.3 (2002), pp. 175–190 (cit. on pp. 150, 196, 198).
- [173]J. E. Lisman and A. M. Zhabotinsky. “A model of synaptic memory: a CaMKII/PP1 switch that potentiates transmission by organizing an AMPA receptor anchoring assembly”. In: *Neuron* 31.2 (2001), pp. 191–201 (cit. on pp. 196, 198).
- [174]No authors listed. “The ADHD-200 Consortium: A Model to Advance the Translational Potential of Neuroimaging in Clinical Neuroscience”. In: *Front Syst Neurosci* 6 (2012), p. 62 (cit. on p. 43).
- [175]L. Lu, V. Timofeyev, N. Li, et al. “Alpha-actinin2 cytoskeletal protein is required for the functional membrane localization of a Ca²⁺-activated K⁺ channel (SK2 channel)”. In: *Proc. Natl. Acad. Sci. U.S.A.* 106.43 (2009), pp. 18402–18407 (cit. on p. 153).
- [176]A. R. Luria. *Higher Cortical Functions in Man*. Springer US, 1980 (cit. on pp. 41, 85).
- [177]H. Ma, B. Li, and R. W. Tsien. “Distinct roles of multiple isoforms of CaMKII in signaling to the nucleus”. In: *Biochim. Biophys. Acta* (2015) (cit. on pp. 111, 150).
- [178]D. Mantini, A. Gerits, K. Nelissen, et al. “Default mode of brain function in monkeys”. In: *J. Neurosci.* 31.36 (2011), pp. 12954–12962 (cit. on p. 43).
- [179]D. Mantini, M. Corbetta, G. L. Romani, G. A. Orban, and W. Vanduffel. “Evolutionarily novel functional networks in the human brain?” In: *J. Neurosci.* 33.8 (2013), pp. 3259–3275 (cit. on p. 43).
- [180]D. S. Margulies, J. L. Vincent, C. Kelly, et al. “Precuneus shares intrinsic functional architecture in humans and monkeys”. In: *Proc. Natl. Acad. Sci. U.S.A.* 106.47 (2009), pp. 20069–20074 (cit. on p. 43).
- [181]J. A. Martin, Z. Hu, K. M. Fenz, J. Fernandez, and J. S. Dittman. “Complexin has opposite effects on two modes of synaptic vesicle fusion”. In: *Curr. Biol.* 21.2 (2011), pp. 97–105 (cit. on pp. 102, 147).
- [182]L. J. Martin, A. A. Zurek, J. F. MacDonald, et al. “Alpha5GABAA receptor activity sets the threshold for long-term potentiation and constrains hippocampus-dependent memory”. In: *J. Neurosci.* 30.15 (2010), pp. 5269–5282 (cit. on p. 149).
- [183]C. Martínez-Cué, B. Delatour, and M. C. Potier. “Treating enhanced GABAergic inhibition in Down syndrome: use of GABA α 5-selective inverse agonists”. In: *Neurosci Biobehav Rev* 46 Pt 2 (2014), pp. 218–227 (cit. on p. 150).
- [184]M. Matsuzaki, N. Honkura, G. C. Ellis-Davies, and H. Kasai. “Structural basis of long-term potentiation in single dendritic spines”. In: *Nature* 429.6993 (2004), pp. 761–766 (cit. on pp. 111, 153).

- [185]K. A. McKiernan, J. N. Kaufman, J. Kucera-Thompson, and J. R. Binder. “A parametric manipulation of factors affecting task-induced deactivation in functional neuroimaging”. In: *J Cogn Neurosci* 15.3 (2003), pp. 394–408 (cit. on p. 39).
- [186]A. Meneses. “Effects of the 5-HT7 receptor antagonists SB-269970 and DR 4004 in autoshaping Pavlovian/instrumental learning task”. In: *Behav. Brain Res.* 155.2 (2004), pp. 275–282 (cit. on p. 150).
- [187]M. Mennes, B. B. Biswal, F. X. Castellanos, and M. P. Milham. “Making data sharing work: the FCP/INDI experience”. In: *Neuroimage* 82 (2013), pp. 683–691 (cit. on p. 43).
- [188]M. Mennes, C. Kelly, S. Colcombe, F. X. Castellanos, and M. P. Milham. “The extrinsic and intrinsic functional architectures of the human brain are not equivalent”. In: *Cereb. Cortex* 23.1 (2013), pp. 223–229 (cit. on p. 40).
- [189]S. Mesmoudi, V. Perlberg, D. Rudrauf, et al. “Resting state networks’ corticotopy: the dual intertwined rings architecture”. In: *PLoS ONE* 8.7 (2013), e67444 (cit. on pp. 83–85, 87, 90, 99, 110, 115, 117, 172, 179).
- [190]M. M. Mesulam, A. Guillozet, P. Shaw, et al. “Acetylcholinesterase knockouts establish central cholinergic pathways and can use butyrylcholinesterase to hydrolyze acetylcholine”. In: *Neuroscience* 110.4 (2002), pp. 627–639 (cit. on p. 41).
- [191]B. Milner, M. Petrides, and M. L. Smith. “Frontal lobes and the temporal organization of memory”. In: *Hum Neurobiol* 4.3 (1985), pp. 137–142 (cit. on pp. 41, 85).
- [192]P. K. Moghadam and M. B. Jackson. “The functional significance of synaptotagmin diversity in neuroendocrine secretion”. In: *Front Endocrinol (Lausanne)* 4 (2013), p. 124 (cit. on pp. 101, 146).
- [193]Z. Mukamel, G. Konopka, E. Wexler, et al. “Regulation of MET by FOXP2, genes implicated in higher cognitive dysfunction and autism risk”. In: *J. Neurosci.* 31.32 (2011), pp. 11437–11442 (cit. on p. 156).
- [194]J. D. Murray, A. Bernacchia, D. J. Freedman, et al. “A hierarchy of intrinsic timescales across primate cortex”. In: *Nat. Neurosci.* 17.12 (2014), pp. 1661–1663 (cit. on pp. 85, 99).
- [195]C. Narain, S.K. Scott, R.J.S. Wise, et al. “Defining a Left-lateralized Response Specific to Intelligible Speech Using fMRI”. In: *Cerebral Cortex* 13.12 (2003). cited By 144, pp. 1362–1368 (cit. on p. 182).
- [196]M. E. Newman. “Modularity and community structure in networks”. In: *Proc. Natl. Acad. Sci. U.S.A.* 103.23 (2006), pp. 8577–8582 (cit. on pp. 29, 31, 37, 45).
- [197]M. E. J. Newman. “Detecting community structure in networks”. In: *The European Physical Journal B - Condensed Matter* 38.2 (2004), pp. 321–330 (cit. on p. 45).
- [198]K. B. Nooner, S. J. Colcombe, R. H. Tobe, et al. “The NKI-Rockland Sample: A Model for Accelerating the Pace of Discovery Science in Psychiatry”. In: *Front Neurosci* 6 (2012), p. 152 (cit. on p. 43).
- [199]G. Northoff and F. Bermpohl. “Cortical midline structures and the self”. In: *Trends Cogn. Sci. (Regul. Ed.)* 8.3 (2004), pp. 102–107 (cit. on p. 41).
- [200]K. N. Ochsner, K. Knierim, D. H. Ludlow, et al. “Reflecting upon feelings: an fMRI study of neural systems supporting the attribution of emotion to self and other”. In: *J Cogn Neurosci* 16.10 (2004), pp. 1746–1772 (cit. on p. 41).

- [201]T. P. O'Connor, K. Cockburn, W. Wang, et al. "Semaphorin 5B mediates synapse elimination in hippocampal neurons". In: *Neural Dev* 4 (2009), p. 18 (cit. on pp. 112, 154).
- [202]K. K. Ogden, A. Khatri, S. F. Traynelis, and S. A. Heldt. "Potentiation of GluN2C/D NMDA receptor subtypes in the amygdala facilitates the retention of fear and extinction learning in mice". In: *Neuropsychopharmacology* 39.3 (2014), pp. 625–637 (cit. on p. 149).
- [203]K. D. Oikonomou, M. B. Singh, M. T. Rich, S. M. Short, and S. D. Antic. "Contribution of extrasynaptic N-methyl-d-aspartate and adenosine A1 receptors in the generation of dendritic glutamate-mediated plateau potentials". In: *Philos. Trans. R. Soc. Lond., B, Biol. Sci.* 370.1672 (2015) (cit. on p. 149).
- [204]K. Okamoto, T. Nagai, A. Miyawaki, and Y. Hayashi. "Rapid and persistent modulation of actin dynamics regulates postsynaptic reorganization underlying bidirectional plasticity". In: *Nat. Neurosci.* 7.10 (2004), pp. 1104–1112 (cit. on pp. 111, 153).
- [205]A. K. Pandey, L. Lu, X. Wang, R. Homayouni, and R. W. Williams. "Functionally Enigmatic Genes: A Case Study of the Brain Ignorome". In: *PLoS ONE* 9.2 (2014), e88889 (cit. on p. 7).
- [206]R. J. Pasterkamp and R. J. Giger. "Semaphorin function in neural plasticity and disease". In: *Curr. Opin. Neurobiol.* 19.3 (2009), pp. 263–274 (cit. on pp. 112, 155).
- [207]V. Perlbarg, G. Marrelec, J. Doyon, et al. "NEDICA: Detection of group functional networks in fMRI using spatial independent component analysis". In: *2008 5th IEEE International Symposium on Biomedical Imaging: From Nano to Macro*. IEEE, 2008 (cit. on pp. 37, 44).
- [208]B. D. Philpot, K. K. Cho, and M. F. Bear. "Obligatory role of NR2A for metaplasticity in visual cortex". In: *Neuron* 53.4 (2007), pp. 495–502 (cit. on p. 148).
- [209]R.A. Poldrack. "Can cognitive processes be inferred from neuroimaging data?" In: *Trends in Cognitive Sciences* 10.2 (2006). cited By 561, pp. 59–63 (cit. on p. 175).
- [210]C. G. Pontrello and I. M. Ethell. "Accelerators, Brakes, and Gears of Actin Dynamics in Dendritic Spines". In: *Open Neurosci J* 3 (2009), pp. 67–86 (cit. on p. 153).
- [211]M. C. Potier, J. Braudeau, L. Dauphinot, and B. Delatour. "Reducing GABAergic inhibition restores cognitive functions in a mouse model of Down syndrome". In: *CNS Neurol Disord Drug Targets* 13.1 (2014), pp. 8–15 (cit. on pp. 149, 150).
- [212]J. D. Power, K. A. Barnes, A. Z. Snyder, B. L. Schlaggar, and S. E. Petersen. "Spurious but systematic correlations in functional connectivity MRI networks arise from subject motion". In: *Neuroimage* 59.3 (2012), pp. 2142–2154 (cit. on p. 42).
- [213]J. D. Power, D. A. Fair, B. L. Schlaggar, and S. E. Petersen. "The development of human functional brain networks". In: *Neuron* 67.5 (2010), pp. 735–748 (cit. on p. 42).
- [214]E. Premi, F. Cauda, R. Gasparotti, et al. "Multimodal fMRI resting-state functional connectivity in granulin mutations: the case of fronto-parietal dementia". In: *PLoS ONE* 9.9 (2014), e106500 (cit. on p. 84).
- [215]T. M. Preuss. "Evolutionary Specializations of Primate Brain Systems". In: *PRIMATE ORIGINS: Adaptations and Evolution*. Springer US, 2007, pp. 625–675 (cit. on p. 43).
- [216]Y. Qu, R. Curtis, D. Lawson, et al. "Differential modulation of sodium channel gating and persistent sodium currents by the beta1, beta2, and beta3 subunits". In: *Mol. Cell. Neurosci.* 18.5 (2001), pp. 570–580 (cit. on pp. 100, 145).

- [217]M. E. Raichle, A. M. MacLeod, A. Z. Snyder, et al. “A default mode of brain function”. In: *Proc. Natl. Acad. Sci. U.S.A.* 98.2 (2001), pp. 676–682 (cit. on pp. 39, 41, 85).
- [218]P. Rakic and J. L. Rubenstein, eds. *Cellular Migration and Formation of Neuronal Connections*. Oxford, UK: Academic Press, 2013 (cit. on p. 7).
- [219]P. Rakic, A. E. Ayoub, J. J. Breunig, and M. H. Dominguez. “Decision by division: making cortical maps”. In: *Trends Neurosci.* 32.5 (2009), pp. 291–301 (cit. on p. 7).
- [220]B. G. Rash, S. Tomasi, H. D. Lim, C. Y. Suh, and F. M. Vaccarino. “Cortical gyrification induced by fibroblast growth factor 2 in the mouse brain”. In: *J. Neurosci.* 33.26 (2013), pp. 10802–10814 (cit. on p. 155).
- [221]A. Raznahan, R. Toro, E. Daly, et al. “Cortical anatomy in autism spectrum disorder: an in vivo MRI study on the effect of age”. In: *Cereb. Cortex* 20.6 (2010), pp. 1332–1340 (cit. on pp. 3, 194).
- [222]J. Richiardi, A. Altmann, A. Milazzo, et al. “Correlated gene expression supports synchronous activity in brain networks”. In: *Science* 348.6240 (2015), pp. 1241–1244 (cit. on pp. 4, 143).
- [223]R. Romaniello, F. Arrigoni, M. T. Bassi, and R. Borgatti. “Mutations in α and β -tubulin encoding genes: implications in brain malformations”. In: *Brain Dev.* 37.3 (2015), pp. 273–280 (cit. on p. 154).
- [224]J. D. Rudie, L. M. Hernandez, J. A. Brown, et al. “Autism-associated promoter variant in MET impacts functional and structural brain networks”. In: *Neuron* 75.5 (2012), pp. 904–915 (cit. on pp. 156, 196).
- [225]T. J. Ryan and S. G. Grant. “The origin and evolution of synapses”. In: *Nature reviews. Neuroscience* 10.10 (2009), pp. 701–712 (cit. on pp. 142, 166).
- [226]M. Safran, I. Dalah, J. Alexander, et al. “GeneCards Version 3: the human gene integrator”. In: *Database* 2010.0 (2010), baq020–baq020 (cit. on p. 173).
- [227]M. Sanhueza, G. Fernandez-Villalobos, I. S. Stein, et al. “Role of the CaMKII/NMDA receptor complex in the maintenance of synaptic strength”. In: *J. Neurosci.* 31.25 (2011), pp. 9170–9178 (cit. on p. 148).
- [228]S. N. Sansom and F. J. Livesey. “Gradients in the brain: the control of the development of form and function in the cerebral cortex”. In: *Cold Spring Harb Perspect Biol* 1.2 (2009), a002519 (cit. on pp. 83, 110).
- [229]J. Savitz, I. Lucki, and W. C. Drevets. “5-HT(1A) receptor function in major depressive disorder”. In: *Prog. Neurobiol.* 88.1 (2009), pp. 17–31 (cit. on p. 150).
- [230]J. B. Savitz and W. C. Drevets. “Imaging phenotypes of major depressive disorder: genetic correlates”. In: *Neuroscience* 164.1 (2009), pp. 300–330 (cit. on p. 150).
- [231]R. Saxe and N. Kanwisher. “People thinking about thinking people. The role of the temporo-parietal junction in “theory of mind””. In: *Neuroimage* 19.4 (2003), pp. 1835–1842 (cit. on pp. 41, 85).
- [232]D. L. Schacter, D. R. Addis, and R. L. Buckner. “Remembering the past to imagine the future: the prospective brain”. In: *Nat. Rev. Neurosci.* 8.9 (2007), pp. 657–661 (cit. on pp. 41, 85).
- [233]B. L. Schlaggar. “Mapping genetic influences on cortical regionalization”. In: *Neuron* 72.4 (2011), pp. 499–501 (cit. on pp. 83, 110).

- [234]J. D. Schmahmann, D. N. Pandya, R. Wang, et al. “Association fibre pathways of the brain: parallel observations from diffusion spectrum imaging and autoradiography”. In: *Brain* 130.Pt 3 (2007), pp. 630–653 (cit. on p. 26).
- [235]S.K. Scott, C. Catrin Blank, S. Rosen, and R.J.S. Wise. “Identification of a pathway for intelligible speech in the left temporal lobe”. In: *Brain* 123.12 (2000). cited By 645, pp. 2400–2406 (cit. on p. 182).
- [236]T. J. Sejnowski, P. S. Churchland, and J. A. Movshon. “Putting big data to good use in neuroscience”. In: *Nat. Neurosci.* 17.11 (2014), pp. 1440–1441 (cit. on pp. 2, 3).
- [237]A. Semyanov, M. C. Walker, D. M. Kullmann, and R. A. Silver. “Tonically active GABA A receptors: modulating gain and maintaining the tone”. In: *Trends Neurosci.* 27.5 (2004), pp. 262–269 (cit. on p. 149).
- [238]J. Sepulcre, M. R. Sabuncu, T. B. Yeo, H. Liu, and K. A. Johnson. “Stepwise connectivity of the modal cortex reveals the multimodal organization of the human brain”. In: *J. Neurosci.* 32.31 (2012), pp. 10649–10661 (cit. on pp. 38, 39, 84).
- [239]J. Sepulcre, H. Liu, T. Talukdar, et al. “The organization of local and distant functional connectivity in the human brain”. In: *PLoS Comput. Biol.* 6.6 (2010), e1000808 (cit. on pp. 24, 25, 38, 99).
- [240]W. R. Shankle, A. K. Romney, B. H. Landing, and J. Hara. “Developmental patterns in the cytoarchitecture of the human cerebral cortex from birth to 6 years examined by correspondence analysis”. In: *Proc. Natl. Acad. Sci. U.S.A.* 95.7 (1998), pp. 4023–4028 (cit. on p. 87).
- [241]C. Shelley, M. Farrant, and S. G. Cull-Candy. “TARP-associated AMPA receptors display an increased maximum channel conductance and multiple kinetically distinct open states”. In: *J. Physiol. (Lond.)* 590.Pt 22 (2012), pp. 5723–5738 (cit. on pp. 101, 146).
- [242]G. M. Shepherd. *Handbook of Brain Microcircuits*. UK: Oxford University Press, 2010 (cit. on p. 140).
- [243]G. M. Shepherd. *Neurobiology*. UK: Oxford University Press, 1994 (cit. on p. 7).
- [244]J. R. Simpson, A. Z. Snyder, D. A. Gusnard, and M. E. Raichle. “Emotion-induced changes in human medial prefrontal cortex: I. During cognitive task performance”. In: *Proc. Natl. Acad. Sci. U.S.A.* 98.2 (2001), pp. 683–687 (cit. on p. 39).
- [245]P. Skudlarski, K. Jagannathan, V. D. Calhoun, et al. “Measuring brain connectivity: diffusion tensor imaging validates resting state temporal correlations”. In: *Neuroimage* 43.3 (2008), pp. 554–561 (cit. on p. 39).
- [246]K. S. Smith, S. V. Mahler, S. Pecina, and K. C. Berridge. “Hedonic hotspots: Generating sensory pleasure in the brain”. In: *Pleasures of the brain* (2010). Oxford University Press, 27–49 (cit. on p. 40).
- [247]S. M. Smith, P. T. Fox, K. L. Miller, et al. “Correspondence of the brain’s functional architecture during activation and rest”. In: *Proc. Natl. Acad. Sci. U.S.A.* 106.31 (2009), pp. 13040–13045 (cit. on pp. 24, 25, 28, 38, 45, 84, 85, 99, 110).
- [248]C. D. Smyser, T. E. Inder, J. S. Shimony, et al. “Longitudinal analysis of neural network development in preterm infants”. In: *Cereb. Cortex* 20.12 (2010), pp. 2852–2862 (cit. on p. 42).
- [249]M. E. Soden, G. L. Jones, C. A. Sanford, et al. “Disruption of dopamine neuron activity pattern regulation through selective expression of a human KCNN3 mutation”. In: *Neuron* 80.4 (2013), pp. 997–1009 (cit. on pp. 100, 145).

- [250]M. Somel, H. Franz, Z. Yan, et al. “Transcriptional neoteny in the human brain”. In: *Proc. Natl. Acad. Sci. U.S.A.* 106.14 (2009), pp. 5743–5748 (cit. on p. 141).
- [251]T. C. Sudhof. “Neurotransmitter release: the last millisecond in the life of a synaptic vesicle”. In: *Neuron* 80.3 (2013), pp. 675–690 (cit. on pp. 101, 146).
- [252]M. K. Sun and D. L. Alkon. “The “memory kinases”: roles of PKC isoforms in signal processing and memory formation”. In: *Prog Mol Biol Transl Sci* 122 (2014), pp. 31–59 (cit. on p. 153).
- [253]R.K. Sunahara, H.-C. Guan, B.F. O’Dowd, et al. “Cloning of the gene for a human dopamine D5 receptor with higher affinity for dopamine than D1”. In: *Nature* 350.6319 (1991). cited By 656, pp. 614–619 (cit. on p. 181).
- [254]K. Supekar, L. Q. Uddin, K. Prater, et al. “Development of functional and structural connectivity within the default mode network in young children”. In: *Neuroimage* 52.1 (2010), pp. 290–301 (cit. on p. 42).
- [255]M. Takemura, T. Mishima, Y. Wang, et al. “Ca²⁺/calmodulin-dependent protein kinase IV-mediated LIM kinase activation is critical for calcium signal-induced neurite outgrowth”. In: *J. Biol. Chem.* 284.42 (2009), pp. 28554–28562 (cit. on p. 151).
- [256]J Talairach. *Referentially oriented cerebral MRI anatomy : an atlas of stereotaxic anatomical correlations for gray and white matter*. Stuttgart New York New York: G. Thieme Verlag Thieme Medical Publishers, 1993 (cit. on p. 174).
- [257]B. Thirion, G. Varoquaux, O. Grisel, C. Poupon, and P. Pinel. “Principal component regression predicts functional responses across individuals”. In: *Med Image Comput Comput Assist Interv* 17.Pt 2 (2014), pp. 741–748 (cit. on p. 84).
- [258]P. M. Thompson, J. L. Stein, S. E. Medland, et al. “The ENIGMA Consortium: large-scale collaborative analyses of neuroimaging and genetic data”. In: *Brain Imaging Behav* 8.2 (2014), pp. 153–182 (cit. on p. 4).
- [259]M. A. Tischfield and E. C. Engle. “Distinct alpha- and beta-tubulin isotypes are required for the positioning, differentiation and survival of neurons: new support for the ‘multi-tubulin’ hypothesis”. In: *Biosci. Rep.* 30.5 (2010), pp. 319–330 (cit. on p. 154).
- [260]G. Tononi. “An information integration theory of consciousness”. In: *BMC Neurosci* 5 (2004), p. 42 (cit. on p. 24).
- [261]R. Toro, P. T. Fox, and T. Paus. “Functional coactivation map of the human brain”. In: *Cereb. Cortex* 18.11 (2008), pp. 2553–2559 (cit. on p. 62).
- [262]R. Toro, M. Konyukh, R. Delorme, et al. “Key role for gene dosage and synaptic homeostasis in autism spectrum disorders”. In: *Trends Genet.* 26.8 (2010), pp. 363–372 (cit. on pp. 3, 194).
- [263]H. Toyoda, M. G. Zhao, V. Mercaldo, et al. “Calcium/calmodulin-dependent kinase IV contributes to translation-dependent early synaptic potentiation in the anterior cingulate cortex of adult mice”. In: *Mol Brain* 3 (2010), p. 27 (cit. on p. 152).
- [264]T. S. Tran, M. E. Rubio, R. L. Clem, et al. “Secreted semaphorins control spine distribution and morphogenesis in the postnatal CNS”. In: *Nature* 462.7276 (2009), pp. 1065–1069 (cit. on p. 155).
- [265]H.T. Uchiyama, D.N. Saito, H.C. Tanabe, et al. “Distinction between the literal and intended meanings of sentences: A functional magnetic resonance imaging study of metaphor and sarcasm”. In: *Cortex* 48.5 (2012). cited By 19, pp. 563–583 (cit. on p. 182).

- [266]K. R. Van Dijk, M. R. Sabuncu, and R. L. Buckner. “The influence of head motion on intrinsic functional connectivity MRI”. In: *Neuroimage* 59.1 (2012), pp. 431–438 (cit. on p. 42).
- [267]D. C. Van Essen and D. L. Dierker. “Surface-based and probabilistic atlases of primate cerebral cortex”. In: *Neuron* 56.2 (2007), pp. 209–225 (cit. on p. 43).
- [268]D.C. Van Essen. “Surface-based approaches to spatial localization and registration in primate cerebral cortex”. In: *NeuroImage* 23.SUPPL. 1 (2004). cited By 99, S97–S107 (cit. on p. 172).
- [269]G. W. Van Hoesen. “The modern concept of association cortex”. In: *Curr. Opin. Neurobiol.* 3.2 (1993), pp. 150–154 (cit. on p. 24).
- [270]C. G. Vanoye, J. D. Kunic, G. R. Ehring, and A. L. George. “Mechanism of sodium channel NaV1.9 potentiation by G-protein signaling”. In: *The Journal of General Physiology* 141.2 (2013), pp. 193–202 (cit. on pp. 100, 145).
- [271]F. Varela, J. P. Lachaux, E. Rodriguez, and J. Martinerie. “The brainweb: phase synchronization and large-scale integration”. In: *Nat. Rev. Neurosci.* 2.4 (2001), pp. 229–239 (cit. on p. 24).
- [272]J. L. Vincent, I. Kahn, A. Z. Snyder, M. E. Raichle, and R. L. Buckner. “Evidence for a frontoparietal control system revealed by intrinsic functional connectivity”. In: *J. Neurophysiol.* 100.6 (2008), pp. 3328–3342 (cit. on pp. 25, 39, 99).
- [273]J. L. Vincent, G. H. Patel, M. D. Fox, et al. “Intrinsic functional architecture in the anaesthetized monkey brain”. In: *Nature* 447.7140 (2007), pp. 83–86 (cit. on p. 38).
- [274]A. C. Vogel, J. D. Power, S. E. Petersen, and B. L. Schlaggar. “Development of the brain’s functional network architecture”. In: *Neuropsychol Rev* 20.4 (2010), pp. 362–375 (cit. on p. 42).
- [275]K. Vogeley and G. R. Fink. “Neural correlates of the first-person-perspective”. In: *Trends Cogn. Sci. (Regul. Ed.)* 7.1 (2003), pp. 38–42 (cit. on p. 41).
- [276]N.D. Volkow, G.-J. Wang, D. Tomasi, and R.D. Baler. “Obesity and addiction: Neurobiological overlaps”. In: *Obesity Reviews* 14.1 (2013). cited By 85, pp. 2–18 (cit. on p. 181).
- [277]H. Wang, G. G. Stradtman, X. J. Wang, and W. J. Gao. “A specialized NMDA receptor function in layer 5 recurrent microcircuitry of the adult rat prefrontal cortex”. In: *Proc. Natl. Acad. Sci. U.S.A.* 105.43 (2008), pp. 16791–16796 (cit. on pp. 196, 197).
- [278]H. Wang, H. Fukushima, S. Kida, and M. Zhuo. “Ca²⁺/calmodulin-dependent protein kinase IV links group I metabotropic glutamate receptors to fragile X mental retardation protein in cingulate cortex”. In: *J. Biol. Chem.* 284.28 (2009), pp. 18953–18962 (cit. on p. 148).
- [279]M. Wang and A. F. Arnsten. “Contribution of NMDA receptors to dorsolateral prefrontal cortical networks in primates”. In: *Neurosci Bull* 31.2 (2015), pp. 191–197 (cit. on p. 111).
- [280]M. Wang, Y. Yang, C. J. Wang, et al. “NMDA receptors subserve persistent neuronal firing during working memory in dorsolateral prefrontal cortex”. In: *Neuron* 77.4 (2013), pp. 736–749 (cit. on pp. 111, 196, 197).
- [281]X. J. Wang. “Synaptic basis of cortical persistent activity: the importance of NMDA receptors to working memory”. In: *J. Neurosci.* 19.21 (1999), pp. 9587–9603 (cit. on pp. 196, 197).
- [282]X. J. Wang. “Synaptic reverberation underlying mnemonic persistent activity”. In: *Trends Neurosci.* 24.8 (2001), pp. 455–463 (cit. on pp. 196, 197).

- [283]D. Warde-Farley, S.L. Donaldson, O. Comes, et al. “The GeneMANIA prediction server: Biological network integration for gene prioritization and predicting gene function”. In: *Nucleic Acids Research* 38.SUPPL. 2 (2010). cited By 283, W214–W220 (cit. on p. 173).
- [284]Kenneth M. Warwick and Alain Morineau. *Multivariate Descriptive Statistical Analysis*. New York, NY, USA: John Wiley & Sons, Inc., 1984 (cit. on pp. 86–89, 113).
- [285]G. A. Wayman, H. Tokumitsu, M. A. Davare, and T. R. Soderling. “Analysis of CaM-kinase signaling in cells”. In: *Cell Calcium* 50.1 (2011), pp. 1–8 (cit. on pp. 111, 150).
- [286]G. A. Wayman, Y. S. Lee, H. Tokumitsu, et al. “Calmodulin-kinases: modulators of neuronal development and plasticity”. In: *Neuron* 59.6 (2008), pp. 914–931 (cit. on pp. 111, 150).
- [287]E. J. Weeber, C. M. Atkins, J. C. Selcher, et al. “A role for the beta isoform of protein kinase C in fear conditioning”. In: *J. Neurosci.* 20.16 (2000), pp. 5906–5914 (cit. on p. 153).
- [288]J. Weeds and D. Weir. “Co-occurrence Retrieval: A Flexible Framework for Lexical Distributional Similarity”. In: *Comput. Ling.* 31.4 (2005), pp. 439–475 (cit. on pp. 58, 76).
- [289]N. Weiss, S. Hameed, J. M. Fernandez-Fernandez, et al. “A Ca(v)3.2/syntaxin-1A signaling complex controls T-type channel activity and low-threshold exocytosis”. In: *J. Biol. Chem.* 287.4 (2012), pp. 2810–2818 (cit. on pp. 101, 146).
- [290]Susan Weller. *Metric scaling correspondence analysis*. Newbury Park, Calif: Sage Publications, 1990 (cit. on pp. 86, 87).
- [291]L. Wolf, C. Goldberg, N. Manor, R. Sharan, and E. Ruppin. “Gene expression in the rodent brain is associated with its regional connectivity”. In: *PLoS Comput. Biol.* 7.5 (2011), e1002040 (cit. on p. 83).
- [292]H. Yan, X. N. Zuo, D. Wang, et al. “Hemispheric asymmetry in cognitive division of anterior cingulate cortex: a resting-state functional connectivity study”. In: *Neuroimage* 47.4 (2009), pp. 1579–1589 (cit. on pp. 41, 84, 99, 110).
- [293]X. Yang, P. Cao, and T. C. Sudhof. “Deconstructing complexin function in activating and clamping Ca²⁺-triggered exocytosis by comparing knockout and knockdown phenotypes”. In: *Proc. Natl. Acad. Sci. U.S.A.* 110.51 (2013), pp. 20777–20782 (cit. on pp. 102, 111, 147).
- [294]T. Yarkoni, R.A. Poldrack, D.C. Van Essen, and T.D. Wager. “Cognitive neuroscience 2.0: Building a cumulative science of human brain function”. In: *Trends in Cognitive Sciences* 14.11 (2010). cited By 58, pp. 489–496 (cit. on pp. 172, 174, 176).
- [295]T. Yarkoni, R. A. Poldrack, T. E. Nichols, D. C. Van Essen, and T. D. Wager. “Large-scale automated synthesis of human functional neuroimaging data”. In: *Nat. Methods* 8.8 (2011), pp. 665–670 (cit. on pp. 8, 56, 57, 74, 75, 175, 176).
- [296]B. T. Yeo, F. M. Krienen, J. Sepulcre, et al. “The organization of the human cerebral cortex estimated by intrinsic functional connectivity”. In: *J. Neurophysiol.* 106.3 (2011), pp. 1125–1165 (cit. on pp. 24, 25, 38–40, 84, 99).
- [297]H. Zeng, E. H. Shen, J. G. Hohmann, et al. “Large-scale cellular-resolution gene profiling in human neocortex reveals species-specific molecular signatures”. In: *Cell* 149.2 (2012), pp. 483–496 (cit. on pp. 7, 83, 142, 172).
- [298]F. Zhang, B. Su, C. Wang, et al. “Posttranslational modifications of β -tubulin in alzheimer disease”. In: *Transl Neurodegener* 4 (2015), p. 9 (cit. on p. 193).

- [299]Q. Zhang, Y. Li, and R. W. Tsien. “The dynamic control of kiss-and-run and vesicular reuse probed with single nanoparticles”. In: *Science* 323.5920 (2009), pp. 1448–1453 (cit. on pp. 101, 111, 146).
- [300]J. Zimmermann, T. Trimbuch, and C. Rosenmund. “Synaptobrevin 1 mediates vesicle priming and evoked release in a subpopulation of hippocampal neurons”. In: *Journal of Neurophysiology* 112.6 (2014), pp. 1559–1565 (cit. on pp. 102, 147).

List of Figures

1.1	Spatiotemporal multiscale organization of the cortex	1
1.2	The spatiotemporal domain of neuroscience	2
1.3	Stairway to memory formation	13
1.4	The question to answer	13
1.5	Plan of the dissertation	17
2.1	Mapping and representativeness of RSNs and similarities in two different populations	27
2.2	RSN \times TBN overlap matrix	29
2.3	RSN \times BA overlap matrix	30
2.4	Mapping of VSA and PTF families	32
2.5	The dual intertwined rings architecture	48
2.6	Long distance cortical connections closing the PTF ring	49
2.7	Intertwining scheme	50
3.1	Neurosynth webpage	56
3.2	Neurosynth pipeline	57
3.3	Lexical map	59
3.4	Topographic map	61
3.5	The 21 anatomo-functional regions	64
3.6	Anatomo-functional regions versus cognitive networks I	65
3.7	Anatomo-functional regions versus cognitive networks II	65
3.8	Parietal gradients	67
3.9	Temporal gradients	69
3.10	Frontal gradients	71
3.11	The two intertwined rings	73
4.1	The two intertwined rings corresponding to different type of temporal processing.	84
4.2	Differential distribution of gene expression: CA analysis	91
4.3	DiCA analysis: regions factor scores histogram.	92
4.4	Heatmap representing the correlations between the 938 genes used in DiCA.	93
4.5	Bootstrap ratios for the genes for the Dimension extracted by DiCA	94
4.6	Map of the bootstrap ratios for the 161 genes, analyzed with DiCA, grouped per family and per class of neuronal function.	96

4.7	Scatter plot of the gene factor scores of the discriminant dimension extracted by the DiCA analyses performed on the 161 genes measured on Specimens H0352001 (horizontal) and H0352002 of ABA.	97
4.8	Example of cortical mapping of gene expression with extreme bootstrap ratios in PTF or VSA	98
4.9	Summary of the temporal properties of proteins that most differentiate between the two rings and their correspondence with the preferred information processing modes of the rings.	104
4.10	Genes correlation versus regions correlation	105
5.1	Cerebral and cortical anatomo-functional regions	114
5.2	Expression profiles: SATB2 and DRD1	116
5.3	Cerebral regions' organization based on gene expression	118
5.4	Cortical regions' organization based on gene expression	119
5.5	Ionic channels: cerebral and cortical distribution	122
5.6	Neurotransmitter release: cerebral and cortical distribution	124
5.7	Neurotransmitter receptors: cerebral and cortical distribution	126
5.8	Neuromodulators receptors: cerebral and cortical distribution	128
5.9	Short term memory: cerebral and cortical distribution	130
5.10	Long term memory: cerebral and cortical distribution	132
5.11	Cell-cell interaction: cerebral and cortical distribution	134
5.12	Growth factors: cerebral and cortical distribution	136
5.13	CaMKs family: differential distribution	137
5.14	Cortical gradients of gene expression	138
5.15	The differential stoichiometry of cortical synapses	144
5.16	VSA versus PTS memorization	152
5.17	Cladogram of taxonomic groups and origins of synaptic components	165
5.18	Phylogenetic relationships of mammals and their basic plan of cortical organization	167
6.1	Mapping of the networks corresponding to the cognitive functions "syllables production", "pure tone" and "lips movement"	177
6.2	3D and 2D mapping of the expression profile across the 947 brain regions for the Microtubule-associated Protein Tau (MAPT) gene	177
6.3	3D and 2D mapping of the regions of maximal expression for Microtubule-associated protein tau (MAPT) and Myelin basic protein (MBP) genes	178
6.4	2D mapping of the cognitive network "facial expression" in green	179
6.5	Topographical similarities (overlap) between "speech function" (nodes in magenta) and the 300 cognitive tasks	180
6.6	Mapping of the cognitive and sensorimotor functions related to the VSA ring, and some cognitive functions that reconstruct the PTF ring	181

6.7	Mapping of the regions where the genes coding for oxytocin receptor (OXTR) and dopamine receptor D5 (DRD5) are the most expressed	184
6.8	Mapping of the networks corresponding to the cognitive functions “speech” and “sentences”	185
6.9	Topographical similarities (overlap) between the ICN7 network (colored nodes) and the 300 cognitive tasks	185
7.1	Figure a shows the memory cascade with different proteins which interact within each synapse with two symmetrical dynamics: the effect of activation on memory, and the effect on memory on activation. These proteins have several subunits and isoforms. Our results show that these subunits or isoform can be differentially expressed across different regions of the cerebral cortex. They form different synapses and memory cascades specialized by regions as shown in Figure b). The figure illustrates four types of synapses organized along the two main gradients of genetic expression (VSA-PTF and temporo-frontal): the congruence between the synapses and the functional specialization of the different anatomo-functional cortical regions are presented in Chapters 4 and 5.	191
7.2	AD propagation patterns and tubulin subunits cortical gradients	192
7.3	ASD: comparison of cognitive networks and distribution for implicated genes	195
A.1	Differential distribution of gene expression: CA analysis on H0351.2002	227
A.2	DiCA analysis: regions factor scores histogram for H0351.2002	230
A.3	Brain H0351.2002 (161 genes) DiCA bootstrap ratios	231

List of Tables

4.1	The 161 genes coding for proteins forming ionic channels or involved in neurotransmitter release.	95
A.1	Brain H0351.2001 CA regions factor scores for Dimensions 1 and 2 and bootstrap ratios for Dimension 1	227
A.2	Brain H0351.2002 CA regions factor scores for Dimensions 1 and 2 and bootstrap ratios for Dimension 1	228
A.3	Brain H0351.2001 (938 genes) DiCA confusion matrix, fixed effect model	228
A.4	Brain H0351.2002 (983 genes) DiCA confusion matrix, fixed effect model	228
A.5	Brain H0351.2001 (938 genes) DiCA confusion matrix, random effect model	228
A.6	Brain H0351.2002 (983 genes) DiCA confusion matrix, random effect model	228
A.7	Brain H0351.2001 DiCA: Bootstrap ratios for the 938 genes	228
A.8	Brain H0351.2002 DiCA: Bootstrap ratios for the 938 genes.	228
A.9	Brain H0351.2001 (161 genes) DiCA confusion matrix, fixed effect model	228
A.10	Brain H0351.2001 (161 genes) DiCA confusion matrix, random effect model	229
A.11	Brain H0351.2002 (161 genes) DiCA confusion matrix, fixed effect model	229
A.12	Brain H0351.2002 (161 genes) DiCA confusion matrix, random effect model	229
A.13	Brains H0351.2001 and H0351.2002 DiCA: Bootstrap ratios for the 161 genes	229

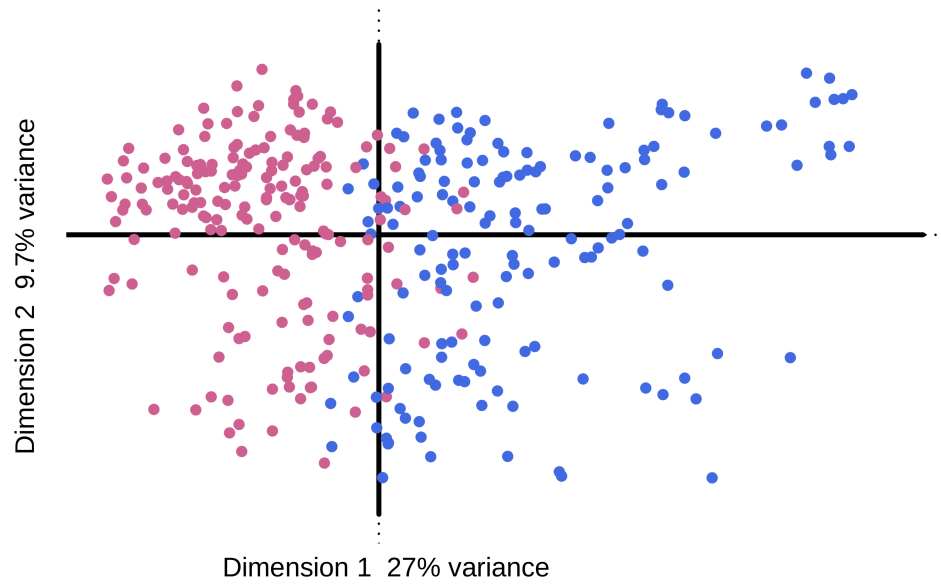


Fig. A.1.: Differential distribution of gene expression: CA analysis on H0351.2002

<http://journals.plos.org/plosone/article/asset?unique&id=info:doi/10.1371>

Tab. A.1.: Brain H0351.2001 CA regions factor scores for Dimensions 1 and 2 and bootstrap ratios for Dimension 1

<http://journals.plos.org/plosone/article/asset?unique&id=info:doi/10.1371/journal.pone.0171111>

Tab. A.2.: Brain H0351.2002 CA regions factor scores for Dimensions 1 and 2 and bootstrap ratios for Dimension 1

	VSA actual	PTF actual
VSA predicted	123	29
PTF predicted	45	197

Tab. A.3.: Brain H0351.2001 (938 genes) DiCA confusion matrix, fixed effect model. Confusion matrix for the fixed effect assignments of the ROIs to the rings. The columns represent the a priori assignment and the rows the actual (a posteriori) model assignment. Diagonal entries represent correct assignments.

	VSA actual	PTF actual
VSA predicted	177	12
PTF predicted	10	138

Tab. A.4.: Brain H0351.2002 (983 genes) DiCA confusion matrix, fixed effect model. Confusion matrix for the fixed effect assignments of the ROIS to the rings. The columns represent the a priori assignment and the rows the actual (a posteriori) model assignment. Diagonal entries represent correct assignments.

	VSA actual	PTF actual
VSA predicted	123	30
PTF predicted	45	196

Tab. A.5.: Brain H0351.2001 (938 genes) DiCA confusion matrix, random effect model. Confusion matrix for the random effect assignment of the ROIS to the rings. The columns represent the a priori assignment and the rows the (a posteriori) model assignment. Diagonal entries represent correct assignments.

	VSA actual	PTF actual
VSA predicted	176	13
PTF predicted	11	137

Tab. A.6.: Brain H0351.2002 (983 genes) DiCA confusion matrix, random effect model. Confusion matrix for the random effect assignment of the ROIS to the rings. The columns represent the a priori assignment and the rows the (a posteriori) model assignment. Diagonal entries represent correct assignments.

<http://journals.plos.org/plosone/article/asset?unique&id=info:doi/10.1371/journal.pone.0171111>

Tab. A.7.: Brain H0351.2001 DiCA: Bootstrap ratios for the 938 genes

<http://journals.plos.org/plosone/article/asset?unique&id=info:doi/10.1371/journal.pone.0171111>

Tab. A.8.: Brain H0351.2002 DiCA: Bootstrap ratios for the 938 genes.

	VSA actual	PTF actual
VSA predicted	132	34
PTF predicted	36	192

Tab. A.9.: Brain H0351.2001 (161 genes) DiCA confusion matrix, fixed effect model. Confusion matrix for the fixed effect assignments of the ROIS to the rings. The columns represent the a priori assignment and the rows the actual (a posteriori) model assignment. Diagonal entries represent correct assignments.

	VSA actual	PTF actual
VSA predicted	130	35
PTF predicted	38	191

Tab. A.10.: Brain H0351.2001 (161 genes) DiCA confusion matrix, random effect model. Confusion matrix for the random effect assignment of the ROIS to the rings. The columns represent the a priori assignment and the rows the (a posteriori) model assignment. Diagonal entries represent correct assignments

	VSA actual	PTF actual
VSA predicted	169	13
PTF predicted	18	137

Tab. A.11.: Brain H0351.2002 (161 genes) DiCA confusion matrix, fixed effect model. Confusion matrix for the fixed effect assignments of the ROIS to the rings. The columns represent the a priori assignment and the rows the actual (a posteriori) model assignment. Diagonal entries represent correct assignments.

	VSA actual	PTF actual
VSA predicted	168	13
PTF predicted	19	137

Tab. A.12.: Brain H0351.2002 (161 genes) DiCA confusion matrix, random effect model. Confusion matrix for the random effect assignment of the ROIS to the rings. The columns represent the a priori assignment and the rows the (a posteriori) model assignment. Diagonal entries represent correct assignments.

<http://journals.plos.org/plosone/article/asset?unique&id=info:doi/10.1371>

Tab. A.13.: Brains H0351.2001 and H0351.2002 DiCA: Bootstrap ratios for the 161 genes

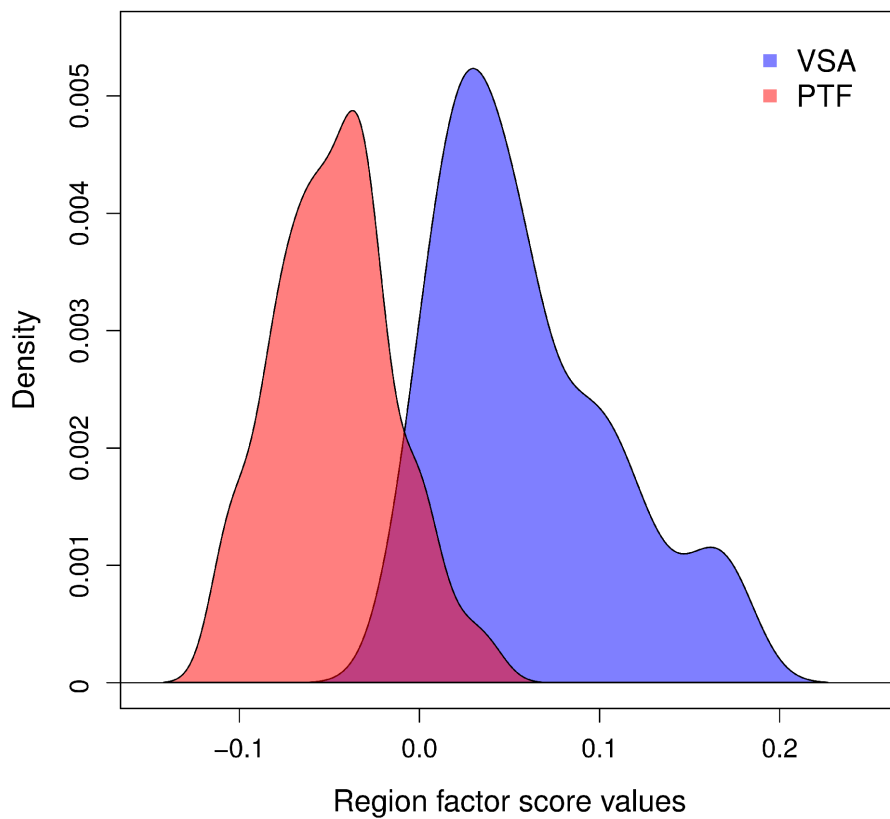


Fig. A.2.: DiCA analysis: regions factor scores histogram for H0351.2002. We plot the histogram of the factor score values—obtained for the 337 regions by the DiCA analysis—as a function of the number of regions a priori assigned to the VSA (blue) or the PTF (red) ring

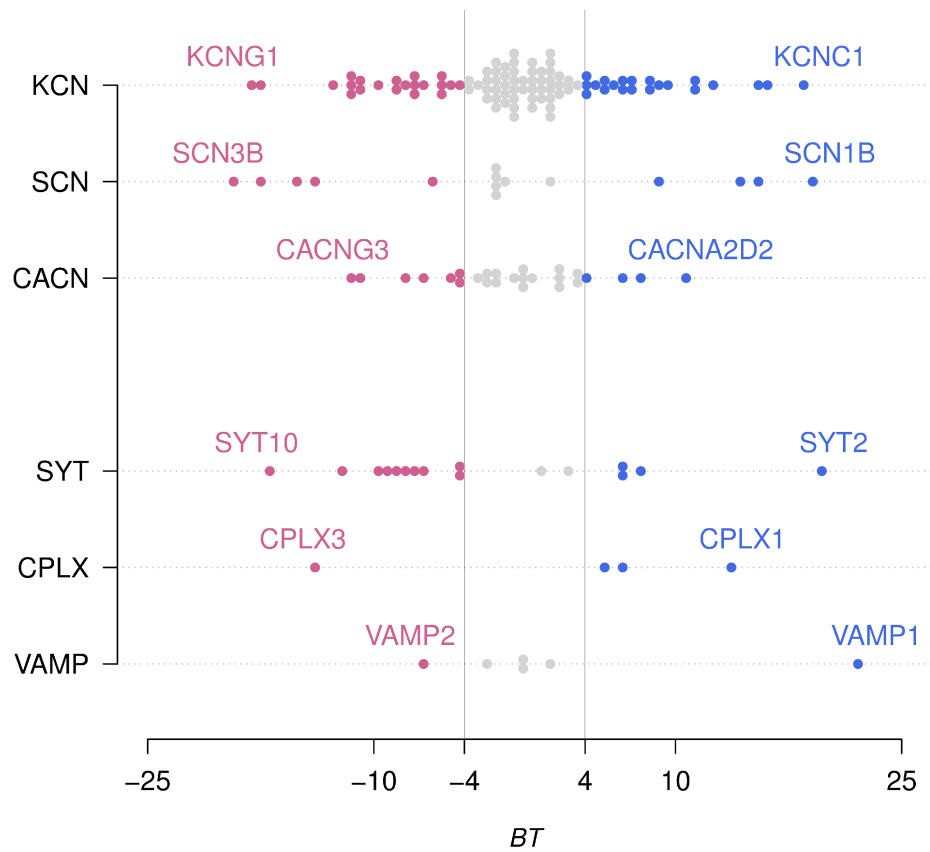


Fig. A.3.: Brain H0351.2002 (161 genes) DiCA bootstrap ratios. In blue are represented genes with significant positive bootstrap ratios ($BT > 4.00$) associated with the VSA ring and in red, genes with significant negative bootstrap ratios ($BT < -4.00$) associated with the PTF ring. For each family, extreme genes are identified. These genes are the most preferentially expressed in either VSA or PTF.